2015

# The age and provenance of Cambro-Ordovician sedimentary rocks of the Murrawong Creek Formation, southern New England Orogen, Australia

Carly S. Roder
*University of Wollongong*

Follow this and additional works at: https://ro.uow.edu.au/thsci

## Recommended Citation

# The age and provenance of Cambro-Ordovician sedimentary rocks of the Murrawong Creek Formation, southern New England Orogen, Australia

## Abstract

The Murrawong Creek and overlying Pipeclay Creek formations are a volcaniclastic sedimentary sequence containing some of the oldest fossil assemblages (Middle Cambrian to Ordovician) in the southern New England Orogen (NEO). These ages contrast markedly with the younger Devonian units that comprise most of the neighbouring Gamilaroi (Tamworth Group) and Djungati (Woolomin Group) terranes. Some researchers suggest that the fossils date allochthonous limestone blocks that slumped into younger deep marine basins. This project aims to test these competing hypotheses by utilizing detrital zircon geochronology (U-Pb SHRIMP dating) to establish the maximum depositional age by determining the youngest population of detrital zircons. Previous attempts to extract zircons from pre-Devonian rocks have been unsuccessful, but through targeting Zr-rich sandstone layers using a handheld XRF in the field, six detrital zircons were extracted from the Murrawong Creek Formation. All zircons show minimal rounding indicating minimal residence in sediment systems and are devoid of inherited cores derived from older melted crust. The youngest population of two zircons in the Murrawong Creek Formation have an age of 450 ±10 Ma indicating a maximum depositional age of ca. 460 – 440 (early Late Ordovician). The Pipeclay Creek Formation yielded thousands of zircons with a unimodal detrital zircon population of 443.4 ± 4.3 Ma, indicating a maximum depositional age in the latest Ordovician to earliest Silurian. This is consistent with the slightly older age of the Murrawong Creek Formation. These two formations still represent the oldest sedimentary units in the NEO, albeit younger than the age inferred from biostratigraphy.

In a broader tectonic framework, two tectonic models explaining the Gamilaroi terrane currently exist: 1. the island arc is an exotic terrane which accreted onto the eastern margin of Gondwana via east directed subduction, 2. the island arc developed just outboard of Gondwana and was later merged onto the Gondwanan margin via continuously west directed subduction. The lack of 'Gondwanan' Precambrian zircon grains suggest that the sediments are sourced from an island arc receiving no sedimentary influence from Gondwana. Point counting results plotted in QFL diagrams confirm that these quartz-poor sediments were sourced from an undissected arc. Geochemical analysis identified calc-alkaline, tholeiitic, boninitic and MORB-like clasts within the conglomerate. Together with chert clasts, this suggests that sediment deposition occurred within a forearc basin of an intra-oceanic island arc that was eroding detritus derived from old, offscraped accretionary wedge material and the adjacent island arc volcanic edifice. This explains the mixture of Cambrian shallow water fauna from older accreted volcanic seamounts with Ordovician-Silurian zircons in the same formations. It is likely that these represent portions of a forearc basin from the earliest stage of development of the Gamilaroi terrane somewhere in the Panthalassan Ocean. The arc evolved to more felsic composition throughout the Late Ordovician whereby the erosional unroofing of arc plutonic rocks occurred, resulting in the increasing presence of monzonitic clasts and zircons in the Pipeclay Creek Formation. Subsequent arc rifting in the Devonian was followed by collision and accretion onto the Gondwanan margin during the latest Devonian.

## Degree Type
Thesis

## Degree Name
International Bachelor of Science

## Department
School of Earth & Environmental Sciences

# The age and provenance of Cambro-Ordovician sedimentary rocks of the Murrawong Creek Formation, southern New England Orogen, Australia

**Carly Sue Roder**

A thesis submitted in part fulfilment of the requirements of the Honours degree of International Bachelor of Science in the School of Earth and Environmental Sciences, University of Wollongong 2015

The information in this thesis is entirely the result of investigations conducted by the author, unless otherwise acknowledged, and has not been submitted in part, or otherwise, for any other degree or qualification.

**Carly Roder**
**22<sup>nd</sup> April 2015**

# __ABSTRACT__

The Murrawong Creek and overlying Pipeclay Creek formations are a volcaniclastic sedimentary sequence containing some of the oldest fossil assemblages (Middle Cambrian to Ordovician) in the southern New England Orogen (NEO). These ages contrast markedly with the younger Devonian units that comprise most of the neighbouring Gamilaroi (Tamworth Group) and Djungati (Woolomin Group) terranes. Some researchers suggest that the fossils date allochthonous limestone blocks that slumped into younger deep marine basins. This project aims to test these competing hypotheses by utilizing detrital zircon geochronology (U-Pb SHRIMP dating) to establish the maximum depositional age by determining the youngest population of detrital zircons. Previous attempts to extract zircons from pre-Devonian rocks have been unsuccessful, but through targeting Zr-rich sandstone layers using a handheld XRF in the field, six detrital zircons were extracted from the Murrawong Creek Formation. All zircons show minimal rounding indicating minimal residence in sediment systems and are devoid of inherited cores derived from older melted crust. The youngest population of two zircons in the Murrawong Creek Formation have an age of 450 ±10 Ma indicating a maximum depositional age of ca. 460 – 440 (early Late Ordovician). The Pipeclay Creek Formation yielded thousands of zircons with a unimodal detrital zircon population of 443.4 ± 4.3 Ma, indicating a maximum depositional age in the latest Ordovician to earliest Silurian. This is consistent with the slightly older age of the Murrawong Creek Formation. These two formations still represent the oldest sedimentary units in the NEO, albeit younger than the age inferred from biostratigraphy.

In a broader tectonic framework, two tectonic models explaining the Gamilaroi terrane currently exist: 1. the island arc is an exotic terrane which accreted onto the eastern margin of Gondwana via east directed subduction, 2. the island arc developed just outboard of Gondwana and was later merged onto the Gondwanan margin via continuously west directed subduction. The lack of 'Gondwanan' Precambrian zircon grains suggest that the sediments are sourced from an island arc receiving no sedimentary influence from Gondwana. Point counting results plotted in QFL diagrams confirm that these quartz-poor sediments were sourced from an undissected arc. Geochemical analysis identified calc-alkaline, tholeiitic, boninitic and MORB-like clasts within the conglomerate. Together with chert clasts, this suggests that sediment deposition occurred within a forearc basin of

an intra-oceanic island arc that was eroding detritus derived from old, offscraped accretionary wedge material and the adjacent island arc volcanic edifice. This explains the mixture of Cambrian shallow water fauna from older accreted volcanic seamounts with Ordovician-Silurian zircons in the same formations. It is likely that these represent portions of a forearc basin from the earliest stage of development of the Gamilaroi terrane somewhere in the Panthalassan Ocean. The arc evolved to more felsic composition throughout the Late Ordovician whereby the erosional unroofing of arc plutonic rocks occurred, resulting in the increasing presence of monzonitic clasts and zircons in the Pipeclay Creek Formation. Subsequent arc rifting in the Devonian was followed by collision and accretion onto the Gondwanan margin during the latest Devonian.

# Table of Contents

# Table of Figures and Tables

# <u>ACKNOWLEDGEMENTS</u>

x

# Chapter 1.      Introduction

## 1.1    Introduction

The Murrawong Creek Formation (Cawood 1980) consists of massive, volcaniclastic sandstone and conglomerate interbedded with minor banded chert (Cawood 1980). It is considered the basal unit of the Gamilaroi terrane (Aitchison *et al.* 1988), within the southern New England Orogen (NEO). The conglomerate of the Murrawong Creek Formation consists of a volcaniclastic matrix which hosts pebble to boulder sized clasts of volcanic rock and fossiliferous limestone which hold the first definitive Cambrian fauna found within eastern New South Wales (Cawood 1980). The Murrawong Creek Formation is conformably overlain by the Pipeclay Creek Formation (Crook 1961), which comprises bedded argillites, sandstones and lenses of limestones and conglomerate (Cawood 1980). Conodont fauna from within cherts of unknown nature of the Pipeclay Creek Formation were found to be of late Middle Cambrian age (Stewart 1995).

The two formations are located approximately 30 km south east of Tamworth in central north-eastern New South Wales. The volcanic clasts of both formations are interpreted to have been transported by gravity flows from a western source (Leitch & Cawood 1987). It is inferred that they are inner-submarine-fan deposits within a forearc basin, adjacent to a volcanic arc, most likely intra-oceanic (Cawood 1980; Leitch & Cawood 1987). The current accepted age for the sedimentary rocks is Middle Cambrian, assuming the fossiliferous limestone clasts and chert layers are syndepositional with the host-matrix (e.g.,Cawood 1976; Cawood 1980; Stewart 1995). This project will attempt to constrain the age of the host-matrix of the Murrawong and Pipeclay Creek Formations through the use of detrital zircon geochronology. This will provide the first successful attempt at radiometric dating of the volcaniclastic matrix of the Early Paleozoic rocks of the New England Orogen and determine whether the fossiliferous limestone was formed simultaneously.

Volcaniclastic conglomerates often contain samples of source-rocks as their clasts (Leitch & Cawood 1987), making them effective sedimentary sequences to undertake provenance analysis. Sedimentary provenance studies are aimed at reconstructing and inferring the sedimentation history to determine the conditions under which the sediments formed, namely the tectonic setting (Weltje & von Eynatten 2004). Provenance analysis will

further determine the tectonic setting of the Murrawong (and Pipeclay) Creek Formation, providing more information for the geological history of the southern New England Orogen during the Early Paleozoic, and its association to the eastern margin of Gondwana.

## 1.2    Aims and Objectives

The aim of this project is to describe and date what are considered to be the oldest known sedimentary sequences within the southern NEO, specifically the Murrawong Creek and Pipeclay Creek formations. The use of detrital zircon geochronology should provide a better understanding of the Early Paleozoic evolution of the southern NEO.

The age and provenance of these ?Cambrian-Silurian? volcaniclastic rocks will place tighter temporal and spatial constraints on the initiation of sedimentation in the proto-NEO and contribute to the resolution of long held disputes over continental growth methods for eastern Australia. The project is divided into several objectives:

i.    Map and sample key sections of the Murrawong Creek and Pipeclay Creek formations to create a detailed geological map using ArcGIS and Google Earth

ii.    Produce a detailed stratigraphic column incorporating my own mapping, sampling and zircon geochronology with previous mapping by Cawood (1980) and biostratigraphy (Cawood 1976; Stewart 1995; Brock 1998a, b, 1999; Furey-Greig 2003; Sloan & Laurie 2004)

iii.    Undertake standard petrographic sandstone analysis using the QFL methods of Dickinson and Suczek (1979) to determine provenance

iv.    Undertake whole rock geochemistry (XRF and ICP-MS) of volcaniclastic units and interbedded volcanics to discriminate the tectonic setting of formation

v.    Extract and date detrital zircons from the Murrawong Creek and overlying Pipeclay Creek formations for U-Pb dating using the SHRIMP at ANU. The zircon age data can be compared with previous fossil ages and, on the basis that the youngest detrital zircon population age represents the maximum depositional age, can be used to test if the fossils represent the depositional age or whether they are older rocks that have slumped into younger sequences

vi.    Use the petrological, geochemical and geochronological data to determine whether volcaniclastic rocks of the Murrawong Creek Formation are affiliated with the Gondwanan continental margin, or whether they represent an exotic terrane, which has later collided with Gondwana.

## 1.3 Background

### 1.3.1 The New England Orogen

The New England Orogen (NEO) exhibits complex geology typical of ancient convergent margins, and extends for more than 1500 km from Bowen in north Queensland to Newcastle in central New South Wales (Aitchison *et al.* 1992a). The NEO is divided by the Clarence-Moreton Basin into northern and southern parts, which are then further divided into 3 provinces; Yarrol, Gympie and New England. The NEO represents the eastern most tectonic element of the Tasmanides or Terra Australis Orogen (Cawood 2005), a group of orogenic belts that formed the eastern portion of Gondwana (Glen 2005). The NEO is composed of Early Cambrian to Triassic subduction-related rocks exhibiting a zonation from west to east of a volcanic arc-forearc-subduction complex system (Scheibner 1996). The oldest rocks are Cambrian dismembered ophiolitic rocks incorporated into the serpentinite mélange of the Weraerai terrane. These ophiolites are interpreted to be derived from an exotic terrane formed in the ancient Panthalassan Ocean (Aitchison & Ireland 1995). This exotic terrane is considered to have accreted onto the continental margin of Gondwana during the Carboniferous and is therefore allochthonous to the Gondwana continent (Aitchison *et al.* 1992a).
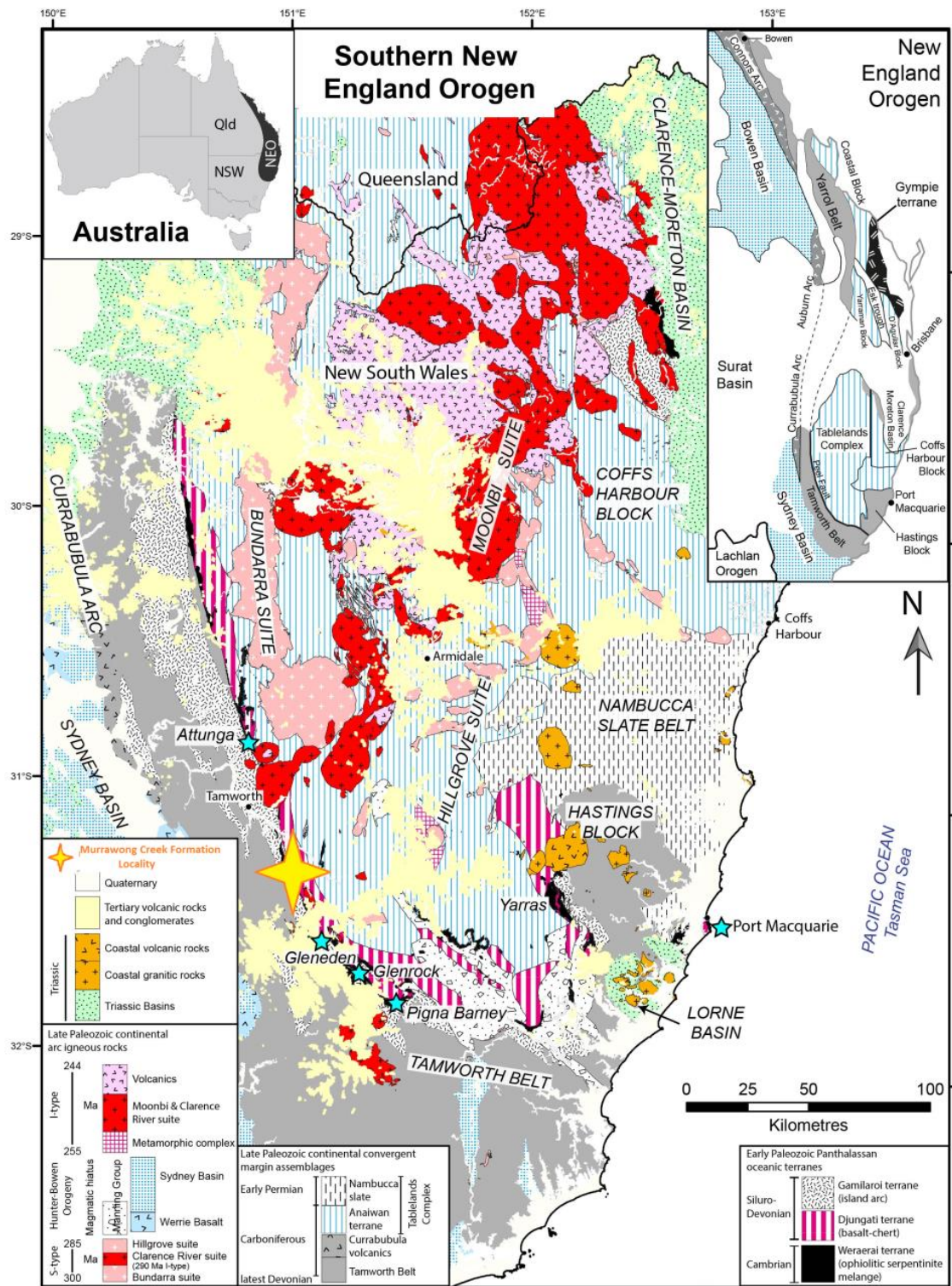
*Figure 1.1 - a) Tectonostratigraphic map of the New England Province, New England Orogen, with yellow star indicating study locality; b) Synthesis of the New England Orogen. Map taken from Nutman et al. (2013)*

The Peel Fault of the southern NEO has long been recognised as a fundamental geological discontinuity (Benson 1918), thought to be connected with the Yarrol fault in the north, creating the Peel-Yarrol Fault System (PYFS). The PYFS exhibits lenses of serpentinite along its length and is a break between two contrasting zones of the NEO: (1) a western, coherent, weakly deformed sequence with age constraints from scattered macrofauna and conodonts; and (2) an eastern, strongly deformed, zone including mélange sequences lacking widespread age constraints (Murray 1997).

Early tectonic models suggested that the NEO formed as an Andean continental margin with continuous west-directed subduction (Leitch 1974, 1975; Cawood 1976, 1980; Leitch & Cawood 1980; Cawood 1983). The next major paradigm shift was the exotic terrane model initiated by Aitchison *et al.* (1988) and Aitchison *et al.* (1992a) whereby the NEO was an exotic terrane during the Late Silurian to Devonian, which was then superimposed onto the Gondwana continental margin in the Carboniferous. Scheibner (1973) suggested that the NEO had multiple, episodic west-dipping subduction zones, while Leitch (1975) proposed the evolution of a single west-dipping subduction zone with subduction beginning in the Devonian. These early models led to the 'consensus' model for the evolution of the New England Orogen, which still exists today; a Devonian to Carboniferous convergent plate margin with westward-dipping subduction that evolved to an extensional regime in the Permian (Murray 1997).

The presence of Early Paleozoic rocks throughout the southern portion of the NEO has been a topic of debate over the past few decades. Cawood (1976) first mapped the oldest rocks in the Woolomin area, where both a Cambrian ophiolite sequence and a volcaniclastic sequence with Cambrian and Ordovician limestones exist on either side of the Peel Fault (Murray 1997). A wide range of macrofauna was dated to give Cambrian and Ordovician ages (e.g., Cawood 1976; Engelbretsen 1993; Brock 1998a). Some researchers have disputed these age constraints on the basis that the fossiliferous limestone is allochthonous and thus the biostratigraphy does not provide an accurate age of deposition (Murray 1997).

The southern region or New England province (Figure 1.1) provides the focus for this review, which is considered to have been dominated by an eastern convergent boundary with a west-dipping subduction zone during the Paleozoic (Cawood 1983). This model of a convergent tectonic setting results from sequences interpreted from west to east as a

continental margin arc, fore arc basin and an accretionary wedge (Korsch *et al.* 2009). Leitch (1974) divided the southern NEO into two longitudinal zones, separated by the Peel Fault System. Zone A is a thick sequence of clastic sedimentary rocks west of the Peel Fault which accumulated in a subsiding marine basin, closely associated with a magmatic arc. These sedimentary rocks have two distinct ages with Early Paleozoic bedded argillite, volcaniclastic sandstones and conglomerates underlying a Middle Paleozoic succession of volcanogenic clastic sedimentary rocks from siltstone through to conglomerate intercalated with basalts, dolerite, keratophyre and various chert and limestone lenses (Cawood 1980). The volcanic arc provides the sediment source, and has been considered to have a long-lived history, from the Middle Cambrian to Early Permian. Zone B refers to those successions east of the Peel Fault, which have undergone higher grades of metamorphism. Age data suggests that these sequences were deposited coevally, with Zone B representing a subduction complex assemblage (Cawood 1983). Previously it has been thought that this tectonic setting remained fairly uniform throughout the Paleozoic (Leitch 1974, 1975; Cawood 1976, 1980, 1983; Leitch & Cawood 1987). It has since been proposed that the complexity of the terranes suggest a changing subduction-related environment with the introduction of allochthonous material (Aitchison *et al.* 1992a; Aitchison & Flood 1994; Stratford & Aitchison 1996).

Aitchison *et al.* (1988) divided the southern NEO into eleven terranes, with this nomenclature generally followed in this thesis. The Cambrian Weraerai terrane (Figure 1.1) is situated along the Peel Fault, and contains the oldest rocks in the New England Orogen. It consists of a disrupted ophiolitic sequence bounded by faults in contact with the adjacent Gamilaroi terrane (Aitchison & Ireland 1995). The Gamilaroi terrane, the focus of this thesis, is an Upper Silurian-Devonian intra-oceanic island arc sequence that is bordered to the east by the Peel-Manning Fault System (PMFS). The Djungati terrane lies immediately to the east of this, and consists of an intensely deformed Devonian ocean-floor sequence of basalt, chert and sediments. Structurally underlying the Djungati terrane is the Anaiwan terrane, a sequence of thrust slices of basalt, chert and tuffaceous sedimentary rocks of Late Devonian to Early Carboniferous age (Aitchison *et al.* 1988). The convergent plate boundary changed from a relatively high-angle subduction zone into a transform or oblique convergent margin by the Early Permian. This resulted in the rapid infilling of sedimentary basins along the PMFS (Aitchison & Flood 1992; Buckman 1993). These sedimentary rocks are assigned to the Manning Group (Voisey

1957). The three terranes most spatially relevant to this thesis are: the Weraerai terrane, the Gamilaroi terrane and the Djungati terrane, as all have units adjacent to the PMFS.

### 1.3.2 The Weraerai terrane

The Weraerai terrane is a disrupted ophiolite sequence hosted in a serpentinite matrix mélange (Aitchison *et al.* 1992b). It was injected diapirically along the PMFS and consists of the oldest rocks of the NEO (Aitchison *et al.* 1992b). The Weraerai terrane is juxtaposed against the Gamilaroi terrane and was initially thought to be of a similar age to the adjacent basal strata of the Gamilaroi terrane, the Murrawong and Pipeclay Creek formations. However magmatic zircons of 'plagiogranite' inclusions in the serpentinites have yielded ages of 530 ± 6 Ma (Aitchison *et al.* 1992b), which Aitchison *et al.* (1992b) considered to be much older than those strata.

Aitchison *et al.* (1992b) suggested that younger terranes were thrust westward over eastern Australia during the mid-Paleozoic, with the Weraerai terrane acting as a basement upon which they were thrust. The ophiolite sequence is interpreted to have been exposed by later deformational events in the Early Permian, resulting in ophiolite emplacement at higher structural levels due to faulting (Aitchison *et al.* 1992b).

### 1.3.3 The Gamilaroi Terrane

Flood, Aitchison and Stratford extensively studied the Gamilaroi terrane. The Gamilaroi terrane is the western-most terrane of the southern NEO, representative of an intra-oceanic island arc system (Aitchison *et al.* 1992a; Stratford & Aitchison 1997). The Gamilaroi terrane is within Zone A of Leitch (1974) and includes the Tamworth Group, the overlying Baldwin Formation and the Mostyn Vale Formation (Flood & Aitchison 1992). This divides the original sequence, the Tamworth Belt, into a Devonian intra-oceanic arc sequence (Gamilaroi terrane) and a Carboniferous Gondwana continental margin arc sequence (Aitchison *et al.* 1992a; Aitchison *et al.* 1992b; Flood & Aitchison 1992; Aitchison & Flood 1994; Stratford & Aitchison 1996, 1997).

The Gamilaroi terrane is bounded to the east by the PMFS and is a sequence of volcaniclastic rocks with intercalated meta-andesites, rhyolites, dacites and spilites (Aitchison & Flood 1994). The Tamworth Group, as defined by Crook (1961), is considered the lowermost strata of the Gamilaroi terrane (Aitchison & Flood 1994). Detrital modal analysis of sandstone by Cawood (1983) found these rocks possess an

island arc signature. This was clarified for the basal units of the Gamilaroi terrane, the Murrawong Creek and Pipeclay Creek formations, whereby Leitch and Cawood (1987) determined deposition was most likely within a forearc basin of intra-oceanic arc. High sedimentation rates of volcanic detritus coupled with intercalated island-arc basalts are consistent with an island arc interpretation (Aitchison & Flood 1994). Upper Silurian to Middle Devonian basalts of the Gamilaroi terrane exhibit geochemical features characteristic of intra-oceanic island arc magmas in a supra-subduction zone setting (Offler & Gamble 2002). This has been further clarified by Offler and Murray (2011), whereby geochemical signatures offer an interpretation of a rifted intra-oceanic island arc, with the volcanic rocks in the Nundle area forming at a distal spreading centre, possibly in a  back arc setting.

The age of the Tamworth Group has been interpreted to be early Paleozoic based on biostratigraphic interpretation of fossiliferous clasts (Cawood 1976, 1983; Engelbretsen 1993; Stewart 1995; Engelbretsen 1996; Furey-Greig 2003; Sloan & Laurie 2004). However, Aitchison and Flood (1994) state that the age of the clasts do not necessarily indicate the age of the units that contain the clasts. Instead, Aitchison *et al.* (1992a) argued that the entire Gamilaroi terrane is Devonian in age based on radiolarian data .

It is thought that the island arc of the Gamilaroi terrane underwent rifting during the Devonian due to the presence of keratophyric rocks closely associated with basalt and E-type MORB (Flood & Aitchison 1992). Offler and Gamble (2002) reported the occurrence of Middle to Upper Devonian basalts with a back-arc basin signature potentially produced during the rifting of the arc. The evolution of the arc has been outlined by Stratford and Aitchison (1996), whereby the arc is submarine and active, followed by decreased volcanic activity and depth with the start of carbonate platform development, and then an initiation of arc rifting in the early Middle Devonian with rapid subsidence of platforms as a result of normal faulting and an increase in volcanism.

The strata unconformably overlying the Gamilaroi terrane marks the transition into a foreland basin succession, signifying the accretion of the Gamilaroi terrane onto the eastern margin of Gondwana (Aitchison & Flood 1994). Aitchison and Flood (1994) outlined a tectonic model whereby the Gamilaroi terrane was an allochthonous island arc sequence throughout the Devonian, with east-dipping subduction occurring underneath the arc. This is consistent with modern analogues of arc-continent collision, such as the Izu-

Bonin-Marianas arc, whereby subduction occurs underneath the arc rather than the continent. In this model the Gamilaroi terrane is thrust onto the Gondwana continental margin in the Carboniferous as a result of a collisional event (Aitchison & Flood 1994). A subduction polarity flip ensued, forming a west-dipping subduction zone (Aitchison & Flood 1994). This tectonic model contrasts previous models outlining the entire Tamworth Belt to be the result of a long-lived westward dipping subduction zone, with the Gamilaroi terrane separated from Gondwana by only a small back-arc basin (Leitch 1974, 1975; Cawood 1976, 1980, 1983).

Offler and Gamble (2002) disagree with this interpretation stating that the presence of a supra-subduction zone indicates that a back arc basin is associated with the arc. They propose that the Gamilaroi is related to the regional basin setting of the Lachlan Fold Belt to the west during the Middle Silurian. Thus, the polarity of arc and back arc basin suggests the subduction zone dipped to the west (Offler & Gamble 2002). Offler and Murray (2011) however, suggest that obduction was the driving mechanism of arc emplacement onto the Gondwanan continent. This generally supports Aitchison and Flood's (1994) model although they state that both a west and east dipping subduction zone existed during the Devonian.

### 1.3.4 The Djungati terrane

The Djungati terrane comprises the Woolomin Group, Wisemans Arm Formation and Watonga Formation, and was deposited in a widespread ocean basin (Aitchison *et al.* 1992a; Buckman *et al.* 2015). Rocks of the Djungati terrane (Aitchison *et al.* 1988) are extremely deformed, with the depositional age constrained by radiolarian data to be from the latest Silurian into the youngest Carboniferous (Aitchison & Flood 1992; Aitchison *et al.* 1992a).

The Djungati terrane consists of a basal unit of meta-basalts, conformably overlain by red ribbon-bedded radiolarian chert, making up the Woolomin Group (Aitchison *et al.* 1988). These are overlain by green siliceous tuffs, arc derived sediments and olistoliths of chert, basalt and limestone, comprising the Wisemans Arm Formation (Leitch & Cawood 1980). The Watonga Formation, previously thought to be related to the Woolomin Formation is a tectonic mélange of ocean floor basalts, cherts and siliceous sediments (Och *et al.* 2005), which has been found to be younger than the Woolomin Formation through biostratigraphic ages of conodont fauna (Och *et al.* 2007).

It has been suggested that the volcaniclastic sediments of the sequence were deposited as a result of increased volcanism or erosion of an offshore island arc, which fed into the sediment-starved accretionary complex as it migrated shoreward in the Late Devonian (Cawood 1980; Aitchison & Flood 1992; Aitchison *et al.* 1992a). The Weraerai and Djungati terranes are tectonically contrasting units with very different ages. Thus, their spatial affinity must have occurred subsequent to the volcaniclastic deposition in the Late Devonian, highlighting the tectonic complexity of the region (Aitchison *et al.* 1992a).

### 1.3.5   *Macquarie Arc, Lachlan Orogen*

The Macquarie Arc exists as interspersed volcanic belts across central and into southern New South Wales. It represents a supra-subduction zone element of the Lachlan Orogen, originating as an intra-oceanic island arc offshore from Gondwana (Aitchison & Buckman 2012; Glen *et al.* 2012). Three major belts and one minor belt is recognised, comprising mafic to intermediate volcanic and volcaniclastic rocks, with limestones and intrusions (Glen *et al.* 2012). The Macquarie Arc has been dated as Ordovician using both biostratigraphic and radiometric methods. Correlations have been made between the Lachlan and New England orogens, often through the inclusion of Lachlan Orogen Ordovician limestones as allochthonous clasts in Siluro-Devonian (Gamilaroi terrane) rocks in the NEO (e.g., Cawood 1980; Leitch & Cawood 1980; Furey-Greig 1999, 2000, 2003; Quinn & Percival 2010). Little has been agreed upon in terms of tectonic models for the Macquarie Arc, with the stacking of arc phases and occurrence of flanking sediments both east and west of the arc proving it to be different from standard superimposed intra-oceanic arcs (Glen *et al.* 2012).

It is possible that the Murrawong Creek Formation is exotic to the New England Orogen, forming part of an early Paleozoic fragment related to the Macquarie Arc (Leitch & Cawood 1987). Similarities can be drawn with the age of the Macquarie Arc, Ordovician, and the ages discussed in this thesis. The Murrawong Creek Formation consists of volcaniclastic sediment derived from an andesitic and basaltic source, similar to that produced in volcanism from the Macquarie Arc (Glen *et al.* 2012). Volcaniclastic sediments were deposited on emerging islands during phase one of Macquarie Arc magmatic evolution, a possible scenario for the deposition of the Murrawong Creek Formation.

### 1.3.6 Continental Growth Mechanisms

An understanding of the tectonic evolution of the NEO provides insight into those mechanisms that developed the eastern Australian Gondwanan continental margin. It is currently agreed that this is the site of an ancient convergent margin, where by oceanic lithosphere was subducted in proximity to the Gondwanan continent, however, the mechanisms and polarity of subduction is still disputed (Aitchison & Buckman 2012). There are two fundamentally different tectonic models for the Murrawong Creek Formation, whereby it formed as part of a forearc-accretionary terrane on the eastern edge of Gondwana (Leitch 1974, 1975; Cawood 1976, 1980, 1983; Engelbretsen 1993, 1996; Sloan & Laurie 2004), or it formed as an exotic, allochthonous unit resulting from an intra-oceanic rifted island arc (Aitchison *et al.* 1992a; Aitchison & Flood 1994). Collins (2002) and Cawood *et al.* (2009) provided models for the New England Orogen whereby plate coupling is the main driving factor leading to episodic crustal shortening and orogeny (accordion model). This model does not provide an explanation for the introduction of allochthonous terranes, unlike the models proposed by Aitchison and Flood (1994) and Aitchison and Buckman (2012).

An explanation of the two opposing models is provided using the Ordovician Macquarie Arc as an example, whereby the mechanisms of arc collision with Gondwana are disputed. The rocks of the Murrawong Creek Formation may be related to the Macquarie Arc; otherwise these models may provide an explanation for the allochthonous nature of the rocks that are the Murrawong Creek Formation.
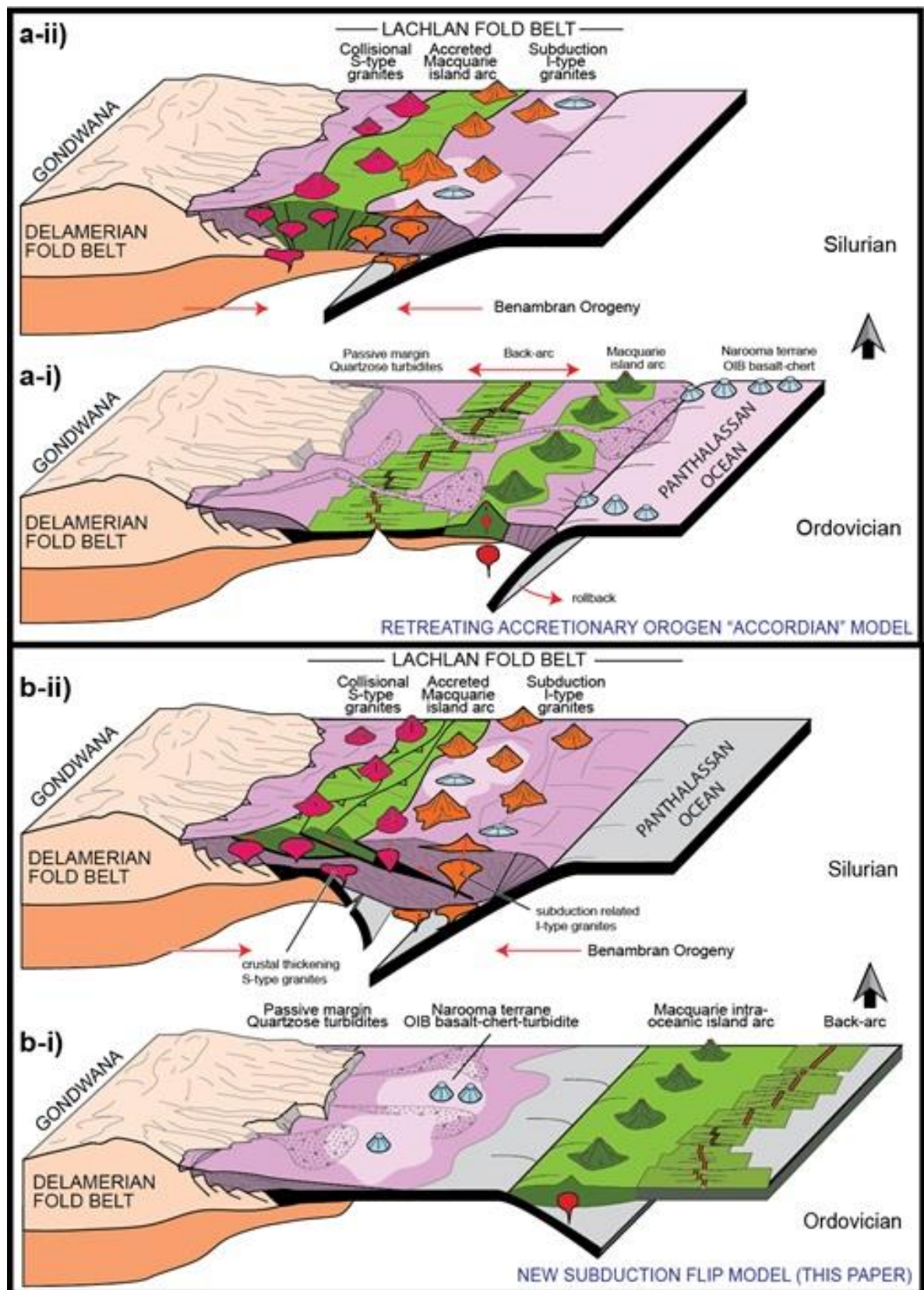
*Figure 1.2 - Two opposing models for the addition of material to continental margins: a) retreating accretionary orogen, accordion tectonics and b) subduction flip quantum tectonics. From Aitchison and Buckman (2012)*

The 'accordion' tectonic model (Figure 1.2) outlines the process whereby back arc extension, coupled with episodic contractional events lead to the introduction of material onto Gondwana (Collins 2002). Here, back arc basin extension forms new MORB-style crust, and then contractional events provide a mechanism by which the arc becomes attached to the continental margin. Thus, Panthalassan oceanic lithosphere was continuously subducted underneath the Gondwanan continent with a westward dipping subduction zone and temporal plate coupling (Aitchison & Buckman 2012).

Other models indicate that growth was via the addition of material at continental margins whereby offshore elements are added episodically (Dewey 2005; Aitchison & Buckman 2012). The 'quantum tectonic' model (Figure 1.2) recently proposed by Aitchison and Buckman (2012) suggests that the Macquarie Arc was allochthonous to the Gondwanan continent with eastward subduction consuming oceanic lithosphere that existed between the plates. This consumption of oceanic crust led to the obduction of the arc onto the Gondwanan continental margin and subsequently subduction flip, to create a west-dipping subduction zone. This model is consistent with Aitchison and Flood's (1994) proposed Gamilaroi terrane model.

### 1.3.7    Sedimentation at Island Arcs

The term *volcaniclastic* was implemented by Fisher (1961) to describe those rocks that are somewhat in-between volcanic and sedimentary in composition, including all siliclastic sedimentary rocks enriched in volcanic fragments (Fisher & Smith 1991; Frolova 2008; Boggs 2009). In sedimentary basins proximal to widespread igneous source regions, volcanic edifices that emerge above sea-level often provide a high proportion of the clastic sediment entering sedimentary basins (Fisher & Smith 1991). Volcaniclastic rocks are extremely varied in composition, lithology and structure depending on the nature and composition of the volcanic source and any underlying basement rocks exposed to erosion. Depositional environments in volcanic archipelagos can vary from shallow marine with fringing reefs to deep submarine canyons and abyssal plains within only a matter of 10's of kilometres. Thus, the difficulties in classifying these rocks has been a hindrance to their understanding in the past (Frolova 2008). Volcaniclastic rocks can often be confused as being of igneous origin, as in the example poorly sorted, angular greywackes, which often resemble porphyritic lavas. The distinction is that volcaniclastic rocks are a result of igneous processes but are deposited in a sedimentary fashion. This is usually identifiable

in thin-section petrography whereby there is a lack of interlocking phenocrysts or trachytic type textures that are common in igneous rocks (Boggs 2009).

Plate tectonics is the main control on sedimentation in deep marine conditions, as it directly affects both the source and the basin in which sediments accumulate (e.g., Dickinson & Suczek 1979; Boggs 2011). Climate also influences sediment composition due to the varying rates of weathering on land and the presence of carbonate reefs. However, this effect is minimal for deep marine sedimentation, unless those sediments have been transported extensively across terrestrial environments before ending up in marine environments. In this case, less weatherable minerals such as quartz reflect the continental influence.

In areas of intense volcanism, such as active volcanic arcs, large amounts of sediments rapidly accumulate in geographic lows, causing the sedimentary record to fluctuate under short periods of time unseen elsewhere. This rapid influx of material provides a record of volcanism at the time, often reflecting the tectonic setting of the region. Thus, volcaniclastic rocks can prove to be extremely useful for understanding the tectonic regime and plate dynamics of a region (Fisher & Smith 1991). Sediments deposited in subduction-related settings are almost always volcaniclastic in nature, derived from the nearby volcanic arc, with the three most important depositional settings including: deep-sea trenches, forearc basins (Figure 1.3) and back arc basins (e.g., Dickinson *et al.* 1983; Marsaglia 1995; Boggs 2011). The arc side of the trench axis often produces an accretionary wedge, or an uplifted, deformed belt of trench and oceanic pelagic sediments (Leeder 1982).

Intra-oceanic island arcs in subduction-related environments consist of assemblages of volcanic lava flows, pyroclastic falls and pyroclastic flows, which are often intermingled with basin sediments on the edge of a forearc basin (Leeder 1982). The associated epiclastic deposits are a thick fill of extensively reworked and redeposited products of slumps, slides, debris flows and turbidity currents whereby water is the dominant agent of sediment transport (e.g., Lowe 1982; Reading 1996; Nichols 2009). Submarine slopes of stratovolcanoes are particularly susceptible to resedimentation because of steep regional gradients, high seismicity and rapid sediment accumulation, resulting in small but frequent slides (Reading 1996). These are preferentially preserved on steep seafloor surfaces, such as flanking the volcano or in submarine canyons (Underwood *et al.* 1995).
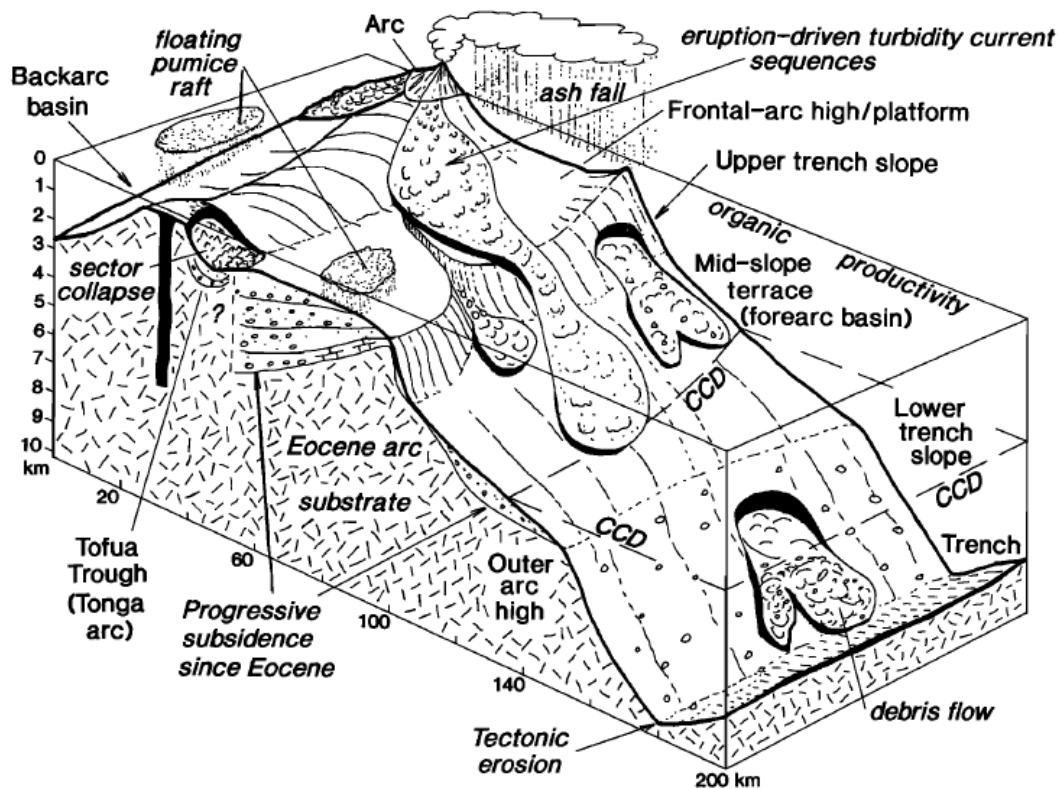
*Figure 1.3 - Major depositional processes in oceanic forearc environments, from Underwood et al. (1995)*

Turbidity currents are sediment flows in which the grains are suspended by turbulence, and can be divided into three particle size populations; 1) clay, silt, fine-medium sand-size particles; 2) coarse-grained sand to small pebble sized gravel and; 3) pebble and cobble sized clasts (Lowe 1982). Those sediments in group 2 and 3 are likely to be transported in large masses of concentrated flows and deposited rapidly (Lowe 1982). These flows deposit sediment through a series of sedimentation waves; the first depositing the coarsest gravel through traction and suspension sedimentation, the second wave depositing finer gravel and sand by traction sedimentation, and the third is a residual low-density current which forms the Bouma divisions (Lowe 1982).

Grading is often a key indicator of source and energy regime in sedimentary environments, however it is difficult to determine given the varied and active nature of subduction-related environments. Gravity-flow deposits may produce normal grading, however extensive mixing of materials of different ages and sources often occurs (Underwood *et al.* 1995). This heterogeneity is often the key to recognising a debris-flow deposit whereby the sedimentary rock often has large clast sizes, poor sorting, matrix support and a variety of clast lithologies (Underwood *et al.* 1995).

Sedimentation at island arcs often involves deposition in a submarine environment, and therefore many of these deposits are associated with marine carbonate facies (e.g., Watkins 1985; Reid *et al.* 1996; Nichols 2009) . The incorporation of carbonates into the sedimentary succession may vary, from a conformably overlying succession (e.g., Watkins 1985) to being present as allochthonous blocks and clasts within volcaniclastic rocks (Underwood *et al.* 1995).

## 1.4   Location

The Murrawong Creek Formation is located approximately 20km north-east of Nundle and 30km south east of Tamworth (Figure 1.5). The formation is situated on the eastern edge, approximately in the middle of the Tamworth Belt and probably part of the Gamilaroi terrane, NEO (Figure 1.1). The outcrop at this locality is poor, and rarely in situ, resulting in mapping undertaken within creek beds running across strike (Figure 1.4).

The Pipeclay Creek Formation stratigraphically overlies the Murrawong Creek Formation, and was studied at both the above location and adjacent to Chaffey Dam, approximately 43km southeast of Tamworth (Figure 1.5). Similar to the previous location, the outcrop is poorly exposed, with a variety of volcaniclastic sediments and volcanic rocks. A small roadside quarry has been used for road fill, exposing a conglomerate lens of the Pipeclay Creek Formation, which was used as the basis for this study (Figure 1.4).
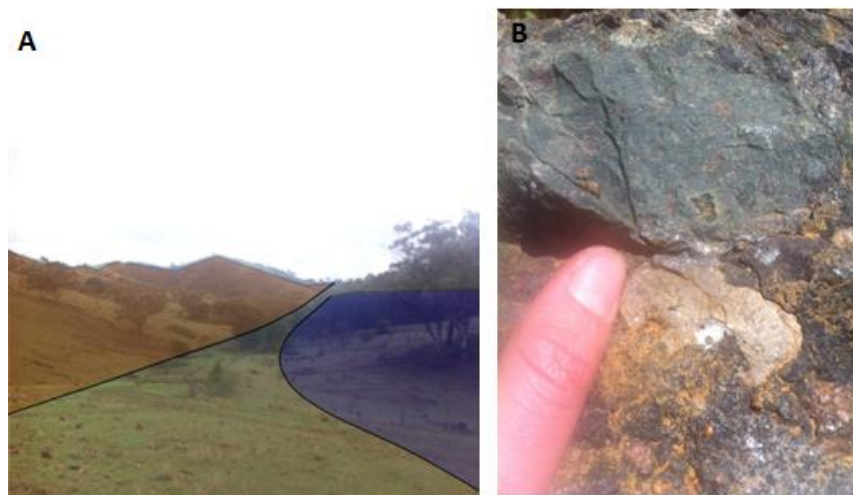


*Figure 1.4 -  A) Photograph of the Peel  and Sandy Creek faults, looking north from the Murrawong Creek Formation, whereby the Djungati terrane is to the east (blue) of the Peel fault, and the Gamilaroi terrane is to the west (orange) of the Sandy Creek Fault. The middle section is the Bog Hole Formation. B) Photograph of Pipeclay Creek Formation conglomerate with limestone, chert, volcanic and plutonic clasts.*

*Figure 1.5 - Location Map showing sample and mapping locations, with the MCF at Location 1 and the PCF at Location 2. Map from Spatial Information Exchange, NSW Government https://maps.six.nsw.gov.au/*

# Chapter 2. Field Relations and Stratigraphy

## 2.1 Introduction

This chapter outlines the geological relations and stratigraphy of the Murrawong Creek and Pipeclay Creek formations. These rocks contain the oldest known fossils of any sedimentary sequence within the NEO, indicating Middle Cambrian age for the lowermost Murrawong Creek Formation (Cawood 1976) and late Middle Cambrian age for the Pipeclay Creek Formation (Stewart 1995). These old Cambro-Ordovician ages contrast with the predominantly Devonian-Carboniferous age of most of the rocks of the NEO. The early detailed mapping of Cawood (1980) provides an excellent framework of the relationships between different units, including volcaniclastic sandstones, conglomerates, cherts, siltstones, occasional mafic lava flows and more felsic keratophyres that may represent later stage sills or dykes (Figure 2.2). Outcrop is patchy and best along ridge tops, creek beds or along the flanks of steeply incised gullies. The poor outcrop means that it is difficult to determine via field relations whether the fossil bearing units occur within autochthonous or allochthonous units. However, it is clear that some coarse-grained conglomerate units contain large rounded clasts of fossiliferous limestone (Figure 2.1) along with clasts of red chert and abundant volcanic and plutonic detritus. Thus, clasts of shallow marine limestone are being mixed in with clasts of deep marine facies in a deep-water mass flow deposit. Given the geological uncertainties associated with limited and patchy outcrop this project has focussed on extracting detrital zircons from the volcaniclastic sandstones for U-Pb dating to compare with previous biostratigraphic age constraints. This section outlines previous biostratigraphic results presented in the literature, in context with mapping and sampling.

*Figure 2.1 – Left photograph: Pipeclay Creek Conglomerate location, road-side quarry. Right photograph: Field photo of limestone clast within Pipeclay Creek Conglomerate.*

### 2.1.1   Biostratigraphy

To date, biostratigraphy has been the key method in determining age constraints on the stratigraphic section west of Woolomin. Biostratigraphy is an excellent dating technique; however the major problem of biostratigraphic age dating for these volcaniclastic rocks is the assumption that the fossiliferous limestone clasts are of the same age as the enclosing sedimentary matrix. A key objective of this thesis is to compare the available biostratigraphic data with the detrital zircon U-Pb age data collected at ANU, for both the Murrawong and Pipeclay Creek formations. This section reviews the significant fauna documented in both formations and provides spatial and stratigraphic context.

**Murrawong Creek Fauna**

Cawood (1976) was the first to document Cambrian fauna in eastern NSW, where he recorded trilobites, inarticulate brachiopods and simple conodonts from limestone clasts immediately west of the Peel Fault. The key fauna documented include *Ptychagnostus (Goniagnostus) fumicola* Öpik and *Glyptagnostus* sp. aff. *G. stolidotus* Öpik from the basal strata of the Murrawong Creek Formation. Following this, Cawood (1980) corrected his identification of key species not to be *G. stolidotus,* but *Ptyagnostus aceleatus* or *P. puncuosus,* limiting the limestones to a late Middle Cambrian age. He also noted the presence of Middle Ordovician conodonts in limestone blocks in the upper levels of Unit 1 of the Murrawong Creek Formation (Cawood 1976). These conodonts were used as a

basis for his age determination, stating the age of the fauna are most likely simultaneous with deposition of the host-sediment due to an absence of mixing of Cambrian and Ordovician faunas at stratigraphic levels (Cawood 1976).

Following Cawood's work (1976, 1980, 1983), subsequent authors debated as to whether the fossiliferous limestones are contemporaneous in age with the host matrix of the sedimentary rocks. The following authors documented Middle Cambrian ages for allochthonous fossiliferous limestone clasts within the Murrawong Creek Formation, with faunas ranging from coralmorphs to brachiopods, conodonts and trilobites. Engelbretsen (1993) recorded a possible cnidarian *Tretocylichne perplexa* gen. et sp. nov followed by lingulate brachiopods *Treptotreta jucunda, Amictocracens teres* and others (Engelbretsen 1996). Brock (1998a) documented articulate brachiopods *Nisusia metula* n. sp. and *Yorkia* sp. indet. and *Arctohedra austrina* n. sp. *Yorkia*, and molluscs including *Latouchella accordionata, L. aliciae* nov. sp., *Yochelcionella daleki* plus others. Trilobites were explored by Sloan and Laurie (2004) with some of the fauna including *Utagnostus trispinulus* and *Hypagnostus parvifrons*. All of these fauna were collected from Cawood's (1976) L1 locality. Cawood (1980) notes that these fauna provide only the *maximum* age constraint for the Murrawong Creek Formation with the *minimum* age constraint derived from the unconformable overlying Ordovician Haedon Formation.

**Pipeclay Creek Fauna**

Fossiliferous limestone has not been studied in the conformably overlying Pipeclay Creek Formation. Aitchison *et al.* (1992a) recorded the presence of radiolarian fauna assignable to *Ceratoikiscum* across several exposures of siliceous rocks, providing an age range from Early Silurian to Carboniferous. He stated that it along with the Murrawong Creek Formation, are unlikely to be Cambrian but rather Silurian or Devonian. This was disputed by Stewart (1995) who detailed paraconodonts, including *Muellerodus, Herzina, Prooneotodus* and *Furnishina* obtained from chert within the Pipeclay Creek Formation. This finding led Stewart (1995) to conclude a Middle Cambrian to early Late Cambrian age for the Pipeclay Creek Formation, supporting Cawood's (1980) interpretation of Cambrian age for the deposition of the Murrawong Creek and Pipeclay Creek formations. Details regarding the chert from which the conodonts were sampled are ambiguous as to the allochthonous or autochthonous nature, being only described as spiculitic.

## Ordovician Fauna in the southern New England Orogen

This section outlines the occurrence of Ordovician fauna within the southern New England Orogen, in order to allow for correlations between formations and the possibility of a common source. The Haedon Formation is a laterally discontinuous lens of conglomerate that unconformably overlies both the Murrawong Creek and the Pipeclay Creek formations (Figure 2.4) (Furey-Greig 2003). Cawood (1976) originally found *Periodon aculeatus* in allochthonous limestone blocks at Copes Creek. Furey-Greig (2003) recorded the occurrence of conodont fauna including *Ansella jemtlandica* (LÖFGR EN), *Oistodus lanceolatus* (PANDER), and also *Periodon aculeatus* (HADDING), confirming an Early-Middle Ordovician age. Cawood suggested that this is the most likely age of the upper units of the Murrawong Creek Formation, however remained confident that the lower units are of Middle Cambrian age (Cawood 1976).

Unconformably overlying the Haedon Formation is the Drik Drik Formation with an olistromal mode of occurrence of limestones throughout (Furey-Greig 2000). The Drik Drik Formation is thought to be early Devonian (Mawson *et al.* 1995), however the allochthonous limestone hosts Late Ordovician conodonts including, *Belodina confluens, Phragmodus undatus, Yaoxianognathus ani, Y. tunguskaensis* and *Drepanoistodus suberectus* (Furey-Greig 2000). Furey-Greig (2000) suggests the fauna might be related to the Wisemans Arm Formation and fauna recorded from the north-eastern part of the Lachlan Fold Belt; however the source of the allochthonous limestone blocks remains enigmatic.

Furey-Greig (1999) documented Late Ordovician fauna including *Panderodus gracilis* and *Belodina confluen*s from allochthonous limestone blocks in the Wisemans Arm Formation. The fauna is correlated with Late Ordovician fauna found in the Uralba Beds east of Manilla and the Trelawney Beds south-east of Tamworth (Furey-Greig 1999). Furey-Greig (1999) refers to the Uralba Beds as olistromal limestones which should be reclassified as part of the Wisemans Arm Formation. The Uralba Beds have yielded a fauna almost identical to that mentioned from the Wisemans Arm Formation, including *Taoqupognathus tumidus* (Trotter & Webby), *Panderodus nodus* (Zhen *et al.*) and *Yaoxianognathus ani* (Zhen *et al.*; Furey-Greig 1999).
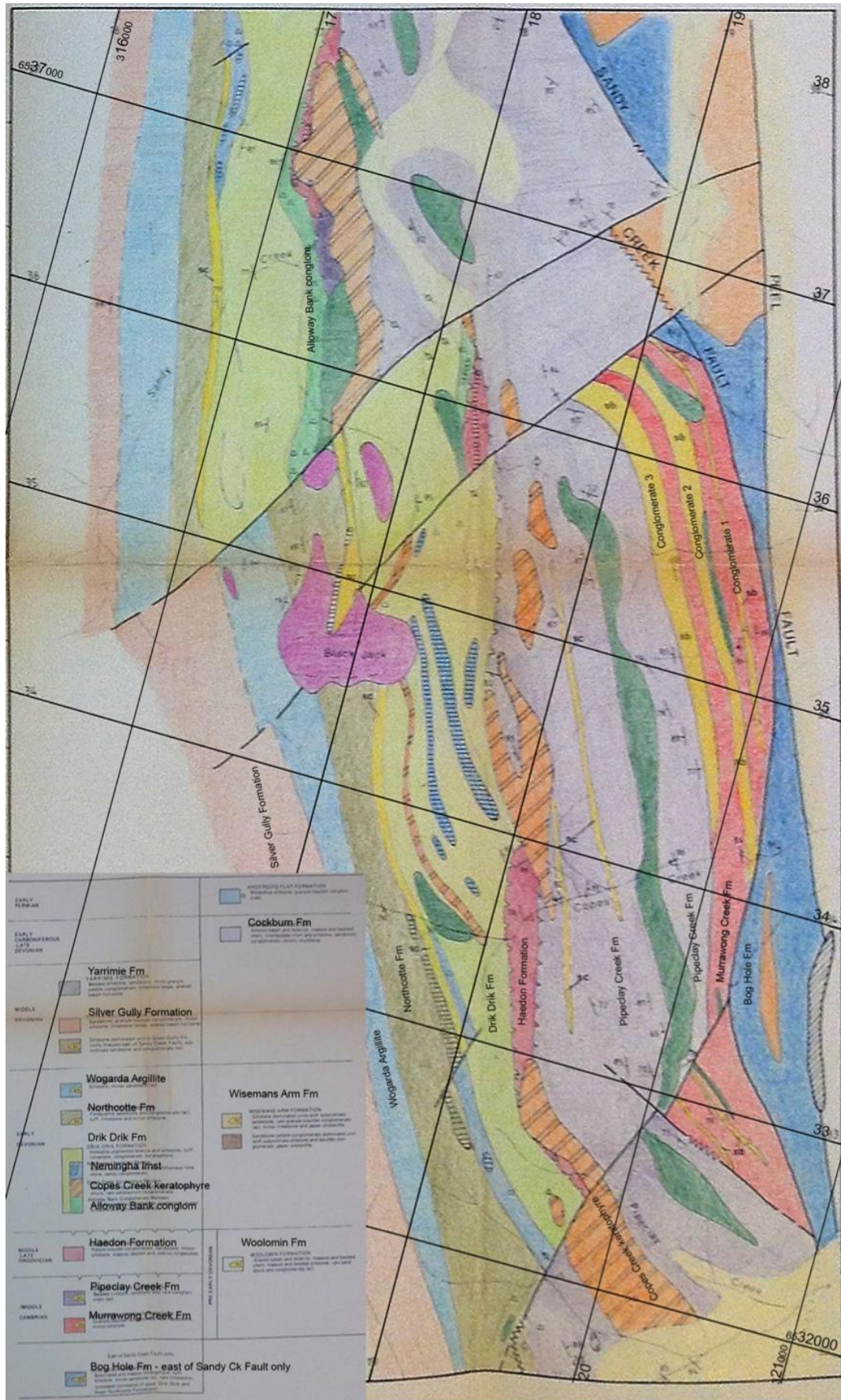
*Figure 2.2 - Detailed Geology Map from Cawood (1980)*

Hall (1975) found corals and conodonts from limestones within the Uralba and Trelawney Beds, which were the oldest known NEO strata at that time. The fauna is dominated by the following genera: *Palaeophyllum, Cyathophylloides* and *Crenulites* with a variety of new species named in this paper. The fossils were collected from fossiliferous limestones indicative of an Upper Ordovician age.

## 2.2    Field Relations

Geological field mapping was undertaken over five days with the main objective to map contacts, collect samples, and note geological structures. The area had previously been extensively mapped by Cawood (1980) (Figure 2.2), and thus this exercise aimed to check the accuracy of early maps and gain an understanding of the field geology. A combination of Google Earth images and Clino FieldMove was used in the field, whilst ArcGIS was used in the final drawing of maps. Outcrops were mostly restricted to creek beds and often extremely weathered.

Figure 2.5 shows the detailed study area of the Murrawong Creek Formation, near Woolomin NSW. It was noted that in this area the Murrawong Creek Formation does not lie directly adjacent to the Peel Fault, but rather the Sandy Creek Fault, as the Bog Hole Formation exists as a faulted block between the two faults. The volcaniclastic sedimentary rocks of the Murrawong Creek and Pipeclay Creek formations are near vertical or steep dipping to the west, with dips measured between 78° to 89° and a strike of almost exactly north-south. Representative sandstone samples were taken from coarse-grained horizons within the formations and later classified via petrographic analysis. The Murrawong Creek Formation is divided into three units; a basal coarse volcaniclastic unit, an overlying conglomerate unit and a volcanic unit (Figure 2.6).
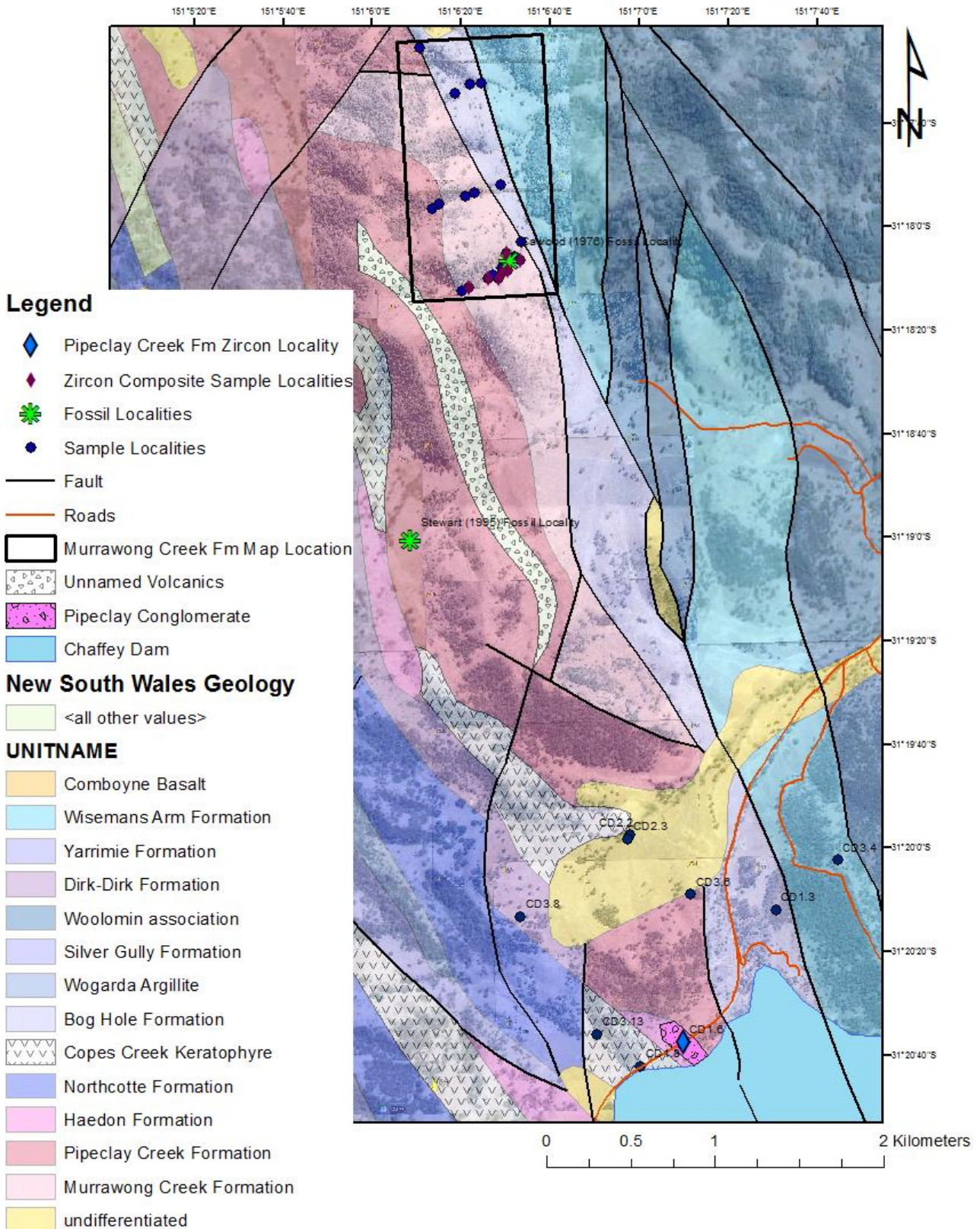
*Figure 2.3 - Map showing the geology of the field study area. The fossil locality within the MCF is Cawood's (1976) L1 locality, which was revisited by numerous researchers. The locality within the PCF is from Stewart (1995). Geological boundaries used are from NSW_250k Geology.*
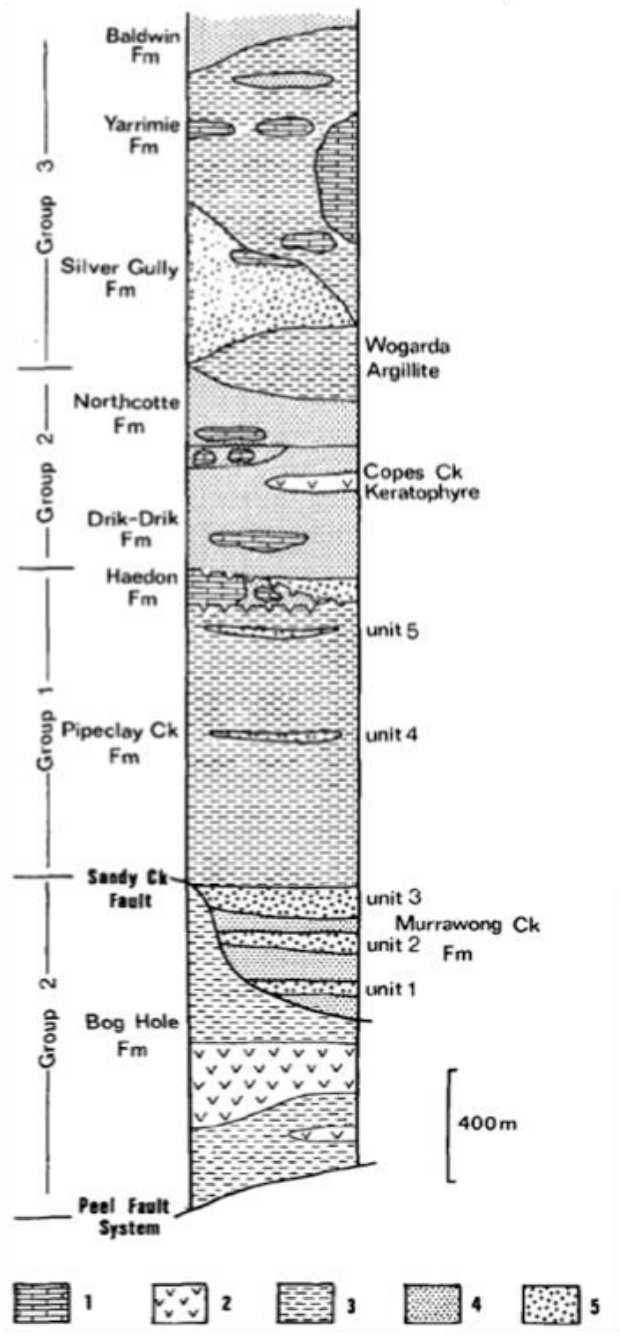
Figure 2. Generalized stratigraphic section for the early to middle Paleozoic strata west of the Peel Fault System, showing the observed regional relationships between rock units and the different petrographic groups to which they are assigned. Key: 1 = limestone; 2 = keratophyre; 3 = siltstone-dominated sequences with interbedded sandstone; 4 = coarse sandstone-dominated sequences with interbedded siltstone; 5 = granule-boulder conglomerate dominated sequences with interbedded sandstone and rare siltstone. Units 1 to 5 refer to mappable stratigraphic horizons recognized in the Murrawong Creek and Pipeclay Creek Formations. The sinuous trend of the Sandy Creek Fault (Fig. 1B) is depicted schematically as a curved line.

*Figure 2.4 - Stratigraphic column of the Early - Middle Paleozoic strata west of the Peel Fault system; from Cawood (1983).*
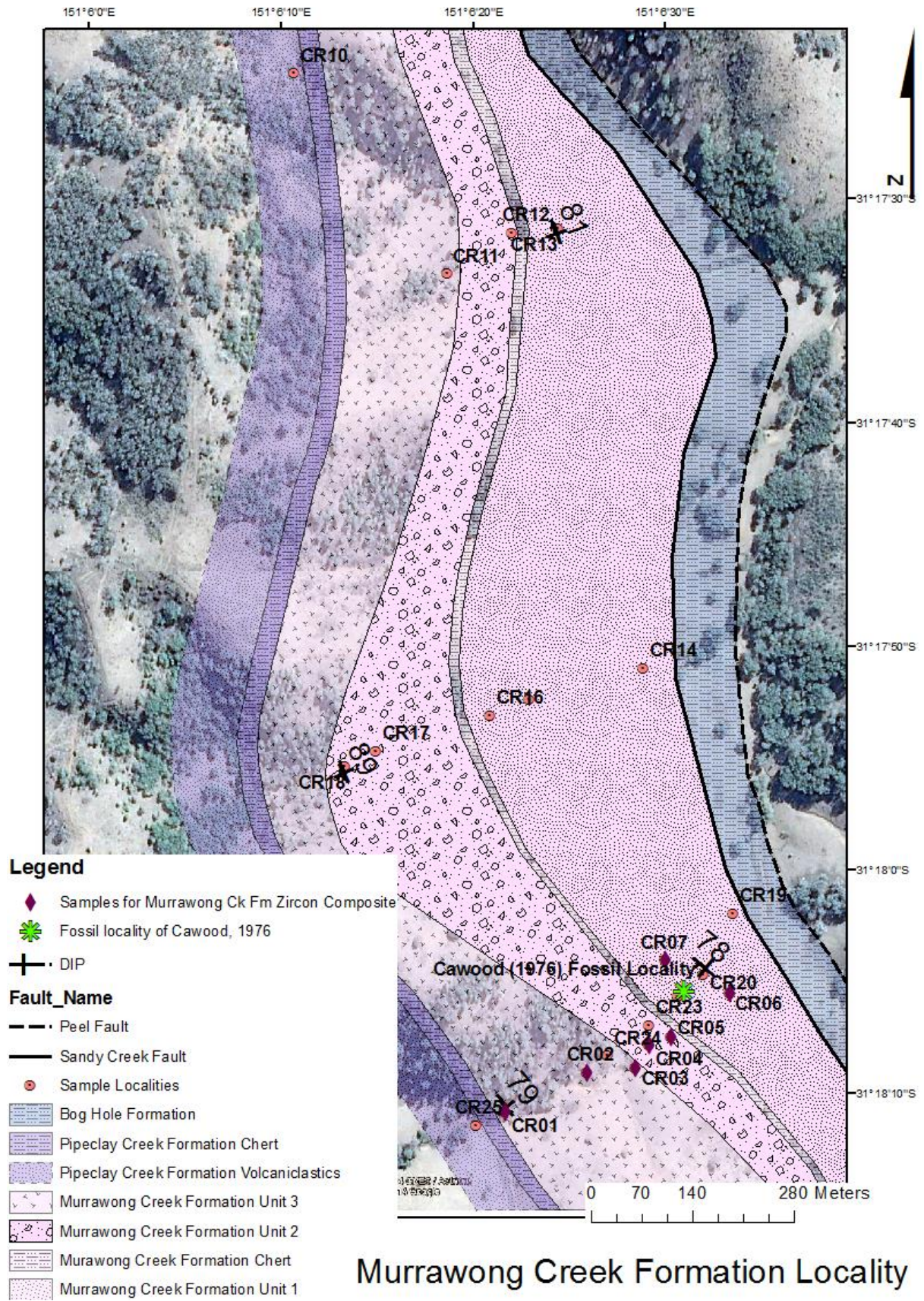
Figure 2.5 -Map of Location 1, using boundaries as mapped in the field.

## 2.2.1 Stratigraphy of Location 1
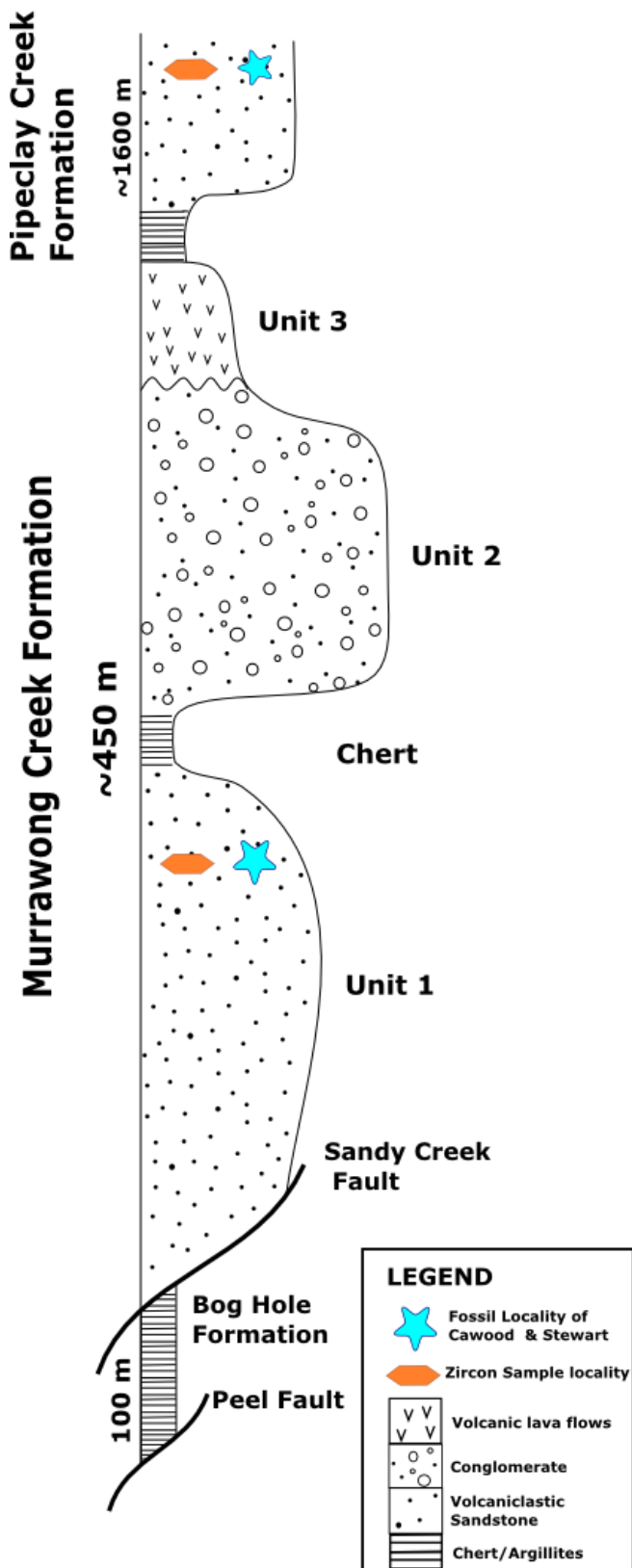


*Figure 2.6 - Stratigraphic column of the Murrawong Creek Formation.*

*Unit 1* - Mapped in the field as coarse lithic sandstone (Figure 2.5), the basal Unit 1 of the Murrawong Creek Formation consists of coarse-grained feldspathic volcaniclastic sandstone with interbedded siltstone, chert and conglomerate layers. The unit is massive bedded and poorly sorted, likely as a result of debris-flow style deposition in a marine basin (Cawood 1980). Clasts consist of feldspars, pyroxenes, limestones and chert. Feldspars show a tabular habit and are white in colour, while pyroxenite clasts are irregular, small black clasts. Interbedded chert layers are sporadic and green-blue in colour. Clast size ranges from 0.5 – 20 mm, with the exception of conglomerate boulders with clast size approximately 5 cm, however these were not *in situ* and their source was not found. Gradation of grain size is observed only locally, with fining upwards to interbedded siltstone layers. Chert exists as thinly bedded, siliceous green-blue chert. The presence of large quartz vein structures indicates episodes of hydrothermal alteration following deposition. It is from this unit that the fossils for previous work were extracted (e.g., Cawood 1976; Engelbretsen 1993; Brock 1998a).

*Unit 2* – Separated from Unit 1 by a massive green-black chert layer, Unit 2 is a volcaniclastic conglomerate layer. This overlying unit is distinctly more coarse-grained than Unit 1, with clast size ranging from 10 –

100 mm. These are massive, poorly sorted sedimentary rocks with interbedded chert layers and no gradational structures observed. They were likely deposited in a high-energy environment, such as debris flows with a proximal volcanic source. Volcanic fragments are the dominant constituents, with secondary alteration producing a chloritic overprint and green colour observed in the field. The matrix is medium-grained Fe-rich sand, which in combination with low Zr (determined using hand-held XRF) indicates a less evolved provenance.

*Unit 3* – Fine grained volcanic unit, separated from Unit 2 by an erosional contact. The presence of small-scale ripple marks and scours along the contact suggests deposition of Unit 2 in a low-energy marine environment followed by basaltic-andesitic lava flows from a proximal volcanic source (Unit 3). Fine-grained phenocrysts range from ~ 0.2 mm to ~1mm. Plagioclase is present as white, tabular crystals against a dark grey groundmass. Pyroxenes and amphiboles are indistinguishable in the field with both observed as small black phenocrysts. These are massive deposits with no volcanic layering observed. This basaltic andesite is dark grey in colour and chert is absent from this layer. The green overprint is interpreted to be a result of chlorite alteration.

*Pipeclay Creek Formation* – The contact between the Murrawong Creek Formation and Pipeclay Creek Formation is not observed, but is inferred by a sudden widespread occurrence of blue-green siliceous, banded chert. Few interbedded medium-grained volcaniclastic sandstone layers are observed with massive habit and fragmented angular clasts (0.2 – 1 mm) deposited in a high-energy environment. The lithic sandstones are quartz-poor with fragments consisting of chert and lithic clasts, suggesting marine deposition in close proximity to a volcanic source.

At location 2, the Pipeclay Creek Formation is an isolated lens of cobble to boulder-sized conglomerate. A sand-sized, volcanic-derived detrital matrix hosts a wide variety of relatively rounded clasts. Chert clasts are relatively small (5 – 100 mm) and consist of blue-green chert as well as red chert possibly sourced from the adjacent Djungati terrane. Volcanic clasts (20 – 50 mm) are mafic, with a predominance of feldspar phenocrysts amongst a dark groundmass. Large plutonic clasts (20 – 100 mm) are coarse grained and dominated by K-feldspars, quartz and biotite (Figure 4.4A). Large limestone clasts (20– 100 mm) show no evidence of macrofauna and are chalky-grey in colour. The array of clasts coexisting in a single rock produces a spectacular conglomerate.

## 2.3 Comments

The mapping undertaken is relatively in accord with those produced by Cawood (1980). Only a few minor contacts differ, most likely as a result of the poor outcrop and need to infer contacts. For example, north of CR11-13 the contacts are inferred, as sampling was not undertaken in this area.

Closer review of the field evidence, especially the understanding of stratigraphic relationships, provides initial clues into the depositional and tectonic environment for the Murrawong Creek and Pipeclay Creek formations. A high energy, debris-flow style of deposition is indicated through the coarse-grained nature of this sedimentary sequence, in combination with massive habit, poor sorting and a mixture of chert, carbonate and igneous clasts. Shallow-marine limestone clasts in combination with deep-marine chert clasts indicate the dynamic nature of the depositional basin, whereby pelagic sediments are uplifted with flanking shallow sediments incorporated via sediment gravity flows. The distance from volcanic activity is interpreted to be proximal given the angular, fragmented clasts and the lithological composition of volcanic fragments and plagioclase feldspars. This is supported by the presence of volcanic flows interbedded with the sediments. The sedimentary rocks were perhaps deposited due to erosion directly off a volcanic system resulting in intercalated volcanic flows from an active volcanic setting.

The fossil locality lying within Unit 1 of the Murrawong Creek Formation (Figure 2.3) is that which was used for the majority of studies aforementioned in *Section 2.1.1*. There is no doubt that the limestone clasts held within Unit 1 of the Murrawong Creek Formation are Middle-Late Cambrian in age. However, the allochthonous nature of the limestone within these debris-flow deposits and the spatial similarity between the key references highlights the significance of this project in determining an age for the sedimentary rocks of the Murrawong and Pipeclay Creek formations. The fossil locality (Figure 2.3) within the Pipeclay Creek Formation is that of Stewart (1995). This reference supported the interpreted Early Paleozoic ages of the Murrawong and Pipeclay Creek Formations. The locality from which samples were collected for detrital zircon geochronology in this project (Figure 2.3) lies along strike to Stewart's (1995) locality, possibly even representing a slither of the Haedon Formation, thus providing an upper age constraint for the Pipeclay Creek Formation.

# Chapter 3. Zircon Geochronology

## 3.1 Introduction

Detrital zircon geochronology is used to generate age determinations of sediment deposition for both the Murrawong and Pipeclay Creek formations using the *Sensitive High Resolution Ion Microprobe* (SHRIMP II). Previous dating of both formations has relied on biostratigraphy. The clastic sediments are thought to have been deposited during the Middle Cambrian, adjacent to an offshore island arc. Preceding authors have unsuccessfully attempted to find zircons from these formations (Korsch *et al.* 2010), however we managed to extract rare zircon from the clastic sediments through the use of a hand held XRF in the field. This chapter will attempt to determine the validity of the current biostratigraphic age constraints, through a detailed comparison of the available data and that generated for this thesis.

### 3.1.1 Detrital zircons

Zircons ($ZrSiO_4$) are mechanically and chemically stable minerals that can survive and record a range of geological processes, making them excellent tools for geochronological analysis. Zircons typically crystallise from felsic magmas with greater than 60% $SiO_2$, and are therefore less common in magmas with lower silica contents (Cawood *et al.* 2012). The geological history of a zircon is often retained through complex zoning allowing for a reconstruction of the minerals provenance. Trace elements uranium and thorium incorporated in zircon upon formation undergoes radioactive decay to form lead isotopes, providing the basis for geochronology by multiple analytical techniques, including the SHRIMP.

Detrital zircons survive weathering during transport to sedimentary depositional sites and subsequently are a minor constituent of clastic sedimentary rocks. For this reason, detrital zircon has been used to determine provenance, including the tectonic setting of the basin in which they are deposited (Cawood *et al.* 2012). Basins lying along plate margins typically experience contemporaneous sediment deposition and tectonic activity, and so the presence or absence of detrital zircons approximating the age of deposition may also indicate proximity of the basin to an active or passive plate margin (Cawood *et al.* 2012). In terms of geochronological analysis, the 'law of detrital zircons' is that the youngest detrital zircon population represents the maximum depositional age of the clastic

sediments, so that sediment accumulation cannot be older than the youngest zircon population. In eastern Australia, Precambrian detrital zircons have two characteristic peaks associated with supercontinent formation, 600-500 Ma and 1300-1000 Ma which represent Gondwanan and Rodinian formation respectively (Fergusson *et al.* 2013, and references therein). Grains of this age provide a paleogeographic tool to assess whether eastern Australian Paleozoic sedimentary rocks formed proximal or distal to the Gondwanan margin.

### 3.1.2 *U-Pb Zircon Dating*

Williams (1998) provides a detailed summary of U-Pb geochronology and the SHRIMP U-Pb zircon methodology, which is outlined here. Zircon has been a mineral of choice for U-Pb dating for many decades due to the natural incorporation of U-Th but not of Pb during mineral formation. Th and U both contain naturally radioactive isotopes, i.e. unstable isotopes spontaneously decay to a form a stable isotope of a different element, in this case, Pb. The rate at which an isotope undergoes radioactive decay is both element and isotope specific, independent of physical or chemical parameters. The probability that radioactive decay will occur at any point in time is known as the decay constant ($\lambda$), whereby the number of decays occurring per unit time is related to how many atoms are present for a given isotope. The most convenient formula used to describe radioactive decay, which measures the ratio of daughter atoms produced (D) to parent atoms remaining (P) after a period of time (t), is as follows:

$$D/P = e^{\lambda t} - 1$$

A half-life ($T_{1/2}$) can be defined as the time it takes for half a given amount of a radioisotope to decay. This is the influential factor determining the suitability of the U-Pb isotopic system over other natural radioisotopes in geochronological analysis. Due to the scale of geological time, the half-life of the radioisotope must be long enough for an adequate amount of daughter isotope to be produced, however not too long that there is not enough original parent radioisotope remaining (Williams 1998). Half-lives of the U-Pb isotopic system are known:

$^{238}$U decays to $^{206}$Pb with a half-life of 4.47 x $10^{9}$yr

$^{235}$U decays to $^{207}$Pb with a half-life of 0.704 x $10^{9}$yr

A key advantage to using the U-Pb isotopic system for geochronological analysis is the paired nature of the system whereby there are two U isotopes that decay to different Pb isotopes at different rates. Thus, a comparison can be made between the ages calculated from both U-Pb isotopes and through a separate measure from the Pb isotopic composition ($^{207}$Pb/$^{206}$Pb). This is particularly advantageous as it allows for the disturbance of the system to be determined, i.e. if it is a closed system or if it is an open system (influenced by secondary processes). A Concordia diagram is used for visualisation of data, whereby those analyses which measure all three isotopic ages as equal plot on the curve and are known as concordant. These represent closed systems. Two bivariate plots are used 'Wetherill' ($^{207}$Pb/$^{235}$U against $^{206}$Pb/$^{238}$U) or 'Tera-Wasserburg' ($^{206}$Pb /$^{238}$U against $^{207}$Pb/$^{206}$Pb) with the latter being advantageous over the former due to direct plotting of measurements rather than calculating and plotting the $^{235}$U value from a given ratio. Hence, the Tera-Wasserburg diagram was chosen for analysis of these results.

During the sputtering processes of the target during SHRIMP analysis, there is fractionation between different elements e.g. U from Pb. Therefore the raw ratios acquired from SHRIMP are not the true values. This requires calibration to a standard, or a zircon of known age. A common standard is TEMORA II, at 416.8 ± 0.3 Ma (Black *et al.* 2003). Common Pb is present in all measurements, and thus must be accounted for to reduce uncertainty in measurement. This is attempted via choice of well-preserved domains in the zircons and rastering of the primary ion beam over each target prior to analysis in order to remove surface contaminant Pb.

## 3.2    Methodology

### 3.2.1    Sample Preparation

When collecting samples of the Murrawong Creek Formation for detrital zircon analysis in the field, the handheld XRF was used as it was thought that the immature sediments hold very few detrital zircons. Walking across strike rocks were intermittently tested using the handheld XRF to seek zirconium concentrations of >80 ppm, creating a 4 kg composite sample combining the zirconium-rich layers. The samples were crushed and separated using the conventional heavy liquid and magnetic techniques at the mineral separation laboratory of the Research School of Earth Sciences at the Australian National University (ANU).

The standard preparation method was used to create a zircon mount, whereby zircon grains were extracted by hand under the binocular microscope, placed in a mould and set using epoxy resin. The epoxy disc included the TEMORA-2 standard for calibration (U-Pb ages concordant at 417 Ma; (Black *et al.* 2003)), and the disc was ground to reveal mid-sections through the grains before being polished. Cathodoluminescence (CL) imaging was undertaken on the zircon grains to provide a 'map' of the zircon mount for easy navigation during SHRIMP analysis along with documenting the character of the zircon grains.

### 3.2.2    *SHRIMP analysis*

Samples were taken to the ANU for analysis of U-Th-Pb isotopic ratios using the SHRIMP II. The SHRIMP releases a focussed high energy oxygen 10 kV beam which smashes particles off a ~20$\mu$m wide by 1-2$\mu$m deep domain of the sample, which are then sent through the instrument to record the number of ions hitting the detector. CL images were used to target analysis sites, and due to the immature nature of the zircon grains, the aim was to find the best preserved grains displaying oscillatory zoning. The analysis of grains was interleaved, such that three to four unknown grains were visited between each TEMORA-2 standard. The youngest grains were visited twice in order to check for reproducibility. The Murrawong Creek and Pipeclay Creek Formation samples were analysed on two separate analytical sessions and reduction of the raw data and calibration was undertaken manually using the ANU software 'PRAWN' and 'Llead'. Reported ages are derived from $^{206}$Pb/$^{238}$U ratios, as is consistent for Phanerozoic grains. The $^{206}$Pb/$^{238}$U calibration error based on the TEMORA-2 standards in the analysis was 2.6%, slightly higher than the desired < 2%, and this uncertainty was incorporated into the age determinations accordingly. Tera-Wasserburg and cumulative Gaussian distribution plots were generated using ISOPLOT (Ludwig 1998). Weighted mean ages reported here are given at the 95% confidence level.

### 3.3 Description of zircons

*Murrawong Creek Formation* – Due to the immaturity of the sediments in the Murrawong Creek Formation, detrital zircon grains were extremely sparse. Despite the use of the hand-held XRF for the collection of zirconium-rich sandstone layers in the field, only 6 grains were separated and extracted from the composite sample. The paucity of zircons given bulk rock Zr >80 ppm is probably because much Zr is held in detrital clinopyroxene. The selected grains are sub rounded, poorly preserved and very small, with an average 40-70 $\mu$m in size (Figure 3.1). Almost all grains show evidence of oscillatory growth zoning, however none are left fully intact and thus the zoning present is truncated. The grains are dark in the Cl images, resulting from higher contents of U and Th (e.g., Fergusson *et al.* (2013).
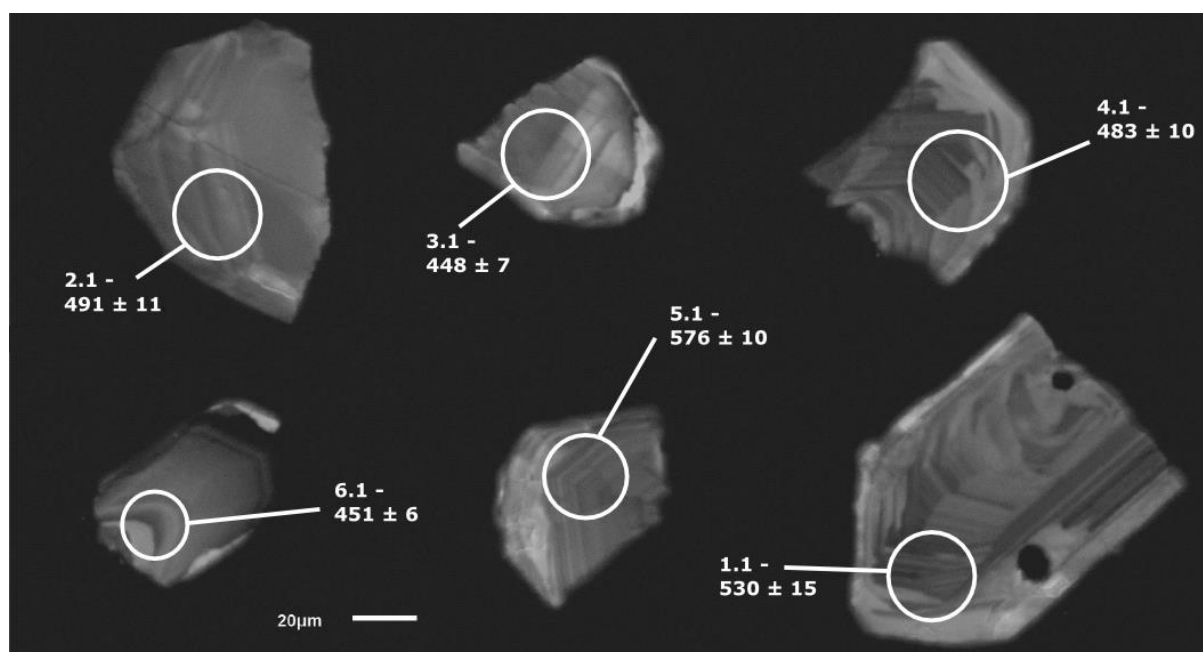


*Figure 3.1 - MCF sample, Mount 29: full suite of the Murrawong Creek Formation zircons with labelled $^{206}Pb/^{238}U$ ages to the nearest Ma.*

*Pipeclay Creek Formation* –This gave a high yield of >500 grains obtained from the 1 kg sample. The selected grains are slightly larger than those of the Murrawong Creek Formation at an average size of 50 – 150 $\mu$m (Figure 3.2). Poorly preserved grains are oval or somewhat rounded grains, with few grains exhibiting euhedral prismatic habit. Many of the selected grains display broad zoning, with the rare euhedral grains often showing oscillatory zoning parallel to the grain margins, whilst some others lack the presence of any zoning. The primary ion beam was targeted to those regions exhibiting zoning structures, or if no zoning was present, the cleanest grains without inclusions or cracks were targeted. The majority of grains have been abraded along grain margins, often truncating internal zoning. Non-luminescent inclusions are present in many of the grains, probably quartz or feldspars.
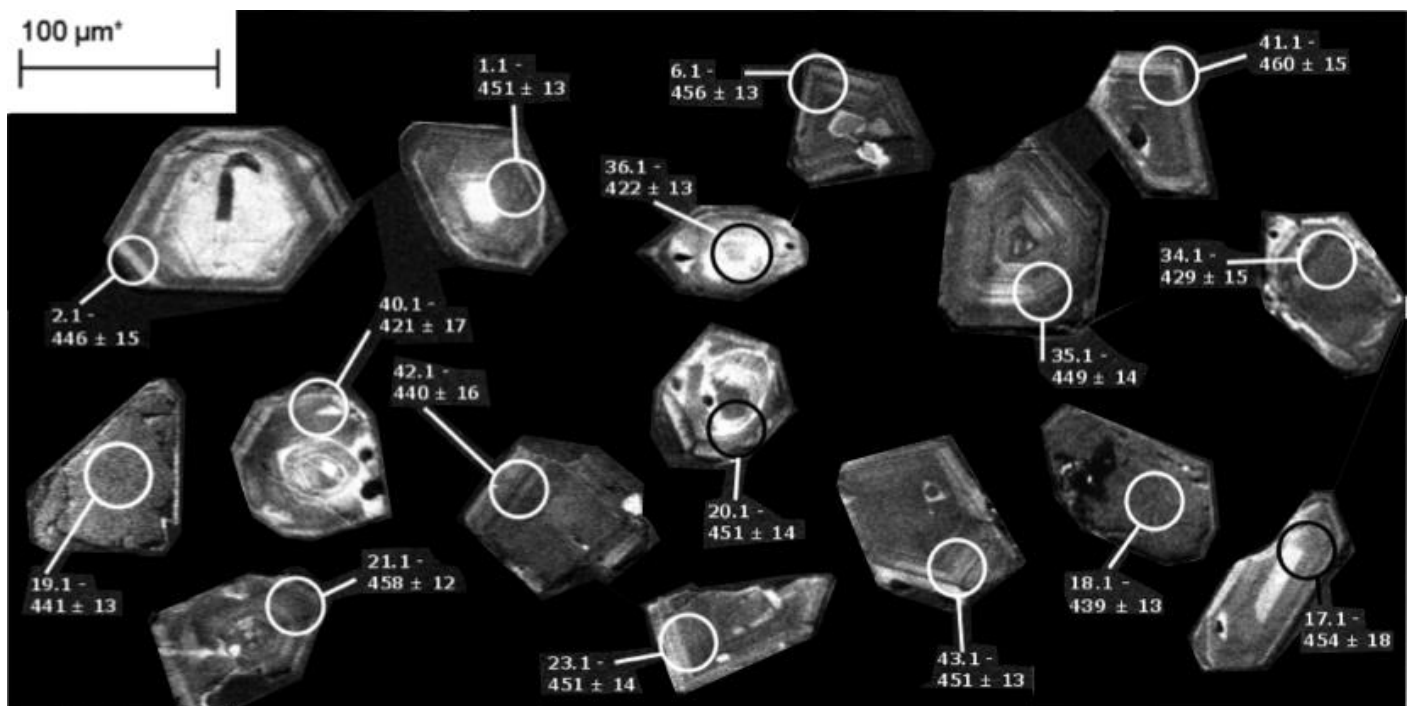


*Figure 3.2 - PCF sample, Mount W34: A random selection of some of the analysed grains, labelled with their $^{206}Pb/^{238}U$ ages to the nearest Ma, see Appendix 2 for full sample set.*

## 3.4 Results

*Murrawong Creek Formation* – All analyses of the six zircons from the Murrawong Creek Formation plot close to concordia (Figure 3.3) indicating that the isotopic system is relatively undisturbed. Common Pb is measured by $^{204}$Pb, which remains reasonably low for all zircons at less than 10 ppb for all measurements. There is no distinct difference between data obtained from the edge or middle of the minerals (Table 3.1). The data set does not produce a single normal population (Figure 3.3) so a final $^{206}$Pb/$^{238}$U weighted mean age is calculated for the two identifiable populations present within the small dataset:

1) $450 \pm 10$ Ma (MSWD = 0.05, to nearest Ma), and
2) $486 \pm 15$ Ma (MSWD = 0.29, to nearest Ma)

$450 \pm 10$ Ma is taken to be the most accurate representative age for the Murrawong Creek Formation, given that the youngest zircon population indicates maximum depositional age. A preliminary result from a single zircon was obtained at an age of $496.0 \pm 18.4$ ($1\sigma$), however given the inconclusive nature of using a single zircon grain from an entire sample, the result had previously been left undocumented. Following this study, it appears that this age is congruent with these results, as it lies within statistical error of the older zircon population and thus has been included in the results in this study to bolster the low zircon yield extracted from the Murrawong Creek Formation.

*Table 3.1 - MCF sample U/Pb SHRIMP analysis*

| Labels | Site | U/ppm | Th/ppm | Th/U | f206% | AGE 6/38 |
|--------|------|-------|--------|------|-------|----------|
| **CRZ-1.1** | m,osc,p,fr | 195 | 80 | 0.41125 | 0.0075 | $529.8 \pm 14.6$ |
| **CRZ-2.1** | e,osc,p,fr | 169 | 107 | 0.63071 | 0.00382 | $490.5 \pm 11.0$ |
| **CRZ-3.1** | e,osc,p,fr | 312 | 70 | 0.22318 | 0.00357 | $448.5 \pm 7.2$ |
| **CRZ-4.1** | osc,p,fr | 271 | 121 | 0.44563 | 0.0021 | $482.5 \pm 10.1$ |
| **CRZ-5.1** | osc,p,fr | 792 | 292 | 0.36863 | 0.00225 | $575.6 \pm 9.5$ |
| **CRZ-6.1** | m,osc,p,fr | 587 | 76 | 0.12872 | 0.00086 | $450.6 \pm 6.5$ |

m = middle, e = edge, osc = oscillatory zoned, p = prismatic, fr = fragment

f206% = the proportion of $^{206}$Pb that is non radiogenic, based on measured $^{204}$Pb and a model common Pb composition.

*Figure 3.3 - Murrawong Creek SHRIMP analyses; a) Terra-Wasserburg plot, b) Non-filtered $^{206}Pb/^{238}U$ age on cumulative Gaussian distribution plot. Diagrams produced by A. Nutman, 2014.*
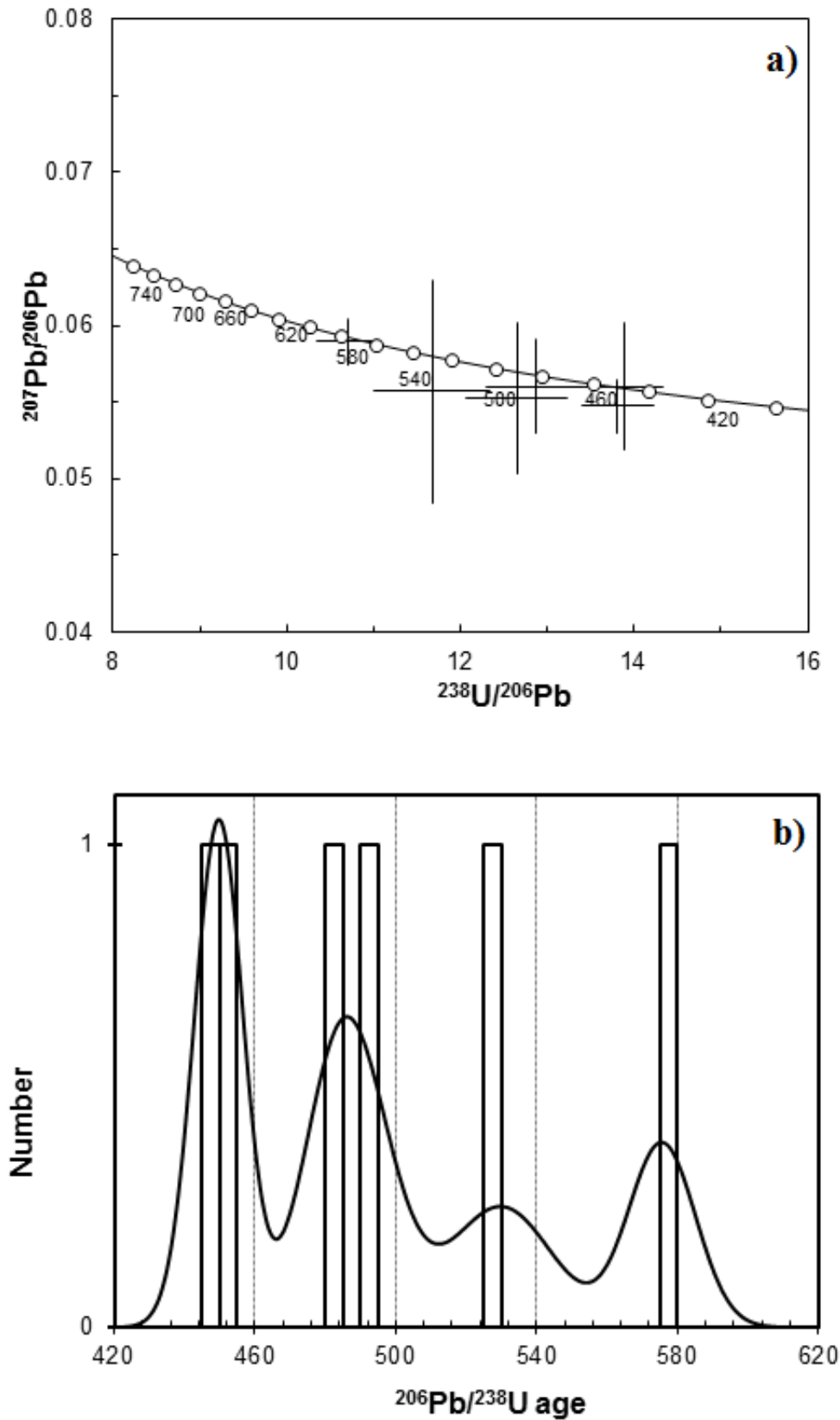
*Table 3.2 - PCF sample, U/Pb SHRIMP analyses.*

| Labels | Site | U/ppm | Th/ppm | Th/U | f206 | 206Pb/238U | ± 6/38 | 207Pb/206Pb | ± 7/6 | AGE 6/38 |
|---|---|---|---|---|---|---|---|---|---|---|
| PCF-1.1 | e,osc,p | 228 | 64 | 0.281 | 0.00297 | 0.0725 | 0.0021 | 0.0547 | 0.0016 | 451.4 ± 12.8 |
| PCF-2.1 | e,osc,p | 318 | 100 | 0.313 | 0.00349 | 0.0717 | 0.0025 | 0.0562 | 0.0015 | 446.2 ± 14.8 |
| PCF-3.1 | m,p | 1134 | 494 | 0.435 | 0.00157 | 0.0708 | 0.0024 | 0.0559 | 0.0009 | 441.2 ± 14.4 |
| PCF-5.1 | e,osc,p | 136 | 56 | 0.411 | 0.01376 | 0.0683 | 0.0031 | 0.0604 | 0.0052 | 425.9 ± 18.9 |
| PCF-6.1 | e,osc,p | 572 | 239 | 0.417 | 0.00167 | 0.0734 | 0.0022 | 0.055 | 0.0012 | 456.5 ± 13.4 |
| PCF-7.1 | m,fr | 1228 | 564 | 0.46 | 0.00034 | 0.0714 | 0.0025 | 0.0561 | 0.0005 | 444.4 ± 14.8 |
| PCF-8.1 | e,osc,fr | 389 | 108 | 0.277 | 0.00276 | 0.0731 | 0.0022 | 0.0538 | 0.0013 | 454.8 ±13.3 |
| PCF-9.1 | e.,osc,p | 399 | 162 | 0.405 | 0.00115 | 0.0705 | 0.0035 | 0.055 | 0.0013 | 438.9 ± 21.2 |
| PCF-10.1 | m,osc,fr | 822 | 293 | 0.356 | 0.00097 | 0.0725 | 0.0021 | 0.0556 | 0.0007 | 451.1 ± 12.7 |
| PCF-11.1 | e,osc,p | 214 | 53 | 0.247 | 0.00002 | 0.0679 | 0.0022 | 0.0589 | 0.0017 | 423.4 ± 13.3 |
| PCF-12.1 | e,osc,p | 467 | 127 | 0.272 | 0.0024 | 0.0688 | 0.002 | 0.0541 | 0.0016 | 428.6 ± 12.1 |
| PCF-12.2 | m,osc,p | 343 | 73 | 0.213 | 0.00002 | 0.0701 | 0.0027 | 0.0564 | 0.0012 | 436.6 ± 16 |
| PCF-13.1 | e,osc,p | 179 | 80 | 0.448 | 0.00803 | 0.0679 | 0.0021 | 0.05 | 0.0027 | 423.5 ± 12.3 |
| PCF-13.2 | m,osc,p | 164 | 58 | 0.352 | 0.0054 | 0.0661 | 0.0025 | 0.0595 | 0.0026 | 412.4 ± 15 |
| PCF-14.1 | e,osc,p | 939 | 365 | 0.389 | 0.00005 | 0.0718 | 0.002 | 0.0554 | 0.0006 | 446.7 ± 12.3 |
| PCF-15.1 | m,osc,p | 297 | 77 | 0.259 | 0.00158 | 0.0749 | 0.0024 | 0.0562 | 0.0016 | 465.4 ± 14.2 |
| PCF-16.1 | e,osc,p | 474 | 172 | 0.364 | 0.00323 | 0.0663 | 0.0108 | 0.0553 | 0.0028 | 413.8 ± 65.6 |
| PCF-17.1 | m,osc,p | 280 | 107 | 0.383 | 0.00216 | 0.0729 | 0.003 | 0.0553 | 0.0017 | 453.7 ± 17.9 |
| PCF-18.1 | m,p | 1948 | 1084 | 0.557 | 0.00071 | 0.0705 | 0.0021 | 0.0556 | 0.0006 | 439.2 ± 12.6 |
| PCF-19.1 | m,fr | 1396 | 624 | 0.447 | 0.00064 | 0.0709 | 0.0021 | 0.0545 | 0.0005 | 441.4 ± 12.6 |
| PCF-20.1 | e,osc,p | 353 | 137 | 0.389 | 0.00355 | 0.0725 | 0.0024 | 0.053 | 0.0014 | 451 ± 14.2 |
| PCF-21.1 | e,osc,fr | 516 | 188 | 0.365 | 0.00013 | 0.0737 | 0.0020 | 0.0557 | 0.0011 | 458.2 ± 12.2 |
| PCF-22.1 | m,p | 2697 | 1432 | 0.531 | 0.00022 | 0.0711 | 0.0023 | 0.0564 | 0.0004 | 442.8 ± 13.8 |
| PCF-23.1 | e,osc,fr | 445 | 147 | 0.329 | 0.0008 | 0.0724 | 0.0023 | 0.0562 | 0.0009 | 450.6 ± 13.7 |
| PCF-24.1 | e,osc,fr | 347 | 93 | 0.268 | 0.0016 | 0.0732 | 0.0021 | 0.0541 | 0.0010 | 455.7 ± 12.8 |
| PCF-25.1 | e,osc,fr | 417 | 112 | 0.269 | 0.00024 | 0.0685 | 0.0021 | 0.057 | 0.0009 | 427.2 ± 12.7 |
| PCF-26.1 | m,osc,p | 241 | 66 | 0.273 | 0.00354 | 0.068 | 0.0023 | 0.0542 | 0.0023 | 424.4 ± 13.6 |
| PCF-26.2 | m,osc,p | 197 | 49 | 0.247 | 0.0161 | 0.0655 | 0.0045 | 0.0548 | 0.0047 | 408.9 ± 27.2 |
| PCF-27.1 | m,osc,fr | 607 | 289 | 0.477 | 0.00223 | 0.0722 | 0.0023 | 0.0537 | 0.0013 | 449.2 ± 13.9 |
| PCF-28.1 | e,osc,fr | 203 | 82 | 0.385 | 0.06745 | 0.0605 | 0.002 | 0.056 | 0.0088 | 378.4 ± 12.1 |
| PCF-29.1 | m.osc,p | 560 | 214 | 0.382 | 0.00076 | 0.0716 | 0.0024 | 0.056 | 0.0012 | 445.9 ± 14.6 |
| PCF-30.1 | m,osc,p | 331 | 122 | 0.368 | 0.00156 | 0.0696 | 0.0021 | 0.056 | 0.0014 | 433.8 ± 12.8 |
| PCF-31.1 | e.osc,p | 340 | 103 | 0.303 | 0.00364 | 0.0724 | 0.0028 | 0.0536 | 0.0015 | 450.8 ± 16.7 |
| PCF-32.1 | e,osc,p | 658 | 231 | 0.351 | 0.00016 | 0.0744 | 0.0058 | 0.0527 | 0.0028 | 462.3 ± 35.1 |
| PCF-33.1 | e,osc,fr | 794 | 292 | 0.368 | 0.00051 | 0.0724 | 0.0021 | 0.0567 | 0.0008 | 450.7 ± 12.8 |
| PCF-34.1 | m,osc,p | 497 | 170 | 0.343 | 0.00009 | 0.0688 | 0.0025 | 0.0568 | 0.0008 | 428.7 ± 15.2 |
| PCF-35.1 | m,osc,p | 369 | 113 | 0.307 | 0.00026 | 0.0722 | 0.0024 | 0.0549 | 0.0012 | 449.2 ± 14.2 |
| PCF-36.1 | m,osc,p | 186 | 66 | 0.352 | 0.00366 | 0.0677 | 0.0022 | 0.0529 | 0.0022 | 422 ± 13.1 |
| PCF-37.1 | e,osc,fr | 404 | 135 | 0.334 | 0.00002 | 0.0728 | 0.0024 | 0.0558 | 0.0008 | 452.9 ± 14.5 |
| PCF-38.1 | e,osc,fr | 593 | 214 | 0.36 | 0.00114 | 0.0715 | 0.0022 | 0.0563 | 0.0013 | 445.4 ± 13 |
| PCF-39.1 | e,fr | 2637 | 1467 | 0.556 | 0.00041 | 0.0693 | 0.0019 | 0.0556 | 0.0004 | 432.1 ± 11.1 |
| PCF-40.1 | e,osc,p | 382 | 123 | 0.324 | 0.00055 | 0.0676 | 0.0029 | 0.0565 | 0.0010 | 421.4 ± 17.4 |
| PCF-41.1 | e.osc,p | 764 | 266 | 0.348 | 0.00014 | 0.074 | 0.0024 | 0.0562 | 0.0006 | 460.5 ± 14.5 |
| PCF-42.1 | e,osc,p | 731 | 238 | 0.326 | 0.00002 | 0.0707 | 0.0026 | 0.0558 | 0.0007 | 440.4 ± 15.7 |
| PCF-43.1 | e,osc,p | 573 | 190 | 0.333 | 0.00089 | 0.0725 | 0.0021 | 0.0564 | 0.001 | 450.9 ± 12.9 |

*Pipeclay Creek Formation* – A closed isotopic system is indicated as all analyses plot close to Concordia and there are low amounts of common Pb (Figure 3.4). No difference was observed between core and rim analysis, with most being within statistical error of one another (Table 3.2). All grains are interpreted to produce a single normal population (Figure 3.4). In an attempt to identify outliers, those analyses reading less than 430 Ma are disregarded (e.g., PCF – 13.2, 16.1, 26.2, 28.1). It is interesting to note that two of these are grains that originally gave inconsistently young ages, and these are second readings giving an even younger age. For this reason it is likely that these are the youngest grains of the sediments. Nevertheless, the youngest population of detrital zircon ages was considered and the calculated weighted mean $^{206}Pb/^{238}U$ age is 443.4 ± 4.3 (MSWD= 0.71; Figure 3.5).

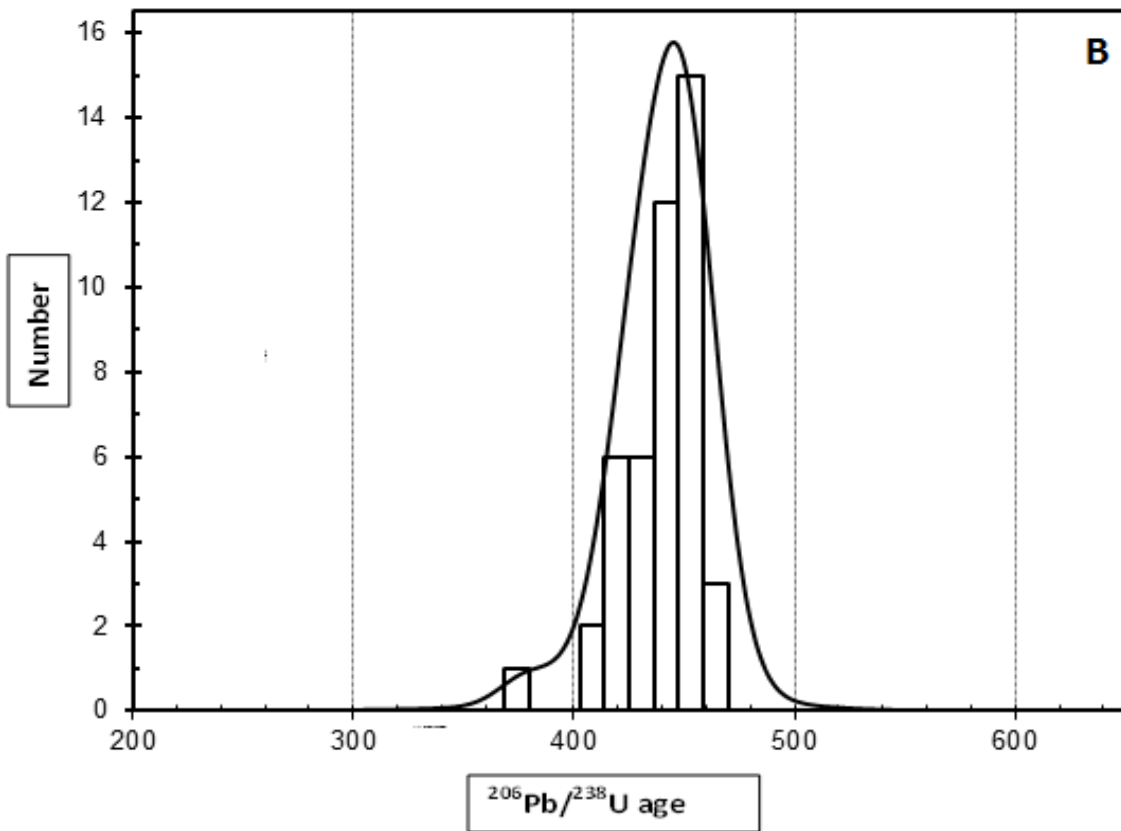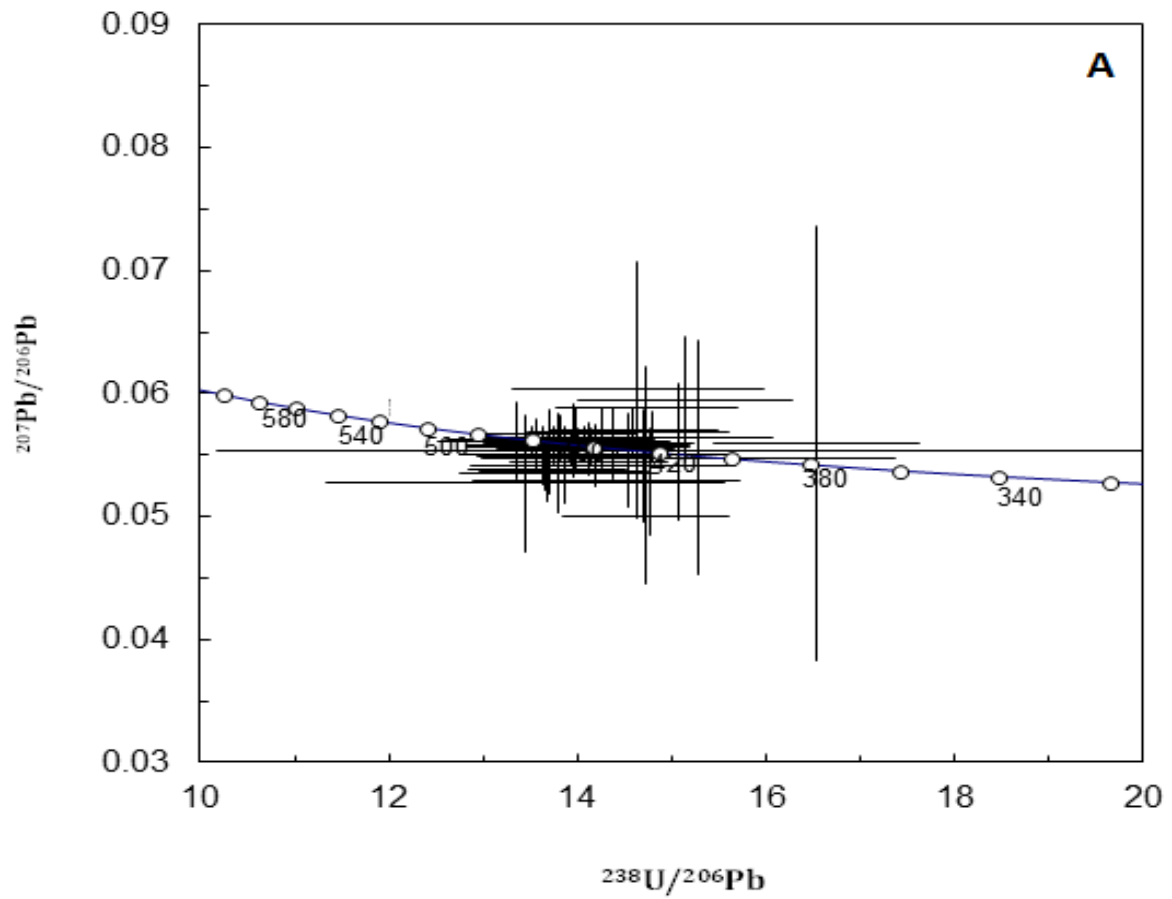*Figure 3.4 - Pipeclay Creek SHRIMP analyses, A: Terra-Wasserburg plot, B: Non-filtered 206Pb/238U age on Cumulative Gaussian distribution plot*
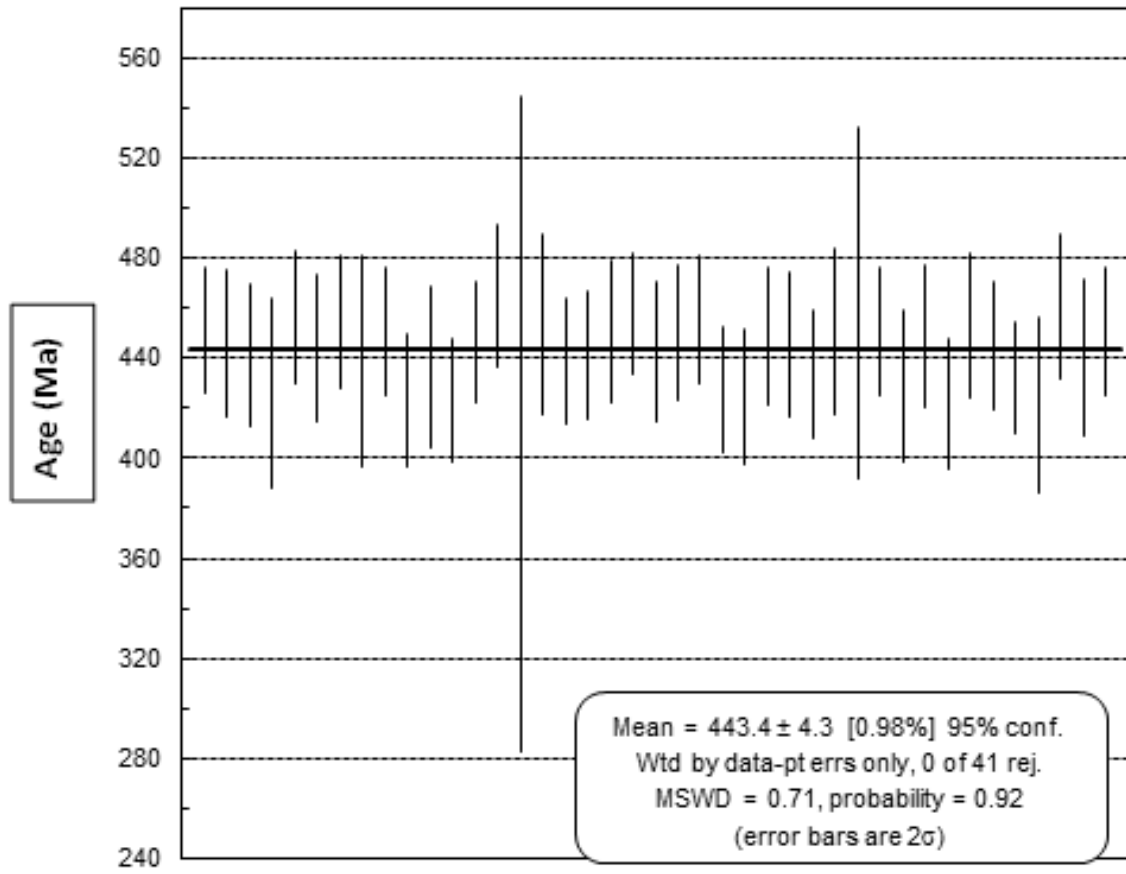
*Figure 3.5 - Age distribution plot. All diagrams produced by A. Nutman, 2014*

## 3.5    Interpretation

The presence of oscillatory zoning in all detrital zircon grains collected from the Murrawong Creek Formation implies the zircons are sourced from magmatic bodies, rather than produced by hydrothermal alteration or in metamorphic environments (Corfu *et al.* 2003). The slightly sub-rounded nature, combined with apparent recrystallization of some rims is interpreted to be resorbed exteriors (Corfu *et al.* 2003), is consistent with pumpellyite-prehnite facies due to burial metamorphism of the succession (Cawood 1983; Engelbretsen 1996). The grains are all extremely fragmented, a result of the laboratory separation process, and it is therefore difficult to determine source from these grains.

The distinct lack of zircons obtained from a large composite sample strongly suggests that the sediments were being eroded from a silica-poor, oceanic source area such as an intra-oceanic island arc or forearc basin setting. The clear absence of any inherited, older 'Gondwanan' zircons supports the hypothesis that these oldest portions of the Gamilaroi terrane were formed proximal to a juvenile island arc well away from the sedimentary influence of Gondwana somewhere in the vast expanse of the Panthalassan Ocean, during the Late Ordovician. The mixture of oscillatory zoned grains and grains with no zoning at all specify an igneous source.

The number of zircon grains extracted from the Pipeclay Creek Formation could indicate either a further distance from the source, or more likely the maturity of the magmatic system feeding the adjacent island arc. Zircons are more likely to crystallise in silica-rich magmas (Cawood *et al.* 2012), which result from ongoing fractionation of minerals in the existing magma chamber. Thus very few zircons crystallised from a predominantly mafic magma source early in the development of the island arc, and therefore few were transported to the Murrawong Creek Formation during the early Late Ordovician. However by the latest Ordovician the arc had matured, resulting in more abundant zircons within the overlying Pipeclay Creek Formation.

The width/length ratio of zircon grains is commonly used to determine source, as crystallization velocity acts as a control on the shape of the zircon (Deer *et al.* 1996; Corfu *et al.* 2003).The majority of grains observed exhibit an almost equant ratio, indicating slow cooling within a fractionated plutonic magma source in the lower crust (Corfu *et al.* 2003). This is confirmed via zoning of individual grains whereby when zoning is present it is typical to that of silica saturated plutonic rocks, namely granite. When zoning is absent

the grains exhibit an irregular sub rounded external appearance, indicating prolonged crystallisation of a deep magma body (Corfu *et al.* 2003). This data is consistent with analysis of hand specimens whereby granitoid clasts exist in the PCF hand samples (Figure 4.4).

The central idea surrounding geochronology of detrital zircons is that the youngest zircon grains are indicative of the oldest possible depositional age, but deposition may well be younger than this. The biostratigraphic record provides different results for the age of these formations whereby both formations have previously been assessed as Middle Cambrian. Despite the small zircon yield for the Murrawong Creek Formation, two of the six grains analysed are Late Ordovician. Although the sample base is small, this represents the only radiometric, non-biostratigraphic age to have been extracted from these extremely juvenile, zircon-poor sedimentary rocks. Thus, this provides the only data at present to test the concept of whether the Cambrian-Ordovician fossil ages represent the age of sedimentation or whether they are older allochthonous blocks that have slumped into younger sediments.

Given there is no valid reason to discount the two Late Ordovician zircon ages it can be concluded that the maximum age of the MCF is that of the youngest population of zircons, i.e., Late Ordovician. This implies that the Cambrian to Early Ordovician fossils previously reported (Cawood 1976; Engelbretsen 1993; Stewart 1995; Engelbretsen 1996; Brock 1998a, b, 1999; Furey-Greig 2003; Sloan & Laurie 2004) are probably extracted from older, allochthonous clasts or rafts of limestone and chert that slumped into younger units. The older zircons are likely sourced from the erosion of the same older Cambrian material that contains the fossils, possibly the Weraerai terrane. These zircons highlight that older Cambrian material was mixed in with the younger Ordovician (450 Ma) material that is probably closer to the true age of sedimentation. This interpretation correlates well with the Cambrian fossils found in Murrawong Creek Formation.

The sample from the Pipeclay Creek Formation provides a more robust dataset, providing a U-Pb age of possible deposition from the latest Ordovician to earliest Silurian. The ages from both formations are younger than the signature ages for Gondwanan Neoproterozoic magma genesis (600 – 500 Ma), further indicating that these rocks have come from an exotic terrane, i.e. an offshore island arc.

In terms of uncertainty in age constraints, it is often more reliable to analyse samples from different levels of a stratigraphic section (Gehrels 2014). Due to limited time and resources, the Pipeclay Creek Formation sample was collected from a single conglomerate locality only, thus may not be representative of the entire formation. However, the sample locality was high in the stratigraphic sequence, providing an upper age constraint. The conglomerate sampled included clasts of limestone, chert, volcanics and plutonic rocks in hand specimen indicating a mixed source, which should be reflected in the detrital zircon population. The Murrawong Creek sample was a composite, satisfying this criterion, however the low zircon yield creates uncertainty as the key to success for detrital zircon geochronology is to analyse a large number of zircon grains to ensure the identification of all significant populations (Williams 1998).

On a more regional scale, this data implies that during the Late Ordovician an immature island arc existed offshore Gondwana, which resulted in the deposition of the Murrawong Creek Formation's volcaniclastic sediments. This arc has then progressed in maturity or alternatively an unroofing of a granitic pluton has occurred during the latest Ordovician and into the Silurian, resulting in the deposition of the Pipeclay Creek Formation.

# Chapter 4.    Petrography

## 4.1    Introduction

Petrographic analysis and point counting of the Murrawong Creek and Pipeclay Creek formations was undertaken to determine the provenance and possible tectonic setting of the sediment source region. Previously, the Murrawong Creek Formation has been thought to be deposited in a submarine fan forming part of a forearc basin and accretionary complex, above a long-lived west dipping subduction zone, east of an active continental margin arc (Leitch 1974, 1975; Cawood 1976, 1980; Leitch & Cawood 1980; Cawood 1983; Leitch & Cawood 1987; Engelbretsen 1993; Sloan & Laurie 2004). An alternative hypothesis proposed by Aitchison et al., (1992, 1994) suggests that these rocks represent the oldest portion of an intra-oceanic island arc (Gamilaroi terrane) that was accreted to the Gondwanan margin as an allochthonous terrane during the latest Devonian. Sandstone petrography along with detrital zircon and geochemical data presented in this study will provide a way of determining both the provenance and age of this sedimentary sequence in order to test the two competing models. The presence of inherited 'Gondwanan' detrital quartz and zircons of Proterozoic age within sedimentary rocks showing a 'transitional continental' signature in a QFL diagram would suggest a close proximity to eastern Gondwana, hence favouring the active continental margin model. Alternatively, a lack of any inherited Proterozoic 'Gondwanan' zircons and continental crust-derived quartz within sedimentary rocks of island arc affinity would more strongly favour accretion of an exotic oceanic terrane. This chapter will systematically present petrographic descriptions and point counting data as QFL diagrams of 19 samples collected across strike at the Murrawong Creek Formation (Figure 2.5) and eight localities from the overlying Pipeclay Creek Formation and surrounding formations near Chaffey Dam, New South Wales (Figure 2.3).

### 4.1.1    Sedimentary Classification

A wide variety of classifications for sedimentary rocks have been developed over the past six decades, receiving varying levels of acceptance (Boggs 2011). Classification of sedimentary rocks is based primarily on framework mineralogy, with few schemes incorporating the relative abundance of matrix (Boggs 2011). Due to the common abundance of framework quartz, feldspars and rock/lithic fragments (QFR) within all sandstones, these make up the key mineralogical constituents for sandstone classification.

Thus the QFR method is particularly useful for clastic sedimentary rocks and conglomerates such as those sampled from the Murrawong Creek and Pipeclay Creek formations.

Two sedimentary classification schemes have been chosen for this chapter; Pettijohn (1954) and Folk (1974), which consider matrix to detrital grain ratios and sorting respectively. These classification schemes are two of the more widely used and are easily applied to point counting data. The Pettijohn (1954) classification is entirely descriptive, taking into account provenance via the feldspar to rock fragment ratio, mineralogical maturity via the quartz to feldspar ratio (since feldspar weathers easily), and fluidity via the sand detritus to interstitial detrital matrix ratio. Shortfalls of this classification scheme are that the feldspar to quartz ratio is less valid for volcaniclastic sediments (Pettijohn 1954), and the term greywacke is outdated due to misuse. Folk's (1974) classification is a ternary QFR diagram, making for easy correlation with point counting data. Provenance is considered through the feldspar to rock fragment ratio, however Folk (1974) provides further classification into daughter diagrams to ensure more accurate provenance association.

### 4.1.2  *Provenance Discrimination*

Plate tectonics is ultimately the major control on sedimentation types in various depositional basins as it determines the dispersal patterns between source (provenance) and sink (basin type) (Dickinson & Suczek 1979). For example, volcaniclastic lithic sands derived from magmatic arcs are present in trenches, forearc basins and marginal seas (Dickinson & Suczek 1979). Detrital framework mode analysis can provide the basis for provenance studies through known mineralogical signatures of specific source regions. The major constituents studied are quartz, feldspars and lithic fragments as these provide a relatively reliable provenance signature. Provenance analysis concentrates on detrital grains, rather than matrix or cement, since the latter mostly result from the processes of diagenesis (Dickinson & Suczek 1979).

Detrital quartz grains inform the worker on various aspects of provenance, for instance sandstones enriched in quartz indicate a continental signature, whilst those sandstones that are quartz-poor imply derivation from a magmatic arc (Dickinson & Suczek 1979). Extremely sparse quartz would indicate intra-oceanic or remnant arc sandstone suites, while continental margin arc suites show a more quartzo-feldspathic signature (Marsaglia

& Ingersoll 1992). The type and amount of feldspars provides clues of provenance; for example potassium feldspar indicates derivation from mature plutonic or metamorphic sources while plagioclase feldspars are indicative of a juvenile, usually volcanic source (Boggs 2011).

One of the most commonly used provenance discrimination diagrams come from Dickinson and Suczek (1979) and Dickinson *et al.* (1983) who created simple diagrams to distinguish the key provenance types: continental block, magmatic arc and recycled orogen. Provenance types were classified through a study of major known sedimentary basins across the globe. A key criticism of their work is that they used both modern and ancient sandstone suites resulting in known and inferred tectonic association respectively (Marsaglia & Ingersoll 1992). In these diagrams undissected arcs refer to those arcs that are immature in nature with a high concentration of feldspars in comparison to lithic fragments, whilst dissected arcs are considered to be more mature and eroded, thus provide a mixed detritus of unroofed plutonic and volcanic source (Dickinson & Suczek 1979).

### 4.2 Methodology

Samples were collected regularly, across strike, in the field on two separate occasions. The preparation of thirty-two standard thin sections was undertaken at the University of Wollongong by laboratory technician, José Abrantes. Petrographic analysis was undertaken using 'Leica DM 2500 P' polarising microscope with images of each sample taken by attached camera, 'Leica DFC 400'.

All thirty-two thin sections were described, with a full sample database in Chapter 8 - Appendix 1. Only thirteen samples from the Murrawong Creek Formation location were analysed using the Gazzi-Dickinson point counting method per Dickinson and Suczek (1979). The low sample number is due to the specific criteria required for point counting:

1. The sample must be sedimentary in nature
2. The sample must be of SAND grain size
3. The sample must not have >25% matrix

Thus, the majority of samples were excluded from this study. A 'Priory, Swift MODEL F' electronic point counter was used; with an attached slide advance mechanism. The major identifiable grains within the sand suite were assigned a 'channel' on the electronic

counter, which recorded the number of counts per channel. Each sample had a total of 500 counts, which were normalised and plotted onto sandstone classification (QFR) and provenance association diagrams (QFL, QmFLt) using the excel software 'TRI-PLOT' and modified using 'Inkscape'.

This method presents sources of error and so must be conducted in conjunction with further provenance studies, such as detrital zircon U-Pb geochronology and whole rock geochemical analysis in Chapter 3 and Chapter 5 respectively. A key issue in petrographic analysis is bias of the worker, and in this case inexperience of the worker, in identifying minerals based on subjective criteria such as colour and relief. This was addressed to the greatest ability through using a variety of reference literature for mineral identification. Thirteen samples is less than the desired amount of data for point counting. Hence, the samples were taken across strike, representing the majority of sediments within the Murrawong Creek Formation. This is in combination with counting each slide to the maximum required count, 500, to ensure the majority of sediment types were covered.

### 4.2.1 Sample Descriptions

The Murrawong Creek Formation consists of a variety of volcaniclastic sedimentary rocks from chert through to boulder conglomerates. The samples are grouped based on field observations as those that are lithologically related and are listed in stratigraphic order. Descriptions move through the three identified units of the Murrawong Creek Formation into the Pipeclay Creek Formation and then to those sequences mapped around Chaffey Dam. Most samples show evidence of alteration, having typical characteristics of prehnite-pumpellyite facies metamorphism. Secondary mineral phases are abundant in the form of chlorite and epidote replacement, sericite alteration, albite after plagioclase, calcite veins and small opaque minerals. The observations reported here are in accord with earlier petrographic analysis by Cawood (1980, 1983); Leitch and Cawood (1987).

N.B., cpx = clinopyroxene, Qz = quartz, Pl = plagioclase, flsp = unidentified feldspar, VF = volcanic fragment, Amb = unidentified amphibole, Ch = chlorite, Ct = chert, Ep = epidote, Olv = olivine, Bi = biotite, He = hematite, Ca = carbonate and Gy = gypsum.
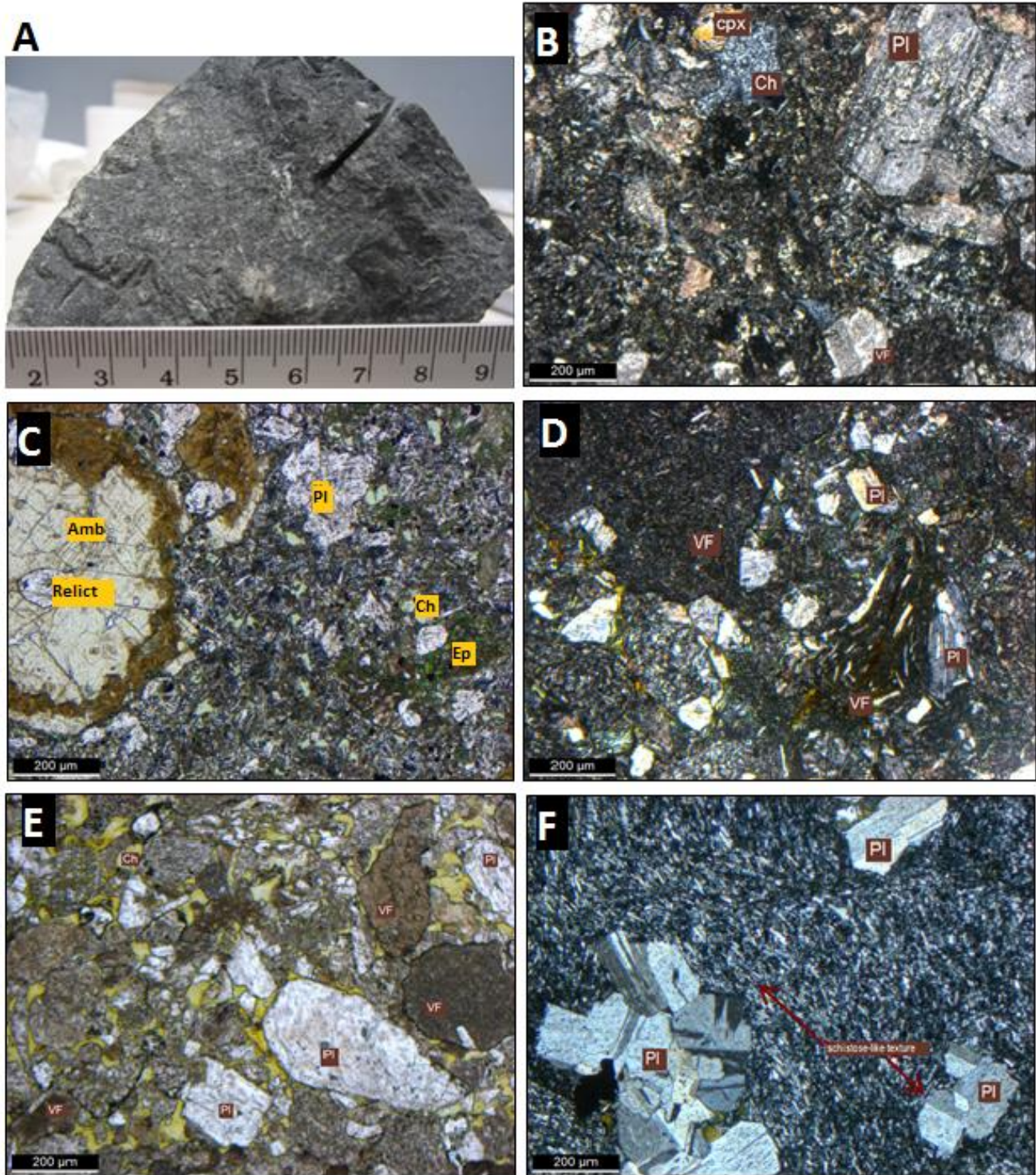
*Figure 4.1* - **MURRAWONG CREEK FORMATION**, Unit 1: volcaniclastic unit of feldspathic coarse sandstone to boulder conglomerate. This unit shows major cementation via chloritic infill and replacement of feldspars by clinopyroxene and epidote coating. Minor to no quartz was observed throughout the section with major constituents including plagioclase, clinopyroxene, volcanic fragments and amphiboles. **(A)** CR16, fine-grained sandstone hand specimen; **(B)** CR12 - XPL, Feldspathic litharenite with feldspars undergoing sericite alteration; **(C)** CR14 - PPL, Arkosic conglomerate; **(D)** CR15 – XPL, Feldspathic litharenite showing extreme chlorite alteration; **(E)** CR15 – PPL, Feldspathic litharenite; **(F)** CR21 – XPL, Volcanic clast from arkosic conglomerate showing glomeroporphyritic clusters of plagioclase.
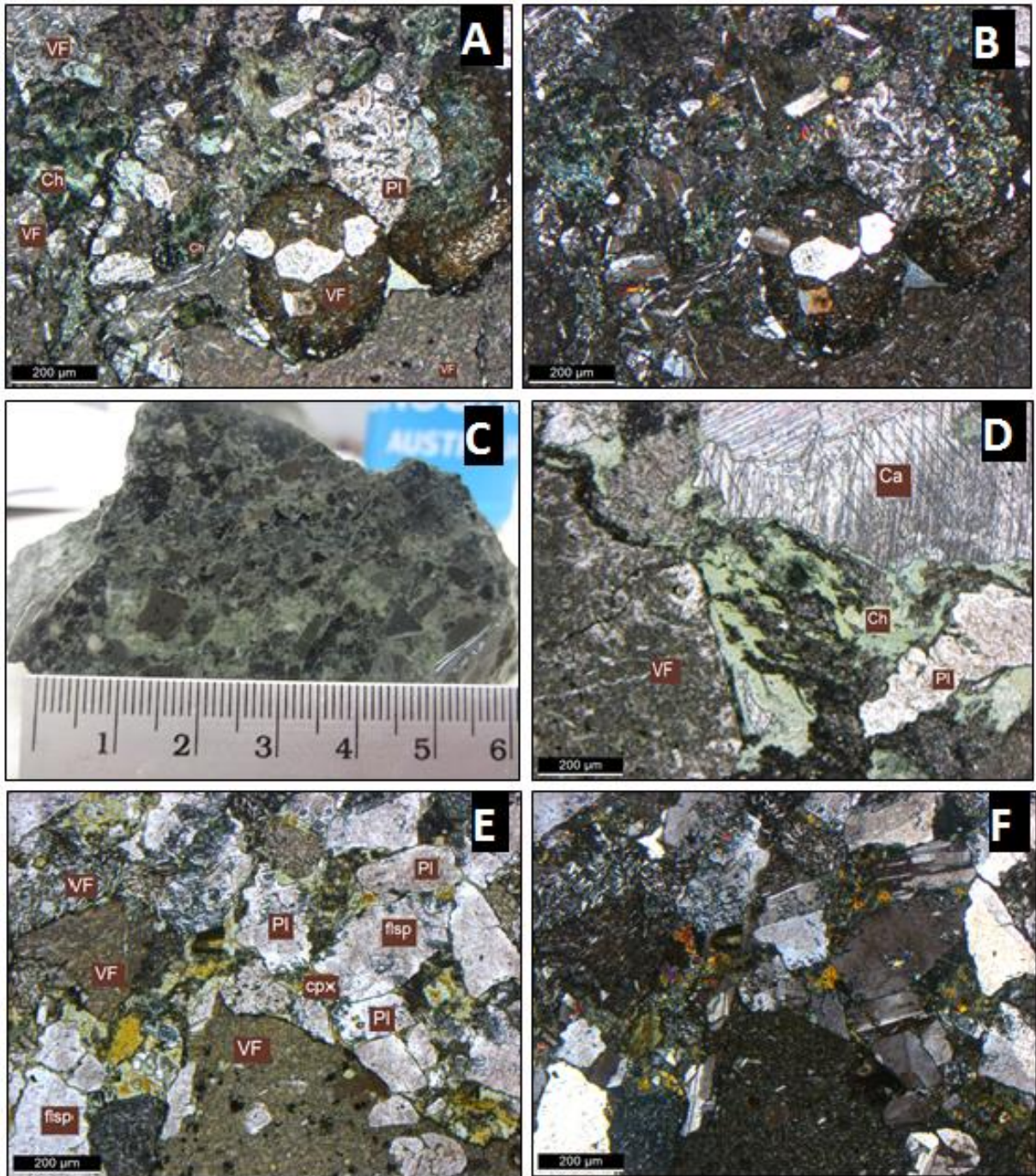
*Figure 4.2* - **MURRAWONG CREEK FORMATION**, Unit 2: This unit is separated from Unit 1 by a chert lens, which was not sampled in the field. A noticeable increase in grain size is evident in this unit, coupled with the move from feldspathic-dominated sediments to lithic-dominated sediments. A lithological variety of grains exist in this unit, as volcanic fragments, clinopyroxene and feldspars comprise the majority of constituents. **(A)** CR17 - PPL, Lithic arkose conglomerate, large rounded clasts of volcanic fragments and plagioclase with infill of pores by chlorite during alteration processes; **(B)** CR17 - XPL; **(C)** CR18, hand specimen with green chlorite cement visible along with large angular clasts; **(D)** CR18 - PPL, Litharenite conglomerate, with chloritic cement and oxide leaching throughout. Carbonates and chalcedony are also products of alteration; **(E)** CR23 - PPL, Lithic arkose conglomerate with relatively intact plagioclase, minor epidote; **(F)** CR23 – XPL.
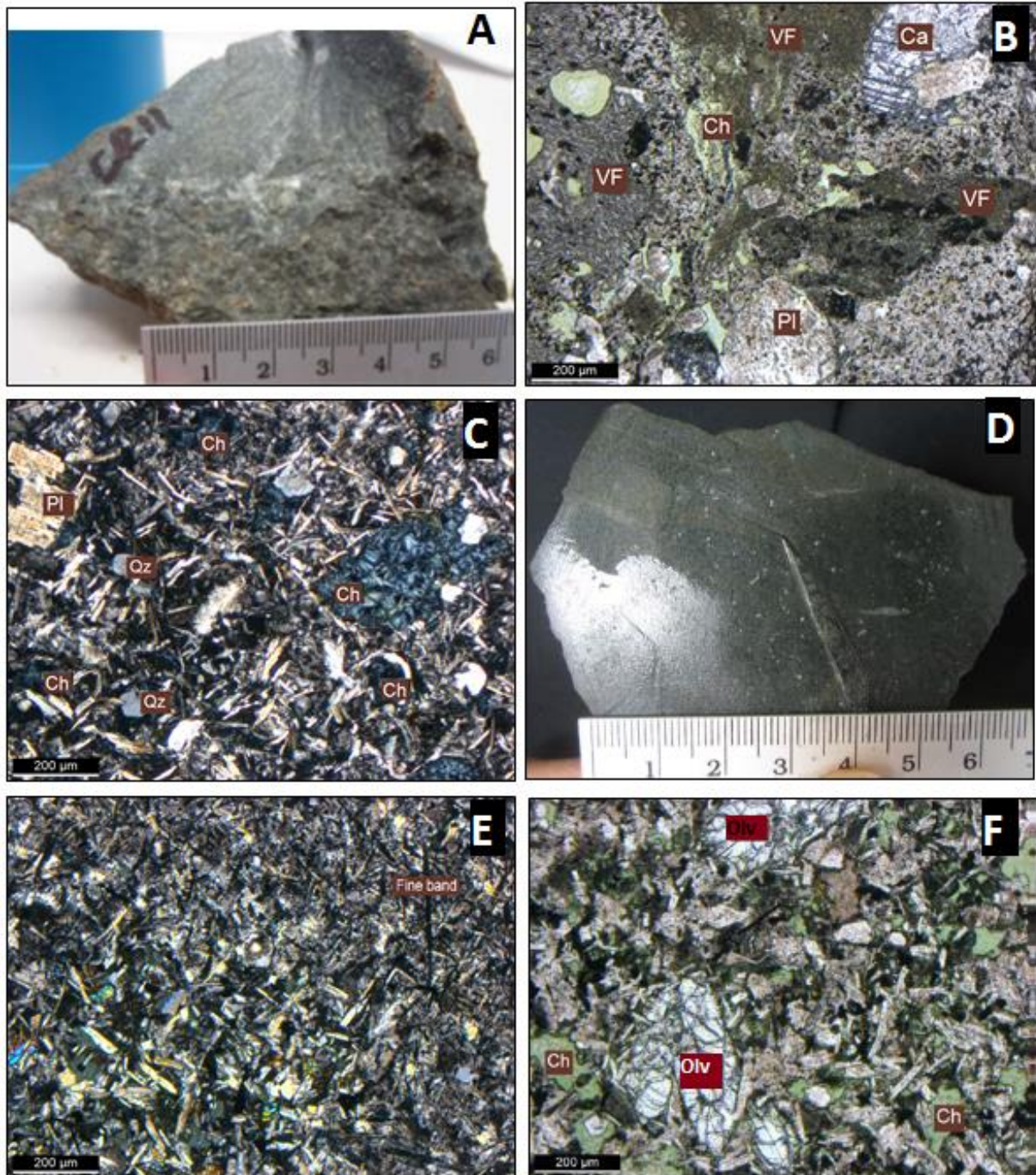
*Figure 4.3* - **MURRAWONG CREEK FORMATION**, Unit 3: Possible move into Pipeclay Creek Formation. Grouped together in the field as fine lithic sand, however with closer petrographic analysis it appears that the fine-grained component of CR11 and CR24 consists of volcanic rock, interpreted to be basaltic andesite. **(A)** CR11, Hand specimen showing boundary of volcaniclastic sandstone and fine-grained volcanic rock; **(B)** CR11 - PPL, Feldspathic litharenite, with large clasts of plagioclase, volcanic fragments and carbonates; **(C)** CR11 - XPL, Basaltic andesite, plagioclase and minor volcanic quartz phenocrysts in a mostly plagioclase groundmass; **(D)** CR24, hand specimen, fine grained volcanic rock with feldspar phenocrysts visible as white specks; **(E)** CR24 - XPL, Basaltic andesite, fine plagioclase groundmass with chlorite infill; **(F)** CR24 – PPL, large olivine phenocrysts and abundant chlorite infill resulting from hydrothermal alteration.
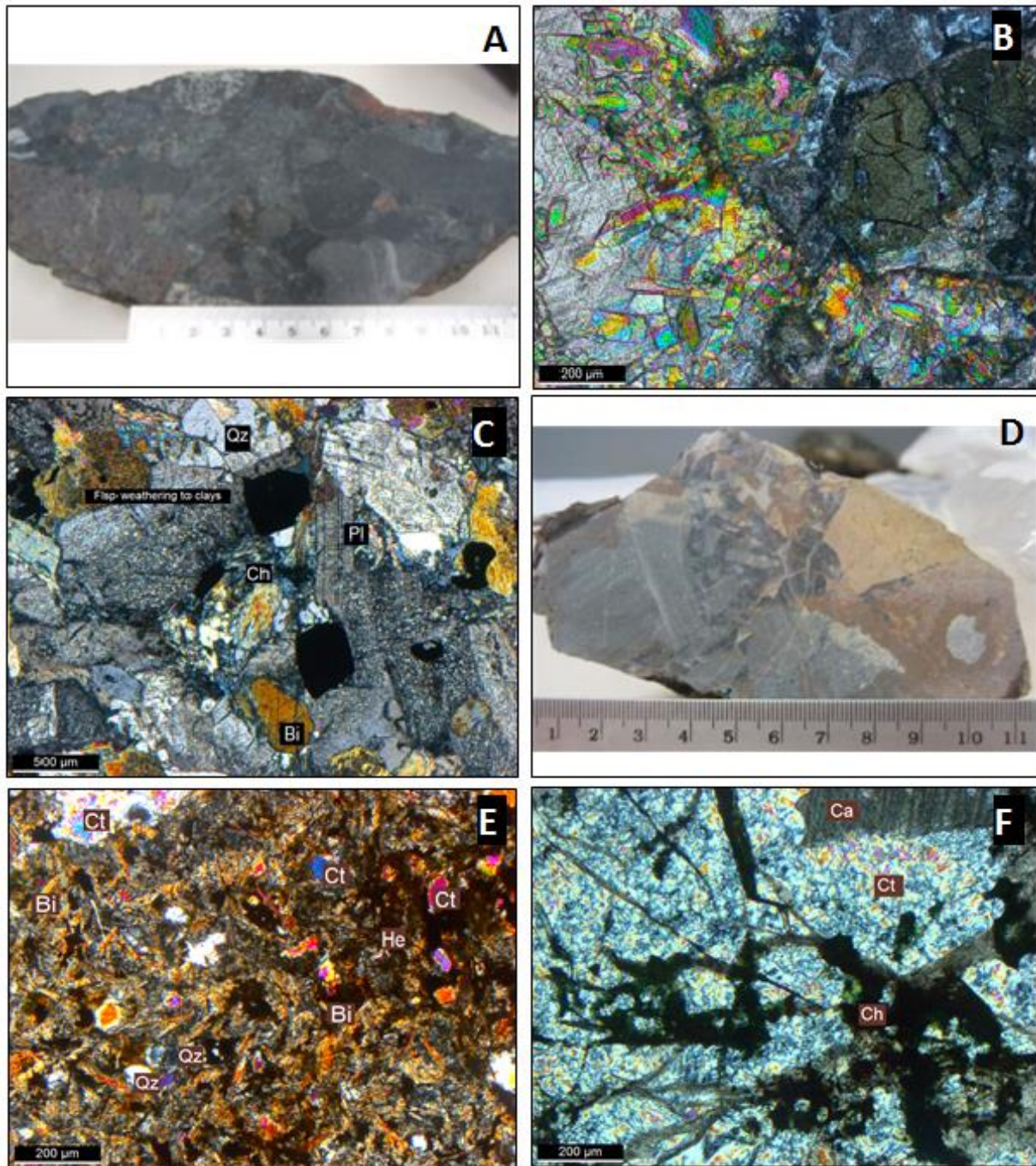
*Figure 4.4* - **PIPECLAY CREEK FORMATION**: Massive conglomerate lens with a wide variety of large clasts. PCF5 has both plutonic and extrusive volcanic clasts, ranging from boninitic through to monzonites with shoshonitic affinities; with a large array of lithologies. **(A)** PCF5, Hand specimen showing the assortment of clasts; **(B)** PCF5.1a - XPL, Boninitic clast with large orthopyroxene clast surrounded by epidote and carbonates **(C)** PCF5.7c – XPL, plutonic clast undergoing sericite alteration dominated by feldspars, micas and amphibole; CD1.6 has only volcanic clasts, interpreted to be andesitic in origin bound by a chalcedonic matrix. **(D)** CD1.6, Hand specimen with alteration rinds around the clasts supporting sulfide mineralisation; **(E)** CD1.6 – XPL, altered volcanic clast with Fe leaching; **(F)** CD1.6 – XPL, chalcedony matrix produced from hydrothermal alteration with needle-like hematite and carbonate.
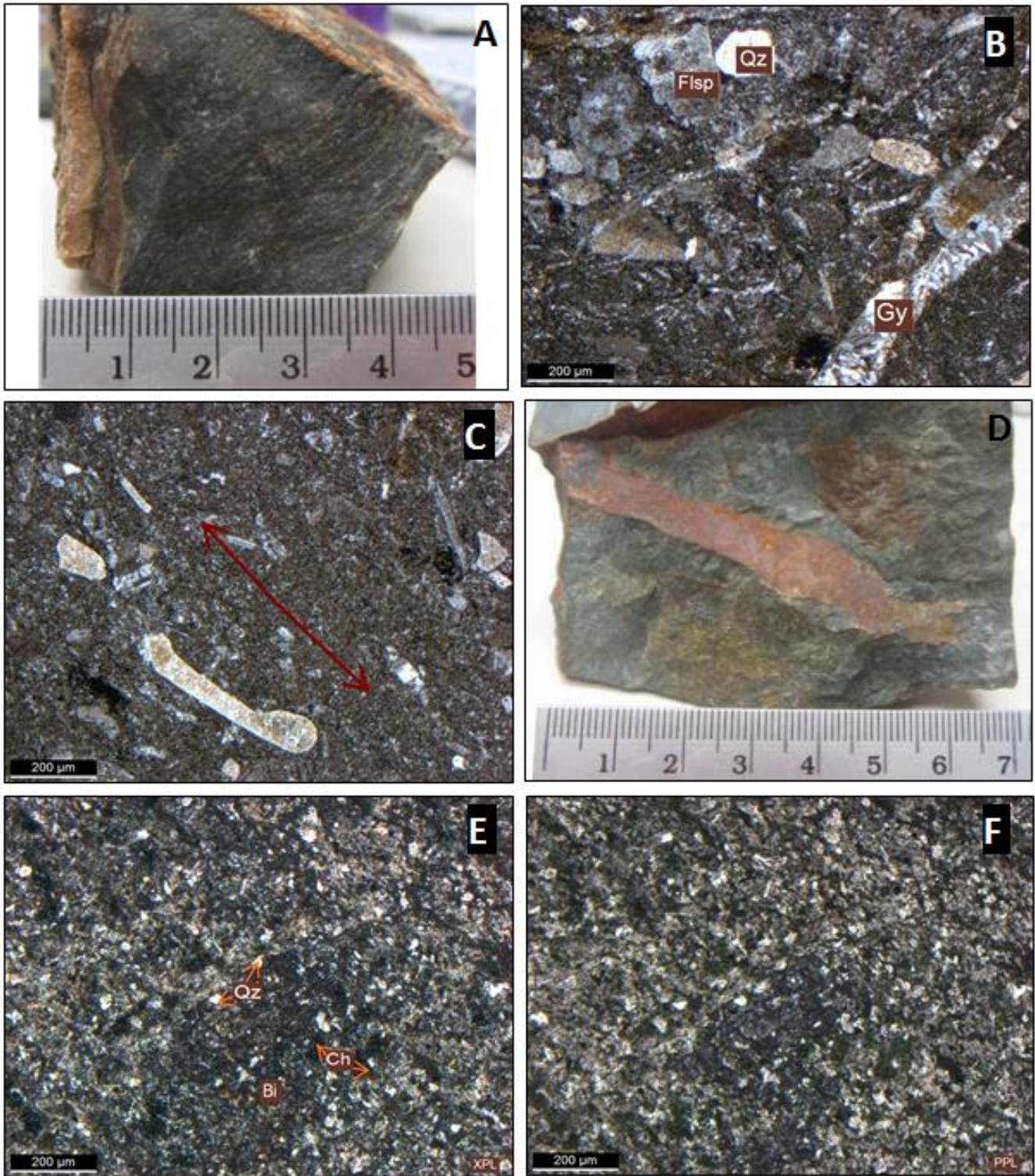
*Figure 4.5* - Extremely fine-grained volcaniclastic unit that is almost too fine for classification with the petrographic microscope, interpreted to be tuffs metamorphosed at low grade. **(A)** CD1.3 – **BOG HOLE FORMATION**, Hand specimen; **(B)** CD1.3 - XPL, Feldspathic metamorphosed tuff undergone epithermal alteration and secondary silicate veining of gypsum; **(C)** CD1.3 – XPL, slight foliation visible; **(D)** CD3.4 – **WISEMANS ARM FORMATION**, Hand specimen; **(E)** CD3.4 - XPL, Volcaniclastic tuff, extremely fine-grained, comprised of mostly mafic minerals including feldspar; **(F)** CD3.4 - PPL
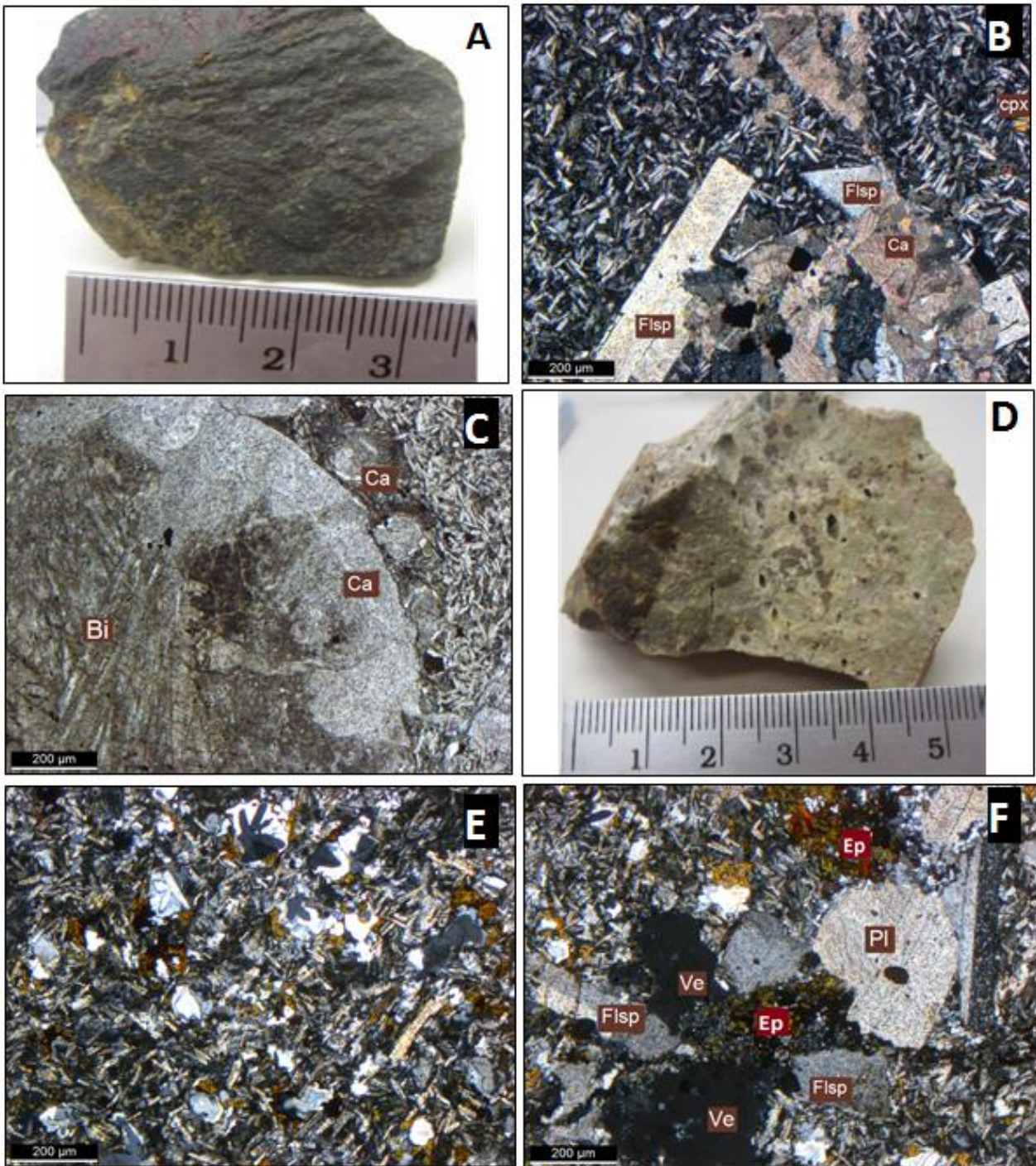
53

*Figure 4.6* - **KERATOPHYRE**, altered volcanic rocks sampled from a lens in the Chaffey Dam area. Major constituents include feldspars and micas with secondary alteration processes including recrystallization of feldspars and chlorite alteration. **(A)** CD1.8, Hand specimen, fine-grained metamorphosed andesite; **(B)** CD1.8 – XPL, epidote and chlorite alteration present, with well-formed tabular feldspar comprising the main constituent; **(C)** CD1.8 - PPL, Spherical phenocryst of calcite and biotite; **(D)** CD2.3, Hand specimen of extremely weathered keratophyre; **(E)** CD2.3 – XPL, trachytic textured altered basaltic-andesitic rock consisting of mostly feldspars and low temperature minerals such as micas; **(F)** CD2.3 – XPL, Epidote and chlorite alteration common as vesicle (Ve) infill, large plagioclase feldspar grains visible.

## 4.3 Results

### 4.3.1 Sandstone Classification

The thirteen samples classed as suitable for point counting were also used for sandstone classification based on Pettijohn (1954) and Folk (1974). The Pettijohn classification resulted in a dominance of feldspathic greywackes, with a few arkose, lithic greywacke and subgreywacke (Table 4.1; Figure 4.7). However, this classification scheme was chosen as less desirable due to the ambiguous use of the term greywacke. Folk's classification resulted in a variety of all the quartz-poor sandstones from arkose to litharenite (Table 4.1; Figure 4.7).

*Table 4.1 - Point Counting results, including percentages of each of the major constituents and sandstone classification*

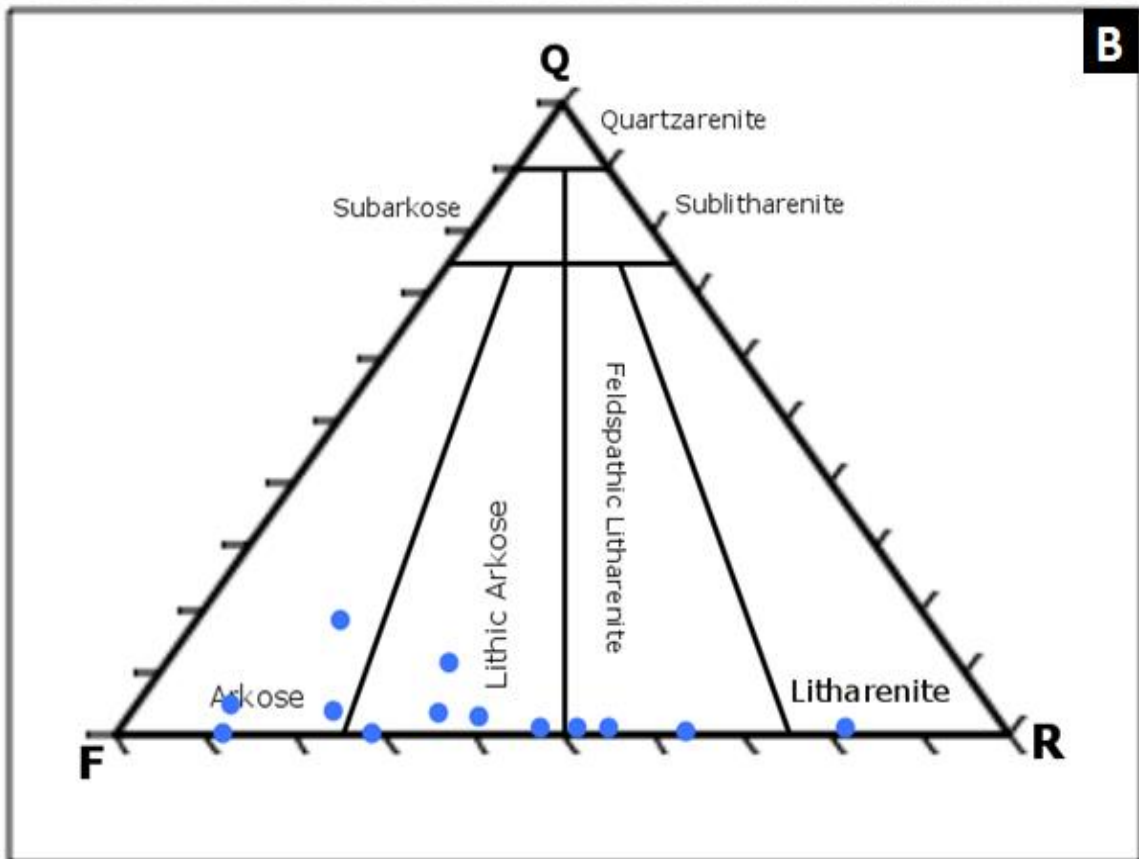| Sample No. | %Q | %Qm | %F | %L | %Lt | QFL total counts | Classification (Pettijohn) | Classification (Folk) |
|---|---|---|---|---|---|---|---|---|
| **CR05** | 20 | 4 | 62 | 18 | 34 | 321 | Feldspathic Greywacke | Lithic Arkose |
| **CR07** | 21 | 19 | 66 | 13 | 15 | 137 | Feldspathic Greywacke | Arkose |
| **CR10** | 10 | 5 | 85 | 5 | 10 | 182 | Feldspathic Greywacke | Arkose |
| **CR11** | 0 | 0 | 36 | 64 | 64 | 247 | Lithic Greywacke | Feldspathic Litharenite |
| **CR12** | 0 | 0 | 49 | 51 | 51 | 280 | Lithic Greywacke | Feldspathic Litharenite |
| **CR14** | 1 | 0 | 88 | 11 | 12 | 199 | Feldspathic Greywacke | Arkose |
| **CR15** | 1 | 0.5 | 44.5 | 54 | 55 | 319 | Subgreywacke | Feldspathic Litharenite |
| **CR17** | 4 | 1 | 52 | 44 | 47 | 251 | Arkose | Lithic Arkose |
| **CR18** | 0 | 0 | 19 | 81 | 81 | 248 | Subgreywacke | Litharenite |
| **CR19** | 11 | 11 | 57 | 32 | 32 | 269 | Arkose | Lithic Arkose |
| **CR21** | 17 | 4 | 74 | 9 | 22 | 167 | Feldspathic Greywacke | Arkose |
| **CR23** | 2 | 0 | 71.5 | 26.5 | 28.5 | 309 | Arkose | Lithic Arkose |
| **CR25** | 9 | 3 | 58 | 33 | 39 | 236 | Feldspathic Greywacke | Lithic Arkose |

*Figure 4.7 – A) Classification of sandstones from Pettijohn (1954); B) Classification of sandstones from Folk (1974). Plots represent point-counted samples.*

*4.3.2   Provenance Discrimination*

Dickinson diagrams provide the basic tool for an initial determination of provenance for sediments. Figure 4.8 plots each sample based on the normalised point counted data from Table 4.1. When observing the QFL diagram the majority of samples plot across the magmatic arc sector with most samples falling within the undissected and transitional arc environment. The QmFLt diagram supports this, where all but four samples plot within the undissected and mostly transitional arc sector. Those few samples plotted within the basement uplift sector are disregarded in this study as a result of human error and/or simplicity of the provenance determination method.
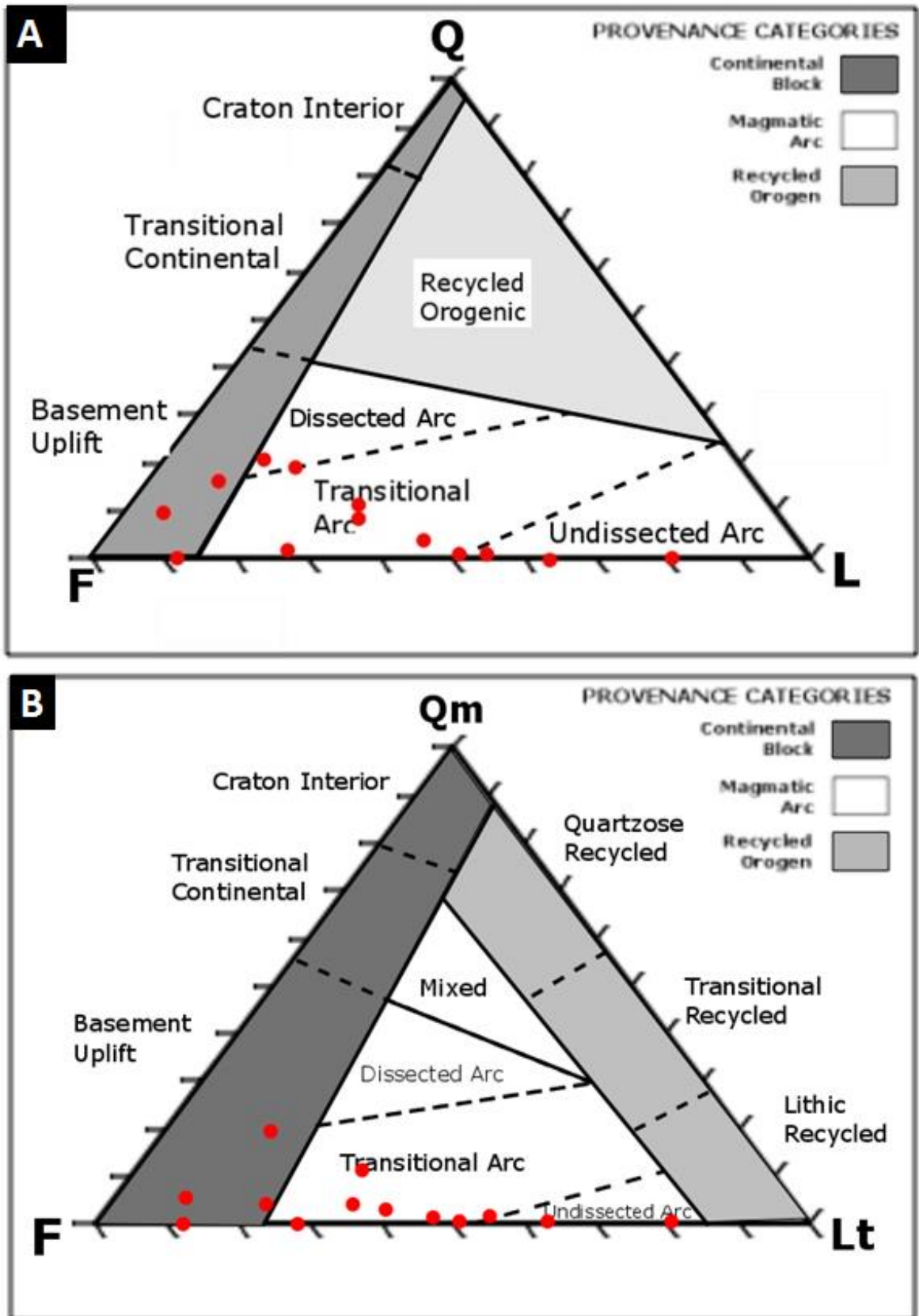
*Figure 4.8 - Provenance discrimination diagrams from Dickinson et al. (1983). A) QFL; B) QmFLt. Plots represent point-counted samples.*

## 4.4 Interpretation

It is the combination of sandstone classification and provenance discrimination diagrams with detailed petrographic analysis that supports a more comprehensive interpretation of provenance. It is evident from the Dickinson diagrams that the Murrawong Creek Formation sedimentary rocks are sourced from a juvenile magmatic arc. The interpretation of a primitive arc is promoted by the lack of data falling within the dissected arc sector. This is confirmed via petrographic analysis whereby the low quartz content in all samples indicates the mineralogical immaturity of the sand (Pettijohn 1954). The presence of large, often tabular feldspars coupled with other unstable ferromagnesian minerals such as clinopyroxene and rare hornblende, biotite and olivine indicate the immature nature of the sediment.

The prevalence of mafic volcanic fragments lends itself to the interpretation of a magmatic arc source with the trend away from the Q pole on the QFL diagram suggesting that the arc is associated with oceanic crust (Dickinson & Suczek 1979). The occurrence of carbonate minerals within the Murrawong Creek sequence suggests the sediments were deposited in either:

1) A submarine basin flanking the volcanic island arc, as small reefs associated with the arc are eroded with the mass flow style of deposition and incorporated into the sediments; or
2) Allochthonous masses, possibly associated with ocean island seamounts, transported to the trench by subduction and accreted onto the overriding plate.

Petrographic descriptions undertaken in this chapter have allowed for a more precise correlation of samples, allowing the confirmation of groups mapped in the field (Figure 2.5). The samples collected from the basal unit (Unit 1) of the Murrawong Creek Formation are feldspathic in nature, thus promoting the interpretation that these sediments are sourced from a proximal volcanic source. Those sediments grouped as Unit 2 of the Murrawong Creek Formation have an increased proportion of volcanic lithic fragments, suggesting that the volcanic source is undergoing a period of erosion, whereby volcanic fragments residing on the volcanic edifice are deposited via mass flow deposits. Unit 3 is an interbedded volcanic sequence, further supporting the proximal affinity to an immature arc setting whereby volcanic rocks are directly deposited in an adjacent sedimentary basin.

The Pipeclay Creek Formation samples that have undergone petrographic analysis are not representative of the whole sequence, but rather a single conglomerate lens. The lithological variety of clasts suggests the arc has undergone a period of erosion, possibly exposing the batholithic core of the volcanic system. The mixture of extrusive and intrusive volcanic rock clasts within this conglomerate lens, coupled with the Dickinson diagram trend of the Murrawong Creek Formation samples into the transitional and dissected arc sectors, suggests an erosional plutonic unroofing with increasing arc maturity. An increase in chert incorporated into the sediments suggests that deep marine sequences are being uplifted and eroded into the depositional basin, possibly from a nearby accretionary complex in a tectonically active environment.

It is evident that the Murrawong Creek and Pipeclay Creek formations have undergone low-grade metamorphism, likely due to hydrothermal alteration. This is indicated via the presence of epidote coatings, chlorite infill and sericite alteration. These minerals highlight the convergent setting where compressional forces have resulted in epithermal (low temperature) alteration styles. This hydrothermal alteration indicates that seawater formed hydrothermal fluids, suggesting an oceanic arc affinity. The presence of glauconite (CR19) supports the interpretation of sediment deposition flanking an intra-oceanic volcanic arc, as it indicates marine diagenesis in relatively shallow waters (Deer *et al.* 1996).

Keratophyres and basalt flows are interbedded with the sedimentary rocks and as a result are good indicators of tectonic setting. The presence of plagioclase feldspars in good condition indicates the juvenile nature of the arc system, supported by unstable ferromagnesian minerals of biotite and clinopyroxene.

When considering the Dickinson diagrams alone, it is evident that there is a small continental influence in some of the samples. However, when considered in conjunction with detrital zircon analysis (Chapter 3) and geochemical analysis (Chapter 5) it becomes apparent that this is not the case. These results are in accord with petrographic analysis undertaken by (Cawood 1980, 1983; Leitch & Cawood 1987). Cawood (1983) described an association with an undissected magmatic arc of Dickinson and Suczek (1979), noting minor quartz and the move from feldspar to lithic dominated rocks within the Murrawong Creek Formation.

# Chapter 5. Geochemistry

## 5.1 Introduction

### 5.1.1 Background

Whole-rock geochemistry provides a well-established method of determining the composition and tectonic setting of formation of igneous and sedimentary rocks of unknown origin (Rollinson 1993). A wide variety of methods have been developed over the past forty years, which use both major and trace element abundances to determine a likely source for volcanic, plutonic and sedimentary rocks (e.g., Pearce & Cann 1973; Miyashiro 1974; Pearce 1982; Bhatia 1983; Pearce *et al.* 1984). Only a decade after the widespread acceptance of plate tectonics, it became evident that specific tectonic settings often display a distinct geochemical signature reflecting the different mechanisms responsible for partial melting as well as the effects of magmatic fractionation and/or contamination.

X-ray fluorescence (XRF) is the most widely used geochemical analytical method for major and some trace elements due to its non-destructive nature, broad range of elemental analysis rates and speed (Rollinson 1993). The method involves a primary X-ray beam aimed at the sample. This excites electrons so that they emit secondary X-rays with wavelengths characteristic to the elements present in the sample. The intensity of these secondary X-rays are measured to deconvolve the elemental abundances (Rollinson 1993). The method detects major and trace elements of geological interest as low as a few parts per million (ppm). A drawback is that the method cannot detect elements lighter than Na (Rollinson 1993). Furthermore, in hand-held rather than laboratory-based instruments, the lower energy of the primary X-ray beam means that Na cannot be measured and Mg is marginal (has large analytical errors).

Major elements are measured as oxides using both hand-held (HH-XRF) and laboratory-based or whole-rock (WR-XRF) and consist of Si, Ti, Al, Fe, Mn, Mg, Ca, Na, K and P. The samples analysed have undergone a period of burial metamorphism, and thus have been subjected to secondary alteration processes. Trace elements are those elements that are present in a rock with less than 0.1 wt % or 1000 ppm. They provide important provenance information (Rollinson 1993) because many are relatively immobile and

resistant to alteration processes e.g., $Al_2O_3$, $TiO_2$, FeO*, V and heavy rare earth elements (HREEs).

### 5.1.2 Island Arc Geochemistry

Island arc settings tend to display geochemical results of increased complexity due to the extremely varied geological processes occurring at these sites (Winter 2010). In subduction zones, mantle melting occurs through the addition of hydrous fluids to the mantle wedge, released as a result of the dehydration of the subducting oceanic crust and its associated sediments (Figure 5.1) (e.g., Wilson 1989; Defant *et al.* 1991; Pearce & Parkinson 1993). Pelagic sediments may be subducted since they accumulate on oceanic crust in oceanic basins, which have higher densities than the conserved plate and thus are 'attached' to the down-going slab and potentially contribute to melt genesis.

Upon melting of the mantle, the elements from both the aqueous phase due to subduction dehydration and the partially melted mantle wedge peridotites mix. Trace elements demonstrate a preference towards either the melt phase (known as incompatible elements) or towards the solid phase (compatible elements) (Rollinson 1993). Those elements that are of small ionic radius, but highly charged are known as high field strength (HFS) cations, while large cations of small charge are referred to as large ion lithophile elements (LILE) (Rollinson 1993). These element groups behave differently with respect to magma composition and thus geochemical analysis of trace elements provides a robust method for inferring the tectonic setting of igneous rocks through the use of well-recognised discrimination diagrams (Rollinson 1993).

The magmas produced in these settings can be subdivided into low-K tholeiitic, medium-K calc-alkaline and high-K mixed magma series (Winter 2010). These are characterised by their enrichment in LILE relative to HFS elements, indicating there is a detectable slab contribution to the source of arc volcanism (Pearce & Peate 1995; Winter 2010). Tholeiitic magma series are derived from magma chambers at shallow depths, so with increasing depth a shift into calc-alkaline magmas occurs (Albarède 2003). The principle source of island arc magmas appears to be dominated by fluid-fluxed depleted mantle, however enrichment may occur through the incorporation of enriched lithosphere or arc-rifting processes (Pearce & Peate 1995; Winter 2010).
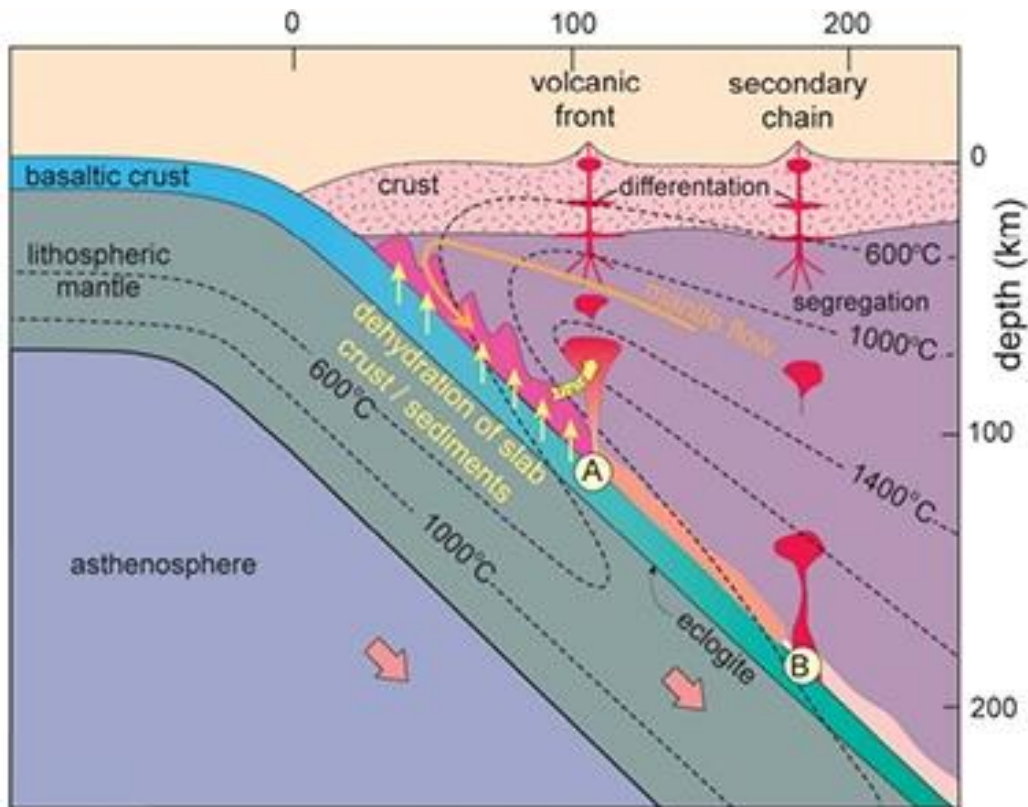
*Figure 5.1 - Schematic diagram of proposed model for subduction zone magmatism, from Tatsumi (1989).*

### 5.1.3    Sedimentary Rock Geochemistry

Similar to and correlated to the modal composition of sedimentary rocks, the geochemical composition of sandstones is controlled by the tectonic regime under which it was deposited (e.g., Pettijohn *et al.* 1974; Bhatia 1983). These processes of sedimentation are covered in Section 1.3.6. Major elements are the key parameters used in sedimentary geochemistry, with sediments showing a progressive decrease in $Fe_2O_3$ + MgO, $TiO_2$, $Al_2O_3/SiO_2$ and an increase in $K_2O/Na_2O$ and $Al_2O_3/(CaO + Na_2O)$ from oceanic island arc through to passive margins (Bhatia 1983).

This chapter aims to complement petrographic analysis and detrital zircon geochronology in source and provenance determination for the Murrawong Creek and Pipeclay Creek formations. Igneous and sedimentary rocks are first classified in terms of lithological nomenclature, and then their tectonic setting is discriminated based on their chemical composition and elemental abundances.

## 5.2 Methodology

Murrawong Creek and Pipeclay Creek formations conglomerates with considerable sized clasts were mapped (Figure 5.2) and analysed using the HH-XRF gun. This was done by holding the HH-XRF on volcanic and plutonic clasts for 120 seconds each, with most samples being analysed a minimum of two times, in order to check for variability. This is necessary because some of the clasts are coarse-grained (few millimetres) relative to the analytical window with a diameter of 6 mm. The multiple analyses obtained from the HH-XRF were averaged and calibrated to a known standard, the Bumbo Latite Member (Figure 5.3). A limitation in the use of HH-XRF is its inability to measure light element oxides, including $Na_2O$, or some trace elements, which are often required for the interpretation of data using discrimination diagrams.
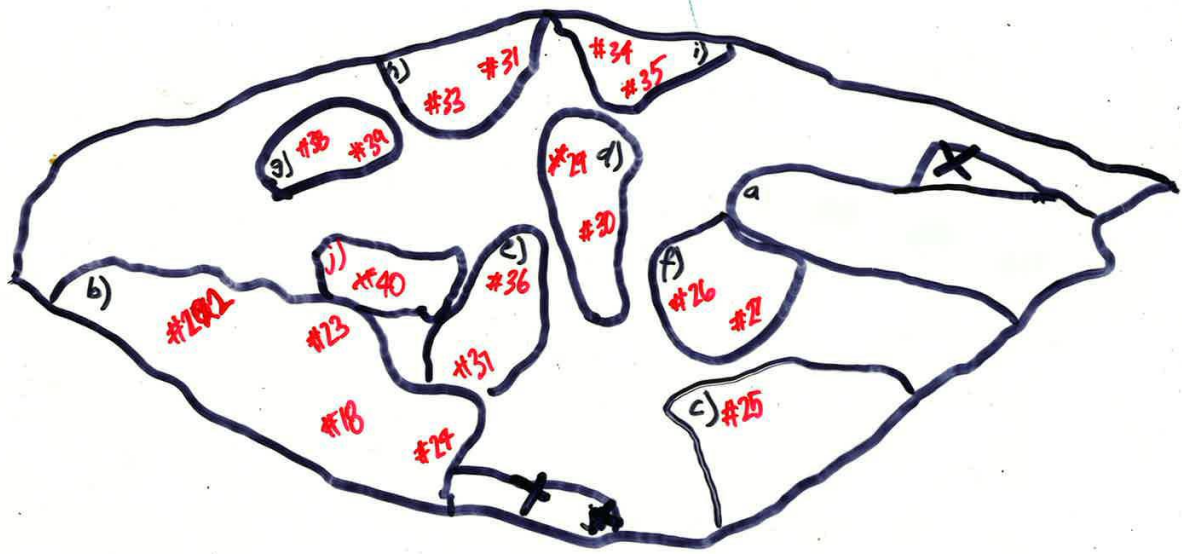
*Figure 5.2 - Map of clasts (upper image) analysed by HH-XRF for sample PCF5 (lower image), with letters representing the number of the clast, whilst numbers represent the HH-XRF analytical value.*
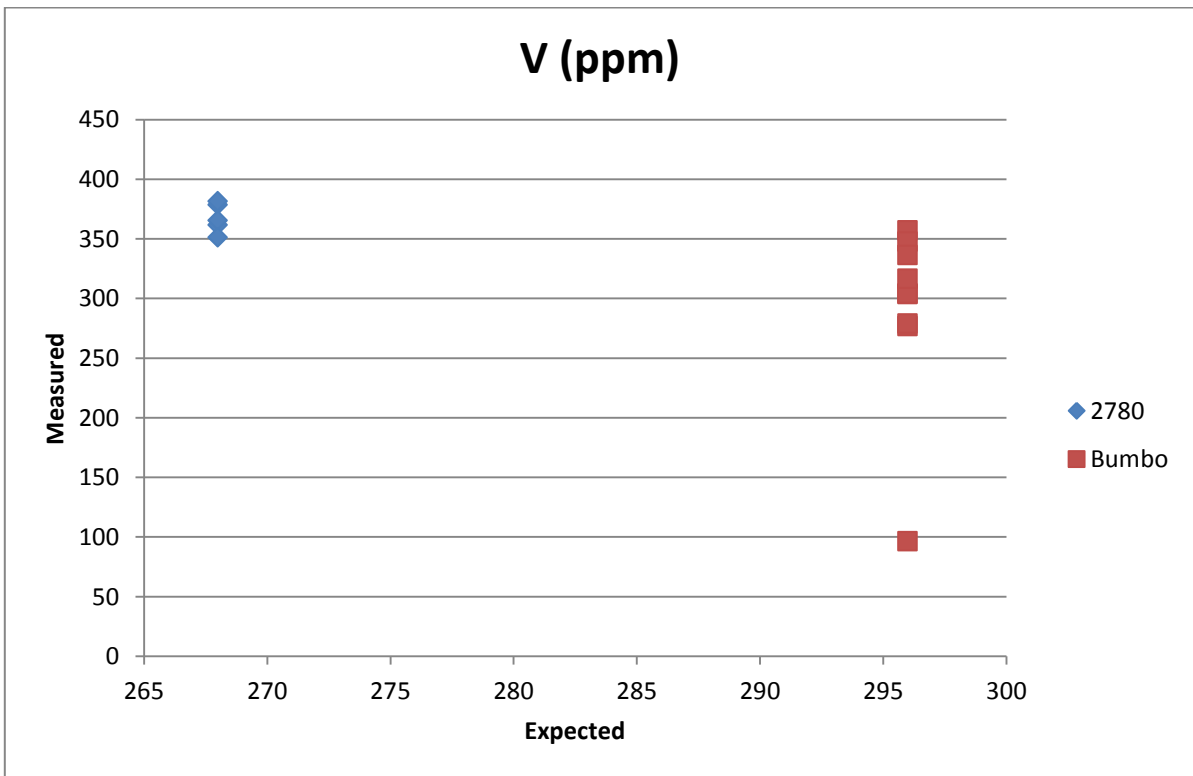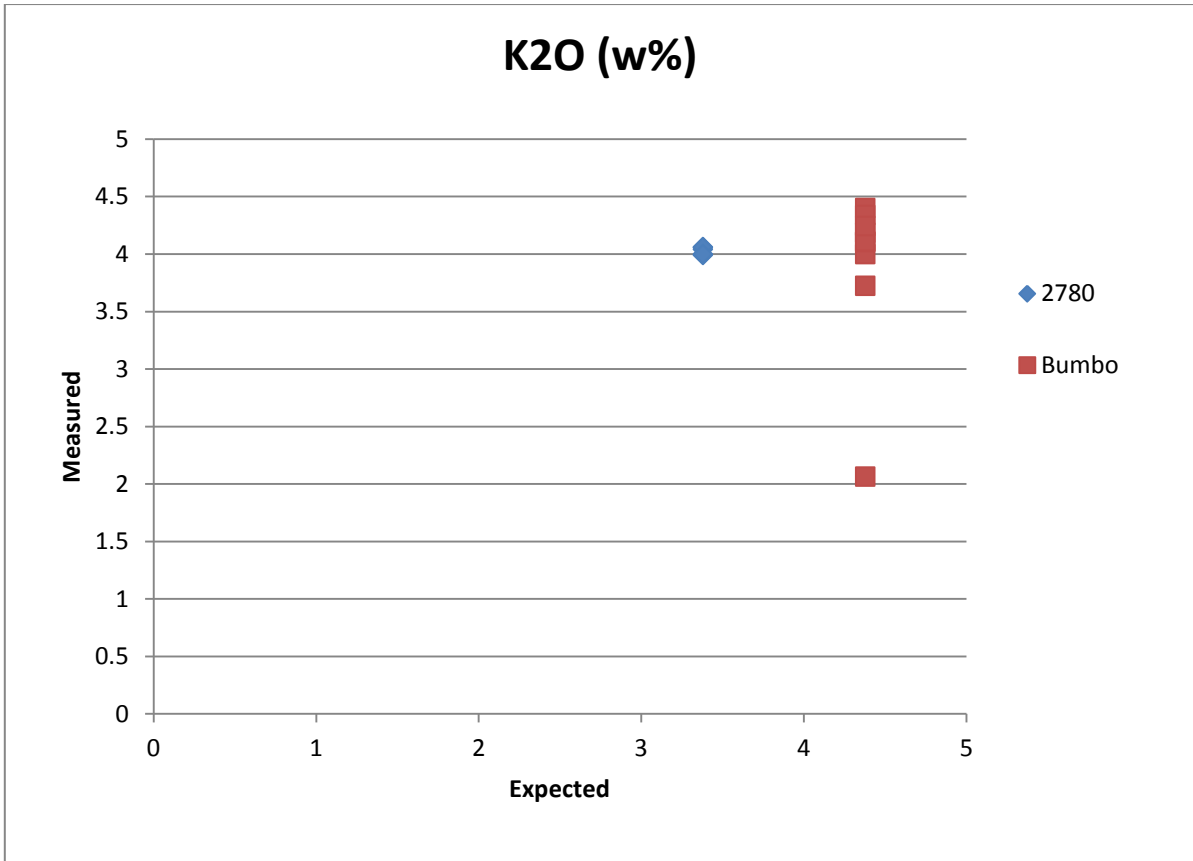
*Figure 5.3 - Graphs of XRF measurements against expected standard values. A consistent outlier led to the removal of this measurement from the data set.*

Whole-rock XRF (WR-XRF) was undertaken on a random selection of these clasts for comparison between the HH-XRF and WR-XRF results. Also analysed were sedimentary rocks from the Murrawong Creek Formation, volcanic rocks identified as keratophyres and a sedimentary sample later determined to be from the Wisemans Arm Formation. WR-XRF analysed major and trace elements using a SPECTRO XEPOS energy dispersive polarization X-ray fluorescence spectrometer at the University of Wollongong. Pressed pellet samples were prepared, with each sample being crushed in a chromium ring mill, and approximately 5g of the pulverised sample mixed with PVC binder and pressed into an aluminium cap. To account for any contamination, chromium and nickel were excluded from this study. These pressed pellets were placed in an oven at 65°C for 12 hours to remove moisture and then made into quenched pressed glass disks for analysis.

REE analysis was undertaken by the Minerals Division of ALS Global in Brisbane, Queensland. The already pulverised samples were flaxed with lithium borate in a furnace. The resulting melt is then cooled and dissolved in an acid mixture containing nitric, hydrochloric and hydrofluoric acids. This solution is then analysed by inductively coupled plasma - mass spectrometry (ICP – MS).

Geochemical and tectonic discrimination diagrams were created using GCDkit (Janousek *et al.* 2006). For the full set of geochemical data, including clast maps, please refer to Chapter 8, Appendix 3.

## 5.3 Results

*Table 5.1 - Whole-rock XRF data including Major element oxides, trace elements and Ohata & Arai (2007) mafic (M), felsic (F), weathering (W) indicies.*

| Element | CR01 | CR03 | CR10 | CR11 | CR12 | CR14 | CR15 | CR17 | CR18 | CR24 | CD1.6 | CD2.3 | CD3.4 | CD3.13 | PCF1a | PCF5.1a | PCF5.1c | PCF5.3a | PCF5.6 | PCF5.6a | PCF5.8a |
|---|---|---|---|---|---|---|---|---|---|---|---|---|---|---|---|---|---|---|---|---|---|
| SiO2 | 52.5 | 56.2 | 62.1 | 56.8 | 53.3 | 53.5 | 61.5 | 56.5 | 56.4 | 57.5 | 78.1 | 69.9 | 72.8 | 69.6 | 59.6 | 46.7 | 55.4 | 46.0 | 55.1 | 50.7 | 69.2 |
| TiO2 | 0.8 | 0.8 | 0.4 | 0.6 | 0.4 | 0.5 | 0.3 | 0.6 | 0.7 | 0.8 | 0.5 | 0.7 | 0.4 | 0.7 | 0.4 | 0.2 | 0.9 | 0.2 | 0.9 | 1.1 | 0.1 |
| Al2O3 | 16.4 | 15.3 | 18.9 | 15.7 | 18.1 | 14.0 | 14.2 | 16.3 | 15.8 | 14.1 | 8.8 | 14.0 | 12.5 | 14.0 | 12.2 | 15.4 | 16.3 | 15.3 | 16.1 | 14.9 | 10.8 |
| Fe2O3 | 11.0 | 9.9 | 5.9 | 9.3 | 9.2 | 11.0 | 7.0 | 9.3 | 9.4 | 9.7 | 3.8 | 3.2 | 4.3 | 3.9 | 4.8 | 10.6 | 10.1 | 10.1 | 10.1 | 5.7 | 5.4 |
| MnO | 0.2 | 0.1 | 0.0 | 0.1 | 0.1 | 0.2 | 0.1 | 0.1 | 0.2 | 0.1 | 0.0 | 0.1 | 0.1 | 0.1 | 0.1 | 0.3 | 0.2 | 0.3 | 0.2 | 0.3 | 0.1 |
| MgO | 2.9 | 3.8 | 0.9 | 4.2 | 4.2 | 4.3 | 3.8 | 3.5 | 3.6 | 3.6 | 0.2 | 0.5 | 0.6 | 0.8 | 1.2 | 8.7 | 3.8 | 8.4 | 3.6 | 1.6 | 3.9 |
| CaO | 5.5 | 6.4 | 1.7 | 4.8 | 5.3 | 8.1 | 2.2 | 5.6 | 5.7 | 5.8 | 1.3 | 2.7 | 1.6 | 2.8 | 6.9 | 7.9 | 4.7 | 8.3 | 4.7 | 11.2 | 3.7 |
| Na2O | 5.7 | 4.7 | 8.7 | 4.1 | 3.6 | 5.3 | 4.9 | 4.0 | 3.2 | 4.4 | 2.6 | 5.8 | 3.7 | 6.1 | 3.7 | 2.1 | 4.0 | 2.3 | 3.9 | 4.1 | 3.3 |
| K2O | 1.4 | 0.6 | 0.1 | 0.1 | 1.7 | 0.2 | 1.3 | 0.6 | 0.7 | 1.1 | 2.0 | 0.4 | 1.7 | 0.9 | 2.9 | 1.1 | 1.9 | 0.9 | 1.9 | 4.1 | 1.1 |
| LOI | 2.4 | 2.5 | 1.3 | 4.7 | 4.7 | 3.0 | 3.8 | 4.0 | 3.8 | 3.1 | 1.8 | 2.0 | 1.2 | 1.7 | 8.2 | 7.7 | 2.8 | 8.8 | 2.8 | 6.7 | 2.1 |
| P2O5 | 0.2 | 0.2 | 0.1 | 0.2 | 0.1 | 0.1 | 0.1 | 0.2 | 0.1 | 0.2 | 0.3 | 0.3 | 0.1 | 0.3 | 0.1 | 0.0 | 0.3 | 0.0 | 0.3 | 0.4 | 0.0 |
| Total | 99.0 | 100.5 | 100.0 | 100.6 | 100.8 | 100.2 | 99.2 | 100.8 | 99.6 | 100.5 | 99.5 | 99.5 | 99.2 | 100.9 | 100.1 | 100.7 | 100.3 | 100.7 | 99.5 | 100.7 | 99.7 |
| **Ohata & Arai (2007) MFW indices** | | | | | | | | | | | | | | | | | | | | | |
| M | 75.0 | 83.5 | 75.1 | 90.2 | 69.7 | 91.1 | 59.8 | 79.5 | 79.7 | 78.2 | 19.0 | 52.5 | 32.0 | 48.7 | 50.8 | 82.8 | 70.5 | 84.2 | 70.4 | 63.4 | 62.3 |
| F | 13.1 | 7.4 | 11.1 | 2.8 | 15.6 | 4.2 | 20.7 | 9.2 | 8.0 | 10.5 | 46.9 | 30.7 | 40.9 | 34.1 | 37.7 | 7.1 | 12.9 | 6.9 | 12.7 | 26.5 | 23.8 |
| W | 11.9 | 9.1 | 13.8 | 6.9 | 14.7 | 4.7 | 19.5 | 11.3 | 12.2 | 11.3 | ==34.0== | 16.8 | ==27.1== | 17.2 | 11.5 | 10.1 | 16.7 | 8.9 | 16.9 | 10.0 | 13.9 |
| **Trace Elements** | | | | | | | | | | | | | | | | | | | | | |
| Cl | 187.6 | 132.5 | 79.9 | 97.8 | 126.6 | 94.5 | 123.9 | 113.2 | 110.9 | 149.4 | 129.6 | 108.1 | 56.6 | 110.2 | 27.1 | 29.3 | 129.8 | 25.6 | 155.5 | 34.8 | 79.4 |
| V | 250.1 | 378.7 | 274.5 | 261.3 | 314.5 | 346.7 | 225.4 | 251.8 | 260.3 | 373.2 | 67.9 | 82.0 | 32.3 | 66.7 | 75.6 | 246.1 | 231.8 | 248.5 | 248.2 | 272.2 | 106.0 |
| Cu | 80.8 | 199.2 | 105.9 | 108.0 | 138.3 | 164.6 | 92.0 | 77.6 | 92.1 | 188.3 | 11.7 | 24.3 | 13.7 | 26.0 | 16.7 | 32.1 | 85.7 | 6.1 | 76.2 | 123.2 | 11.8 |
| Zn | 99.6 | 89.2 | 90.0 | 96.3 | 79.2 | 78.0 | 65.5 | 130.1 | 94.1 | 84.1 | 48.6 | 82.5 | 84.7 | 105.5 | 43.3 | 164.4 | 100.4 | 171.6 | 97.8 | 122.7 | 15.5 |
| Ga | 15.9 | 15.1 | 14.3 | 12.6 | 13.4 | 13.0 | 11.5 | 13.6 | 13.8 | 12.0 | 10.0 | 13.8 | 12.4 | 10.8 | 11.5 | 9.7 | 16.3 | 9.0 | 15.6 | 11.6 | 9.5 |
| Ge | 3.4 | 2.3 | 1.2 | 1.5 | 1.3 | 2.1 | 1.5 | 1.4 | 1.5 | 1.4 | < 1 | 1.6 | 1.5 | 1.1 | 0.9 | < 1 | 1.9 | < 1 | 1.4 | 1.0 | 0.8 |
| As | 1.9 | 1.6 | 0.9 | 1.5 | 0.7 | < 1 | 2.6 | 2.0 | 1.9 | 1.7 | 1.7 | 3.9 | 2.2 | 1.3 | 0.5 | < 1 | 1.3 | < 1 | < 1 | 1.2 | < 1 |
| Se | < 1 | < 1 | < 1 | < 1 | < 1 | < 1 | < 1 | < 1 | < 1 | < 1 | < 1 | < 1 | < 1 | < 1 | < 1 | < 1 | < 1 | < 1 | < 1 | < 1 | < 1 |
| Br | < 1 | < 1 | < 1 | < 1 | < 1 | < 1 | < 1 | < 1 | < 1 | < 1 | < 1 | < 1 | < 1 | < 1 | < 1 | < 1 | < 1 | < 1 | < 1 | < 1 | < 1 |
| Rb | 13.8 | 3.6 | 0.5 | 1.5 | 16.1 | 2.8 | 12.6 | 7.5 | 8.9 | 6.6 | 17.3 | 5.9 | 29.3 | 5.9 | 34.2 | 19.9 | 32.5 | 17.2 | 32.7 | 35.8 | 21.8 |
| Sr | 210.3 | 127.6 | 43.9 | 127.6 | 338.8 | 119.4 | 150.5 | 294.0 | 693.0 | 173.5 | 189.6 | 92.0 | 176.4 | 378.8 | 256.8 | 63.3 | 487.7 | 63.6 | 491.0 | 299.5 | 154.6 |
| Y | 26.5 | 20.8 | 8.2 | 18.0 | 10.1 | 14.4 | 10.5 | 16.8 | 20.0 | 20.9 | 22.5 | 29.3 | 47.9 | 31.3 | 29.9 | 11.3 | 26.9 | 11.2 | 27.6 | 36.9 | 4.0 |

68

| | | | | | | | | | | | | | | | | | | | | | |
|---|---|---|---|---|---|---|---|---|---|---|---|---|---|---|---|---|---|---|---|---|---|
| **Zr** | 63.0 | 72.5 | 25.8 | 47.9 | 25.7 | 26.0 | 47.7 | 39.5 | 57.2 | 75.0 | 93.0 | 127.7 | 120.8 | 105.6 | 151.0 | 7.8 | 75.9 | 7.1 | 86.4 | 62.9 | 44.5 |
| **Nb** | 1.7 | 1.4 | 1.0 | 0.6 | 0.9 | 0.8 | 2.2 | 0.5 | 1.2 | 1.6 | 3.1 | 3.7 | 2.6 | 3.7 | 4.5 | < 1 | 2.3 | < 1 | 2.2 | 1.4 | 2.5 |
| **Mo** | < 1 | < 1 | < 1 | < 1 | < 1 | < 1 | < 1 | < 1 | < 1 | < 1 | < 1 | < 1 | < 1 | < 1 | < 1 | < 1 | < 1 | < 1 | < 1 | < 1 | < 1 |
| **Cd** | < 2 | < 2 | < 2 | < 2 | < 2 | < 2 | < 2 | < 2 | < 2 | < 2 | < 2 | < 2 | < 2 | < 2 | < 2 | < 2 | < 2 | < 2 | < 2 | < 2 | < 2 |
| **Sn** | < 3 | < 3 | < 3 | < 3 | < 3 | < 3 | < 3 | < 3 | < 3 | < 3 | < 3 | < 3 | < 3 | < 3 | < 3 | < 3 | < 3 | < 3 | < 3 | < 3 | < 3 |
| **Sb** | < 3 | < 3 | < 3 | < 3 | < 3 | < 3 | < 3 | < 3 | < 3 | < 3 | 6.6 | < 3 | 4.0 | < 3 | < 3 | 2.5 | < 3 | < 3 | 5.1 | < 3 | < 3 |
| **Cs** | < 4 | < 4 | < 4 | < 4 | < 4 | < 4 | < 4 | < 4 | < 4 | < 4 | < 4 | < 4 | < 4 | < 4 | < 4 | < 4 | < 4 | < 4 | < 4 | < 4 | < 4 |
| **Ba** | 636.4 | 213.9 | 66.7 | 53.0 | 835.1 | 95.6 | 381.6 | 255.9 | 294.2 | 327.3 | 388.7 | 153.9 | 293.6 | 438.9 | 502.9 | 107.2 | 440.5 | 79.1 | 423.6 | 465.0 | 170.4 |
| **La** | < 4 | 10.7 | 28.7 | < 4 | < 4 | < 4 | 25.2 | 14.8 | 14.3 | 21.4 | < 4 | 17.5 | < 4 | < 4 | 17.6 | 18.8 | 17.1 | 7.5 | 8.9 | < 4 | < 4 |
| **Ce** | < 4 | < 1.1 | < 0.3 | 12.2 | 14.9 | 16.3 | < 4 | < 4 | 4.3 | 31.0 | < 4 | 35.7 | 23.2 | 74.8 | 31.3 | 8.8 | 20.1 | < 4 | < 4 | 37.7 | 23.6 |
| **Hf** | < 2 | < 2 | < 2 | < 2 | < 2 | < 2 | < 2 | < 2 | < 2 | < 2 | < 2 | < 2 | < 2 | < 2 | < 2 | < 2 | < 2 | < 2 | < 2 | < 2 | < 2 |
| **W** | < 1 | < 1 | < 1 | < 1 | < 1 | < 1 | < 1 | < 1 | < 1 | < 1 | < 1 | < 1 | < 1 | < 1 | < 1 | < 1 | < 1 | < 1 | < 1 | < 1 | < 1 |
| **Hg** | < 1 | < 1 | < 1 | < 1 | < 1 | < 1 | < 1 | < 1 | < 1 | < 1 | < 1 | < 1 | < 1 | < 1 | < 1 | < 1 | < 1 | < 1 | < 1 | < 1 | < 1 |
| **Pb** | 1.5 | 9.2 | < 1 | 6.9 | 2.5 | 3.6 | 3.0 | 4.4 | 7.6 | 6.4 | 1.5 | 3.0 | 6.0 | 12.1 | 4.5 | < 1 | 3.5 | 0.8 | 4.3 | 4.1 | 2.8 |
| **Bi** | < 1 | < 1 | < 1 | < 1 | < 1 | < 1 | < 1 | < 1 | < 1 | < 1 | < 1 | < 1 | < 1 | < 1 | < 1 | < 1 | < 1 | < 1 | < 1 | < 1 | < 1 |
| **Th** | 1.6 | 1.1 | < 0.4 | < 0.2 | 0.8 | < 0.3 | 0.9 | < 0.3 | 2.0 | 1.4 | 1.8 | 1.5 | 2.2 | 3.3 | 3.0 | < 1.0 | 2.3 | < 1.0 | 1.4 | 1.6 | 2.8 |
| **U** | < 1.0 | < 1.0 | < 1.0 | < 1.0 | < 1.0 | < 1.0 | < 1.0 | < 1.0 | < 1.0 | < 1.0 | 2.4 | 1.4 | 0.6 | 3.9 | 2.3 | < 1.0 | 0.8 | < 1.0 | < 1.0 | 1.0 | 1.1 |
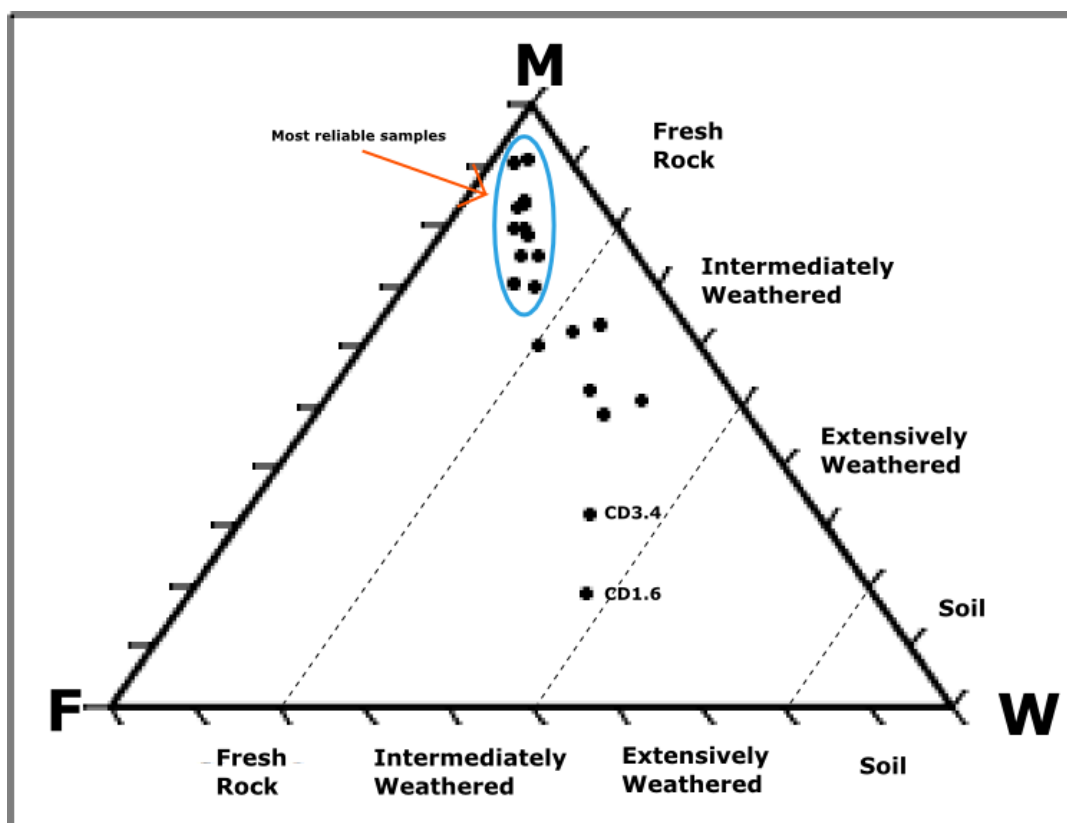
*Figure 5.4 - mafic igneous (M)- felsic igneous (F) - weathering (W) plot of Ohta and Arai (2007). Plots represent WR-XRF analysed samples.*

Both XRF data sets were used together in combination with REE analysis in order to create a larger data set, with the goal of determining trends amongst samples rather than individual plots. ***Table 5.1*** gives an example of the WR-XRF dataset for major elements providing a primitive understanding of the chemistry of the samples. For example, PCF5.1a and PCF5.3a show high concentrations of MgO with low Ti abundances when compared with other samples, suggesting these may be from an alternate source.

The weathering extent of the samples analysed using WR-XRF is shown in Figure 5.4. The majority of samples are fresh volcanic samples, as seen by the cluster of samples at the top of the triangle. Those samples that are more highly weathered are highlighted in Table 5.1, namely CD1.6 and CD3.4. This is evident in petrography whereby the influence of hydrothermal alteration has produced a chalcedonic matrix for CD1.6 and therefore the geochemistry of this sample will reflect the alteration styles imposed rather than the original mineralogy. CD3.4, a sample from the Wisemans Arm Formation, is part of the metasomatised Djungati terrane.

70

### 5.3.1 *General discrimination diagrams*

- **Al$_2$O$_3$ vs TiO$_2$ Diagram**
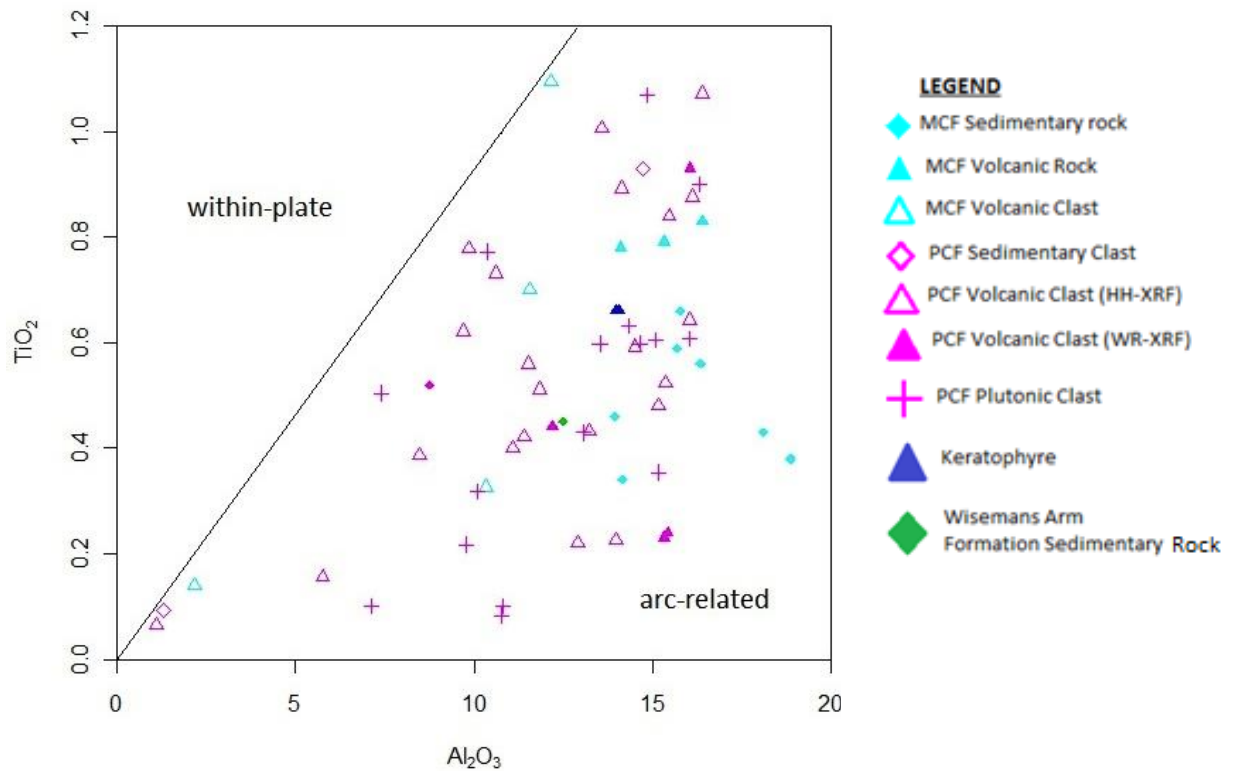


*Figure 5.5 - Al$_2$O$_3$ – TiO$_2$ diagram showing island arc affinity for all samples, adapted from Müller et al. (1992).*

Müller *et al.* (1992) first plotted TiO$_2$ against Al$_2$O$_3$ upon recognition that alkaline samples from within-plate settings contain very high abundances of Ti (a HFS element) comparative to those formed in arc-related settings. The immobile nature of both these elements highlights the validity of this plot for rocks affected by secondary alteration processes. All measured samples plot well within the arc-related spectrum, thus providing an initial arc-source association.

- **Magmatic Affinity Plots**

Following the indication of an arc-affiliated source, the samples were plotted on a FeO*/MgO versus SiO$_2$ diagram to designate magma series affinity (Figure 5.6). Miyashiro (1974) showed with this plot that FeO*/MgO increases with silica during differentiation within a series (Winter 2010). The calc-alkaline series displays enrichment in silica, whilst arc tholeiites tend to show enrichment in Fe producing the most consistent

characteristics for differentiation between the two magma series (Winter 2010). The samples appear to be mostly associated with an arc tholeiite magmatic trend, with only a few mostly Pipeclay Creek Formation plutonic rocks plotting within the calc-alkaline field. The purple arrow indicates that this may be a result of the alteration these samples have undergone. Chlorite alteration leaches silica to form chlorite, which may distort the magmatic affinity from arc calc-alkaline to arc tholeiite. Another factor to consider is the inaccuracy of the HH-XRF in measuring $SiO_2$, which may reduce the validity of some of these sample plots.
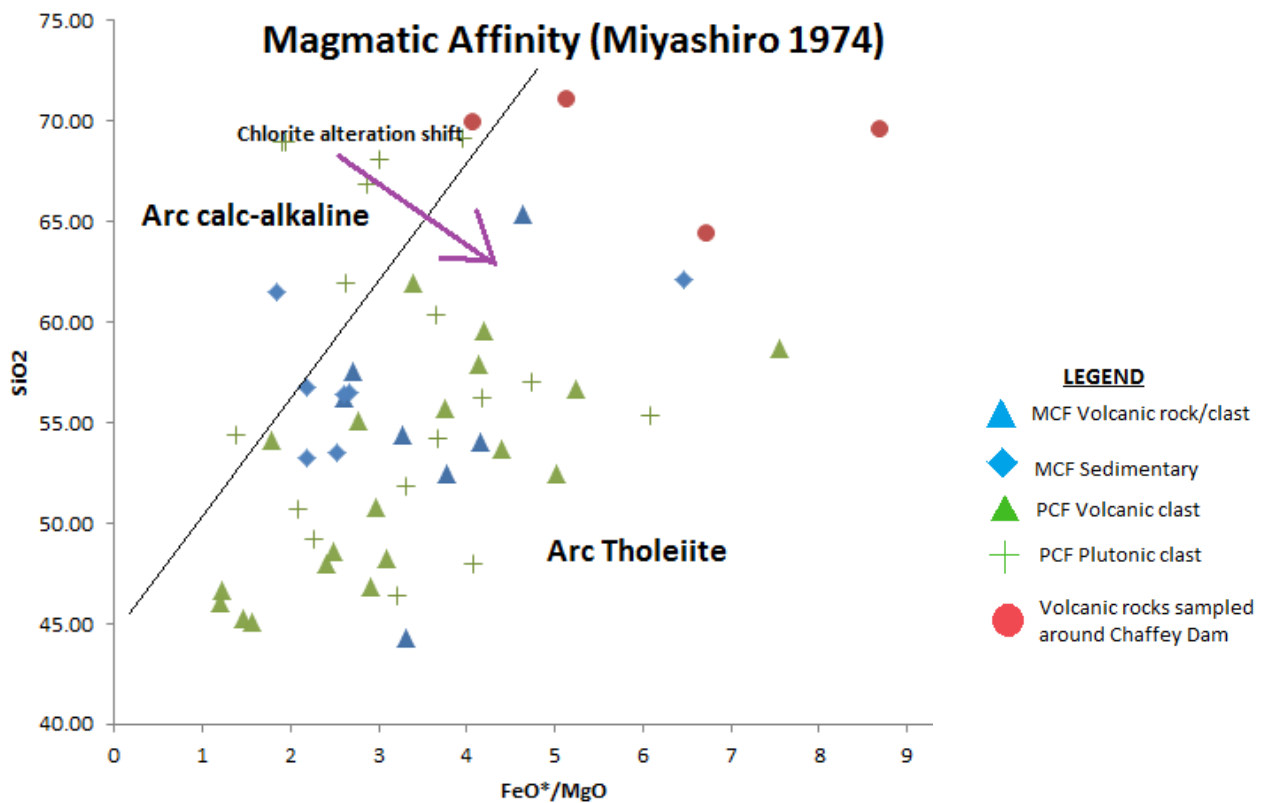


*Figure 5.6 - FeO\*/MgO – SiO2 magmatic affinity plot showing fields of arc calc-alkaline against arc tholeiite, modified from Miyashiro (1974). N.B., FeO\* refers to total Fe, including both Fe₂O₃ and FeO.*

Given the more robust nature of trace elements, trace element data from WR-XRF and ICP-methods has been plotted on Ta/Yb versus Ce/Yb and Th/Yb diagram in order to compare with the results obtained from the FeO*/MgO vs. SiO$_2$ diagram (Figure 5.7). Although they are similarly enriched in within-plate and mid-ocean ridge settings, Ce and Ta are elemental parameters since their mobilities differ in aqueous fluids and thus they behave differently in subduction related environments (Pearce 1982). Here the ratio Ce/Yb is used as it increases with a shift from island arc tholeiites to calc-alkaline basalts and then shoshonitic magmas (Pearce 1982). Th is a relatively immobile element, making it a particularly useful parameter for the study of altered rocks (Pearce 1982).

The samples plot distinctively within the fields of calc-alkaline in Figure 5.7, with the exception of two Pipeclay Creek volcanic samples (PCF5.1a, PCF5.3a) interpreted to be boninitic, and one Pipeclay Creek plutonic sample (PCF5.8a) has plotted within the shoshonitic field on both diagrams. These results are distinctly different to those from Miyashiro (1974) plot, however these can be taken to be more accurate due to the reliability of trace element ratios in low grade altered rocks compared to major element data.
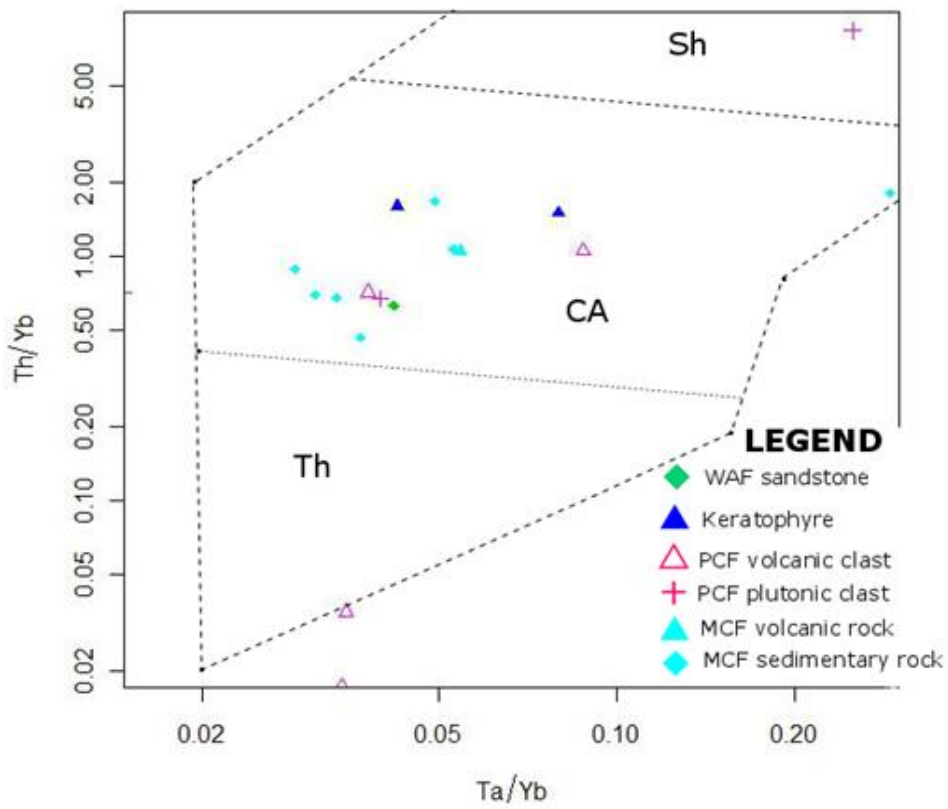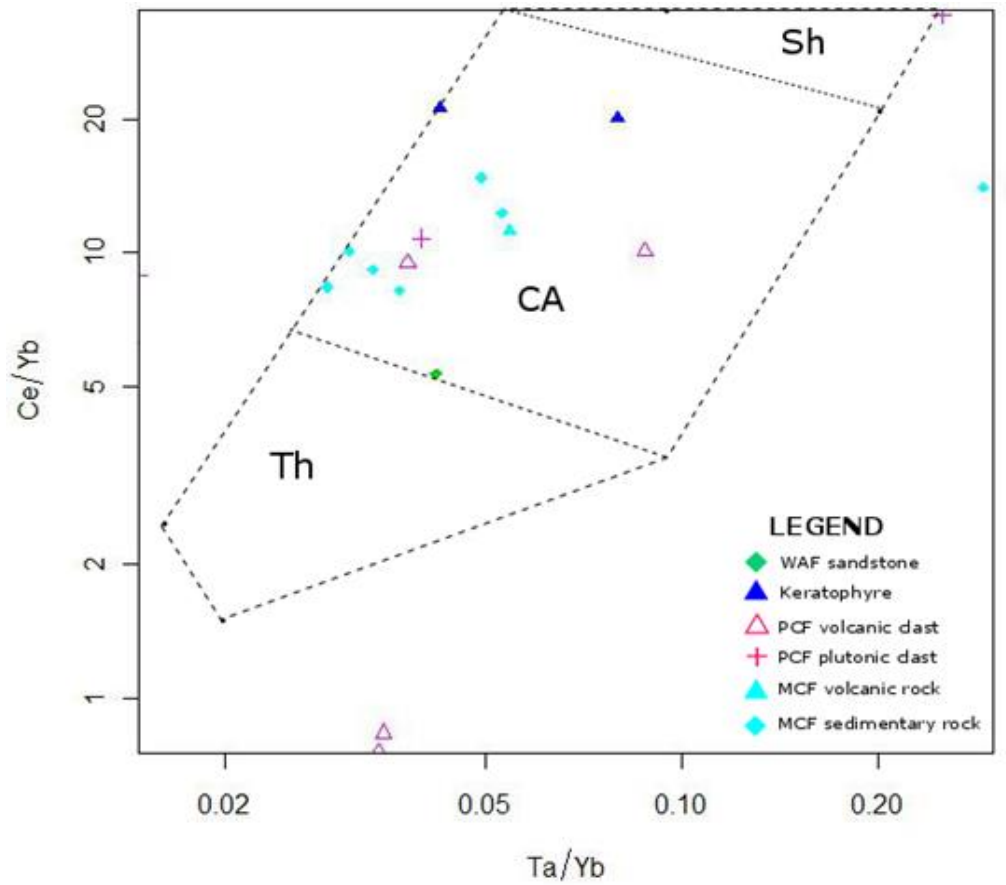
*Figure 5.7 - Magmatic affinity diagrams from Pearce (1982). Fields shown – Th: Arc Tholeiite, CA: arc calc-alkaline, Sh: Shoshonitic*

74

*5.3.2   Volcanic Rock Classification*

The Total Alkalis - Silica ($Na_2O$ + $K_2O$ - $SiO_2$) or TAS diagram (Figure 5.8) has long been used to classify volcanic rocks based on the direct plotting of measured wt % of alkali and silica oxides. Cox *et al.* (1979) stated that if a rock is classified with regard to mineralogical abundance of relative quartz and alkali feldspar, then the same classification scheme can be used at the element oxide level. Many rock-forming minerals have a preference for one alkali over the other (e.g., plagioclase > Na, biotite > K), giving Na and K the potential to fractionate relative to each other (Cox *et al.* 1979). This relative fractionation in combination with the fact that the alkalis are often concentrated into the liquid phase of the melt during crystallisation (e.g., olivine), leads to a positive correlation between the two alkali oxides (Cox *et al.* 1979).

The TAS diagram has been found to be consistent with modal analysis classification (Le Bas *et al.* 1986), and thus is used here for volcanic classification based on geochemical data. The HH-XRF does not detect Na, thus only those igneous samples that were sent for WR-XRF are those that are classified. This diagram is used in conjunction with the immobile element TAS proxy diagram (Figure 5.8), first proposed by Floyd and Winchester (1975) and modified by Pearce (1996), which utilises the immobile element ratios of Zr/Ti and Nb/Y. Combining the diagrams takes into consideration the mobility of the major element oxides ($Na_2O$, $K_2O$ and $SiO_2$), increasing precision in classification.

# Basalt Classification Diagrams
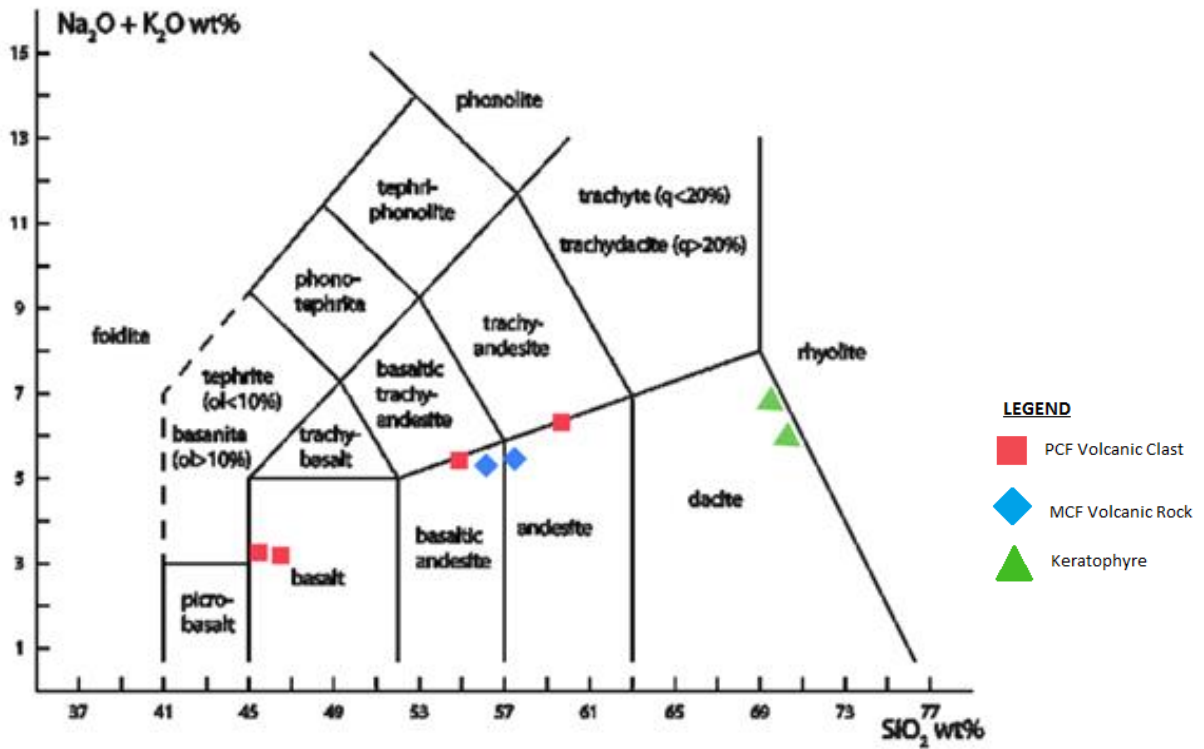


Nb/Y – Zr/Ti plot (modified by Pearce 1996)
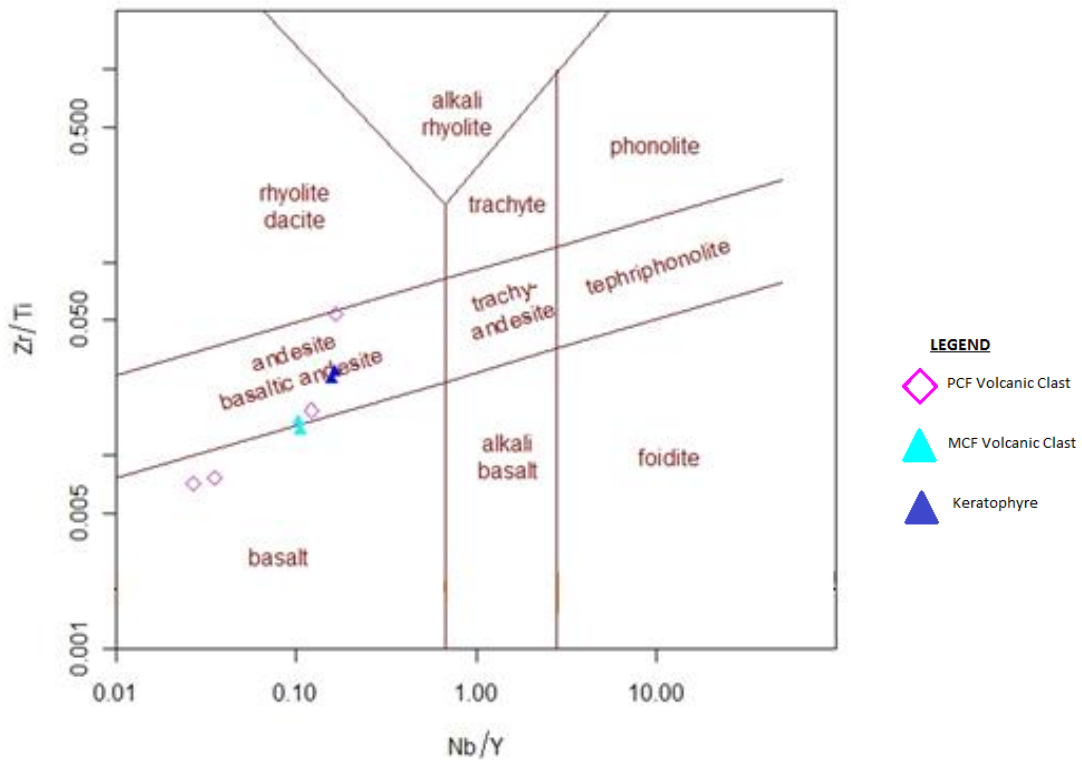


*Figure 5.8 - Basalt classification diagrams; a) TAS diagram from Le Maitre et al. (2002), b) immobile element TAS proxy diagram, from Pearce (1996).*

### 5.3.3 Volcanic Rock Tectonic Discrimination

The field of igneous volcanic geochemistry is well-versed in the literature, with many tectonic diagrams having been produced over the past forty years (e.g., Pearce & Cann 1973; Pearce 1982; Shervais 1982). Tectonic discrimination of basalts using minor or trace element data is expected to have higher accuracy than that of major-element analysis due to widespread overlap of major elements between MORB, back-arc basin tholeiites and volcanic arc basalts (Rollinson 1993).

- **MORB Array Diagrams**
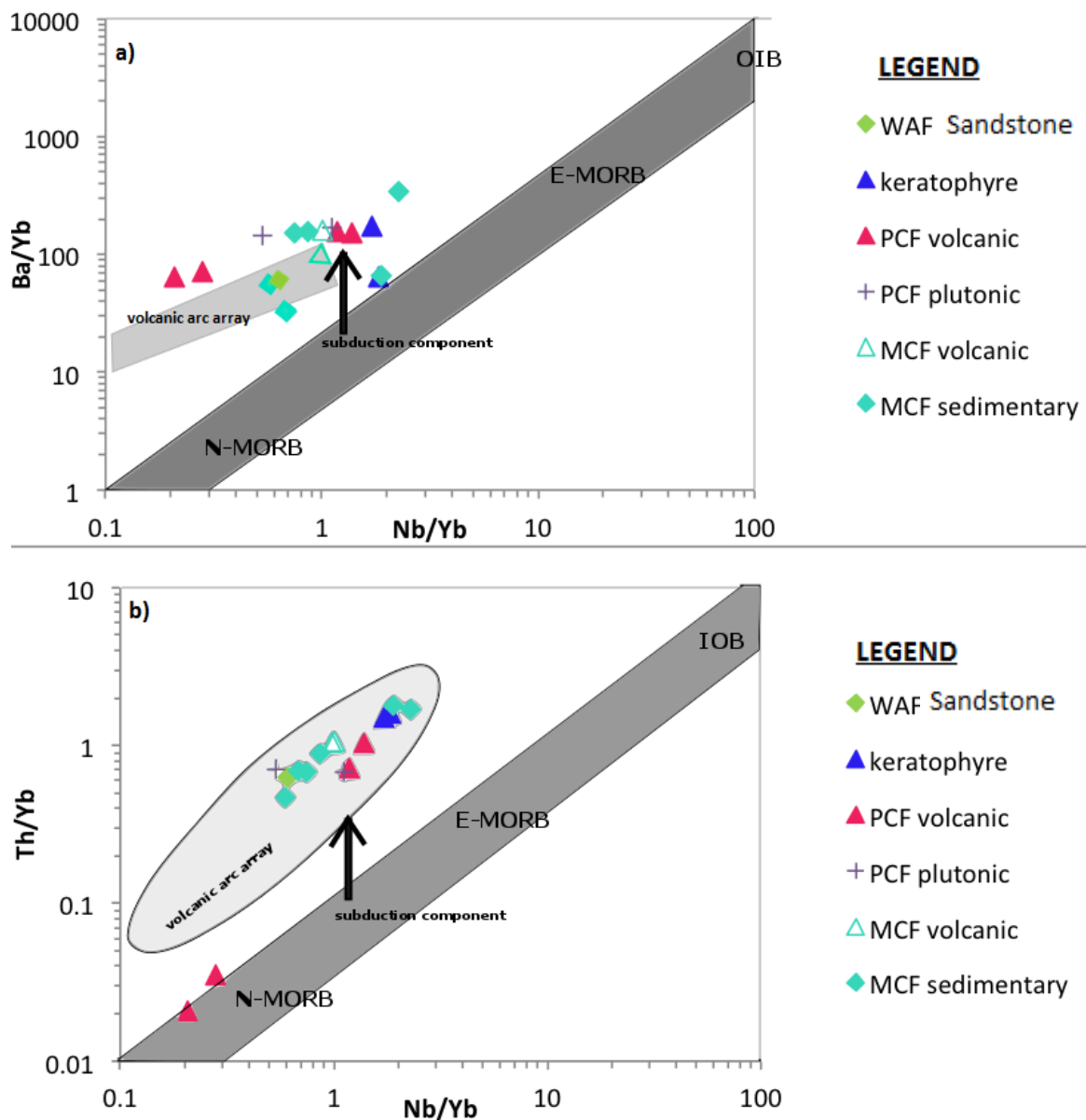


*Figure 5.9 - MORB array diagrams; a) Nb/Yb-Ba/Yb adapted from Leat et al. (2004) and b) Nb/Yb-Th/Yb adapted from Pearce (2014).*

MORB array diagrams (Figure 5.9) provide an insight into the source, whether it was depleted similar to N-MORB or enriched, in conjunction with providing information on the presence of a subduction component and volcanic arc. Yb is used as a normalising factor against Ba, Th and Nb in order to lessen the effects of fractional crystallisation and crystal accumulation in the magma chamber (Leat *et al.* 2004). Ba and Th are mobile elements in a subduction-related setting due to the addition of slab-derived material, and therefore increases in Ba/Yb and Th/Yb ratios reflect addition of slab derived components (Leat *et al.* 2004).

Most samples plot within or nearby the volcanic arc array, again suggesting an arc-related provenance. It is clear that the Murrawong Creek and Pipeclay Creek formations are derived from a subduction-zone related setting. The two anomalous samples are the Pipeclay Creek boninites*,* with the Nb/Yb-Th/Yb diagram indicating they are from a depleted source, similar to that of a NMORB, possibly related to the initiation of subduction. It must be understood that these diagrams are diagnostic for igneous volcanic rocks, and thus plutonic and sedimentary samples are not considered definitive results but rather highlight the cluster of plots in the subduction-related environment, suggesting this is representative of the source area.

- **Tectonic Discrimination Plots**

The following analytical graphs were chosen due to Ti, Zr and V being less mobile elements, which can be measured accurately using both WR-XRF and HH-XRF analysis, giving a larger dataset. The Ti-Zr-Sr diagram (Figure 5.10) assumes relatively fresh samples due to the mobility of Sr under metasomatism during greenschist facies metamorphism (Pearce & Cann 1973; Rollinson 1993),. These samples, however, were metamorphosed at lower grades than that of greenschist facies.

Basalt tectonic discrimination – Pearce and Cann (1973)
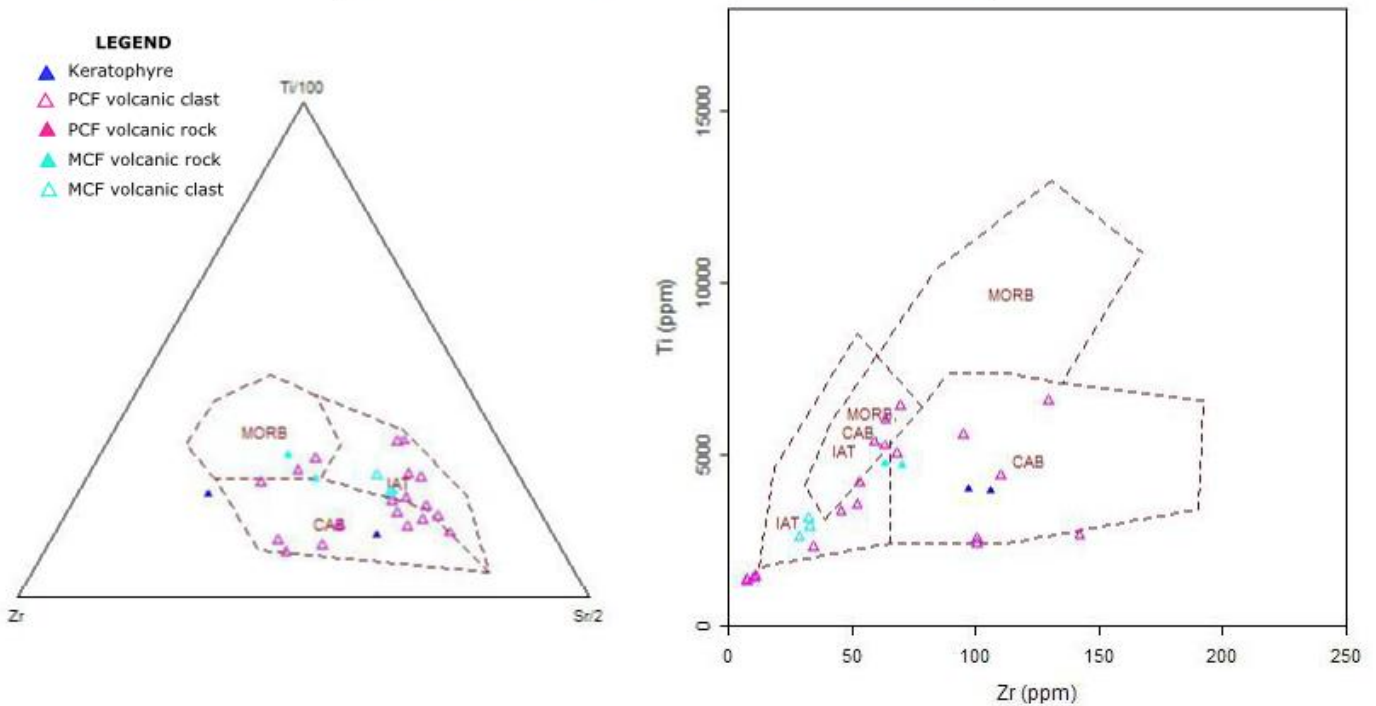
*Figure 5.10 - a) Ti-Zr-Sr ternary diagram for basalts; b) Ti-Zr bivariate basalt discrimination. Fields as follows: IAT, island arc tholeiites; CAB, calc-alkaline basalts; MORB, mid-ocean ridge basalts and a mixed field. Diagrams after Pearce and Cann (1973).*

Only volcanic samples are plotted on discrimination diagrams from Pearce and Cann (1973) determining the magma series from which the rocks are sourced. They are divided into the following fields; island-arc tholeiites, calc-alkali basalts and MORB. These diagrams indicate a mostly island arc tholeiite magma series to be the main source, with a minor calc-alkaline influence. These results are in support of the island arc tholeiite source determined from the FeO*/MgO versus $SiO_2$ diagram of Miyashiro (1974) in Section 5.3.1. Those few samples plotting in MORB on the Ti-Zr-Sr ternary diagram may be a result of the mobility of Sr under alteration processes such as leaching of this element from plagioclase feldspar during weathering. Figure 5.11 is based off the Zr-Ti bivariate diagram of Pearce (1982), classifying the three distinctive tectonic settings from which volcanic rocks may be sourced; island arc lavas, within-plate lavas and MORB. The samples mostly plot within island-arc lavas category, thus confirming the interpretation of an immature island arc source for the Murrawong Creek and Pipeclay Creek formations.

79
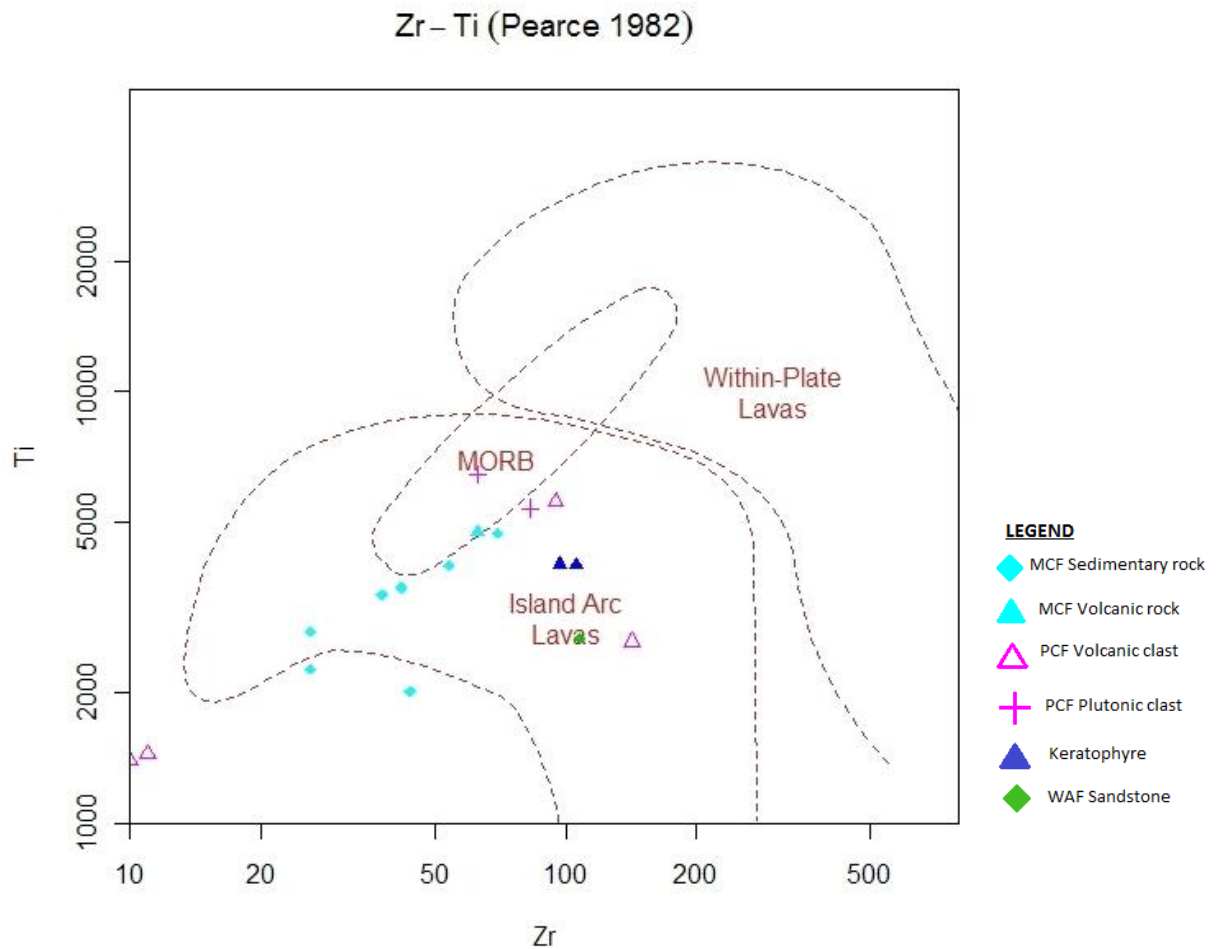
*Figure 5.11 - Zr-Ti bivariate diagram discriminating between lava source, from Pearce (1982).*

One of the most well-recognised tectonic discrimination diagrams for basalts was first proposed by Shervais (1982), which utilises the immobile trace elements vanadium and titanium and their variation in partition coefficients (1<V<1 and Ti <1; Figure 5.12). Ti and V are abundant in more mafic rocks and remain stable over a range of metamorphic processes, highlighting their suitability for geochemical provenance studies (Shervais 1982). Modern volcanic rock associations show diagnostic trends on the Ti/V plot, allowing for a clear categorisation of volcanic rocks into arc related tholeiites, MORB or OIB (Shervais 1982).
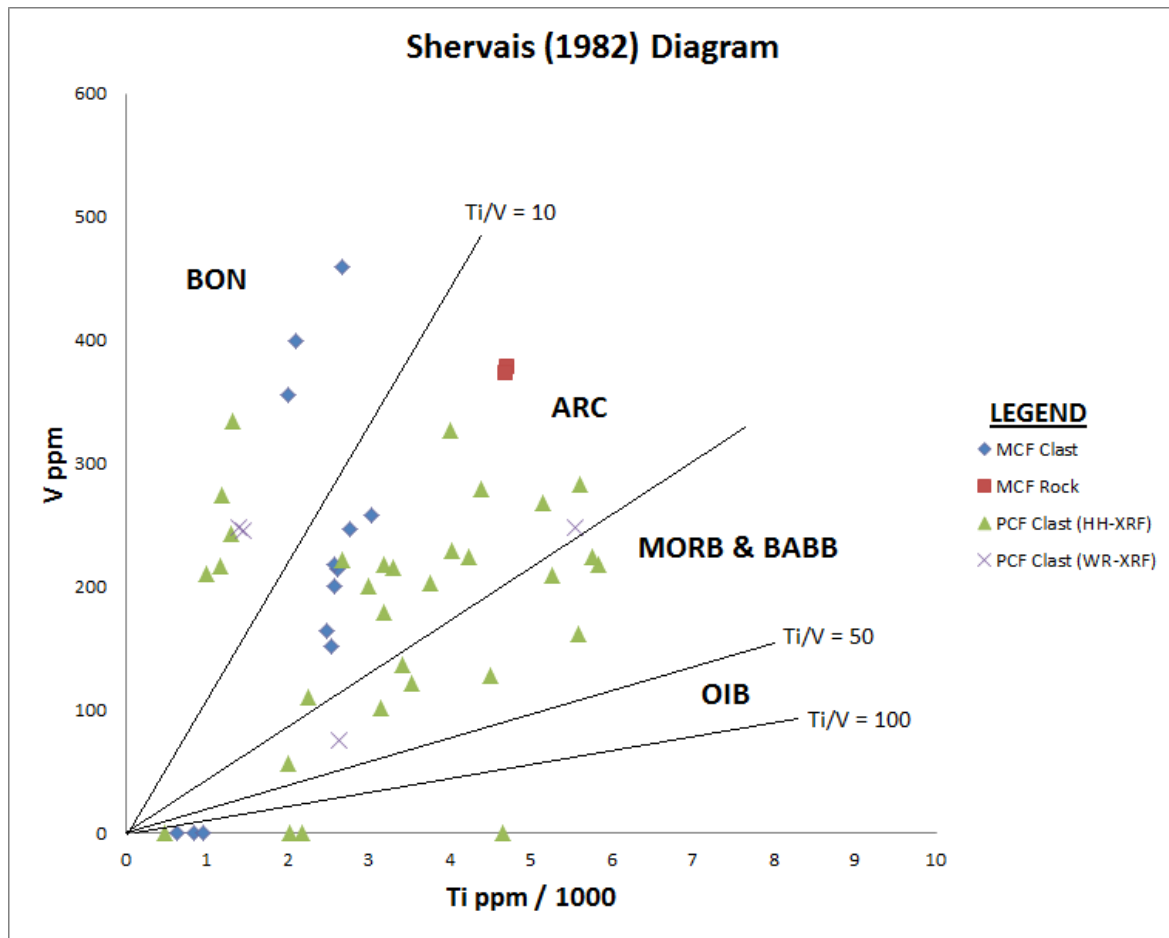
*Figure 5.12 -V-Ti basalt discrimination diagram with fields: BON-boninitic, ART- arc-related tholeiites, MORB & BABB- Mid-ocean ridge basalts & back-arc basin basalts and OIB- ocean island basalts, from Shervais (1982).*

Only those samples that were categorised as mafic to intermediate volcanic rocks, using both HH-XRF and WR-XRF data, were plotted on the Ti-V diagram. The results indicate boninitic rocks are present, which is an indication of a juvenile forearc basin setting for these clasts. A majority of the samples are arc-related tholeiites, while others are associated with MORB or BABB. These may be a result of the arc rifting, or highlighting the primitive nature of the arc, as older oceanic crust, or MORB, is uplifted and possibly eroded into the basin via a nearby accretionary complex.

## 5.3.4 Plutonic Rock Classification

Following the acceptance of volcanic rock classification on the basis of geochemical abundances, the TAS diagram was redesigned in order to accommodate rocks of plutonic origin (Middlemost 1985; Wilson 1989). Figure 5.13 classifies the plutonic clast samples of the Pipeclay Creek Formation to be monzonite, monzodiorite and granodiorite. This agrees with petrographic analysis whereby the samples have a relatively low abundance of quartz.
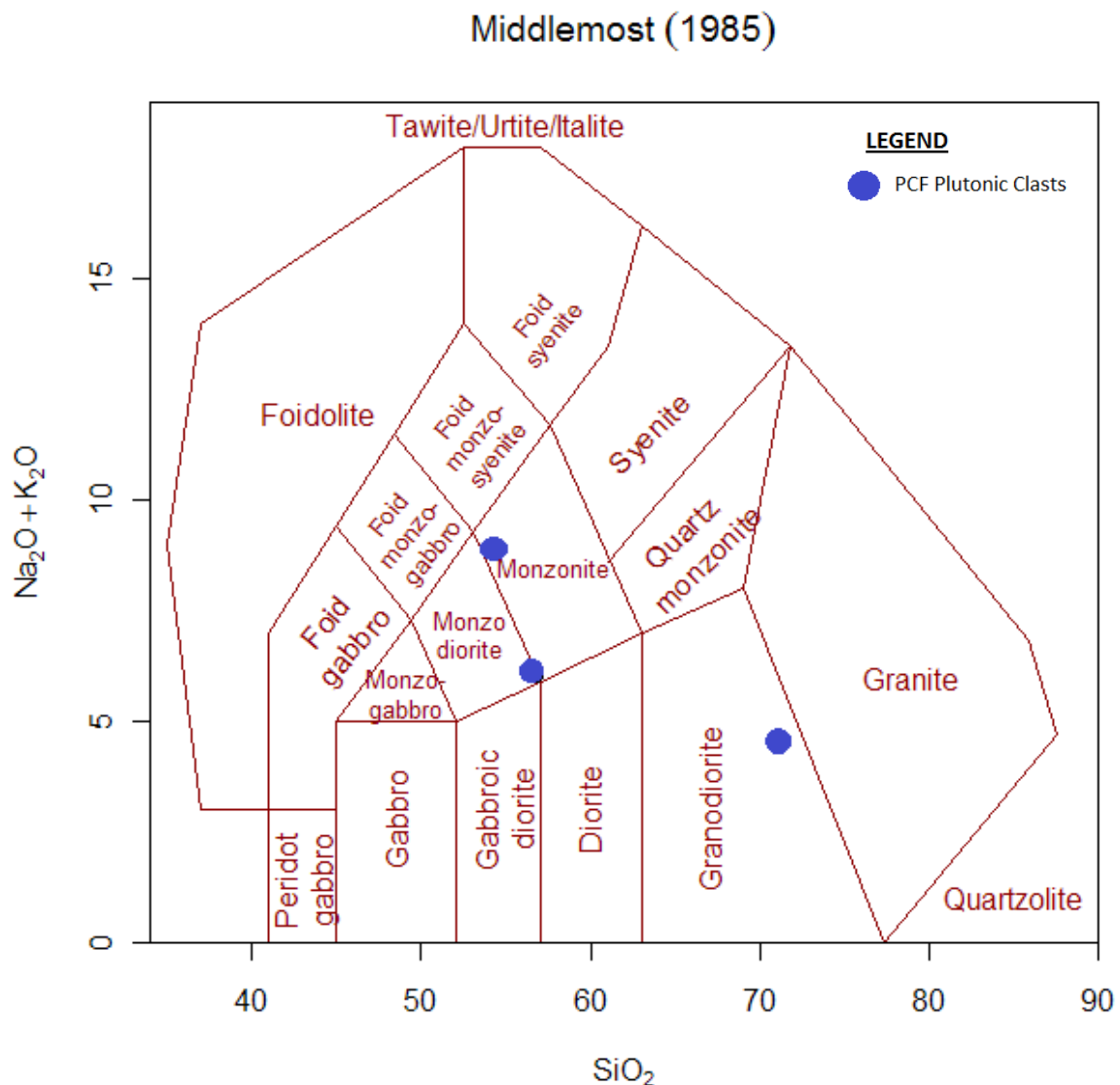


*Figure 5.13 -TAS diagram for the classification of plutonic rocks, from Middlemost (1985).*

*5.3.5   Plutonic Rock Tectonic Discrimination*

Pearce *et al.* (1984) found that the most reliable elements for discriminating between granites from different tectonic settings are Rb, Y, Yb, Nb and Ta, with the exception of post-orogenic granites (Pearce *et al.* 1984; Rollinson 1993). Granites, considered as any plutonic rock containing greater than 5% quartz, were classified into four main categories: 1- Ocean-ridge granites (ORG), 2- volcanic-arc granites (VAG), 3- within-plate granites (WPG) and 4- collisional granites (COLG) (Pearce *et al.* 1984). Both mobile and immobile elements are used in this tectonic discrimination of granites, as Pearce *et al.* (1984) suggest that the low degree of alteration occurring for most granites allows for stability of the elements. Despite the small sample size, it is evident that the granitic clasts from the Pipeclay Creek Formation sediments have formed in a volcanic arc setting (Figure 5.14), thus indicating magmatic association with an oceanic subduction zone (Pearce *et al.* 1984).
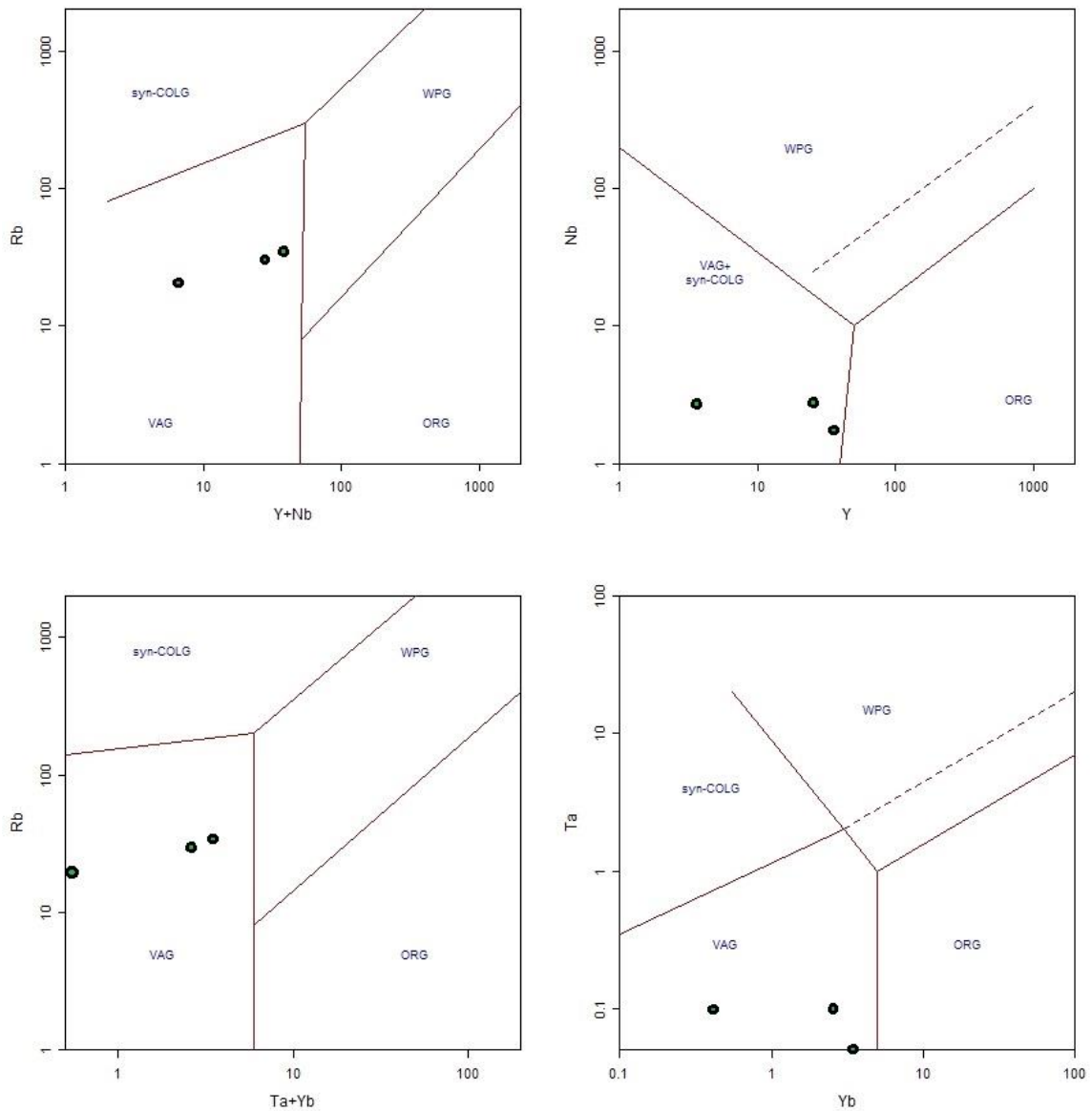
*Figure 5.14 - a) Ta-Yb; b) Rb-(Y + Nb); c) Rb-(Yb + Ta) discrimination diagrams for granitic clasts from the Pipeclay Creek Formation, from Pearce et al. (1984), showing syn-collisional granites (syn-COLG), within-plate granites (WPG), volcanic-arc granites (VAG) and ocean-ridge granites (ORG).*
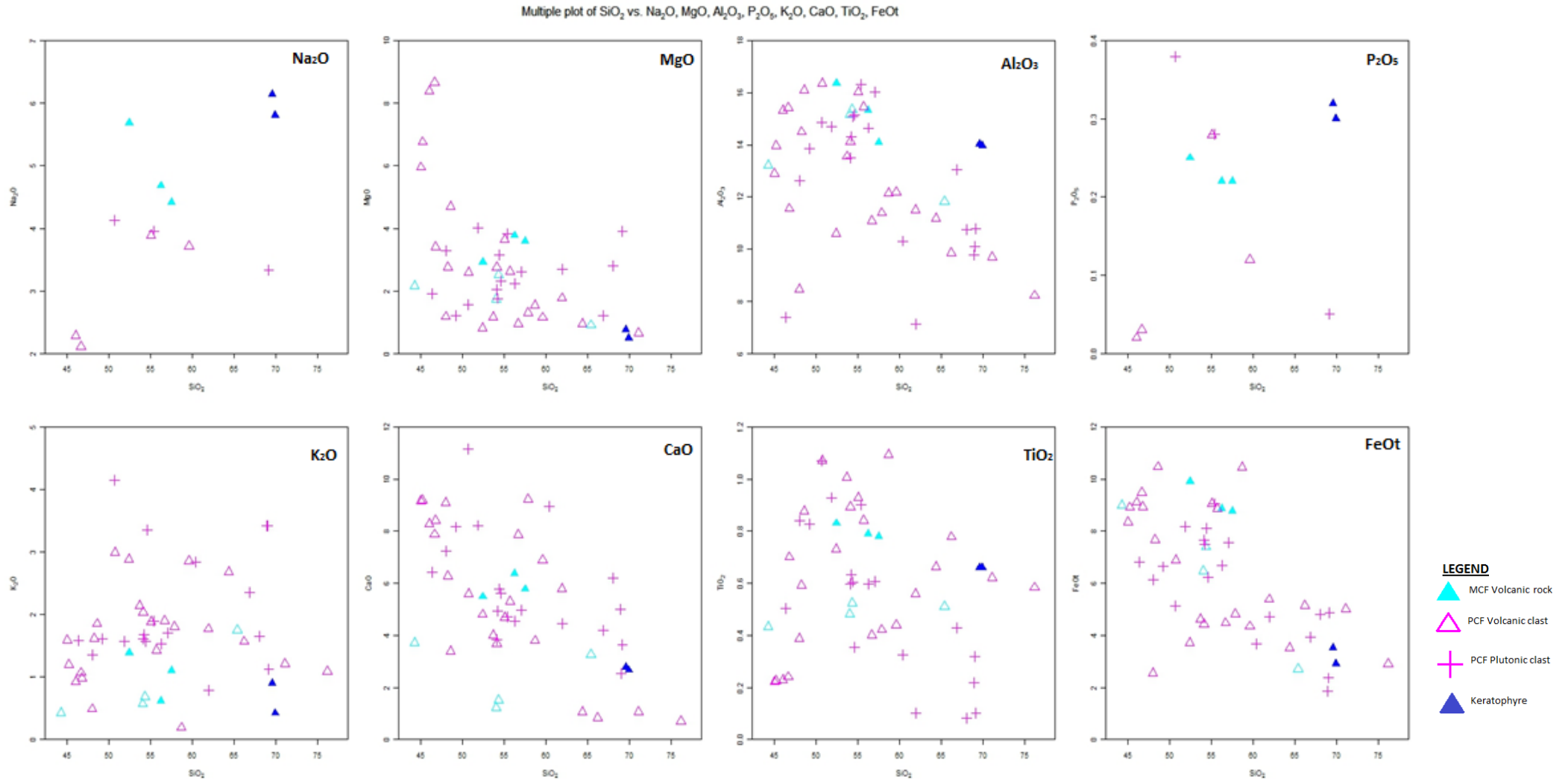
## 5.3.6   Major Element Harker Diagrams



Figure 5.15 - Harker diagrams showing selected major elements plotted against SiO$_2$

FeO$^t$ refers to total Fe measured, as the XRF does not differentiate between Fe$_2$O$_3$ and FeO

Bivariate plots, known as Harker diagrams, plot the major elements using wt % silica as the abscissa since silica increases steadily with magma differentiation (Harker 1909). These diagrams attempt to establish fractionation trends based on crystal fractionation regimes and the uptake of major elements in the magma chamber (Winter 2010). Compatible elements that are incorporated into the crystalline phase show a decreasing trend with increasing silica content, whilst elements that show an increasing trend are considered incompatible. The proportion of incompatible elements increases within the remaining melt, rather than an actual increase of that particular element (Winter 2010).

The lack of data available for $Na_2O$ and $P_2O_5$ results in an inability to make conclusions from these plots, as it is only through trends of multiple analysis that observations can be made. In support of petrographic observations, samples with higher than expected $Na_2O$ concentrations indicate albitisation during low-grade metamorphism since sodium can readily replace calcium. $K_2O$ and $TiO_2$ are largely conserved, and thus have positive slopes as they concentrate in the more evolved melts. The low uptake of $TiO_2$ may represent the minor presence of oxide-mineralisation such as ilmenite. The decrease in $Al_2O_3$, $MgO$, $FeO^t$, and $CaO$ with increasing $SiO_2$ are compatible with fractional crystallisation of plagioclase and mafic phases, such as olivine or pyroxene (Winter 2010).

The key conclusions from observing the Harker diagrams (Figure 5.15) are that despite the samples derivation from the same arc system, these samples are not all derived from the same magma chambers. The clasts analysed vary from volcanic to plutonic, boninitic to shoshonitic, indicating that all aspects of the arc system are incorporated. There may have been separate chambers, or multiple pulses of magma with varying mantle compositions, or some samples may be derived from feeder pipes. Furthermore, varying amounts of alteration has occurred, shifting original compositions, e.g., chlorite overprints result in decreased silica and increased MgO. The chemical differences between the volcanic and plutonic clasts are notable, whereby plutonic clasts indicate more evolved components within the arc system. Lower MgO abundances result from the early fractionation of mafic minerals, while an $Al_2O_3$ rich cluster indicates early removal of feldspars from the system.

Harker diagrams are useful in understanding the development of the magmatic evolution of a system; however it must be noted that scatter may result from analytical errors, in this case particularly the inconsistency of the HH-XRF in measuring $SiO_2$.

## 5.3.7 Sedimentary Rock Tectonic Discrimination

The importance of sedimentary rocks in providing information about source and depositional environments is highlighted by geochemical analysis. Bhatia (1983) was the first to assign geochemical discrimination techniques similar to those used for igneous rocks to sedimentary samples based upon the nature of the geochemical signature acquired due to tectonic setting. Sedimentary discrimination has largely been based on major element oxides, posing the problem of mobility of major elements during sediment weathering and transport (Taylor & McLennan 1985; Rollinson 1993).

Roser and Korsch (1988) used discriminant function analysis of the major element oxides to determine provenance through the following four groups: 1) mafic basalts or andesites, 2) intermediate andesites, 3) felsic plutonic and volcanic and 4) recycled quartzose detritus. They noted that the distinction from 1 through 3 results from changes in petrologic evolution, whereas group 4 is indicative of sedimentary maturation (Roser & Korsch 1988).
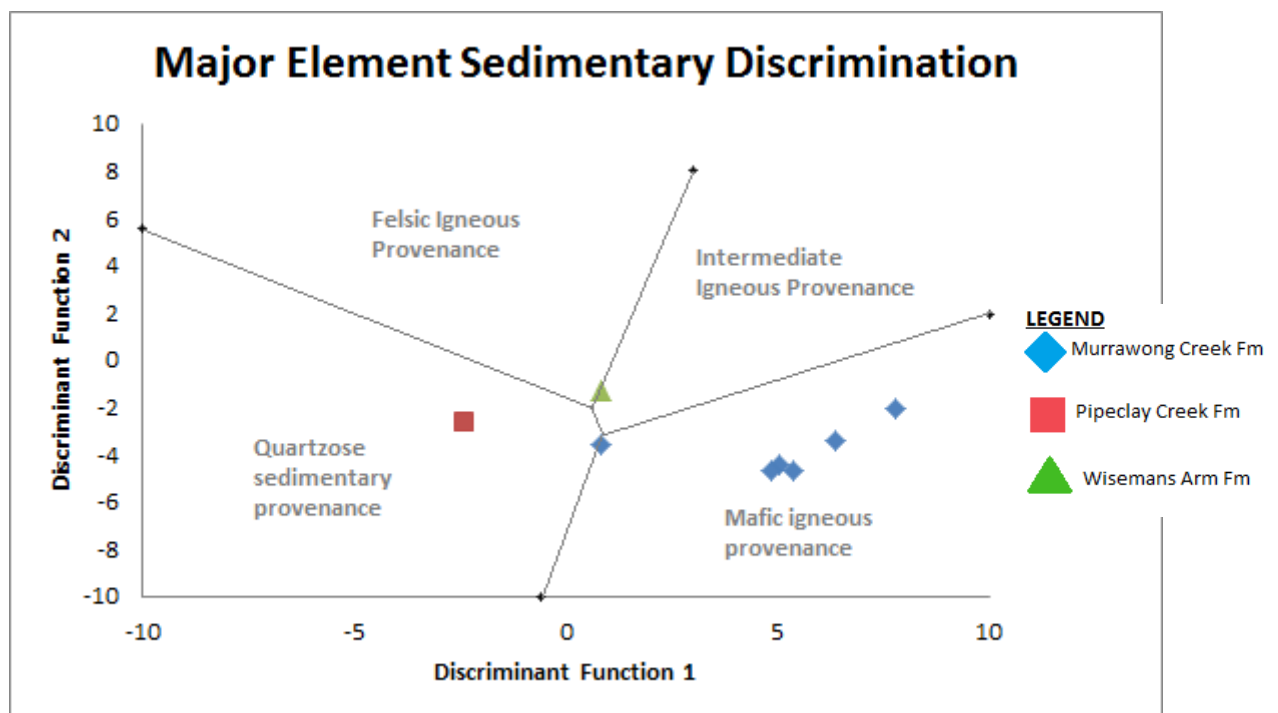


*Figure 5.16 - Major element discriminant function analysis diagram adapted from Roser and Korsch (1988). CD – sample collected by Chaffey Dam, later interpreted to be part of Wisemans Arm Formation.*

87

The discrimination diagram of Roser and Korsch (1988) (Figure 5.16) indicates a mafic igneous provenance for the sediments of the Murrawong Creek Formation, consistent with other findings of basaltic-andesitic source. This alludes to the immature nature of these sediments, indicating their proximal locality of a basic volcanic source. The position of the single Pipeclay Creek sediment cannot be used to make interpretations as it distinguishes only a single, weathered sample (CD1.6), rather than a trend within a sample group.

**Discriminant Function I: $-1.773TiO_2 + 0.607Al_2O_3 + 0.76FeO^t - 1.5MgO + 0.616CaO + 0.509Na_2O - 1.224K_2O - 9.09$.**

**Discriminant Function II: $0.445TiO_2 + 0.07Al_2O_3 - 0.25FeO^t - 1.142MgO + 0.438CaO + 1.475Na_2O + 1.426K_2O - 6.861$.**

Roser and Korsch (1986) used the ratio of $K_2O/Na_2O$ against $SiO_2$ to distinguish between three tectonic settings; passive continental margin, active continental margin and oceanic island arc. They eliminated the degree of variation with grain size to a minimum, noting that volcanic muds were the only sediments misclassified due to their increased $SiO_2$ values (Roser & Korsch 1986; Rollinson 1993). Sedimentary rocks of the Murrawong Creek Formation plot within the oceanic island-arc field (Figure 5.17), whilst Pipeclay Creek and Wisemans Arm formations plot as passive margin and active continental margin respectively.
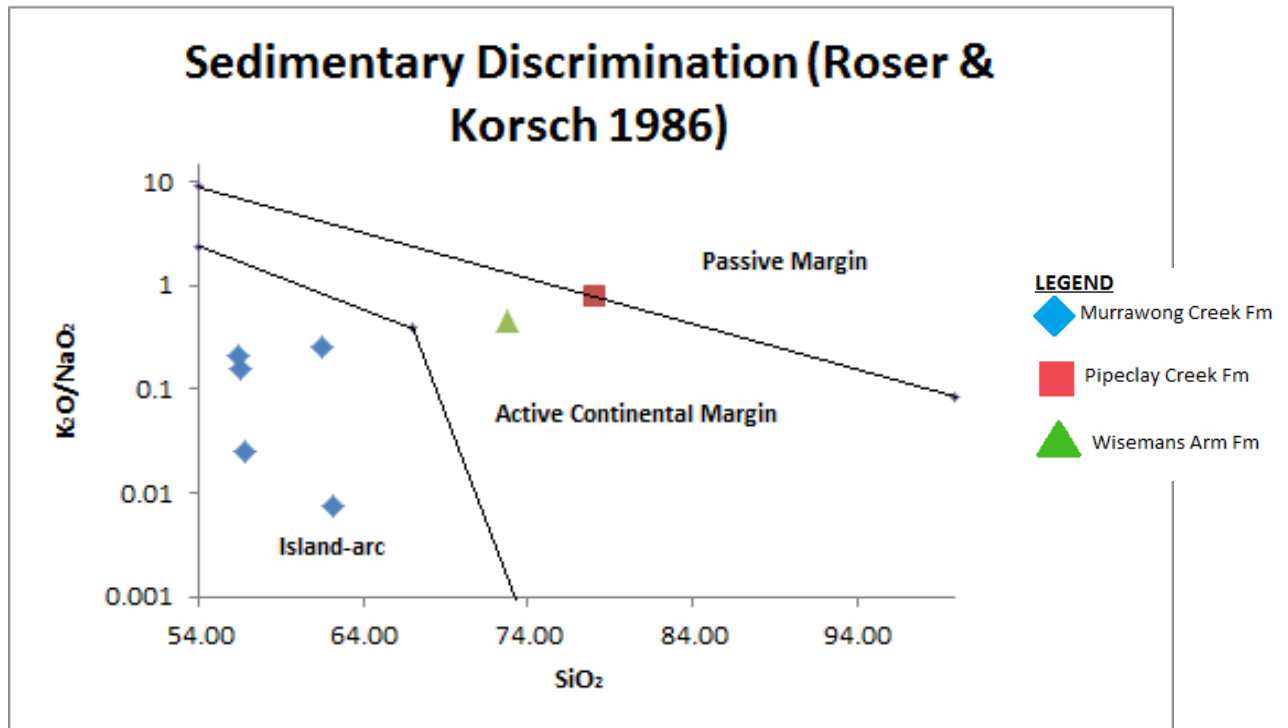
*Figure 5.17 - Tectonic discrimination of sedimentary rocks, adapted from Roser and Korsch (1986). CD – sample collected by Chaffey Dam, later interpreted to be part of Wisemans Arm Formation.*

The sedimentary discriminant analysis diagram of Bhatia (1983) (Figure 5.18), supports the results found in Figure 5.17. The sedimentary rocks of the Murrawong Creek Formation plot within the field defined as oceanic island-arc, suggesting that these sediments are closely associated with an intra-oceanic arc as opposed to an active continental margin or continental island arc. Here oceanic island arc is defined as a sedimentary basin that exists adjacent to an oceanic island arc, with tholeiitic or calc-alkaline volcanic systems (Bhatia 1983).
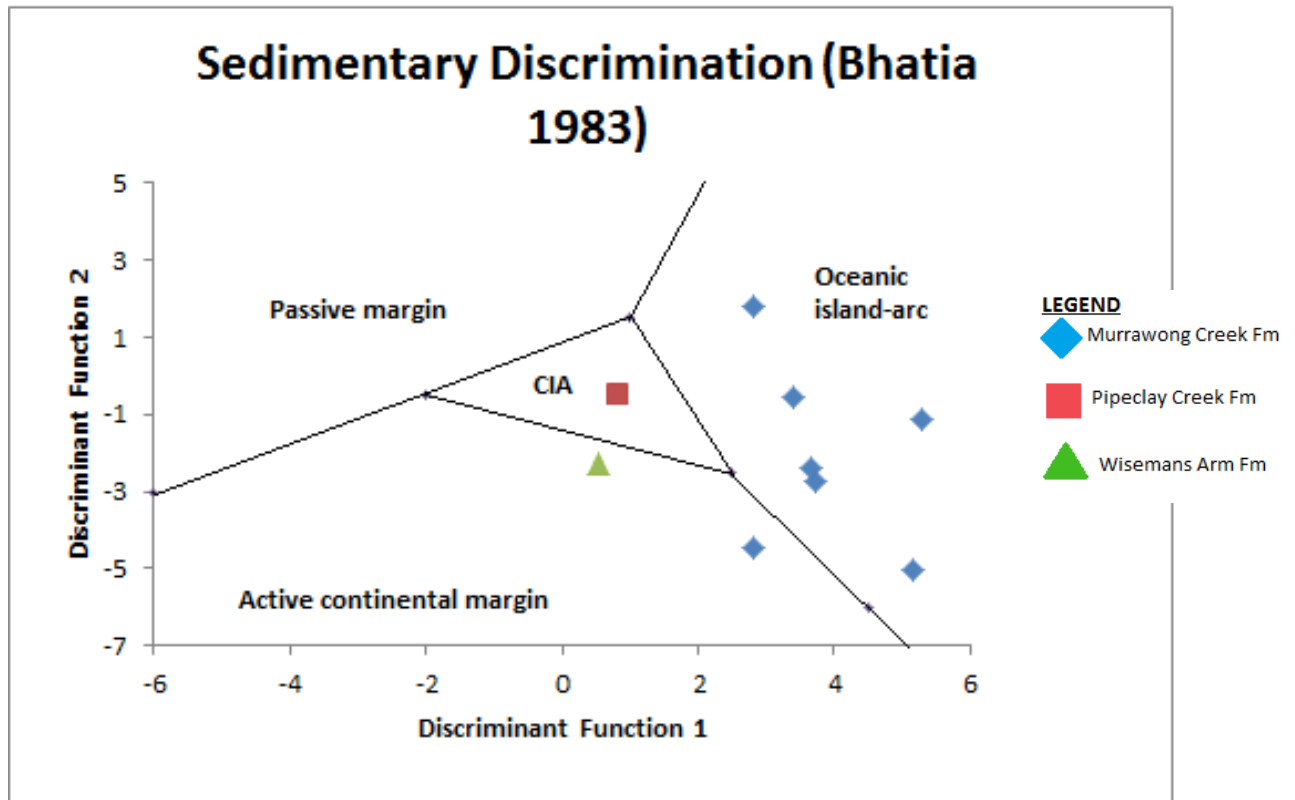
*Figure 5.18 - Tectonic discrimination of sedimentary rocks using discriminant function analysis adapted from Bhatia (1983). CIA – continental margin arc. CD – sample collected by Chaffey Dam, later interpreted to be part of Wisemans Arm Formation.*

**Discriminant Function I: $-0.0447SiO_2 - 0.972TiO_2 + 0.008Al_2O_3 - 0.267Fe_2O_3 + 0.208FeO - 3.682MnO + 0.140MgO + 0.195CaO + 0.719Na_2O - 0.032K_2O + 7.51P_2O_5 + 0.303.$**

**Discriminant Function II: $-0.4215SiO_2 + 1.988TiO_2 - 0.526Al_2O3 - 0.551Fe_2O_3 - 1.610FeO + 2.720MnO + 0.88MgO - 0.907CaO - 0.177Na_2O - 1.840K_2O + 7.244P_2O_5 + 43.57.$**

$FeO$ was determined from $FeO^t$ through classifying the sedimentary rocks to be andesitic, giving an average $Fe_2O_3$ component of 15% of $FeO^t$, whilst taking into consideration the molecular weight value of 1.1113 ($Fe_2O_3$) and 0.89999 ($FeO$). Thus the final equation used:

**$Fe_2O_3 = FeO^t$ x 0.15 x 1.1113**
**$FeO = FeO^t$ x 0.85 x 0.8999**

90

### 5.3.8   REE Geochemistry – MORB normalised abundances

Normalised multiple-element (spider) diagrams group elements that are incompatible with a distinctive mantle mineralogy, in this case N-MORB.  Normalising to MORB was first proposed by Pearce (1983) based on the mobility and incompatibility relative to the mantle with regards to partial melting of garnet hazburgite (Rollinson 1993). Sun and McDonough (1989) also normalise the REEs to MORB with partial melting as the key ordering factor (Winter 2010). When a rock of typical MORB composition is plotted on these diagrams, it is expected that it will produce a flat line about 1.0.

The ordering schemes proposed by Pearce (1983) and Sun and McDonough (1989) are shown in Figure 5.19. Pearce (1983) has mobile LILE located on the left and the more immobile HFSE located on the right. The compatibility of each element relative to the mantle increases outwards from Ba-Th (Rollinson 1993).
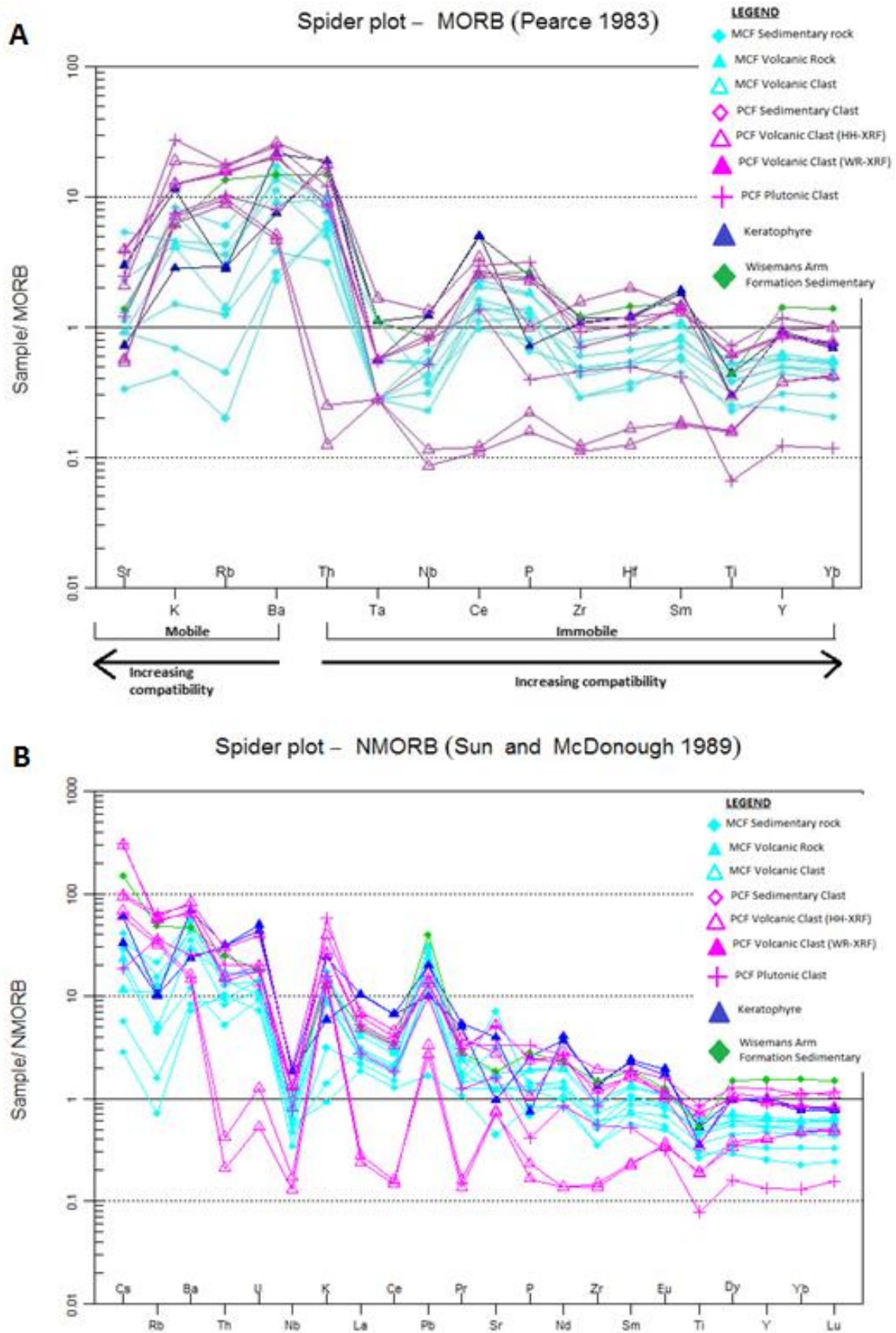
*Figure 5.19 - MORB-normalised multi-element diagrams; A) from Pearce (1983), B) from Sun and McDonough (1989)*

The variation in rock formations, type and characteristics accounts for the vast degree of scatter across Figure 5.19. A trend of enrichment occurs moving up the stratigraphic sequence, with the Murrawong Creek Formation showing evidence of a more depleted source, similar to that of a MORB, while the overlying Pipeclay Creek Formation appears slightly more enriched. Observed trends in spider diagrams are often distinctive of tectonic setting, such as; arc-related enrichment of the LILE, negative Ta-Nb anomalies, depletion of Ti, Y and Yb relative to the MORB and enrichment of Ce and Sm (Pearce *et al.* 1984; Pearce & Peate 1995). These trends can be seen in both of the above diagrams, particularly the negative Ta-Nb anomaly which is established among all samples. The samples show the characteristic depletion of Ti, Y and Yb, and enrichment of Ce relative to the MORB. The small negative Zr anomaly can be attributed to clinopyroxene fractionation in the arc magmas. The negative anomaly of Ti may be accredited to its retention in the sub-arc mantle during melt production and is therefore signature to the arc-related setting (Friend & Nutman 2011).

Two Pipeclay Creek samples, previously classified as basalts, are inconsistent when compared with the other samples on the spider diagrams. They show the island-arc characteristic negative Nb anomaly; however this is coupled with negative anomalies of Th, La, Ce, Pr and enrichment in Y, Yb and Lu. These anomaly types are characteristic of subduction-intiation forearc boninitic basalts (Ishizuka *et al.* 2014). Thus, these samples represent boninitic-affiliated rocks probably formed in the forearc basin of a primitive oceanic island arc.

## 5.4    Interpretation

The geochemical data obtained in this chapter strongly indicates that the Murrawong Creek and Pipeclay Creek formations are closely associated with an island arc, coupled with clasts of chert and basalt with MORB-like affinity that may have been sourced from an accretionary wedge. Bulk sandstone compositions corroborate a juvenile oceanic island arc setting with any link to within-plate sources being disregarded by the $Al_2O_3$-$TiO_2$ diagram (Figure 5.5). The majority of samples are fresh rock within minimal weathering suggesting an active depositional environment.

The magmatic affinity of the clasts of the Murrawong Creek and Pipeclay Creek formations can be interpreted to be mostly calc-alkaline. Tholeiitic magmas exist in a variety of tectonic settings, resulting from shallow partial melting of rising mantle and

therefore shallow differentiation (Winter 2010). Calc-alkaline magmas however are restricted to subduction zones, and thus provide a further indication that the tectonic environment is an arc-related setting.

The tectonic diagrams used for volcanic and plutonic rocks further support the initial interpretation as an island-arc setting. The higher abundance of mobile elements Ba and Th throughout the suite of sampled rocks (excluding boninites) in the MORB array diagrams (Figure 5.9) indicates that the magmatic source is influenced by slab-derived material, thus implying that the source is an arc. These diagrams indicate that the source is slightly more enriched than that of N-MORB, possibly a result of the hydrous phase stimulating depleted primitive mantle. In the Shervais diagram (Figure 5.12) the Murrawong Creek Formation volcanic rocks and clasts clearly plot within the arc-related tholeiites sector, whilst Pipeclay Creek Formation shows a variation between arc-related tholeiites and MORB. The inclusion of clasts with MORB signatures in some of the tectonic discriminant diagrams (Figure 5.9 - Figure 5.12) as well as the older Cambro-Ordovician limestone clasts (Cawood 1976; Engelbretsen 1993; Stewart 1995; Engelbretsen 1996; Brock 1998a, b, 1999; Furey-Greig 2003) may indicate two distinct source rocks: 1) the active island arc (calc-alkaline) and; 2) older MORB-like oceanic crust offscraped into an adjacent accretionary complex.

Sedimentary provenance analysis using tectonic discrimination diagrams has provided a more detailed insight into the sedimentary rock source, interpreted to be an oceanic island arc (Figure 5.17; Figure 5.18). This interpretation is supported by various oceanic-island arc characteristic trends in the spider diagrams (Figure 5.19), for example the enrichment of LILEs compared to HFSEs indicates slab-derived material is incorporated into the partially melted mantle (Ishizuka *et al.* 2014).

Two boninitic clasts within the Pipeclay Creek Formation conglomerate were classified by their characteristic trends on MORB-normalised multiple element diagrams. This interpretation is supported by the presence of a boninitic suite within Figure 5.12, and characteristic petrography of orthopyroxenes and olivine pseudomorphs. This vital information regarding provenance indicates that the sediment was most likely deposited in a forearc basin of a primitive intra-oceanic arc system and the boninitic clasts are being eroded from a nearby uplifting accretionary complex.

The magmatic source of the Murrawong Creek Formation is depleted relative to the mantle, similar to that of MORB, whilst the Pipeclay Creek Formation source was slightly more enriched, suggesting the move to a steady-state of subduction and convection in the mantle wedge (Ishizuka *et al.* 2014). This steady state subduction may have provided a high sediment influx of the subducting slab, resulting in an increase of K to the system. This provides a mechanism to describe the third outlying Pipeclay Creek clast (PCF5.8a), which shows geochemical characteristics of shoshonitic affinity. The presence of these evolved monzonitic magmas lends itself to the interpretation that the Pipeclay Creek Formation is sourced from an arc that has increased in maturity as compared to the sediments of the Murrawong Creek Formation, supporting the results therein Chapter 3 and Chapter 4.

These results largely support the findings of Cawood (1983) whereby through clinopyroxene geochemistry he concluded that the volcanism of a single arc progressed with time from basaltic through to andesitic-dacitic during the Middle Cambrian. The combination of boninitic, tholeiitic, calc-alkaline and shoshonitic related rocks provides excellent provenance association of a primitive oceanic island arc existing during the Late Ordovician which has evolved into the Early Silurian. The sediments have been deposited in a forearc region, confirming the interpretation of Leitch and Cawood (1987). In this setting carbonate reef limestone, accretionary complex basalts (MORBs), primitive supra-subduction zone basalts (boninites), arc-related primitive basalts/andesites through to unroofed plutonic rocks of a more evolved arc system are all incorporated into mass flow style deposits.

# Chapter 6.        Geological Evolution

## 6.1    Geochronology

The detrital zircon ages obtained in this project are younger than the ages obtained by previous biostratigraphic studies (Figure 6.1). While there is no discounting the validity of the Middle to Late Cambrian ages obtained from limestone clasts which host the fossils (Cawood 1976, 1980; Engelbretsen 1993, 1996; Brock 1998a, b, 1999; Furey-Greig 2003; Sloan & Laurie 2004), the Late Ordovician detrital zircon ages obtained from the same units raises questions as to the interpretation that the fossil ages are the same as the depositional age. Both fossiliferous clasts and detrital zircons work on the same principle that the youngest age population represents the maximum depositional age.

Despite the small zircon sample size (6) for the Murrawong Creek Formation, one third of the population resulted in Late Ordovician ages. There is no valid reason to disregard these ages, and thus it is reasonable to say that the Murrawong Creek Formation was deposited at $450 \pm 10$ Ma, during the Late Ordovician. The presence of older zircons within the sample indicates that older, Late Cambrian to Early Ordovician material was being eroded into the sedimentary basin and incorporated into younger sediments prior to deposition. The older zircon population age range coincides with Cawood's (1980) and Stewart's (1995) fossil ages, clarifying these are from a pre-depositional source (Figure 6.1). The oldest Late Cambrian zircons are likely to be sourced from the adjacent Weraerai terrane, representing older oceanic crust that has been incorporated into the sediments via erosion of the accretionary complex. This supports the theory that the limestone clasts are older allochthonous clasts within the conglomerate, most likely from offscraped seamounts also incorporated into and eroded from the accretionary complex or supra-subduction zone ophiolitic basement.
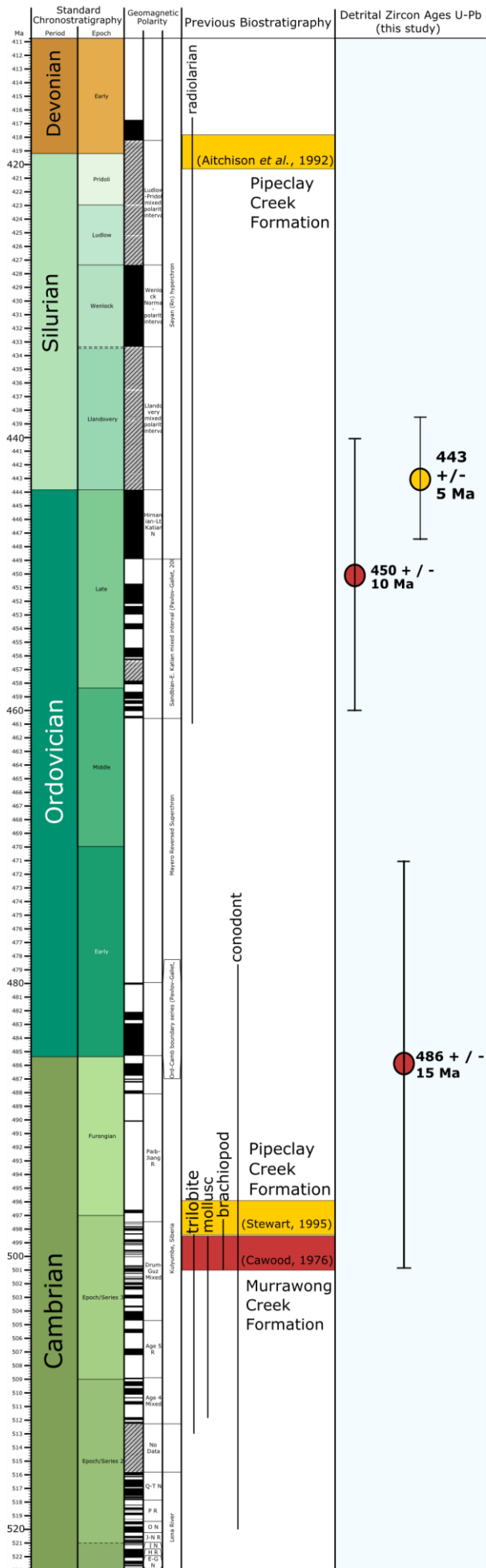
Stewart (1995) argued that the Pipeclay Creek Formation is Late Cambrian in age based on the presence of conodont fauna obtained from thinly bedded dark, spiculitic chert in Copes Creek. However, the field descriptions of the units sampled are not detailed and neither are the conodonts. Given that allochthonous blocks can be several hundreds of metres in length and coupled with the patchy outcrop of the region, it is difficult to confirm whether these units are genuinely autochthonous as argued by Stewart (1995). The youngest detrital zircon age population extracted from the Pipeclay Creek Formation clearly show that the Pipeclay Creek Formation was deposited in latest Ordovician, possibly into the earliest Silurian, at an age of 443.4 ± 4.3 Ma. These results correlate with the age range of the radiolarian fossils found by Aitchison *et al.* (1992), suggesting that this represents the youngest fauna population and therefore maximum depositional age for the Pipeclay Creek Formation (Figure 6.1).

*Figure 6.1 – Timespace plot compares the early biostratigraphic work with the results from this project. This shows that the fossils are obtained from older, allochthonous material that has been incorporated with younger sediments. The minimum age of deposition is indicated by the maximum zircon population ages provided.*

97

## 6.2 Provenance

Previously it has been thought that this volcaniclastic succession is arc-related, with opposing theories as to whether it was an Andean-style continental margin arc (Leitch 1974, 1975; Cawood 1980; Leitch & Cawood 1980; Cawood 1983; Cawood & Leitch 1985) or an intra-oceanic volcanic arc which was later thrust onto the east coast of Gondwana (Leitch & Cawood 1987; Aitchison *et al.* 1992a; Aitchison & Flood 1994). A wide range of geochemical results conclude that these rocks are arc-related, for example; calc-alkaline magma affinity indicates subduction-related magmas, coupled with the high abundance of mobile elements which represent a slab-derived component of the magma. The Shervais (1982) diagram clearly indicates the arc-related nature of these formations with most samples showing arc-related tholeiite affinity along with a boninitic and MORB suite.

The rocks of both the Murrawong and Pipeclay Creek formations have been deposited via sediment-gravity flows, such as debris flows in a submarine environment. Massive bedding is observed throughout the sequence with coarse gravel to boulder grains that are poorly sorted, indicating a mass-flow style of deposition. This lends itself to the interpretation that deposition was under high energy levels and sediment influx eroding off the arc. This interpretation is supported by petrographic identification of glauconite, a mineral characteristic to shallow marine environments. The active tectonic setting of the region results in high volcanic and seismic activity causing small but frequent debris flows off the side of the volcanic arc and into a flanking sedimentary basin, most likely a forearc basin. Active tectonism may have resulted in uplift of the overriding plate, whereby older pelagic sediments from the underlying oceanic crust are incorporated into the newer sediments, explaining the presence of chert and MORB clasts.

Following the determination of an arc-related source, it is important to understand the nature of the volcanic arc; whether it is a continental margin or intra-oceanic arc. The immature nature of the sediment implies an intra-oceanic arc source, given the abundance of tabular feldspars and unstable ferromagnesian minerals. This is coupled with the extremely low abundance of quartz, a mineral likely to be sourced from a continental craton. Sedimentary geochemical analysis produced an oceanic island arc signature on the discrimination diagram from Bhatia (1983) further supporting an intra-oceanic source. The distinct lack of zircons containing a Gondwanan signature age implies the exotic nature of this terrane, indicating that it did not receive any continental detritus input. Thus it is

interpreted that the early Gamilaroi terrane existed as a primitive island arc somewhere within the immense Panthalassan Ocean during the Late Ordovician.

The lithological composition of the sedimentary rocks implies the island arc volcanic source is proximal to the depositional basin. The basal unit (Unit 1) of the Murrawong Creek Formation comprises tabular feldspars indicative of rapid sedimentation. This is followed by Unit 2 of the Murrawong Creek Formation, which comprises mostly angular volcanic lithic fragments, implying that they have been directly deposited off the volcanic arc edifice. This is supported by the presence of interbedded volcanics (Unit 3), keratophyres and basalt flows throughout the area, which are the direct result of localised volcanism. The dominance of volcanic lithic clasts and detritus confirms that deposition of the Pipeclay Creek Formation is also proximal to the volcanic arc.

Cawood (1980) first proposed that the Murrawong Creek Formations volcaniclastic rocks were deposited in a forearc basin of a continental margin arc. He then modified this interpretation to an intra-oceanic island arc in Leitch and Cawood (1987). A forearc basin depositional setting is supported by the results presented in this thesis, whereby the sediments are being shed off the flank of an intra-oceanic island arc and into a proximal depositional basin. The presence of boninitic clasts within the Pipeclay Creek Formation samples, which are rocks characteristic of deposition within a forearc basin of a supra-subduction zone setting, confirm deposition is associated with a forearc basin.

It is apparent that the Murrawong Creek Formation rocks are sourced from an immature, primitive magmatic arc that evolved throughout the Late Ordovician providing the source for the Pipeclay Creek Formation sedimentary rocks. This is supported by the predominance of arc tholeiite and calc-alkaline magma sources for the volcanic clast rocks. The juvenile nature of the arc is highlighted throughout the Murrawong Creek Formations petrographic results, whereby the lithological composition of feldspars, clinopyroxene and amphiboles, coupled with the inherit lack of volcanic quartz confirm that first cycle volcanic detritus was deposited and promptly reworked as mass flows. This mineralogical composition resulted in the sedimentary rocks plotting within the juvenile, undissected arc sector of the Dickinson diagrams. The immature nature of the volcanic source was first realised through the lack of detrital zircons in the sediment, as more evolved, Si-rich magmas are more likely to crystallise zircons. This leads to the interpretation that the Murrawong Creek Formation was deposited adjacent to a primitive volcanic intra-oceanic

island arc, not long after the initiation of subduction of a small tectonic plate under the proto-Pacific plate in the Panthalassan Ocean.

The Pipeclay Creek Formation is sourced from the same volcanic arc, which has progressed into a more evolved source throughout the Late Ordovician. This is evident in hand specimen whereby the presence of granitic clasts amongst a lithological variety of other clasts suggests that the magma has evolved to a more felsic composition. Geochemical analysis expanded on this initial observation in that some of the granitic clasts form monzonites of shoshonitic affinity, highlighting the evolved nature of the magma and possibly indicating an increase in Gondwanan-derived sediments being subducted on the down-going plate and incorporated into the mantle via dehydration. The abundance of zircons with well-developed zoning at almost equal length-width ratios indicate they are sourced from fractionated plutonic magma from the lower crust. This suggests the arc underwent a period of significant erosion, resulting in the unroofing of a plutonic source, possibly the batholithic core of the volcanic system. The plutonic rocks are eroded into the flanking forearc basin and slumped in with the mixture of sediments.

The array of clast types suggests that the Pipeclay Creek Formation clasts are the product of extensively reworked detritus through debris flows. It is apparent that MORB-related and boninitic volcanic rocks are present, suggesting that older oceanic crust has been incorporated into the accretionary complex. The accretionary complex is likely to erode into the forearc basin and hence deposit these older basalts with the younger sediments. The boninitic clasts indicate that reworking of subduction-initiation related forearc rocks is occurring, possibly during uplift of the arc in the late Late Ordovician. The mixture of carbonates, MORBs, boninites, basalts, andesites and granites as erosional clasts within the Pipeclay Creek Formation implies they were deposited via mass flow deposits within a forearc basin of a progressive arc. This supports Cawood (1983) who determined through clinopyroxene geochemistry that these formations were related through deposition in close proximity to a progressive arc. It is likely that the arc system has evolved from subduction-initiation boninitic magmas to arc-tholeiite to calc-alkaline all the way through to shoshonitic magma affinity over the Late Ordovician.

Following deposition, compressional forces due to the convergent margin setting have led to the rocks undergoing epithermal alteration, resulting in low grade pumpellyite-prehnite facies metamorphism. This is shown through characteristic chlorite, epidote and sericite

alteration styles throughout the samples in thin section. It is likely that this island arc setting remained continuous throughout the Silurian and Devonian, and was then thrust onto the continental margin of Gondwana during the Carboniferous (Aitchison *et al.* 1992a; Flood & Aitchison 1992; Aitchison & Buckman 2012).

## 6.3    Regional Correlation

Through these results it appears unlikely that the Murrawong Creek Formation formed as volcaniclastic sediments off the Macquarie Arc, but more likely the result of another subduction zone existing further east in the Panthalassan Ocean (Figure 6.3). The association is dubious due to a lack of zircons of Gondwanan affinity likely to be associated with the Macquarie Arc and the conformable nature of the contact with the early Gamilaroi terrane Pipeclay Creek Formation. It is clear through the zircon dates of both formations that an increase in volcanic activity is occurring around the 450 Ma mark, which is just following the obduction of the Macquarie Arc onto the Gondwanan continent. The Attunga eclogites indicate that subduction was occurring east of Gondwana at 490 Ma (Manton *et al.* In prep.). Following the obduction of the Macquarie Arc, subduction may have increased speed and decreased dip leading to uplift of the overriding plate and the formation of a new volcanic arc that is the early Gamilaroi terrane (Figure 6.3). This interpretation differs from that of  Leitch and Cawood (1987) who, given the proposed Middle Cambrian age of the sequence, suggested that the Murrawong Creek and Pipeclay Creek formations may represent an early phase of the Macquarie arc.

The implications this has on previous tectonic models for the southern NEO are that these results support the hypothesis that multiple subduction zones existed within the Panthalassan Ocean during the Early Paleozoic, as suggested by Scheibner (1973) and Aitchison *et al.* (1988). It seems that the occurrence of a single long-lived westward dipping subduction zone is less likely. This supports the continental growth model of Aitchison and Buckman (2012) and the terrane model of Aitchison *et al.* (1992a), whereby the Gamilaroi terrane existed as an exotic terrane offshore from the Gondwanan continent which was later accreted following westward progression of the arc, likely due to rollback of the subducting plate.
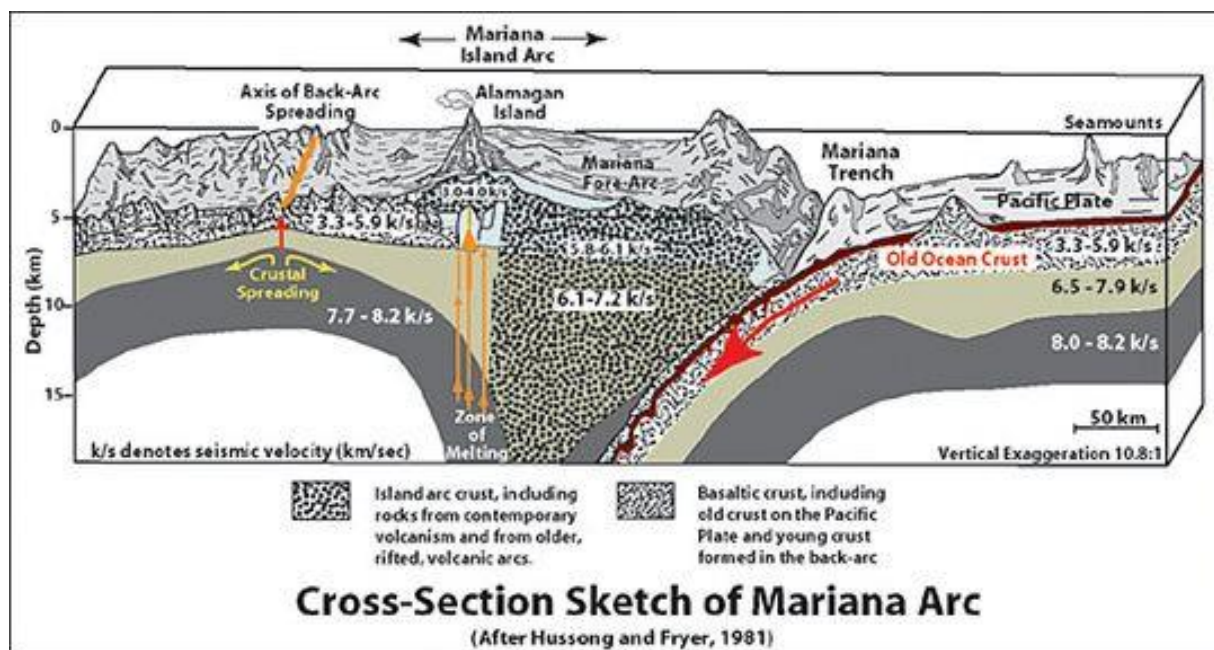
*Figure 6.2 - Marianas subduction zone system, from Schultz (2011).*

A modern analogue of the interpreted tectonic and depositional setting is the Marianas subduction zone and forearc basin (Figure 6.2). The Marianas subduction zone is an intra-oceanic island arc, which shows evidence of rifting, given that arc magmas are found to be depleted and thus formed from extension of crust (Stern & Bloomer 1992). An extrusive sequence of depleted and ultra-depleted magmas produced forearc basalts, boninitic, arc-tholeiite and calc-alkaline related rocks which make up the stratigraphy of the Marianas forearc (Stern & Bloomer 1992; Ishizuka *et al.* 2014). This is similar to that which likely occurred in the forearc basin of the Gamilaroi terrane, whereby rollback is likely to have occurred forming an extensional regime, with the trench advancing towards Gondwana. Extensional arc systems such as this provide a mechanism under which arcs eventually collide, and obduct onto continental margins, commonly followed by a polarity flip in subduction direction (e.g., Cooper & Taylor 1987; Aitchison *et al.* 1999; Dewey 2005). This can be correlated to the quantum tectonic model of Aitchison and Buckman (2012), whereby polarity flip occurs following the obduction of an arc onto a continental margin.
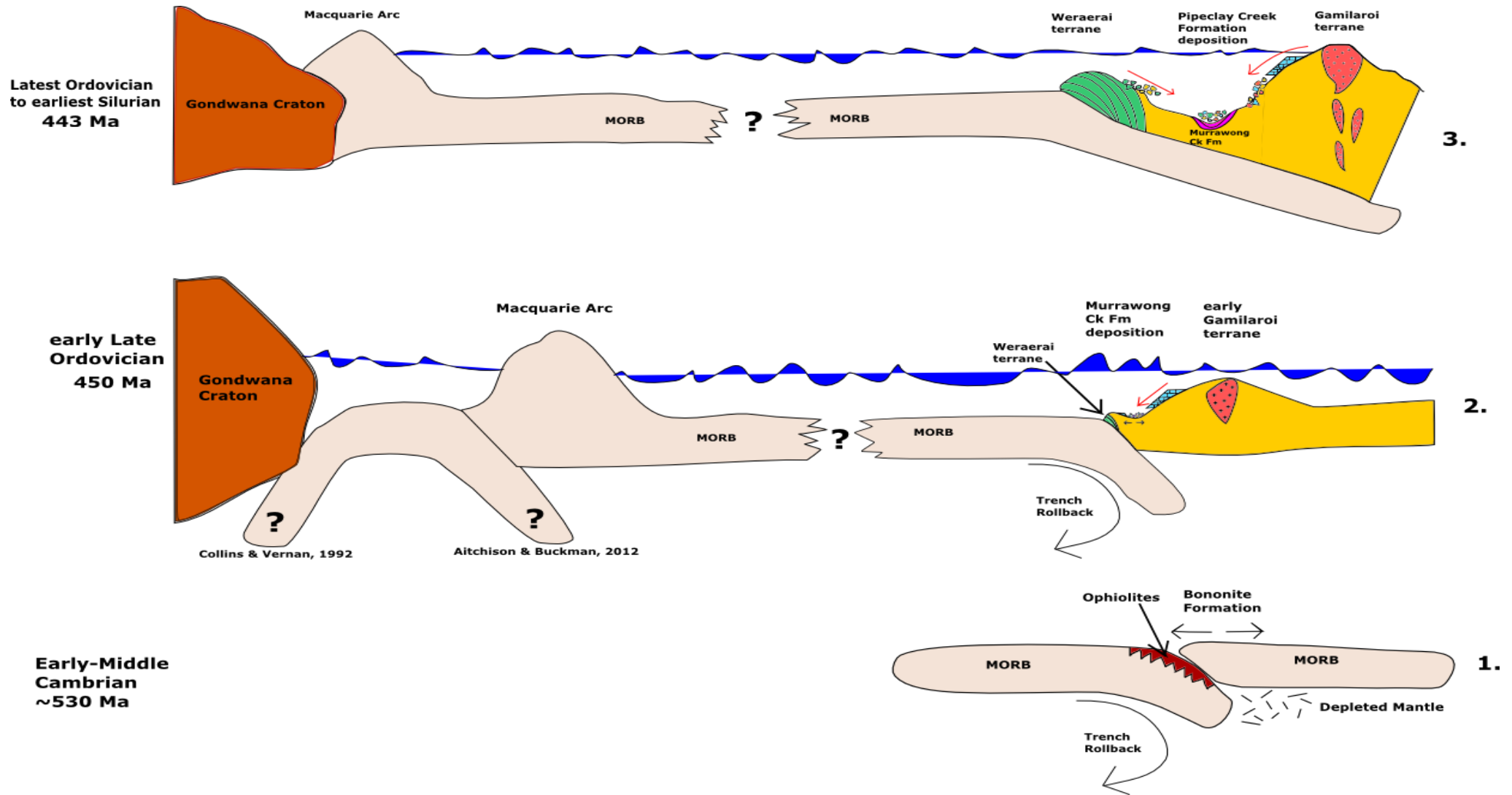
Figure 6.3 - **1.** As denser oceanic crust begins to sink, forming a subduction zone, space is created in the supra-subduction zone. This causes rapid extension to fill the space along with large degrees of partial melting of the mantle. Boninites are formed as a result of this rapid extension, whilst ophiolites are incorporated into the subduction complex mélange. **2.** As the island arc begins to form, older MORB is incorporated into the sediment. The magma is of arc tholeiite to calc-alkaline affinity producing basaltic andesites, which are incorporated into volcanic debris and deposited. **3.** The arc has evolved following the obduction of the Macquarie arc onto Gondwana, giving rise to decreased dip of the subduction zone. The arc is undergoing erosion, exposing the igneous intrusive core. Thus plutonic rocks are incorporated into the system, along with volcanics, carbonates and accretionary complex rocks.

## 6.4   Conclusions

Through detrital zircon geochronology using the SHRIMP at ANU it was determined that the age of the Murrawong Creek Formation is younger than previous estimates of Middle Cambrian age, at 450 ± 10 Ma (early Late Ordovician). There is no doubting that the limestone clasts from which the biostratigraphic age was determined were deposited in the Middle Cambrian, however the results presented here highlight that the age of sediment deposition cannot necessarily be inferred from clast ages. Despite the small yield of only six zircon grains, the detrital zircons were sampled across strike and thus represent the majority of the sequence. There is no valid reason to reject the youngest zircon population, so it can be concluded that the Murrawong Creek Formation is ca. 460 – 440 Ma. Ar-Ar dating of detrital clinopyroxenes within the Murrawong Creek Formation would improve further studies given these immature sediments contain a relatively high abundance of clinopyroxene with a distinct lack of zircons. The Pipeclay Creek Formation yielded thousands of zircons from a conglomerate lens at Chaffey Dam, NSW. From this data it can be said that the Pipeclay Creek Formation is latest Ordovician in age at 443.4 ± 4.3 Ma. This is significantly younger than the biostratigraphic age of Middle Cambrian, however the field relations of the chert in which conodonts were returned are unavailable. Determining the nature of the chert, i.e. allochthonous or autochthonous, would prove useful in further research. The zircons analysed from the Pipeclay Creek Formation sample produced clean data from a location along strike from the conodont location, and therefore should not be disregarded. These results provide the first successful attempt at radiometric dating of the volcaniclastic matrix of the Early Paleozoic rocks of the New England Orogen determining that the fossiliferous limestone was not formed simultaneous with deposition.

A key objective of this project was to test the two opposing provenance models for the depositional setting of the Murrawong and Pipeclay Creek formations: 1) the rocks were deposited in a forearc basin of an oceanic arc situated just off the coast of Gondwana, separated by only a small back-arc basin which closed up during the Late Devonian, resulting in a continental margin arc, or; 2) the rocks formed in an exotic island arc terrane far from Gondwana and were later accreted onto the continent. The absence of Proterozoic Gondwanan-derived zircons within these sedimentary rocks immediately highlights that it is unlikely the sediments have any Gondwanan affinity. This is supported by QFL diagrams, whereby the quartz-poor sediments indicate deposition within an undissected

arc. Boninitic clasts identified via geochemical analysis provide a forearc basin signature for the depositional setting, which is highlighted by the presence of accretionary complex rocks of MORB-like volcanic rocks and cherts. These findings suggest that the Murrawong Creek Formation is an early Gamilaroi terrane sequence from a primitive island arc that came into existence in the Early Ordovician following subduction initiation. With evolution of the arc following the obduction of the Macquarie arc onto the Gondwanan continent in the Late Ordovician, an erosional unroofing of plutonic arc rocks ensued and the Pipeclay Creek Formation was deposited. Simultaneous uplift and erosion of the adjacent accretionary complex occurred and thus clasts of this nature were also incorporated into the sedimentary rocks.

These findings decrease the likelihood of the 'consensus model' of a single long-lived westward dipping subduction zone on the Gondwanan continental margin, however highlight the probability that many island arcs and therefore subduction zones existed in the Panthalassan Ocean during the Early Paleozoic. Following these findings the proposed model for the Gamilaroi terrane is that it was an intra-oceanic island arc that came into existence in the Early Ordovician. The arc migrated westwards due to east-dipping subduction and was accreted onto the Gondwanan continent in the latest Devonian with subsequent west-dipping subduction. Thus, it is unlikely that the island arc was associated with Gondwana through separation by a back-arc basin, but rather it represents an exotic terrane from somewhere in the vast expanse of the Panthalassan Ocean in the Late Ordovician.

# Chapter 7. Reference List

AITCHISON, J. C., BLAKE, M. C., FLOOD, P. G. & MURCHEY, B. L. 1988. New and revised lithostratigraphic units from the south-western New England Fold Belt. *Q.N. Geol. Surv. N.S.W.,* 72**,** 10-16.

AITCHISON, J. C. & BUCKMAN, S. 2012. Accordian vs. quantum tectonics: Insights into continental growth processes from the Paleozoic of eastern Gondwana. *Gondwana Research,* 22**,** 674-680.

AITCHISON, J. C., DAVIS, A. M., STRATFORD, J. M. & SPILLER, F. C. 1999. Lower and middle Devonian radiolarian biozonation of the Gamilaroi terrane New England Orogen, eastern Australia. *Micropaleontology***,** 138-162.

AITCHISON, J. C. & FLOOD, P. G. 1992. Early Permian transform margin development of the southern New England Orogen, eastern Australia (eastern Gondwana. *Tectonics,* 11**,** 1385-1391.

AITCHISON, J. C. & FLOOD, P. G. 1994. Gamilaroi Terrane: A Devonian rifted intra-oceanic island-arc assemblage, NSW, Australia. *Geological Society Special Publication,* 81**,** 155-168.

AITCHISON, J. C., FLOOD, P. G. & SPILLER, F. C. P. 1992a. Tectonic setting and paleoenvironment of terranes in the southern New England orogen, eastern Australia as constrained by radiolarian biostratigraphy. *Pelaeogeography, Palaeoclimatology, Palaeoecology,* 94**,** 31-54.

AITCHISON, J. C., IRELAND, T. R., BLAKE, M. C. & FLOOD, P. G. 1992b. 530Ma zircon age for ophiolite from the New England Orgoen: Oldest rocks known from eastern Australia. *Geology,* 20**,** 125-128.

AITCHISON, J. T. & IRELAND, T. 1995. Age profile of ophiolitic rocks across the Late Palaeozoic New England Orogen, New South Wales: implications for tectonic models. *Australian Journal of Earth Sciences,* 42**,** 11-23.

ALBARÈDE, F. 2003. *Geochemistry: an introduction*, Cambridge University Press.

BENSON, W. 1918. The geology and petrology of the Great Serpentine Belt of New South Wales. Part viii. The extension of the Great Serpentine Belt from the Nundle district to the coast. *Proceedings of the Linnean Society of New South Wales,* 43**,** 593-599.

BHATIA, M. R. 1983. Plate tectonics and geochemical composition of sandstones. *The Journal of Geology***,** 611-627.

BLACK, L. P., KAMO, S. L., WILLIAMS, I. S., MUNDIL, R., DAVIS, D. W., KORSCH, R. J. & FOUDOULIS, C. 2003. The application of SHRIMP to Phanerozoic geochronology; a critical appraisal of four zircon standards. *Chemical Geology,* 200**,** 171-188.

BOGGS, J. S. 2009. *Petrology of Sedimentary Rocks,* Cambridge, Cambridge University Press.

BOGGS, J. S. 2011. *Principles of Sedimentology and Stratigraphy,* USA, Pearson.

BROCK, G. A. 1998a. Middle Cambrian articulate brachiopods from the southern New England Fold Belt, northeastern N.S.W., Australia. *Journal of Paleontology,* 72**,** 604-619.

BROCK, G. A. 1998b. Middle Cambrian molluscs from the southern New England Fold Belt, New South Wales, Australia. *Geobios,* 31**,** 571-586.

BROCK, G. A. 1999. An unusual micromorphic brachiopod from the Middle Cambrian of north-eastern New South Wales, Australia. *Records of the Australian Museum,* 51**,** 179-186.

BUCKMAN, S. 1993. *The Geology north of the Barnard River at Barry Station: Evidence of early Permian strike-slip faulting and basin development.* Bachelor of Science, University of Sydney.

BUCKMAN, S., NUTMAN, A. P., AITCHISON, J. C., PARKER, J., BEMBRICK, S., LINE, T., HIDAKA, H. & KAMIICHI, T. 2015. The Watonga Formation and Tacking Point Gabbro, Port Macquarie, Australia: Insights into crustal growth mechanisms on the eastern margin of Gondwana. *Gondwana Research,* In press.

CAWOOD, P. A. 1976. Cambro-Ordovician strata, northern New South Wales. *Search,* 7**,** 317-318.

CAWOOD, P. A. 1980. *The geological development of the New England Fold Belt in the Woolomin-Nemingha and Wiseman's Arm Regions: the evolution of a Palaeozoic forearc terrane.* PhD, University of Sydney.

CAWOOD, P. A. 1983. Modal composition and detrital clinopyroxene geochemistry of lithic sandstones from the New England Fold Belt (east Australia): A Paleozoic forearc terrane. *Geological Society of America Bulletin,* 94**,** 1199-1214.

CAWOOD, P. A. 2005. Terra Australis Orogen: Rodinia breakup and development of the Pacific and Iapetus margins of Gondwana during the Neoproterozoic and Paleozoic. *Earth-Science Reviews,* 69**,** 249-279.

CAWOOD, P. A., HAWKESWORTH, C. J. & DHUIME, B. 2012. Detrital zircon record and tectonic setting. *GEOLOGY,* 40**,** 875-878.

CAWOOD, P. A., KRÖNER, A., COLLINS, W. J., KUSKY, T. M., MOONEY, W. D. & WINDLEY, B. F. 2009. Accretionary orogens through Earth History. *Geological Society of London Special Publications,* 318**,** 1-36.

CAWOOD, P. A. & LEITCH, E. C. (eds.) 1985. *Accretion and dispersal tectonics of the southern New England Fold Belt, eastern Australia*: Circum-Pacific Council for Energy and Mineral Resources, Earth Science Series.

COLLINS, W. J. 2002. Nature of extensional accretionary orogens. *Tectonics,* 21**,** 6-1 - 6-12.

COOPER, P. & TAYLOR, B. 1987. Seismotectonics of New Guinea: A model for arc reversal following arc‐continent collision. *Tectonics,* 6**,** 53-67.

CORFU, F., HANCHAR, J. M., HOSKIN, P. W. O. & KINNY, P. 2003. Atlas of Zircon Textures. *In:* HANCHAR, J. M. & HOSKIN, P. W. O. (eds.) *Zircon, Reviews in Mineralogy and Geochemistry.* Washington: Mineralogical Society of America.

COX, K. G., BELL, J. D. & PANKHURST, R. J. 1979. *The interpretation of igneous rocks*, G. Allen & Unwin London.

CROOK, K. A. W. 1961. Stratigraphy of the Tamworth Group (Lower and Middle Devonian), Tamworth - Nundle district, N.S.W. *J. Proc. R. Soc. N.S.W.,* 94**,** 173-188.

DEER, W. A., HOWIE, R. & ZUSSMAN, J. 1996. *An Introduction to the Rock Forming Minerals,* Harlow, Prentice-Hall.

DEFANT, M. J., MAURY, R. C., RIPLEY, E. M., FEIGENSON, M. D. & JACQUES, D. 1991. An example of island-arc petrogenesis: geochemistry and petrology of the southern Luzon arc, Philippines. *Journal of Petrology,* 32**,** 455-500.

DEWEY, J. F. 2005. Orogeny can be very short. *Proceedings of the National Academy of Sciences of the United States of America,* 102**,** 15286-15293.

DEWEY, J. F. & BIRD, J. M. 1970. Plate tectonics and geosynclines. *Tectonophysics,* 10**,** 625-638.

DICKINSON, W. R., BEARD, L. S., BRAKENRIDGE, G. R., ERJAVEC, J. L., FERGUSON, R. C., INMAN, K. F., KNEPP, R. A., LINDBERG, F. A. & RYBERG, P. T. 1983. Provenance of North American Phanerozoic sandstones in relation to tectonic setting. *Geological Society of America Bulletin,* 94**,** 222-235.

DICKINSON, W. R. & SUCZEK, C. A. 1979. Plate tectonics and sandstone compositions. *The American Association of Petroleum Geologists Bulletin,* 63**,** 2164-2182.

ENGELBRETSEN, M. 1993. A Middle Cambrian possible cnidarian from the Murrawong Creek Formation, NE New South Wales. *Memoirs of the Association of Australiasian Palaeontologists,* 15**,** 51-56.

ENGELBRETSEN, M. 1996. Middle Cambrian lingulate brachiopods from the Murrawong Creek Formation, northeastern New South Wales. *Historical Biology,* 11**,** 69-99.

FERGUSSON, C. L., NUTMAN, A. P., KAMIICHI, T. & HIDAKA, H. 2013. Evolution of a Cambrian active continental margin: The Delamerian–Lachlan connection in southeastern Australia from a zircon perspective. *Gondwana Research,* 24**,** 1051-1066.

FISHER, R. V. 1961. Proposed classification of volcaniclastic sediments and rocks. *Geological Society of America Bulletin,* 72**,** 1409-1414.

FISHER, R. V. & SMITH, G. A. 1991. *Volcanism, Tectonics and Sedimentation*.

FLOOD, P. G. & AITCHISON, J. C. 1992. Late Devonian accretion of the Gamilaroi Terrane to eastern Gondwana: Provenance linkage suggested by the first appearance of Lachlan Fold Belt-derived quartzarenite. *Australian Journal of Earth Sciences,* 39**,** 539-544.

FLOYD, P. & WINCHESTER, J. 1975. Magma type and tectonic setting discrimination using immobile elements. *Earth and Planetary science letters,* 27**,** 211-218.

FOLK, R. L. 1974. *Petrology of Sedimentary Rocks,* Austin, Texas, Hemphill Publishing Co.

FRIEND, C. & NUTMAN, A. P. 2011. Dunites from Isua, Greenland: A ca. 3720 Ma window into subcrustal metasomatism of depleted mantle. *Geology,* 39**,** 663-666.

FROLOVA, Y. V. 2008. Specific features in the composition, structure, and properties of volcaniclastic rocks. *Moscow University Geology Bulletin,* 63**,** 28-37.

FUREY-GREIG 1999. Late Ordovician conodonts from the olistostromal Wisemans Arm Formation (New England region, Australia). . *Abhandlungen der Geologischen Bundesanstalt,* 54**,** 303-321.

FUREY-GREIG 2000. Late Ordovician (Eastonian) conodonts from the Early Devonian Drik Drik Formation, Woolomin area, eastern Australia. *Records of the Western Australian Museum,* 58**,** 133-143.

FUREY-GREIG 2003. Middle Ordovician conodonts from the Haedon Formation, north-eastern New South Wales. *Courier Forschungsinstitut,* 245**,** 315-325.

GEHRELS, G. 2014. Detrital zircon U-Pb geochronology applied to tectonics. *Annual Reviews of Earth Planetary Sciences,* 42**,** 127-149.

GLEN, R. 2005. The Tasmanides of eastern Australia. *Geological Society, London, Special Publications,* 246**,** 23-96.

GLEN, R. A., QUINN, C. D. & COOKE, D. R. 2012. The Macquarie Arc, Lachlan Orogen, New South Wales: its evolution, tectonic setting and mineral deposits. *Episodes,* 35**,** 177-186.

GOESCH, E. 2011. *Petrology, geochemistry, U-Pb zircon ages and structure of the Yiddah Porphyry Cu-(Au-Mo) prospect of the Late Macquarie Arc, NSW.* Bachelor of Science, University of Wollongong.

HALL, R. Late Ordovician coral faunas from northeastern New South Wales.  J. Proc. R. Soc. NSW, 1975. 75-93.

HARKER, A. 1909. *The natural history of igneous rocks*, Cambridge University Press.

ISHIZUKA, O., TANI, K. & REAGAN, M. K. 2014. Izu-Bonin-Mariana forearc crust as a modern ophiolite analogue. *Elements,* 10**,** 115-120.

JANOUSEK, V., FARROW, C. M. & ERBAN, V. 2006. Interpretation of Whole-rock Geochemical Data in Igneous Geochemistry: Introducing Geochemical Data Toolkit (GCDkit). *Journal of Petrology,* 47**,** 1255-1259.

KACHOVICH, S. 2013. *Significance of Radiolarian biostratigraphy of the southern New England Orogen, New South Wales.* Bachelor of Science Honours, University of Wollongong.

KORSCH, R. J., ADAMS, C. J., BLACK, L. P., FOSTER, D. A., FRASER, G. L., MURRAY, C. G., FOUDOULIS, C. & GRIFFIN, W. L. 2009. Geochronology and provenance of the Late Paleozoic accretion wedge and Gympie Terrane, New England Orogen, eastern Australia. *Australian Journal of Earth Sciences: An International Geoscience Journal of the Geological Society of Australia,* 56**,** 655-685.

KORSCH, R. J., CAWOOD, P. A. & NEMCHIN, A. A. Geochemical and geochronological evolution of the Tamworth Belt, southern New England Orogen. *In:* BUCKMAN, S., ed. New England Orogen, 2010, 2010 University of New England, Armidale. University of New England.

LE BAS, M. J., LE MAITRE, R., STRECKEISEN, A. & ZANETTIN, B. 1986. A chemical classification of volcanic rocks based on the total alkali-silica diagram. *Journal of petrology,* 27**,** 745-750.

LE MAITRE, R. W., STRECKEISEN, A., ZANETTIN, B., LE BAS, M., BONIN, B. & BATEMAN, P. 2002. *Igneous rocks: a classification and glossary of terms: recommendations of the International Union of Geological Sciences Subcommission on the Systematics of Igneous Rocks*, Cambridge University Press.

LEAT, P., PEARCE, J., BARKER, P., MILLAR, I., BARRY, T. & LARTER, R. 2004. Magma genesis and mantle flow at a subducting slab edge: the South Sandwich arc-basin system. *Earth and Planetary Science Letters,* 227**,** 17-35.

LEEDER, M. R. 1982. *Sedimentology: Process and Product,* London, Unwin Hyman Ltd.

LEITCH, E. C. 1974. The geological development of the southern part of the New England Fold Belt. *Journal of the Geological Society of Australia,* 21**,** 133-156.

LEITCH, E. C. 1975. Plate Tectonic Interpretation of the Paleozoic History of the New England Fold Belt. *Geological Society of America Bulletin,* 86**,** 141-144.

LEITCH, E. C. & CAWOOD, P. A. 1980. Olistoliths and debris flow deposits at ancient consuming plate margins; an eastern Australian example. *Sedimentary Geology,* 25**,** 5-22.

LEITCH, E. C. & CAWOOD, P. A. 1987. Provenance determination of volcaniclastic rocks: the nature and tectonic significance of a Cambrian conglomerate from the New England Fold Belt, eastern Australia. *Journal of Sedimentary Research,* 57.

LOWE, D. R. 1982. Sediment gravity flows: II Depositional models with special reference to the deposits of high-density turbidity currents. *Journal of Sedimentary Research,* 52.

LUDWIG, K. 1998. Using Isoplot/Ex Version 1.00 b: A Geochronological Toolkit for Microsoft Excel, Berkeley Geochronology Center. *Spec. Pub*.

MANTON, R., BUCKMAN, S., NUTMAN, A. P., BENNETT, V. & BELOUSOVA, E. In prep. The late Cambrian eclogite at Attunga, New South Wales: Panthlassan juvenile suprasubduction zone crust trapped in Gondwana's eastern margin.

MARSAGLIA, K. 1995. Interarc and backarc basins. *Tectonics of sedimentary basins***,** 299-329.

MARSAGLIA, K. M. & INGERSOLL, R. V. 1992. Compositional trends in arc-related, deep-marine sand and sandstone: A reassessment of magmatic arc provenance. *Geological Society of America Bulletin,* 104**,** 1637-1649.

MAWSON, R., TALENT, J. & FUREY-GREIG, T. 1995. Coincident conodont faunas (late Emsian) from the Yarrol and Tamworth belts of northern New South Wales and central Queensland. *Courier Forschungsinstitut Senckenberg,* 182**,** 421-445.

MIDDLEMOST, E. A. 1985. Magmas and magmatic rocks: An introduction to igneous petrology.

MIYASHIRO, A. 1974. Volcanic rock series in island arcs and active continental margins. *American Journal of Science,* 274**,** 321-355.

MÜLLER, D.-G. D., ROCK, N. & GROVES, D. 1992. Geochemical discrimination between shoshonitic and potassic volcanic rocks in different tectonic settings: a pilot study. *Mineralogy and Petrology,* 46**,** 259-289.

MURRAY, C. G. (ed.) 1997. *From geosyncline to fold belt: a personal perspective on the development of ideas regarding the tectonic evolution of the New England Orogen,* Springwood, NSW: Geological Society of Australia Special Publication.

NICHOLS, G. 2009. *Sedimentology and stratigraphy*, John Wiley & Sons.

NUTMAN, A. P., BUCKMAN, S., HIDAKA, H., KAMIICHI, T., BELOUSOVA, E. & AITCHISON, J. 2013. Middle Carboniferous-Early Triassic eclogite–blueschist blocks within a serpentinite mélange at Port Macquarie, eastern Australia: Implications for the evolution of Gondwana's eastern margin. *Gondwana Research,* 24**,** 1038-1050.

OCH, D. J., LEITCH, E. C., GRAHAM, I. T. & CARPRELLI, G. The geology of the Port Macquarie-Tacking Point coastal tract.  SGGMP-Port Macquarie 2005, First biennial conference, 2005 Port Macquarie. Specialist Group in Geochemistry, Mineralogy and Petrology, Geological Society of Australia, 95-99.

OCH, D. J., PERCIVAL, I. G. & LEITCH, E. C. 2007. Ordovician conodonts from the Watonga Formation, Port Macquarie, northeast New South Wales. *Proceedings of the Linnean Society of New South Wales,* 128**,** 209-216.

OFFLER, R. & GAMBLE, J. 2002. Evolution of an intra-oceanic island arc during the Late Silurian to Late Devonian, New England Fold Belt. *Australian Journal of Earth Sciences,* 49**,** 349-366.

OFFLER, R. & MURRAY, C. 2011. Devonian volcanics in the New England Orogen: tectonic setting and polarity. *Gondwana Research,* 19**,** 706-715.

OHTA, T. & ARAI, H. 2007. Statistical empirical index of chemical weathering in igneous rocks: A new tool for evaluating the degree of weathering. *Chemical Geology,* 240**,** 280-297.

PEARCE, J. 1996. A user's guide to basalt discrimination diagrams.
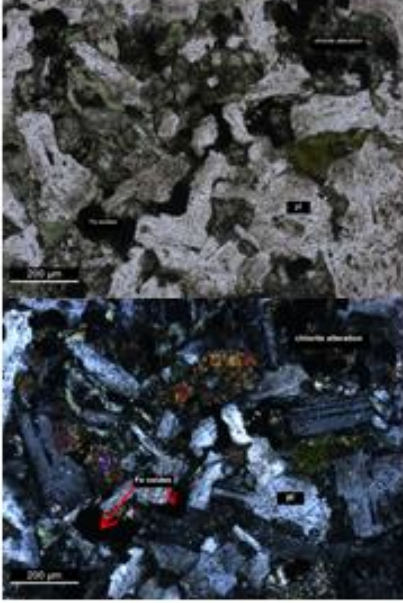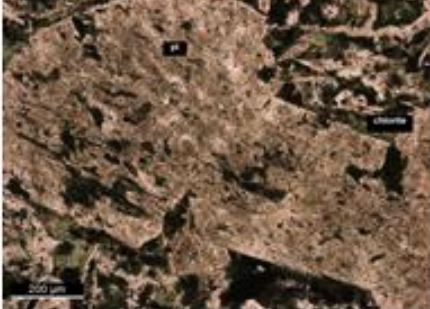
PEARCE, J. & PEATE, D. 1995. Tectonic implications of the composition of volcanic arc magmas. *Annual Review of Earth and Planetary Sciences,* 23**,** 251-286.

PEARCE, J. A. 1982. Trace element characteristics of lavas from destructive plate boundaries. *Andesites***,** 525-548.

PEARCE, J. A. 1983. Role of the subcontinental lithosphere in magma genesis at active continental margins.

PEARCE, J. A. 2014. Immobile Element Fingerprinting of Ophiolites. *Elements,* 10**,** 101-108.

PEARCE, J. A. & CANN, J. 1973. Tectonic setting of basic volcanic rocks determined using trace element analyses. *Earth and planetary science letters,* 19**,** 290-300.

PEARCE, J. A., HARRIS, N. B. & TINDLE, A. G. 1984. Trace element discrimination diagrams for the tectonic interpretation of granitic rocks. *Journal of petrology,* 25**,** 956-983.

PEARCE, J. A. & PARKINSON, I. J. 1993. Trace element models for mantle melting: application to volcanic arc petrogenesis. *Geological Society, London, Special Publications,* 76**,** 373-403.

PETTIJOHN, F., POTTER, P. & SIEVER, R. 1974. Sand and Sandstone. *Soil Science,* 117**,** 130.

PETTIJOHN, F. J. 1954. Classification of Sandstones. *The Journal of Geology,* 62**,** 360-365.

QUINN, C. D. & PERCIVAL, I. G. Correlating Ordovician elements of the Lachlan and New England orogens, eastern Australia. *In:* BUCKMAN, S., ed. New England Orogen 2010, 2010 Armidale. Armidale, NSW: University of New England.

READING, H. G. 1996. *Sedimentary Environments: processes, facies, and stratigraphy*, Blackwell Science.

REID, R. P., CAREY, S. N. & ROSS, D. R. 1996. Late Quaternary sedimentation in the Lesser Antilles island arc. *Geological Society of America Bulletin,* 108**,** 78-100.

ROLLINSON, H. 1993. *Using geochemical data: evaluation presentation, interpretation,* New York, USA, Longman Group UK and John Wiley & Sons, NY.

ROSER, B. P. & KORSCH, R. J. 1986. Determination of Tectonic Setting of Sandstone-Mudstone Suites Using [image] Content and [image] Ratio. *The Journal of Geology,* 94**,** 635-650.

ROSER, B. P. & KORSCH, R. J. 1988. Provenance signatures of sandstone-mudstone suites determined using discriminant function analysis of major-element data. *Chemical Geology,* 67**,** 119-139.

SCHEIBNER, E. 1973. A plate tectonic model of the Palaeozoic tectonic history of New South Wales. . *Journal of the Geological Society of Australia,* 20**,** 405-426.

SCHEIBNER, E. 1996. *Geology of New South Wales - Synthesis: Structural Framework*, Department of Mineral Resources.

SCHULTZ, T. 2011. *The Mariana Trench, The Deepest Part of The Ocean* [Online]. Scienceray. Available: http://scienceray.com/earth-sciences/the-mariana-trench-the-deepest-part-of-the-ocean/#ixzz3Vw7o5eVY [Accessed 31/03 2015].

SHERVAIS, J. W. 1982. Ti-V plots and the petrogenesis of modern ophiolitic lavas. *Earth and Planetary Science Letters,* 59**,** 101-118.

SLOAN, T. R. & LAURIE, L. R. 2004. Middle Cambrian trilobites from allochthonous blocks in the Murrawong Creek Formation, N.S.W. *Memoirs of the Association of Australiasian Palaeontologists,* 30**,** 193-206.

STERN, R. J. & BLOOMER, S. H. 1992. Subduction zone infancy: examples from the Eocene Izu-Bonin-Mariana and Jurassic California arcs. *Geological Society of America Bulletin,* 104**,** 1621-1636.

STEWART, I. 1995. Cambrian age for the Pipeclay Creek Formation, Tamworth Belt, northern New South Wales. *Courier Forschungsinstitut,* 182**,** 565-566.

STRATFORD, J. M. C. & AITCHISON, J. C. 1996. Devonian intra-oceanic arc rift sedimentation - facies development in the Gamilaroi terrane, New England orogen, eastern Australia. *Sedimentary Geology,* 101**,** 173-192.

STRATFORD, J. M. C. & AITCHISON, J. C. 1997. Geochemical evolution within a Devonian intra-oceanic island arc: The Gamilaroi terrane, southern New England orogen, Australia. *The Island Arc,* 6**,** 213-227.

SUN, S.-S. & MCDONOUGH, W. 1989. Chemical and isotopic systematics of oceanic basalts: implications for mantle composition and processes. *Geological Society, London, Special Publications,* 42**,** 313-345.

TATSUMI, Y. 1989. Migration of fluid phases and genesis of basalt magmas in subduction zones. *Journal of Geophysical Research: Solid Earth (1978–2012),* 94**,** 4697-4707.

TAYLOR, S. R. & MCLENNAN, S. M. 1985. The continental crust: its composition and evolution.

UNDERWOOD, M. B., BALLANCE, P. F., CLIFT, P. D., HISCOTT, R. N., MARSAGLIA, K. M., PICKERING, K. T. & REID, R. P. 1995. Sedimentation in forearc basins, trenches, and collision zones of the western Pacific: a summary of results from the Ocean Drilling Program. *Active margins and marginal basins of the Western Pacific***,** 315-353.

VOISEY, A. H. 1957. Further remarks on the sedimentary formations of New South Wales. *J. Proc. R. Soc.,* 91**,** 165-188.

WATKINS, R. 1985. Volcaniclastic and carbonate sedimentation in late Paleozoic island-arc deposits, Eastern Klamath Mountains, California. *Geology,* 13**,** 709-713.

WELTJE, G. J. & VON EYNATTEN, H. 2004. Quantitative provenance analysis of sediments: review and outlook. *Sedimentary Geology,* 171**,** 1-11.

WILLIAMS, I. S. 1998. *U-Th-Pb Geochronology by Ion Microprobe*, Reviews in Economic Geology.

WILSON, B. M. 1989. *Igneous petrogenesis a global tectonic approach*, Springer Science & Business Media.

WINTER, J. D. 2010. *Principles of igneous and metamorphic petrology*, Prentice Hall New York.

# Chapter 8.     Appendices
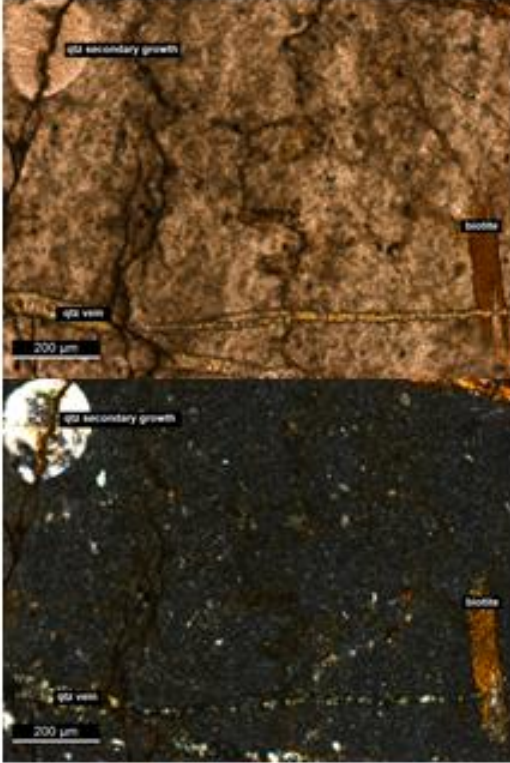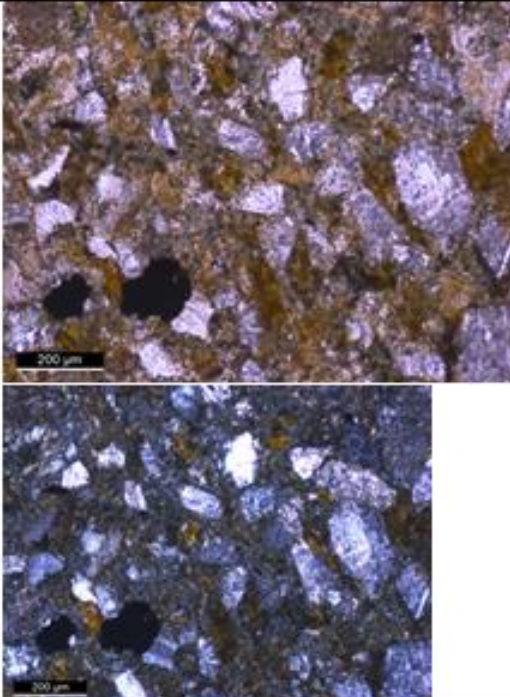
# Appendix 1
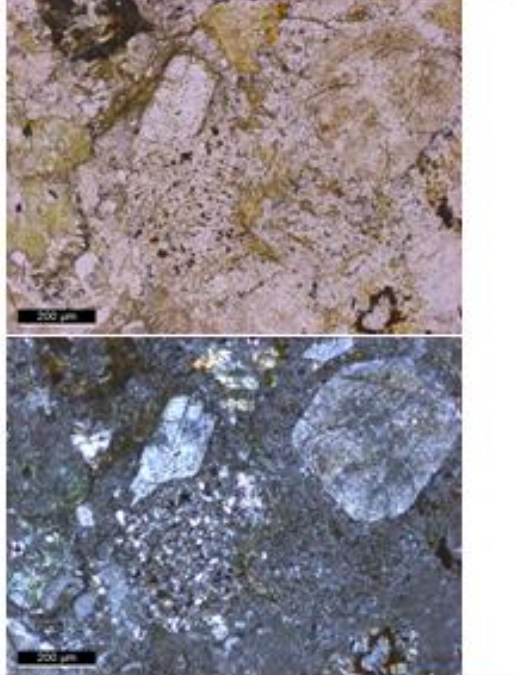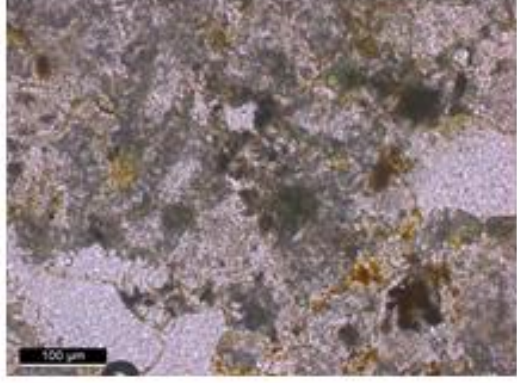
**Sample Database: Hand Specimen and Thin Section Descriptions**
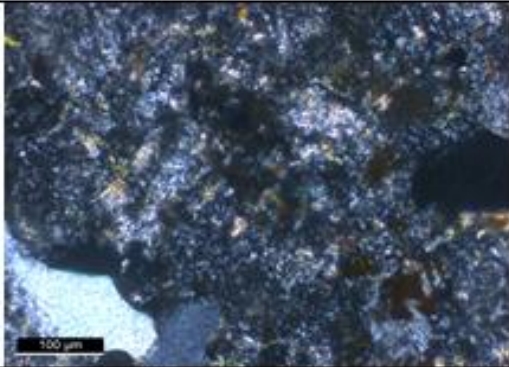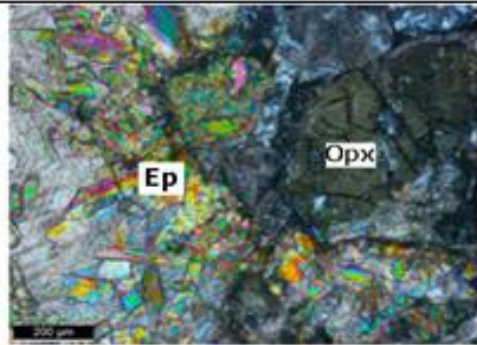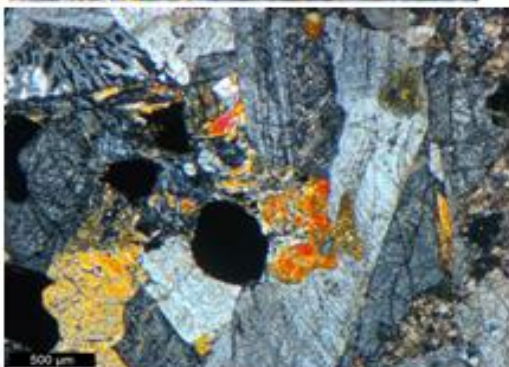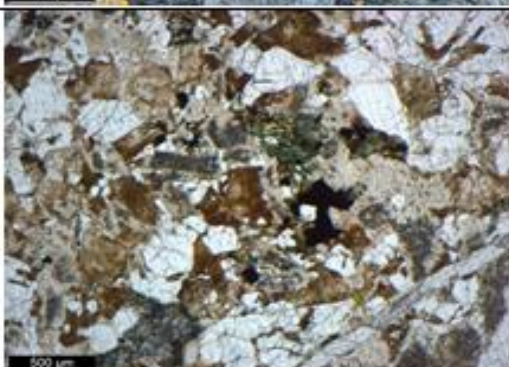
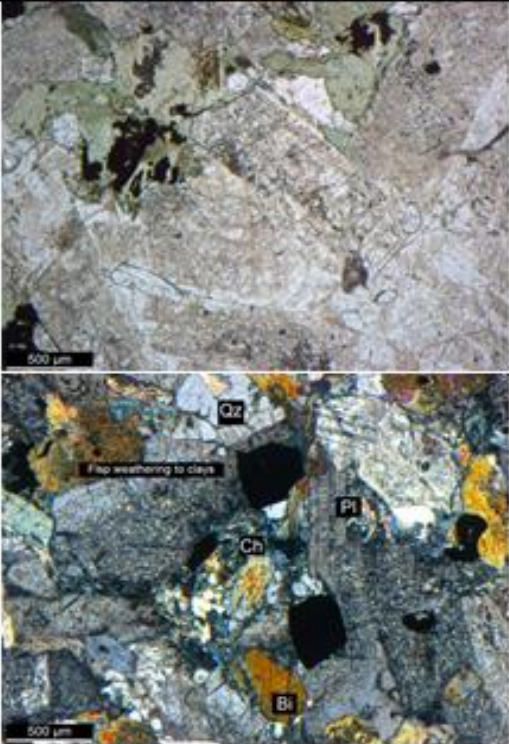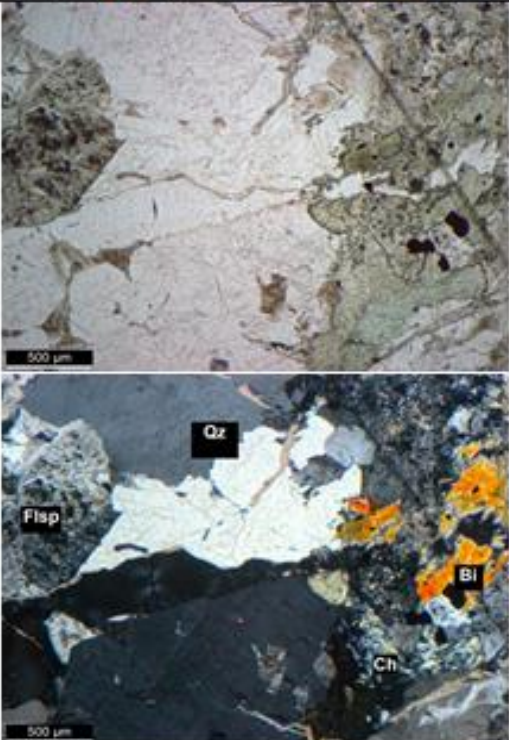| Sample No. | Photograph(s) | Description |
|---|---|---|
| **CR01 –**<br><br>319724<br>6535276<br><br>Hand Specimen |  | Massive coarse grained arkosic sandstone without noticeable clasts. Green-grey in colour, speckled with oblong white minerals, interpreted to be feldspars. Common clinopyroxene observed throughout, average grain size <0.5 – 2 mm. |
| Thin Section |  | Fine-grained andesitic volcanic rock. Major constituents consist of feldspars and clinopyroxene, both of which have undergone alteration via hydrothermal fluids. Secondary replacement of iron oxides and chlorite is common throughout the sample. |
| **CR02**<br><br>319837<br>6535330<br><br>Hand Specimen |  | Very fine grained grey-green rock with sporadic phenocrysts (1 – 3 mm) present. Phenocrysts appear to be volcanic lapilli, feldspars and possible micaceous minerals. Secondary chert vein (~8 mm) cuts through sample. |
| Thin Section |  | Very fine grained basaltic rock, mildly porphyritic in nature with scattered feldspar phenocrysts. Groundmass is predominantly feldspar with chlorite infill. Vesicular, with vesicles having undergone chlorite alteration. Secondary alteration of clinopyroxene to chlorite. |

N.B. All GPS coordinates are GWA-1984, UTM
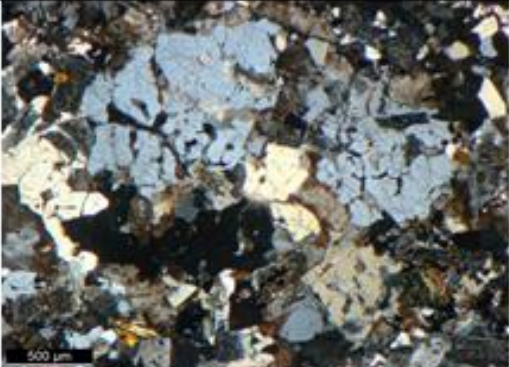
| | | |
|---|---|---|
| |  | |
| **CR03**<br><br>319904<br>6535336<br><br>Hand Specimen |  | Green-grey fine-grained basaltic andesite with sporadic lithic fragments at 2 – 5 mm in size. Less feldspar than other samples, however clinopyroxene abundant homogenously throughout the sample. |
| Thin Section |  | Very fine grained with major constituents of plagioclase and clinopyroxene and minor volcanic glass. Fine-grained laths of these minerals dominate the groundmass. Homogenous interstitial chlorite grains exist through out the sample, with clusters of clinopyroxene and plagioclase phenocrysts. |
| **CR04**<br><br>319922<br>6535368<br><br>Hand Specimen |  | Medium grained arkosic sandstone and green-black siliceous chert. Sample is fairly oxidised, however abundant feldspar and black mineral are identifiable throughout the sandstone, which has no clasts. |

| | | |
|---|---|---|
| Thin Section |  | Very fine grained sandstone, possibly a lithic tuff. Groundmass is a relatively homogenous grey in finer layers with bedding grading into coarser layers. Very weathered, with secondary growth of hematite along tension gashes. Major visible constituents are feldspars and micas, with minor clinopyroxene. Secondary quartz mineralisation is common as veins or surrounding fractures. |
| **CR05**<br><br>319953<br>6535379<br><br>Hand Specimen |  | Fine-grained grey sandstone with slight bedding indicating a coarsening up-sequence. Chert and lithic fragments, with common feldspar fragments throughout. Black mineral has decreased, with fragment size 1 – 6 mm. |
| Thin Section |  | Slightly metamorphosed lithic arkose, with multimineralic volcanic clasts. Plagioclase feldspars clasts are abundant with minor biotite and clinopyroxene. Opaque minerals are present, most likely oxides resulting from secondary alteration. Matrix is very fine, possibly a tuff, however ~40% of the rock is clasts. |

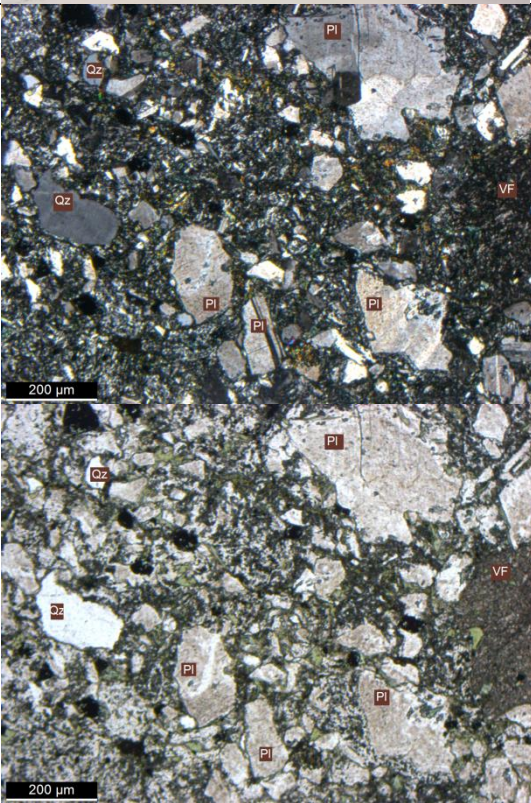| | | |
|---|---|---|
| **CR06**<br><br>320033<br>6535439<br><br>Hand Specimen |  | Course grained sandstone grades into fine-grained lithic sandstone then into siliceous-banded chert. Grain size from < 0.5 – 2 mm, with an abundance of k-feldspars, interpreted as orthoclase with Fe-enrichment. |
| Thin Section |  | Bedded lithic sandstone from very fine to fine-grained with abundant feldspar and clinopyroxene. Minor quartz and pyroxenes observed with secondary mineralization of hematite and chlorite. Grains are mostly rounded, with most undergoing alteration/weathering. Reaction rims are visible, as seen in the bottom right corner, resulting from the low-grade metamorphism. |
| **CR07**<br><br>319945<br>6535485<br><br>Hand Specimen |  | Graded sample of course (0.5-1mm) and fine (<0.5mm) grained lithic sandstone. The fine-grained sandstone composition is unidentifiable in hand specimen, with the coarse grained exhibiting mostly feldspars, and few lithic fragments. |
| Thin Section |  | Very fine grained arkose, possibly an arkosic tuff. Relatively homogenous sample showing signs of weathering and alteration. Significant increase in quartz in comparison to other samples, representing the majority of clasts along with plagioclase feldspars. Secondary replacement by chlorite and hematite throughout. |

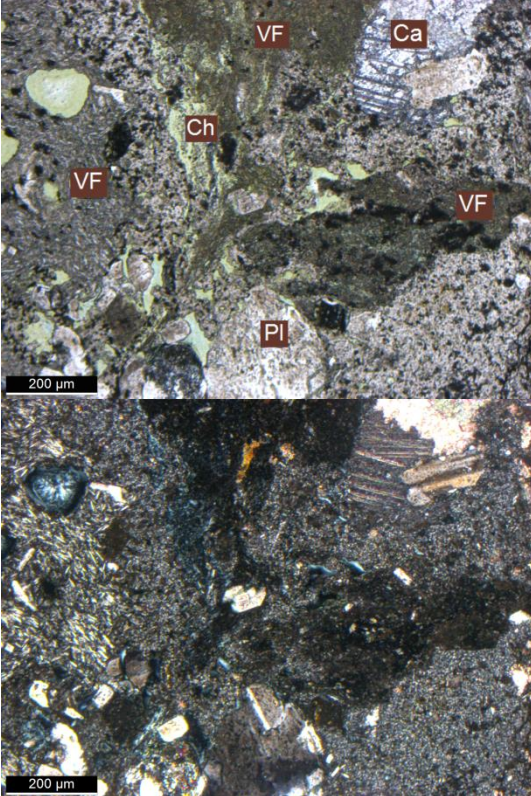| | | |
|---|---|---|
| |  | |
| **PCF5**<br><br>320961<br>6530773<br><br>Hand Specimen |  | Coarse conglomerate with large clast variety and a fine, dark grey matrix. The matrix constitutes <10% of the conglomerate with clast size 5-90 mm. The clasts are mostly rounded and display a spectacular array of limestone, granite, basalt, chert and many other intrusive rocks. |
| **PCF5.1a**<br><br>**Thin Section** |  | Volcanic breccia consists of plagioclase, pyroxenes and myrmekite surrounds a large clast. The clast is a very fine grained, metamorphosed rock, interpreted to be bononite. It is dark green in colour, possibly indicating a chloritic overlay. Olivine pseudomorphs altered to chlorite, showing dusty alteration related to Fe release. Major constituents include chalcedony quartz, orthopyroxene and epidote. Minor opaque minerals and mica phenocrysts throughout the very fine feldspar, mica, epidote groundmass. |
| **PCF5.4d**<br><br>**Thin Section** |  | Coarse-grained plutonic rock dominated by quartz and k-feldspars. Minor clinopyroxene, epidote, plagioclase and amphibole are present. Mostly consists of a granular texture, with feldspars maintaining original tabular shape, although mostly weathering to clay minerals. One region appears porphyroblastic with spherical quartz aggregates. Minor |

N.B. All GPS coordinates are GWA-1984, UTM
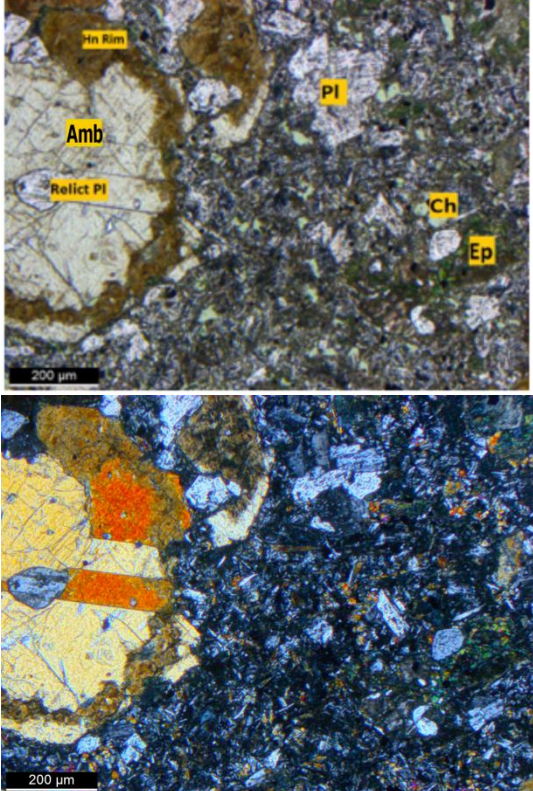
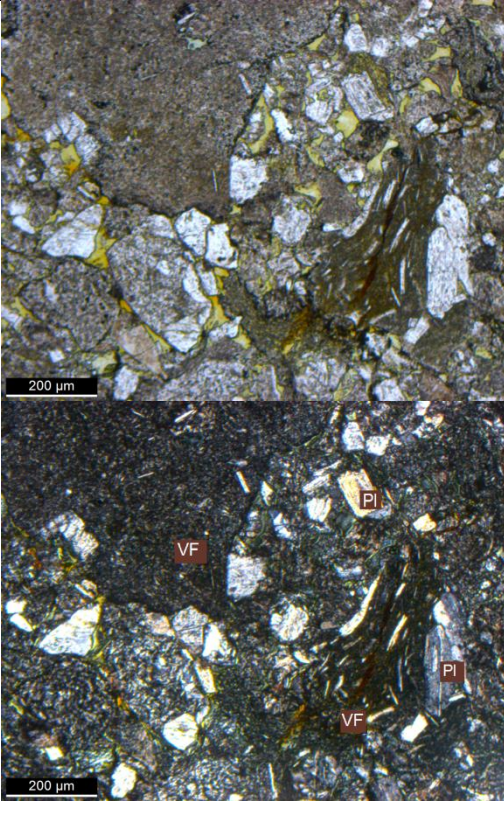| | | |
|---|---|---|
| |  | myrmekite, chlorite and opaque minerals observed. Calcite veining. |
| **PCF5.7c**<br><br>**Thin Section** |  | Plutonic rock dominated by weathered feldspars, micas and amphibole with minor interstitial quartz, opaque minerals and chlorite infill. Feldspars maintain tabular shape, although are weathering to clay minerals due to sericite alteration styles. |
| **PCF5.8a**<br><br>**Thin Section** |  | Monzonite plutonic rock dominated by coarse, equigranular quartz. Weathered feldspars throughout with minor interstitial chlorite, micas, pyroxenes, hornblende and epidote. Zircon mineralisation observed. Quartz grains are fairly rounded with few inclusions of surrounding minerals and calcite veining is common throughout, as well as common chlorite replacement of biotite. Sericite alteration visible throughout, coupled with haematite dusting. |

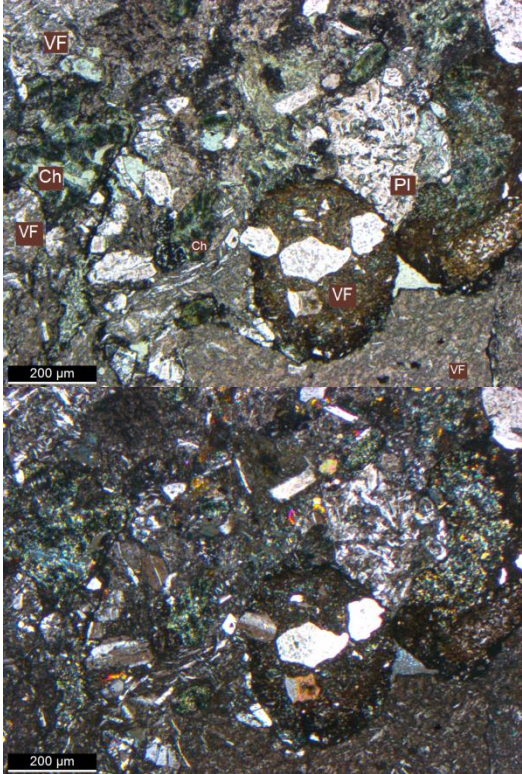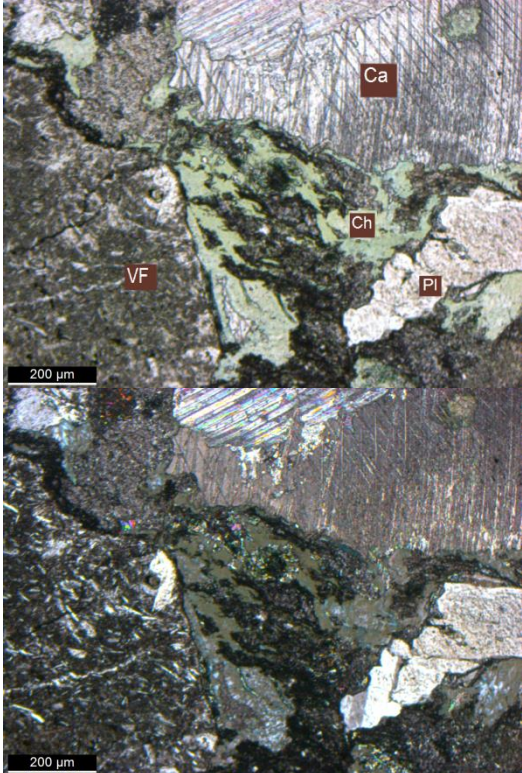N.B. All GPS coordinates are GWA-1984 UTM

The following samples were collected on the main field trip, when mapping was undertaken in October 2014.
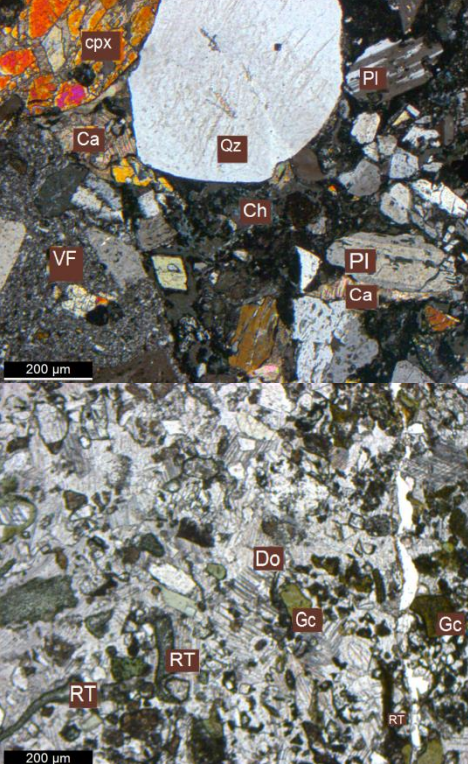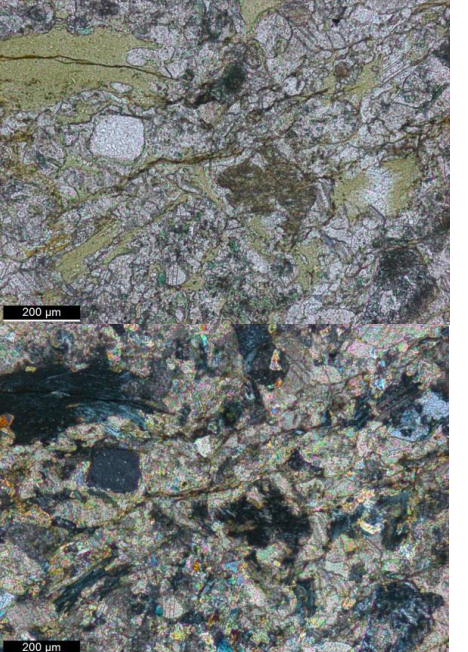
| Sample No. | Photograph(s) | Description |
|---|---|---|
| **CR10**<br>319434<br>6536707<br><br>Hand Specimen |  | Coarse-grained (~1-2mm) massive lithic sandstone. A high proportion of both pink and white feldspars are observed, with grains often exhibiting a tabular habit. Other mineral constituents include lithic fragments and clinopyroxene although lesser of the latter than in previous samples. |
| Thin Section |  | Arkosic sandstone with large clasts in a fine feldspathic matrix. Predominantly plagioclase clasts that exist as mostly fragmented grains, undergoing alteration to clinopyroxene or clay minerals. Multiple twinning abundant on plagioclase clasts. Minor volcanic rock fragments, volcanic quartz and opaque minerals. Secondary chlorite growth through hydrothermal alteration. |
| **CR11**<br>319644<br>6536431<br><br>Hand Specimen |  | Contact exists between fine and coarse-grained feldspathic litharenite sandstones to conglomerates. Appears to be an erosional contact with the presence of ripple marks and scours. The coarse-grained section is massive with lithic fragments (1-10mm) and common feldspar. The fine-grained component is a homogeneous grey-black material (<0.5mm) with scattered lapilli sized feldspars. |

| | | |
|---|---|---|
| Thin Section |  | *Fine Grain*: Plagioclase laths make up bulk of matrix, difficult to determine between volcaniclastic and volcanic rock. Secondary chlorite replacement common throughout sample. A few volcanic quartz and plagioclase clasts.<br>*Conglomerate:* Consists of predominantly volcanic rock fragments and feldspar clasts. Minor calcite and quartz with secondary calcite veins and chlorite. Matrix is very fine consisting of fragments feldspars, clay minerals and possibly illite. |
| **CR12**<br>319733<br>6536487<br><br>Hand Specimen |  | Relatively fine-grained massive conglomerate with 2-10mm clast size, and very fine matrix. Clasts consist of abundant feldspars, lithic fragments, chert and minor epidote. |
| Thin Section |  | Feldspathic Litharenite with reasonably large feldspar clasts and a very fine, possibly tuff, matrix with a chlorite cement. Major constituents include feldspars and volcanic fragments. All fragments are extremely weathered and fragmented with feldspar clasts undergoing major secondary replacement by clinopyroxene, chlorite with minor epidote and calcite replacement. |

| CR13 |  | This sample was not *in situ*, but rather was taken from a boulder, which had been transported down a creek bed going across strike. It may possibly be part of the Pipeclay Creek Formation. Polymict, coarse conglomerate with lapilli clasts of 2-30mm in size and smaller feldspar clasts (~0-8mm) and lithic fragments. One large clast visible that appears to be plutonic in origin. |
|---|---|---|
| 319797 6536493 Hand Specimen | | |
| CR14 319592 6536373 Hand Specimen |  | Fine conglomerate of green sand, with clasts 1-5mm. Many clasts show evidence of vesicles, indicative of volcanic origin, possibly andesitic. Feldspars appear to have been altered to chlorite or epidote with a very fine, dark matrix. |
| Thin Section |  | Coarse-grained arkosic conglomerate with large mostly rounded clasts. Feldspar clasts often form as aggregates of feldspar crystals, with many undergoing secondary chlorite and epidote mineralisation. Clinopyroxene, amphiboles and plagioclase are the major constituent of this sample. Tension gashes, evident by torn feldspars, have crystallised calcite and the very fine matrix existing of predominantly feldspar has chloritic cement. |

| | | |
|---|---|---|
| **CR15**<br>319758<br>6535844<br><br>Hand Specimen |  | Fine-grained feldspathic litharenite. Massive habit with black clasts and abundance of lithic fragments. A single large feldspar clast is visible ~20mm. |
| Thin Section |  | Major constituents include volcanic fragments and feldspars with interstitial volcanic quartz. Grains are mostly rounded, with little to no detrital matrix but chloritic cement. Feldspars appear to have undergone alteration, with little secondary replacement. |
| **CR16**<br>319698<br>6535806<br><br>Hand Specimen |  | Green, coarse-grained sandstone with abundance of feldspars, often oblong shaped, and minor epidote, clinopyroxene, and volcanic clasts. |
| **CR17**<br>319547<br>6535773<br><br>Hand Specimen |  | Greenish polymict conglomerate of massive habit. Clast size 2-30mm, with a single large limestone clast (~30mm) observed. An increase in variety of minerals and clast types, however feldspars and clinopyroxene are still common. Larger chert, volcanic and lithic fragments abundant, with sparse, small (~1mm) red chert clasts scattered. |

| | | |
|---|---|---|
| Thin Section |  | Lithic Arkosic conglomerate consisting of a mixture of volcanic rock fragments and feldspars with chlorite cement matrix. A single large clast appears to be silicified dolomite and includes gypsum, clinopyroxene and quartz clasts within. Overall clasts are mostly rounded with feldspars often as aggregated crystals or exhibiting multiple twinning directions. |
| **CR18**<br>319504<br>6535751<br><br>Hand Specimen |  | Massive conglomerate, very green in colour with <25% matrix. Noticeable increase in grain size, with more common ~15mm sized casts of limestone, basalt, feldspars and chert, all angular in shape. |
| Thin Section |  | Litharenite conglomerate with grey, very fine matrix and chlorite cement. Major component is volcanic lithic fragments with feldspars undergoing extensive replacement by clinopyroxene and chlorite. Minor constituents include calcite and chert, and a minor secondary calcite vein. |

| CR19 |  | Weathered conglomerate with igneous clasts, feldspars and epidote 2-30mm in size. More grey in colour than the green colour of other samples. |
|---|---|---|
| 320038 6535549 | | |
| Hand Specimen | | |
| Thin Section |  | Lithic arkosic conglomerate, with a variety of mineralisation. Two separate photographs are shown, with the top in XPL, and the bottom of a different area in PPL. Abundant rock fragments with both fossiliferous limestone and volcanic rock fragments. Minor constituents include calcite, glauconite, hornblende, quartz and clinopyroxene (as a secondary replacement mineral). Abundant radiolarian tracks and a single fossil observed in carbonate. Varying matrix from chlorite infill to broken down feldspars and opaques. |
| **CR19b** **Thin Section** |  | Limestone clast with major chlorite cement and a fine groundmass of calcite/dolomite. Scattered quartz, feldspar and micas. Quartz grains are fragmented, while feldspars are undergoing weathering. No radiolarian tracks are observed. |

| | | |
|---|---|---|
| **CR20**<br><br>319997<br>6535464<br><br>Hand Specimen |  | Conglomerate with single large limestone clast ~35mm in size. Matrix is fine-grained with abundant feldspars and black mineral, and patchy alteration resulting in green colour. Clasts size 5-50mm, with slight indication of alignment of clasts. Lithic fragments appear to be similar to CR14, with large feldspar clasts. |
| **CR21**<br>319962<br>6535435<br><br>Hand Specimen |  | Weathered conglomerate similar to CR20, however appears to have a singular clast source. Clasts are large and appear to be of volcanic origin, with fine black groundmass and abundant white feldspars. Matrix is relatively coarse (1-2mm) with a variety of minerals however abundance of feldspars and sporadic red chert. |
| Thin Section |  | Arkosic conglomerate slightly metamorphosed as evident by the schistose-like texture of the feldspathic matrix. Consists of fine matrix with few large plagioclase clasts, which often exist as aggregated crystals. Secondary veins have quartz mineralisation. Possible thin section is mostly representative of a volcanic clast from the conglomerate, rather than a true representation of the sediment itself. |
| **CR23**<br>319922<br>6535395<br><br>Hand Specimen |  | Weathered coarse sandstone to fine conglomerate with clast size 0.5-4 mm, and < 25% matrix. A wide variety of clasts are observed, with matrix consisting of ample white feldspars, epidote and clinopyroxene. |

| | | |
|---|---|---|
| Thin Section |  | Coarse lithic arkose, with dominant constituents including volcanic rock fragments and feldspars. Feldspars are fragmented and in the process of secondary replacement by clinopyroxene, epidote and chlorite. Abundant chloritic infill cementing clasts, with matrix other than chlorite appears to be weathered and broken down feldspars but too fine for identification. |
| **CR24**<br><br>319865<br>6535353<br><br>Hand Specimen |  | Very fine-grained (<0.5mm) lithic sandstone with common clinopyroxene. An apparent layering of increased feldspar and slightly coarser grains down sequence is observed. |
| Thin Section |  | Volcanic rock, dominated by feldspars (mostly sanidine) with entire groundmass composed of ~1mm plagioclase laths with abundant chlorite infill. Major constituents are feldspars, which are undergoing alteration to clinopyroxene with few large olivine phenocrysts. Bedding is observed, with a band of finer, darker material containing a needle-like black mineral interpreted to be deerite. This rock is interpreted to be keratophyre. |
| **CR25**<br><br>319684<br>6535257<br>Hand Specimen |  | Medium-grained (<0.2mm) massive, lithic, grey-green sandstone with a decrease in visible feldspars. An increase in red chert fragments observed together with green/black chert fragments, lithic fragments, and clinopyroxene. |

| | | |
|---|---|---|
| Thin Section |  | Coarse lithic arkose with major constituents comprising feldspars, rock fragments and clinopyroxene with minor interstitial opaque minerals and volcanic quartz, all grains are extremely fragmented. Secondary mineralisation of chlorite, rather than chlorite matrix. Matrix too fine for identification. |
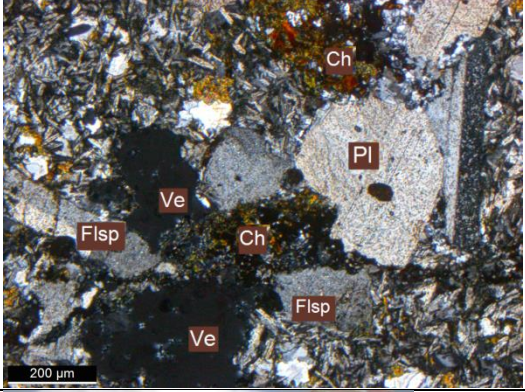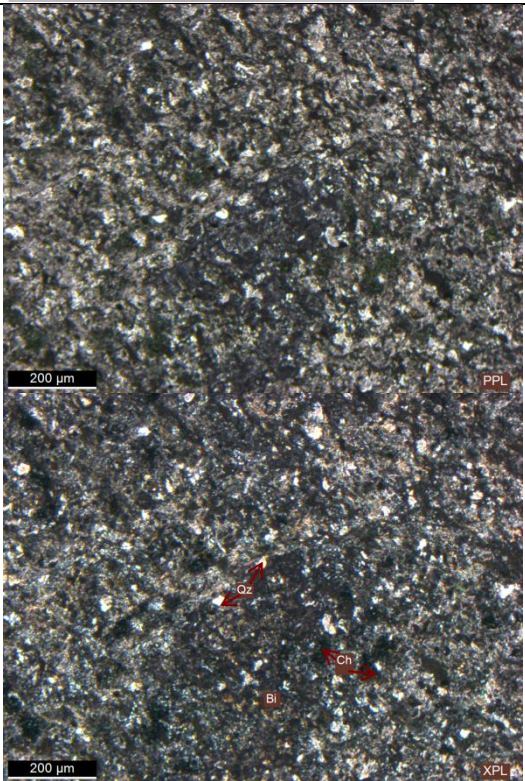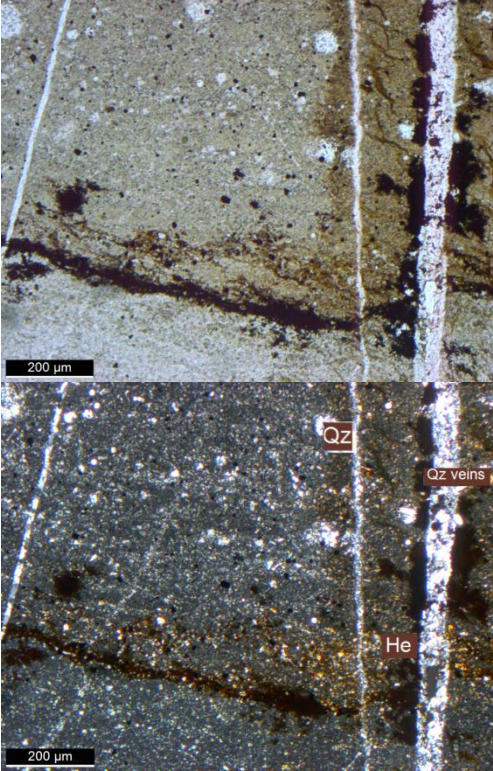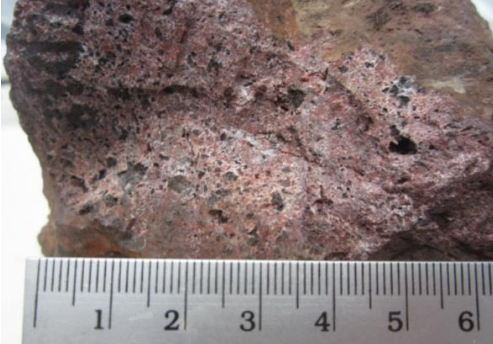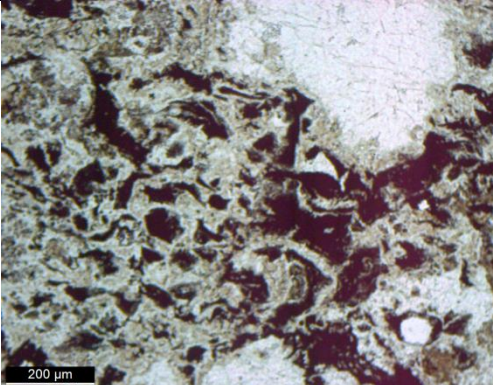
The following samples were collected at Location 2, surrounding Chaffey Dam.
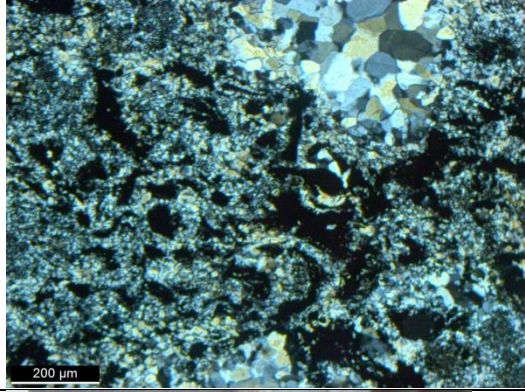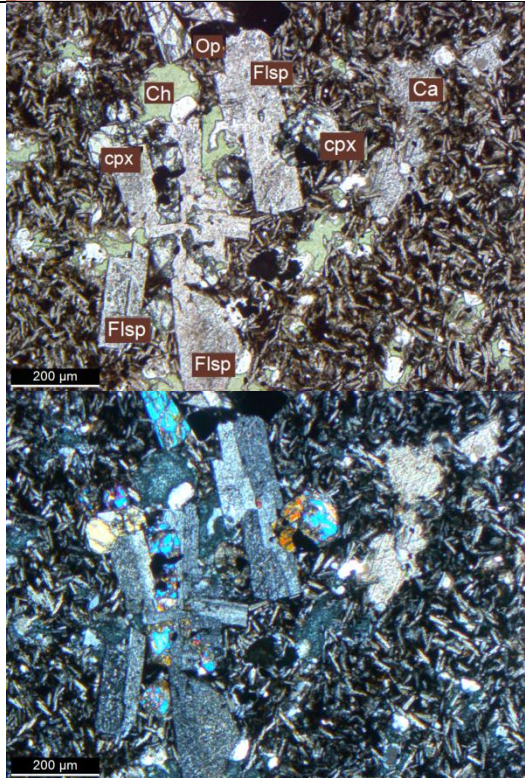
| Sample No. | Photograph(s) | Description |
|---|---|---|
| **CD1.3**<br><br>321550<br>6531577<br><br>Hand Specimen |  | A dark grey very fine-grained (<0.5 mm) lithic sandstone, almost chert-like. Homogenous sample with common feldspar, minor clinopyroxene and oxidised veins or deformation fractures. |
| Thin Section |  | Very fine-grained rock, interpreted to be low-grade metamorphosed tuff. Major constituents comprise feldspars and volcanic quartz with larger clasts aggregated around secondary veining. Quartz grains are mostly rounded with feldspar grains showing signs of degradation, however maintaining original tabular shape. Secondary veining is common throughout the rock, with silicate infill, often gypsum. A general foliation of grain alignment is visible in some parts of the |

| | | section. |
|---|---|---|
| **CD1.6**<br><br>321002<br>6530790<br><br>Hand Specimen |  | Conglomerate with chert matrix holding large clasts (3-50 mm). Fine-grained felsic volcanic clasts show alteration rinds indicating release of Fe and K during hydrothermal alteration. Chalcopyrite or pyrite Cu-sulfide mineralisation is visible in veins and within alteration rinds. |
| Thin Section |  | Large clasts (top photo) in chalcedony matrix (bottom photo) with carbonate (calcite) present. Large clasts (top photo) appear to be a groundmass of recrystallised feldspars, micas and pyroxenes with chalcedony-filled vesicles. Chalcedony matrix has both radiating and amorphous textures and is cut by Fe-oxide veins. Clasts show secondary hematite growth. Laths of biotite visible in clasts groundmass, with some feldspar grains showing silicification rims of chalcedony. Plagioclase shows signs of sericite alteration. |
| **CD1.8**<br><br>320745<br>6530645<br><br>Hand Specimen |  | A volcanic rock, most likely basalt that is homogenous, very fine grained and black. Small lapilli-like clasts exist sporadically throughout the sample. |

| | | |
|---|---|---|
| Thin Section |  | Keratophyre, fine-grained altered basalt with groundmass consisting entirely of feldspar laths with minor clinopyroxene, epidote and chlorite replacement. Common mineral include volcanic quartz, magnetite (associated with phenocrysts) and calcite precipitation with sparse, fragmented phenocrysts of feldspars. A single large spherical clast, possibly lapilli or evaporite, calcite or biotite. Veins mostly have calcite infill. |
| **CD2.2**<br><br>320679<br>6532021<br><br>Hand Specimen |  | Extremely weathered and oxidised fine-medium grained keratophyre. Sample is too weathered for identification of constituents; however there appears to be sporadic, lapilli-like clasts throughout. |
| **CD2.3**<br><br>320672<br>6531997<br><br>Hand Specimen |  | Extremely oxidised & weathered sample collected from a creek bed, same as CD2.2. Identified as volcanic due to the presence of vesicles throughout the rock, which is very fine-grained and light coloured most likely as a result of the weathering. |
| Thin Section |  | Keratophyre basaltic volcanic rock with large sparse vesicles. Groundmass consists of feldspars with common chlorite replacement, interpreted to have a trachytic texture. Grains consist of mostly feldspar with minor volcanic quartz and are generally fragmented and rounded. Common feldspars with many showing signs of within-grain recrystallization, often in k-shapes (top photo). Common low temperature minerals including quartz and micas. |

| **CD3.4**<br><br>321917<br>6531871<br><br>Hand Specimen |  | Siliceous sandstone or chert, very fine-grained. Possible ripple marks in almost indistinguishable bedding characterised by an increased presence of clinopyroxene. Small limestone inclusions and some regions exhibit abundant black lines either at vertical or 45 degree angles, interpreted to be bioturbation. |
| Thin Section |  | Very fine, tuff-like rock with minor constituents of volcanic quartz and feldspars, however nothing else is identifiable. A few darker patches (in centre of photograph) show biotite and chlorite staining. Chlorite is common throughout the section. |

| | | |
|---|---|---|
| **CD3.6**<br><br>321043<br>6531667<br><br>Hand Specimen |  | Black chert with abundant white feldspar mineral throughout. Deformation fractures common and have undergone weathering with iron oxide replacement. |
| Thin Section |  | Interpreted to be a silicified siltstone, as it still has grey colour rather than the high birefringence exhibited by chert. Slightly graded from very fine to fine-grained, with bedding evident and a progressive increase in chert. Constituents are too fine for identification, however opaque minerals, probably iron oxides, are common. Cross cutting quartz veins are common, with abundant secondary hematite staining around veins. |
| **CD3.8**<br><br>320030<br>6531536<br><br>Hand Specimen |  | Red sandstone characterised by interspersed red chert and basalt making a beautiful red and black speckled rock. Massive habit with the largest basalt clast at 5 mm, and white mineral homogenously throughout, interpreted to be quartz. |
| Thin Section |  | Iron-rich chert with fairly equigranular silica crystals with a cloudy opaque overlay. Some clasts of polycrystalline quartz and sparse magnetite. Sporadic radiolarian tracks. |

| | | |
|---|---|---|
| **CD3.13**<br><br>320487<br>6530836<br><br>Hand Specimen |  | Very fine-grained (0.5 – 10 mm) basaltic rock with circular lapilli phenocrysts of red chert, quartz, feldspar and epidote. |
| Thin Section |  | Basalt with groundmass entirely made up of feldspar laths and minor interstitial quartz. Phenocrysts are mostly feldspars, with major chlorite replacement throughout with minor replacement of feldspars to clinopyroxene. Many feldspar phenocrysts maintain tabular shape, whilst sporadic phenocrysts appear spherical, often with reaction rims, interpreted to be lapilli. Diamond-shaped opaque minerals are commonly associated with phenocrysts. |

# Appendix 2

**<u>Zircon U-Pb Geochronology data</u>**

N.B., given the small sample size, all Murrawong Creek Formation geochronology data is shown in text.

**Part 1 – Zircon Mount Map**
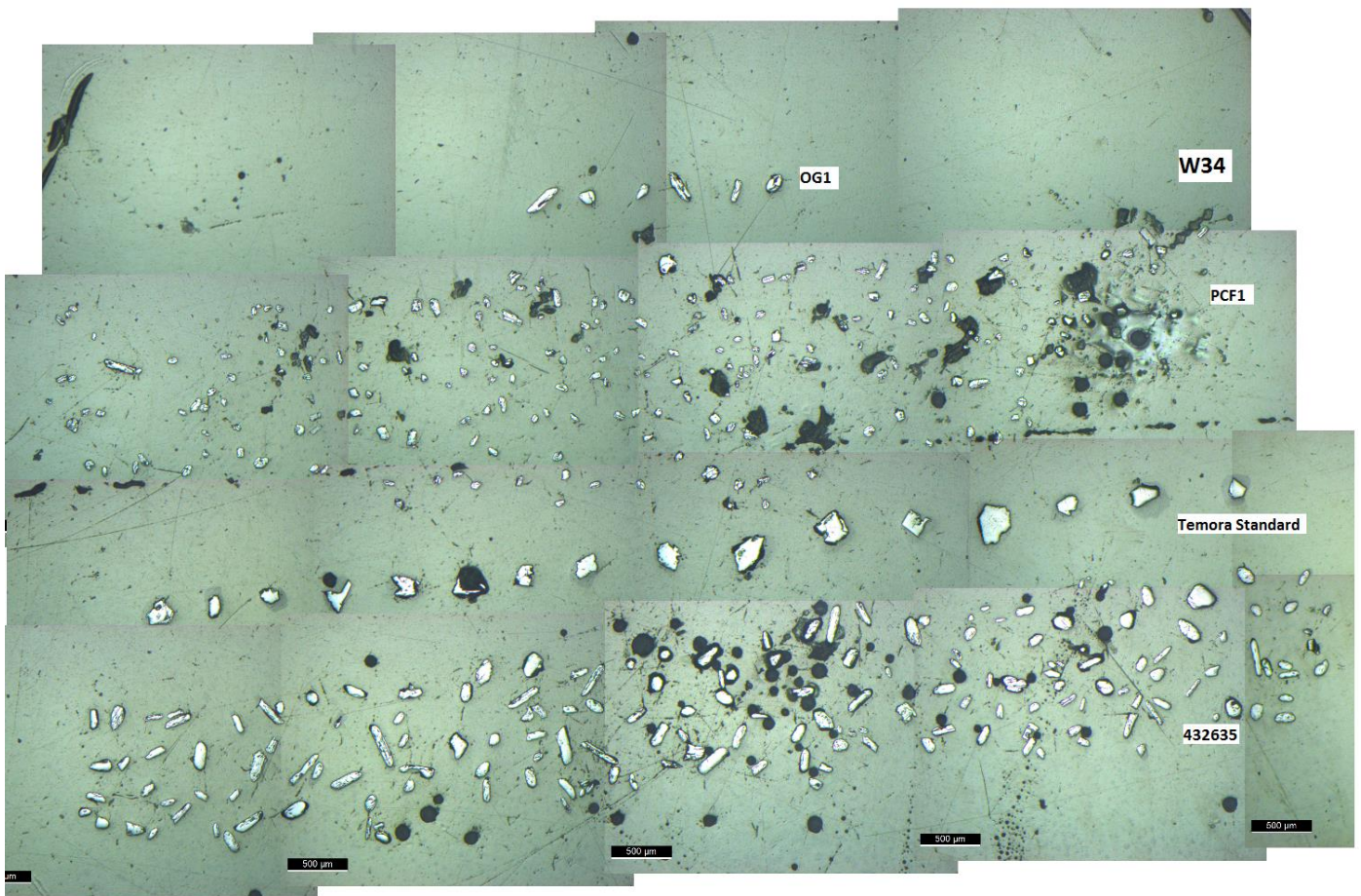


N.B., PCF1 is the Pipeclay Creek Formation zircon sample, whilst 432635 is an unrelated sample on the same mount.

**Part 2 – CLI Images for Pipeclay Creek Formation zircons**

140

146
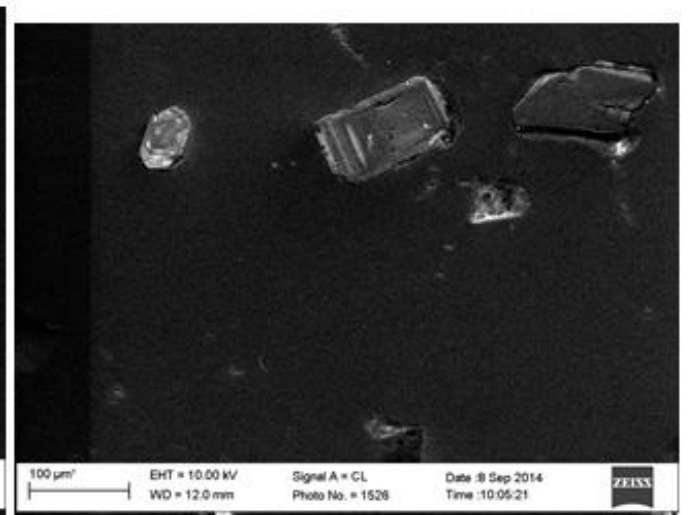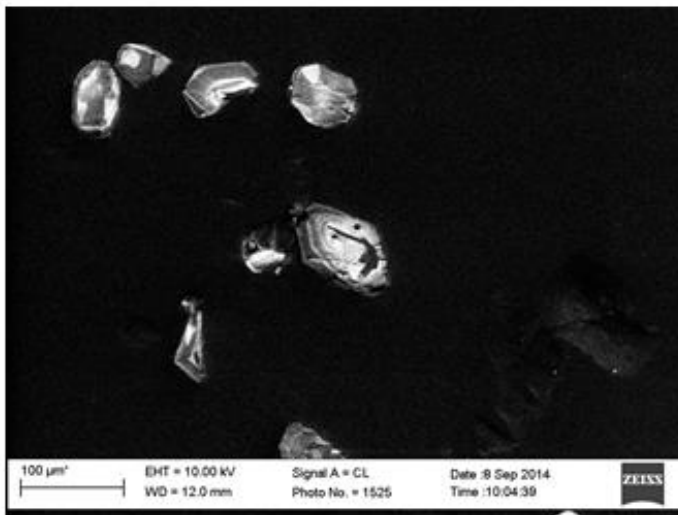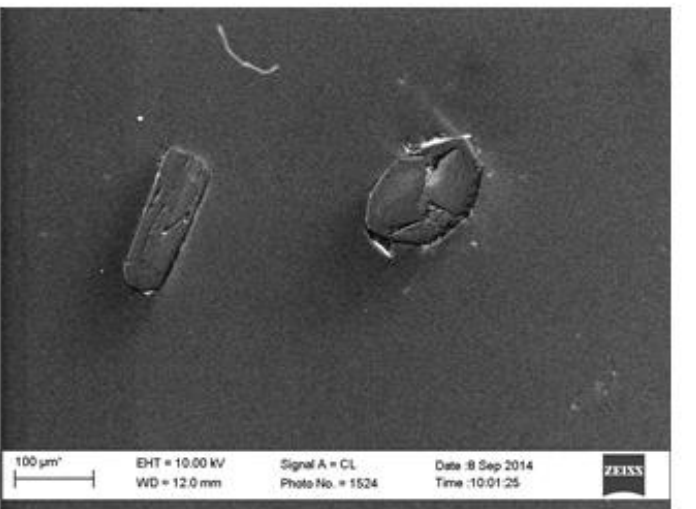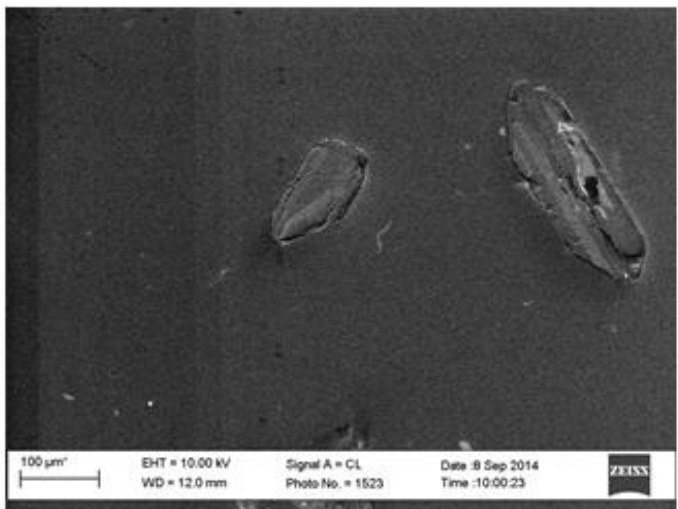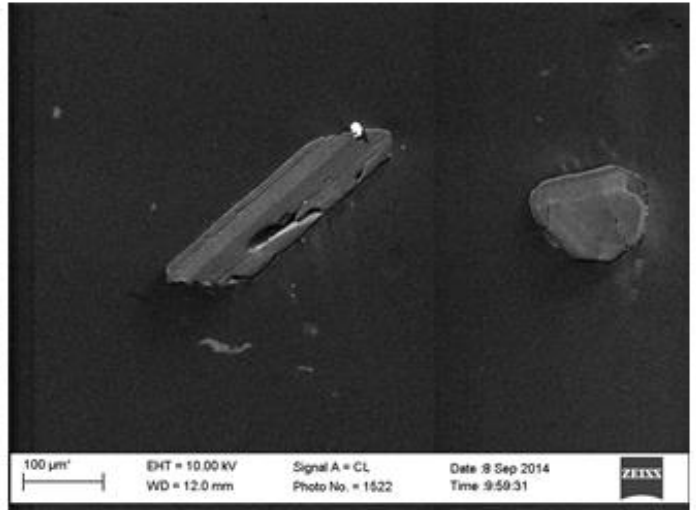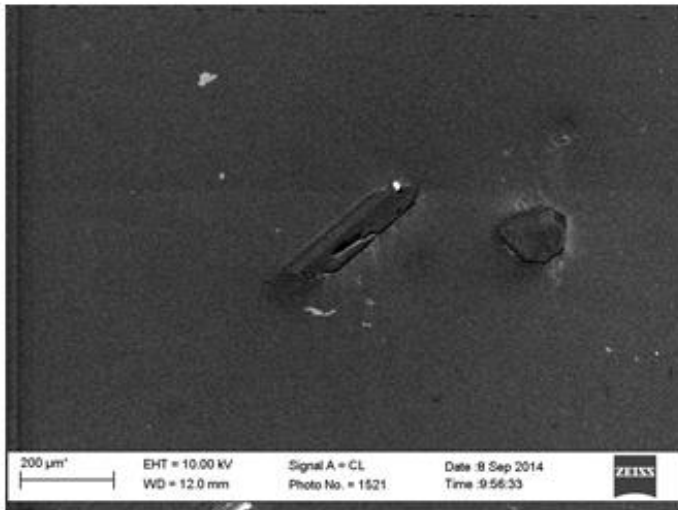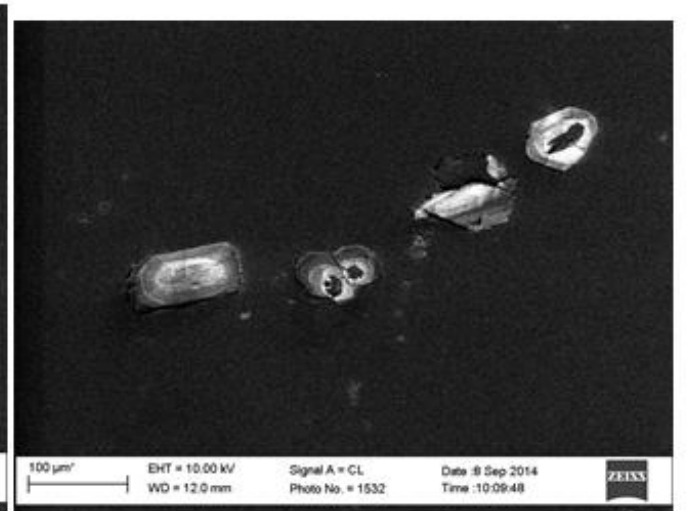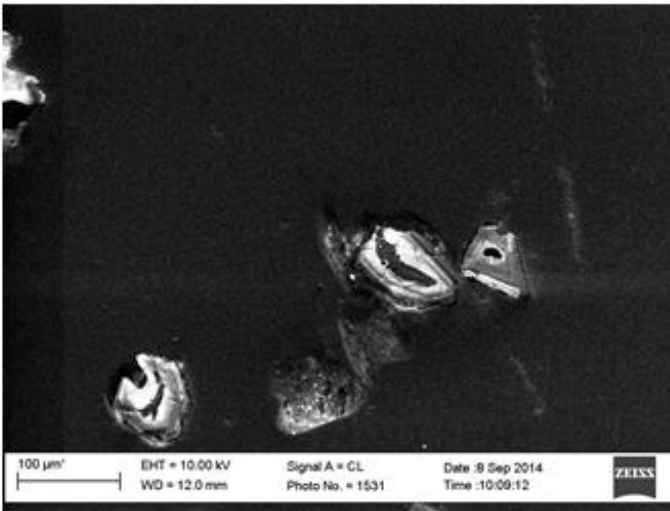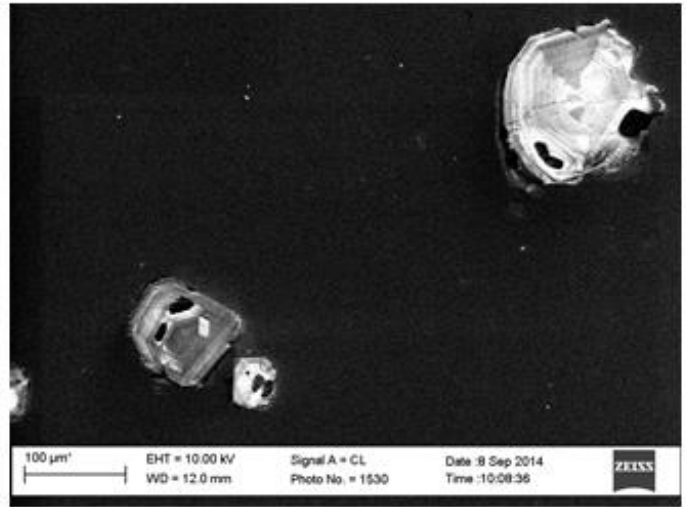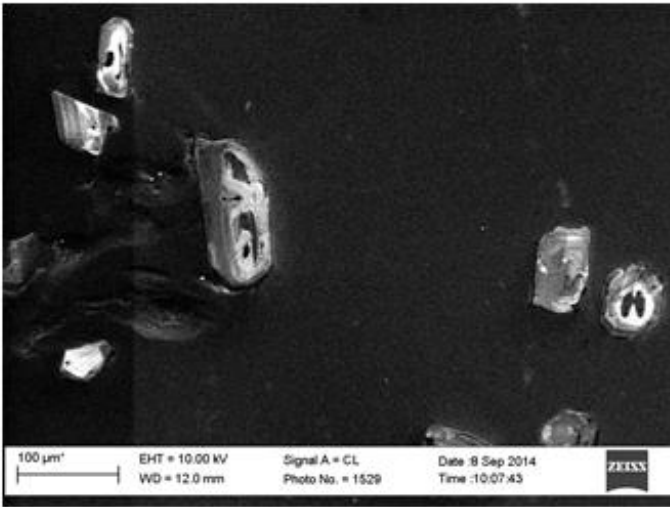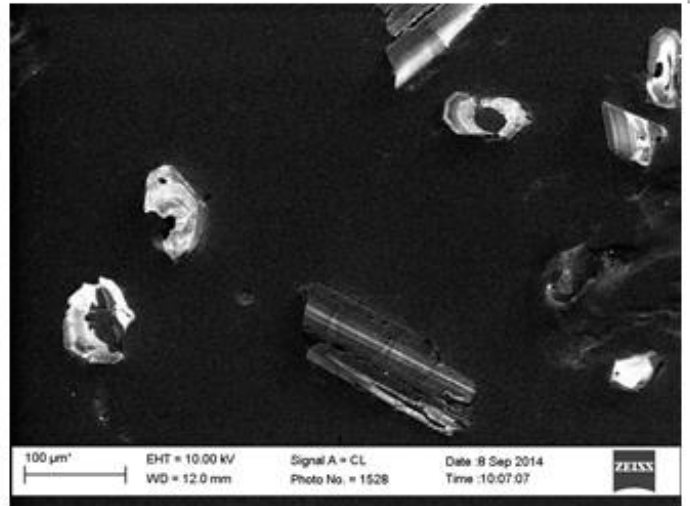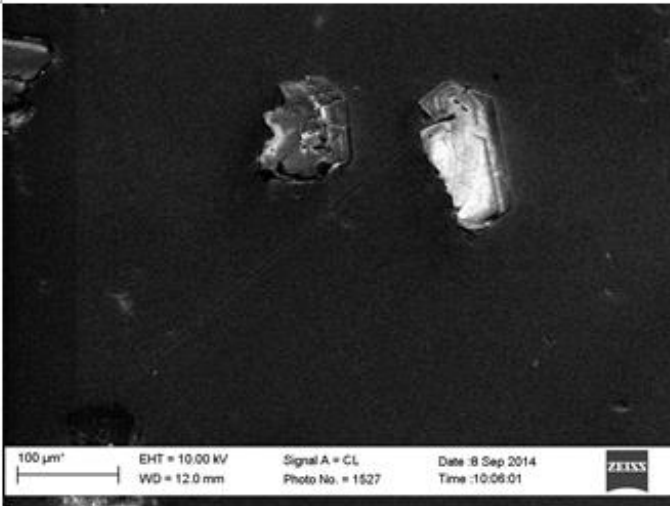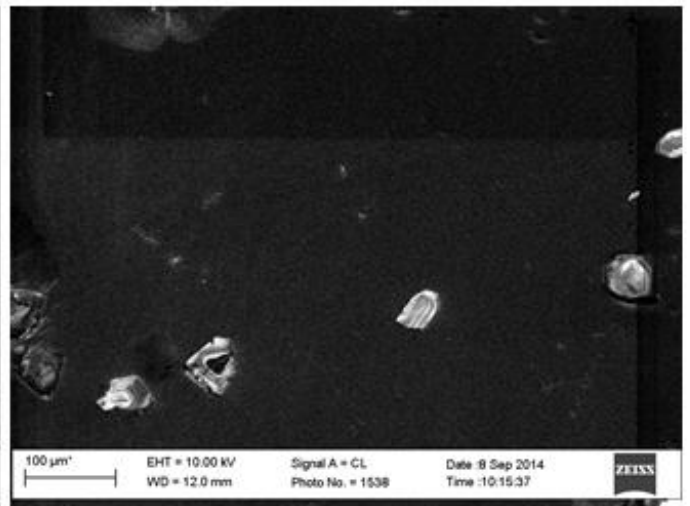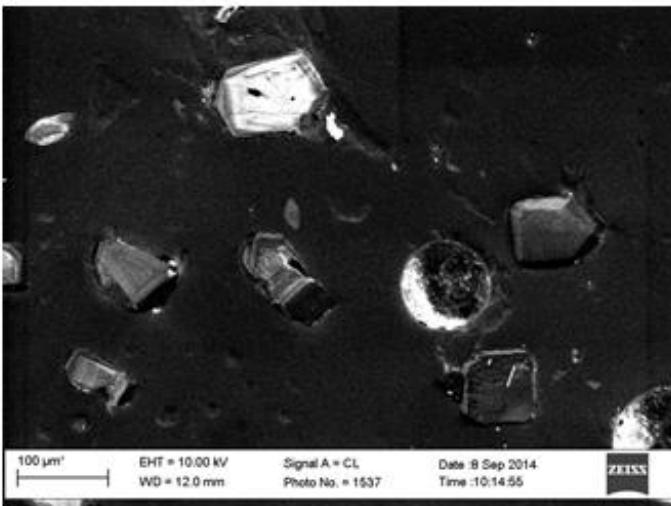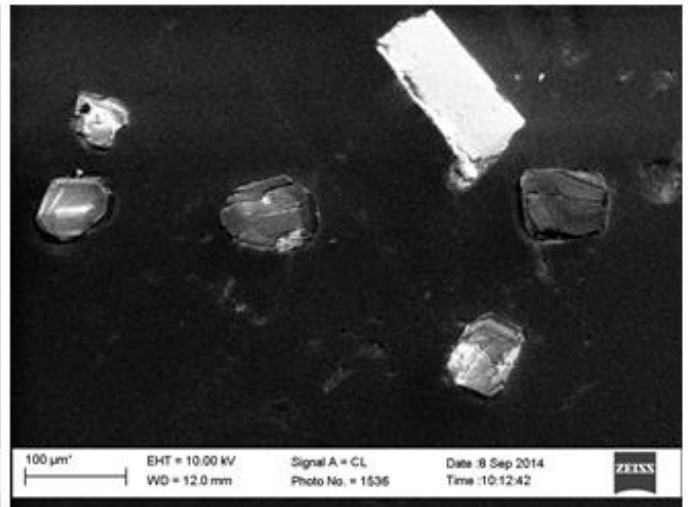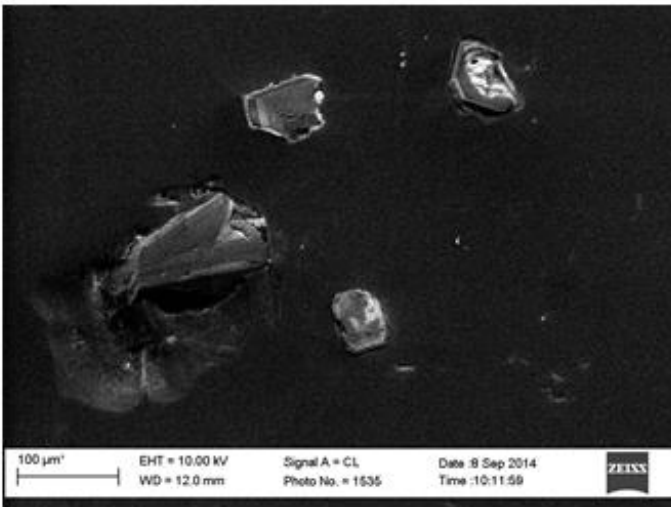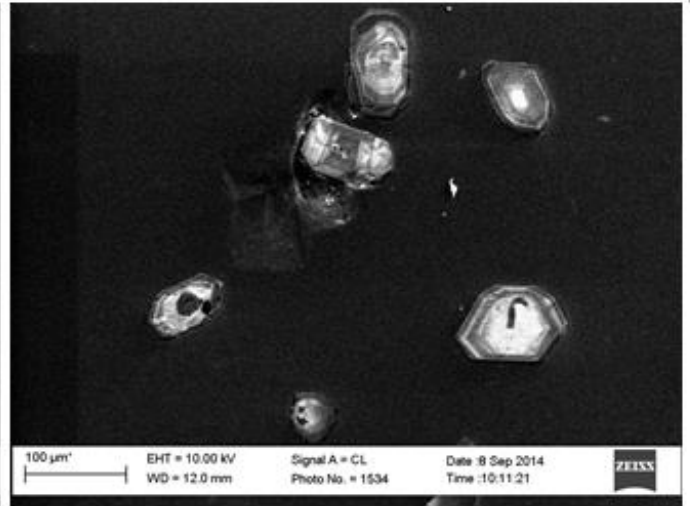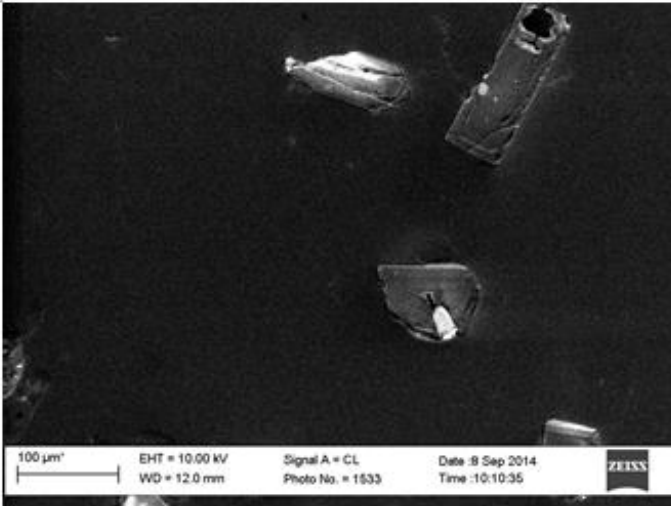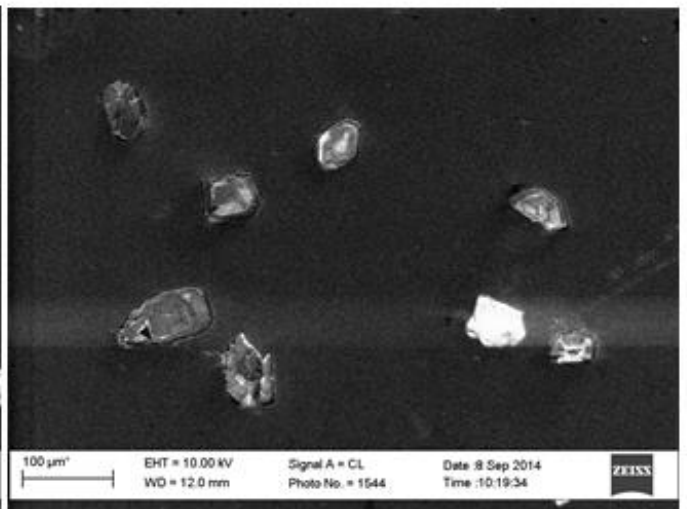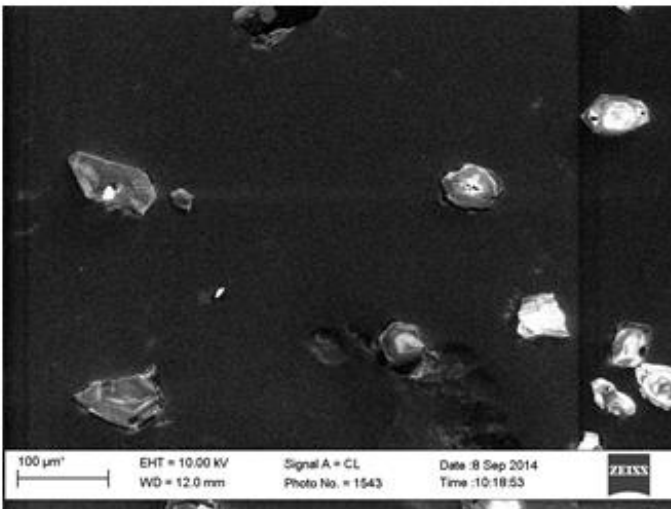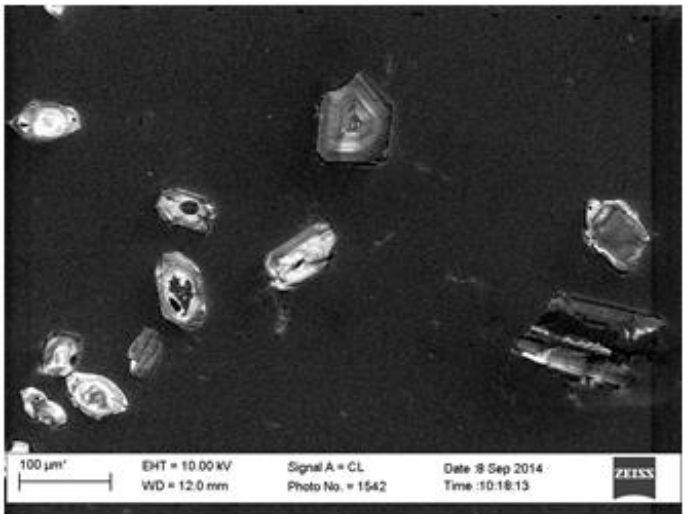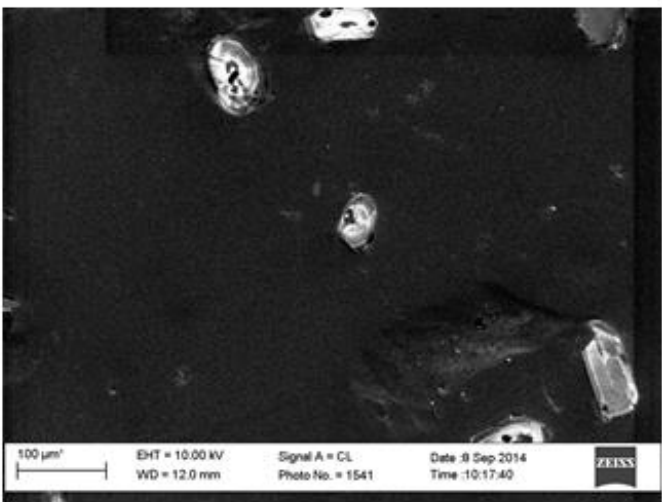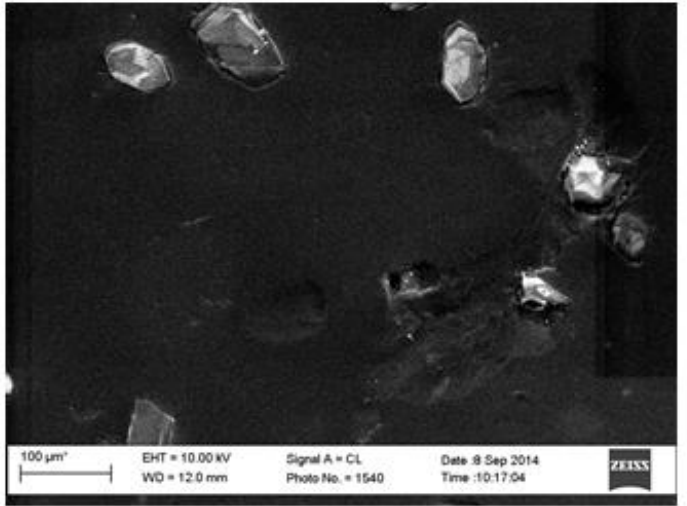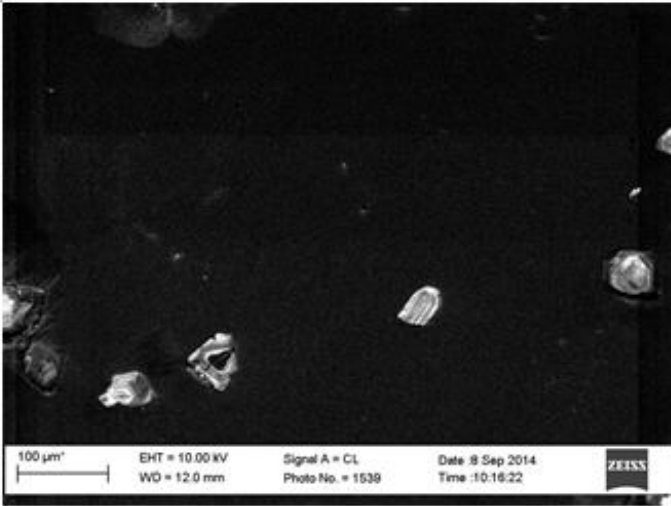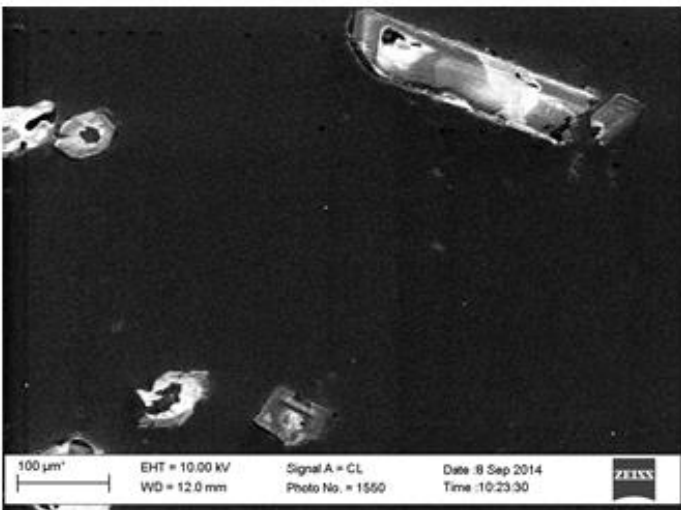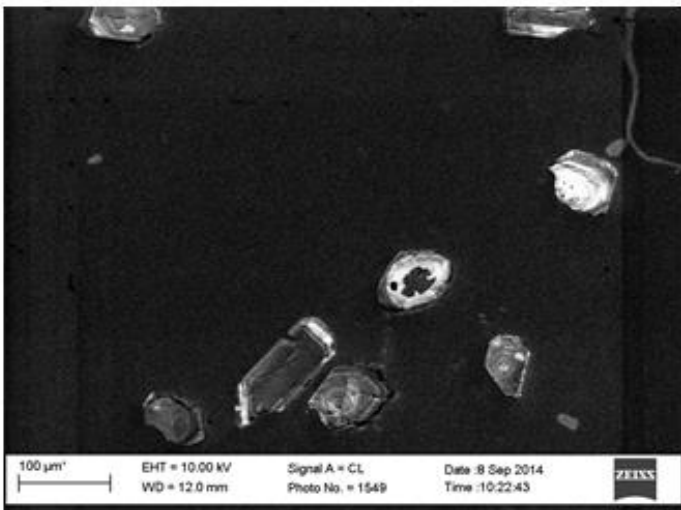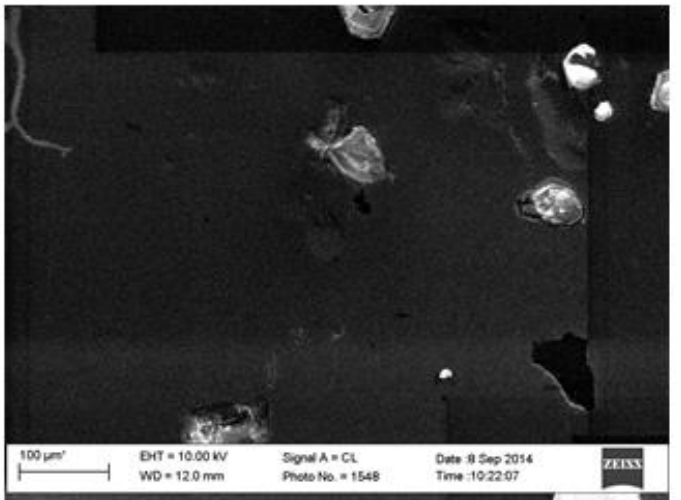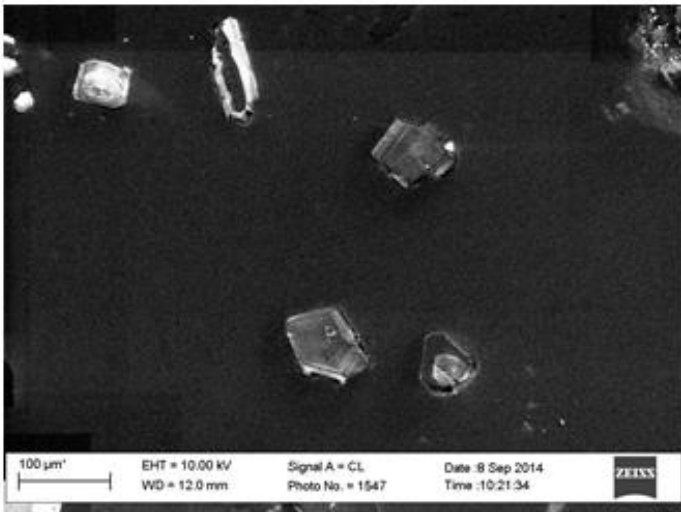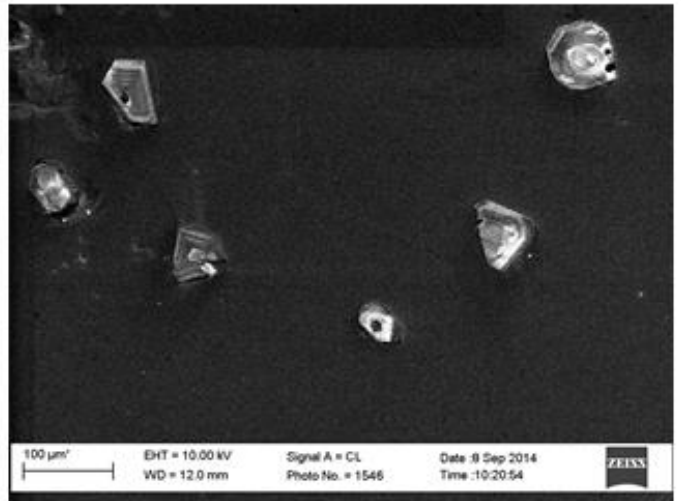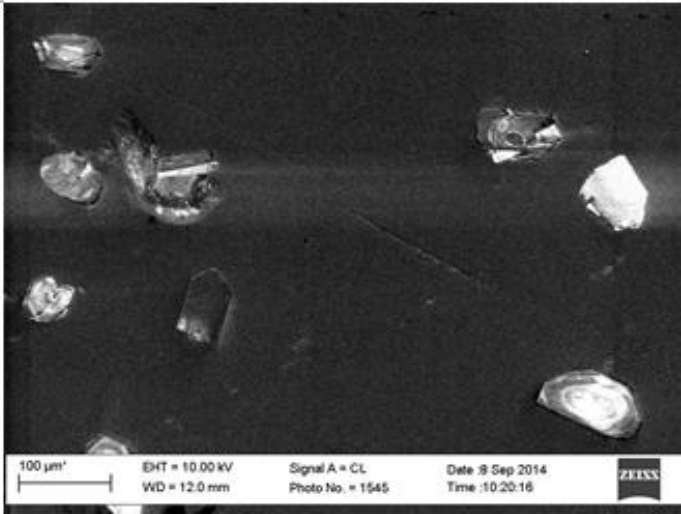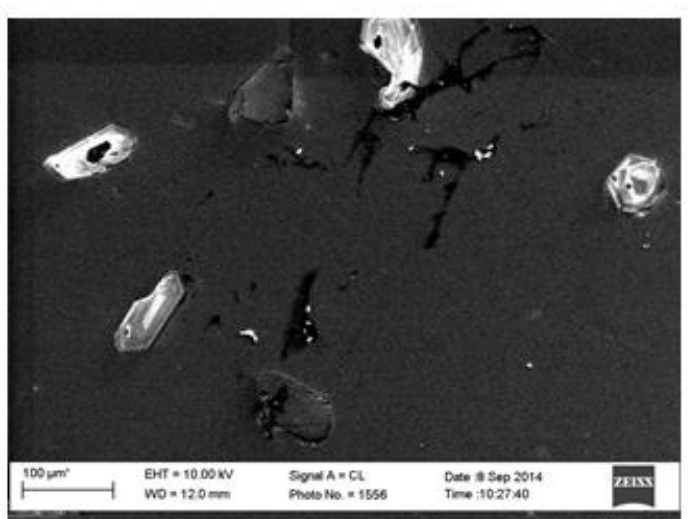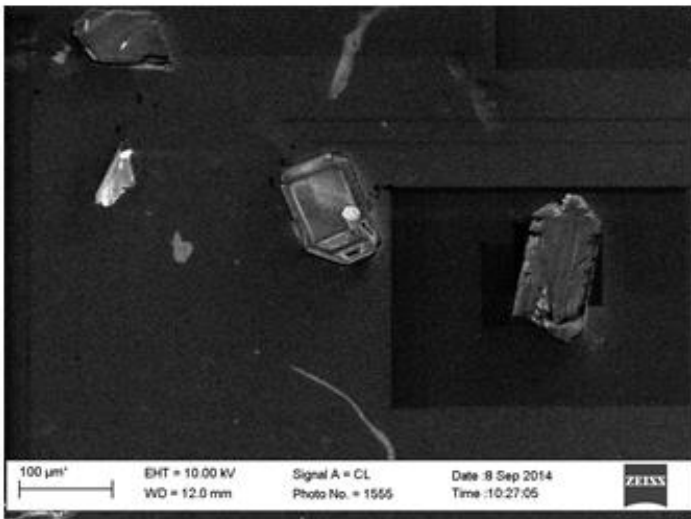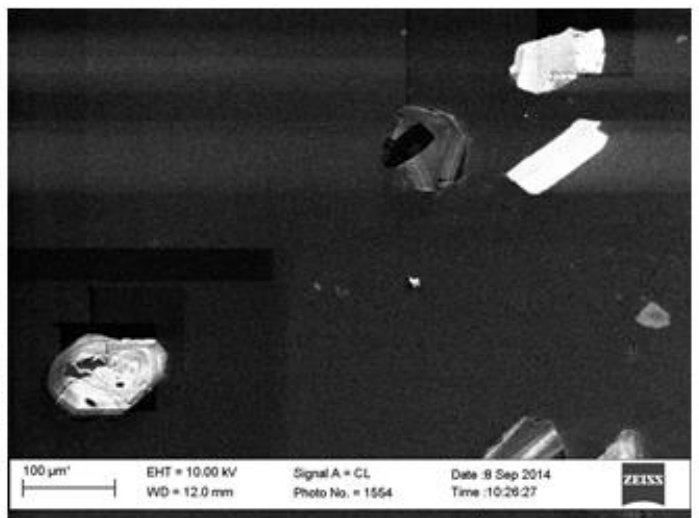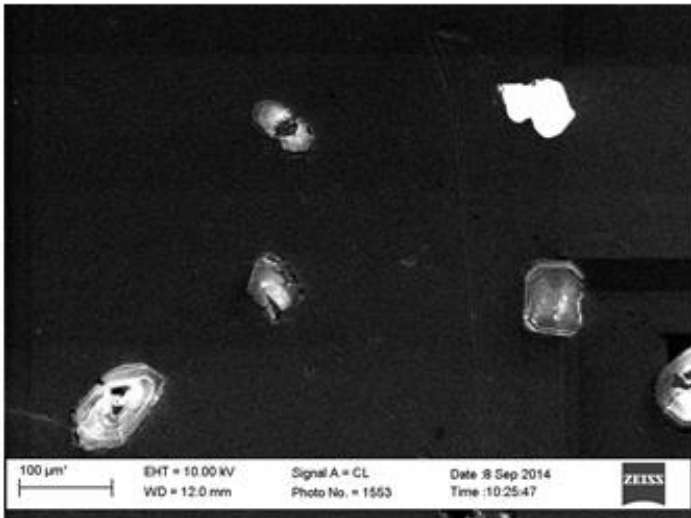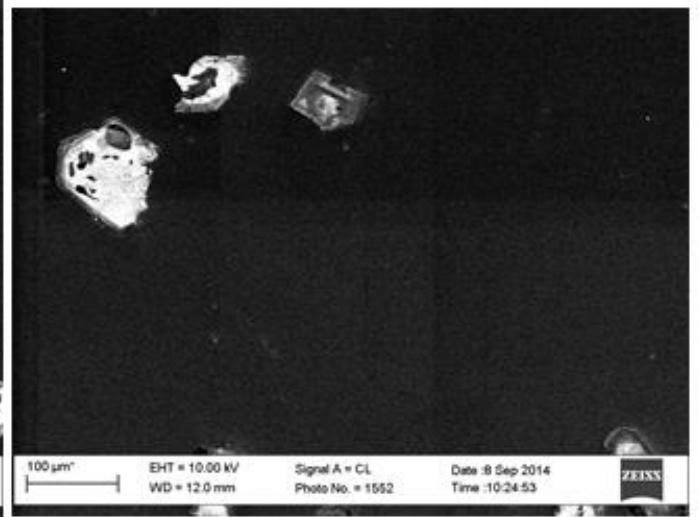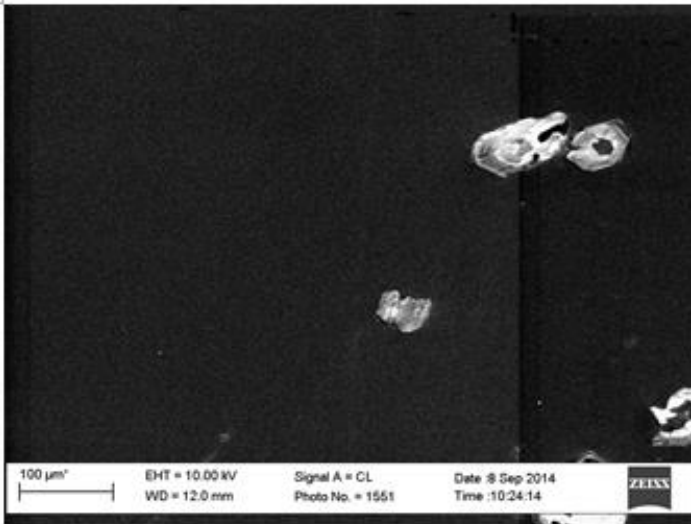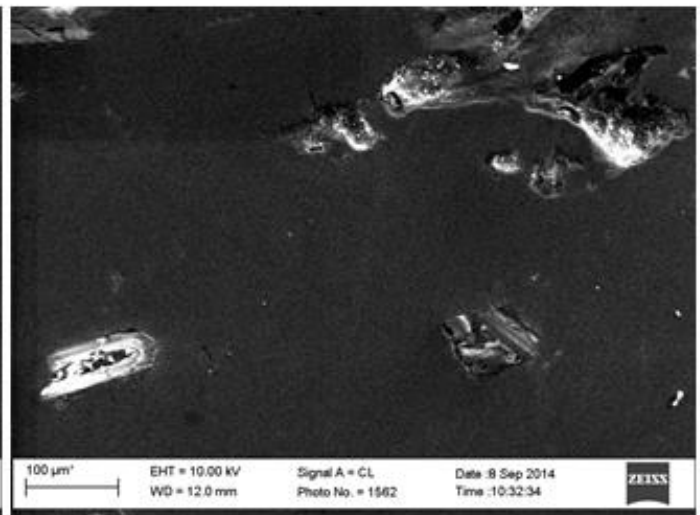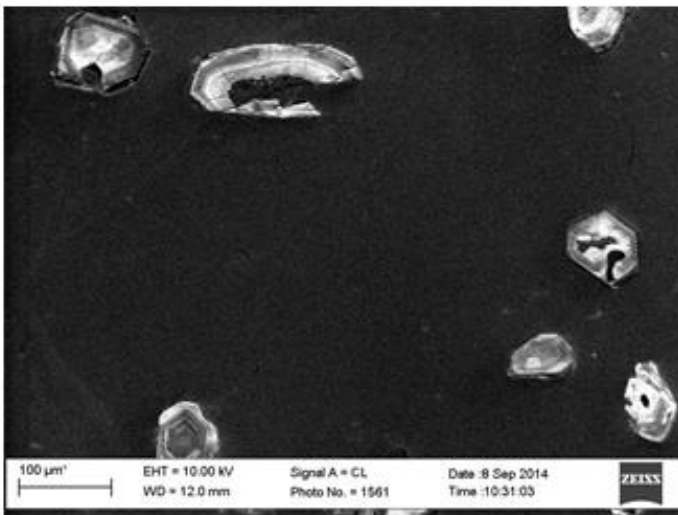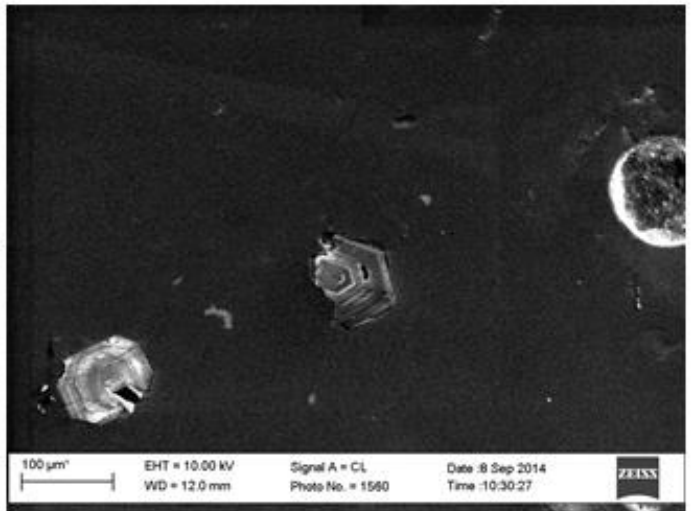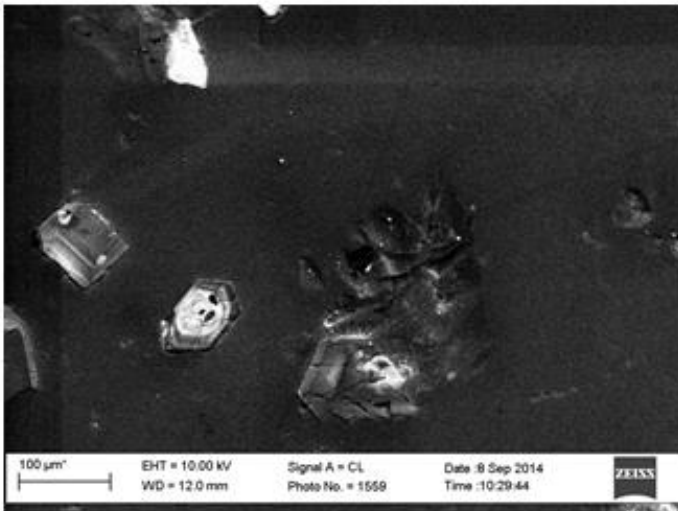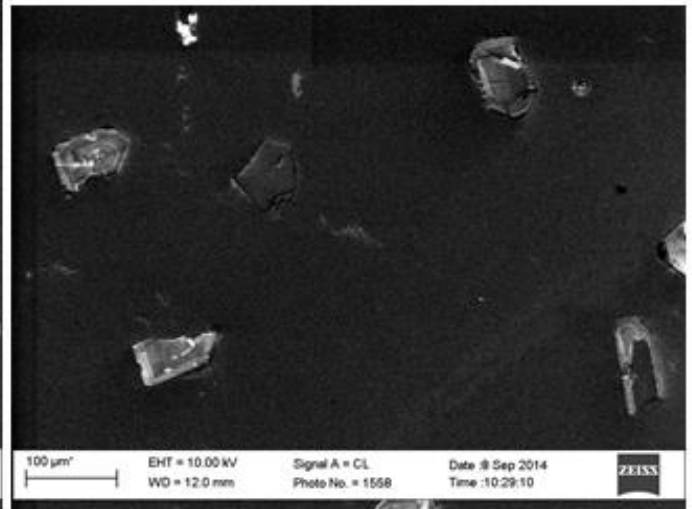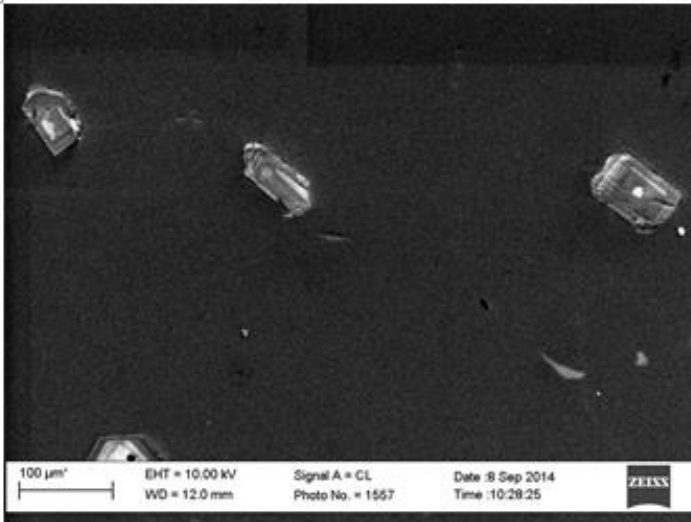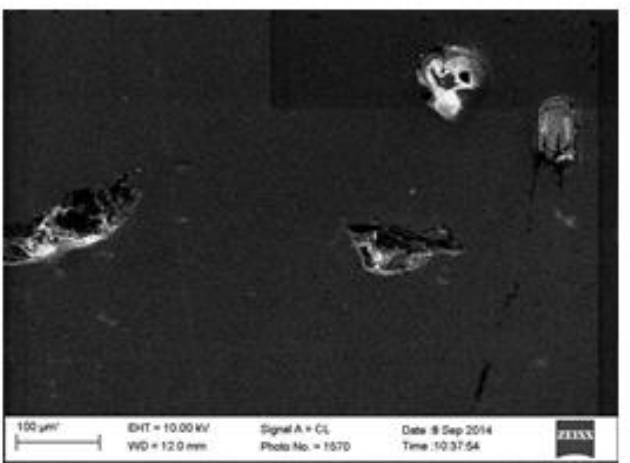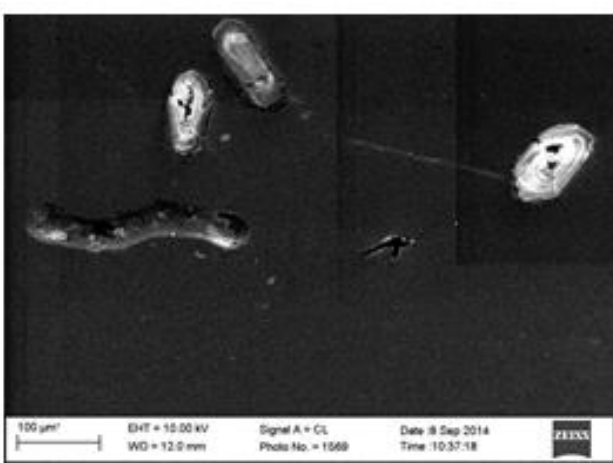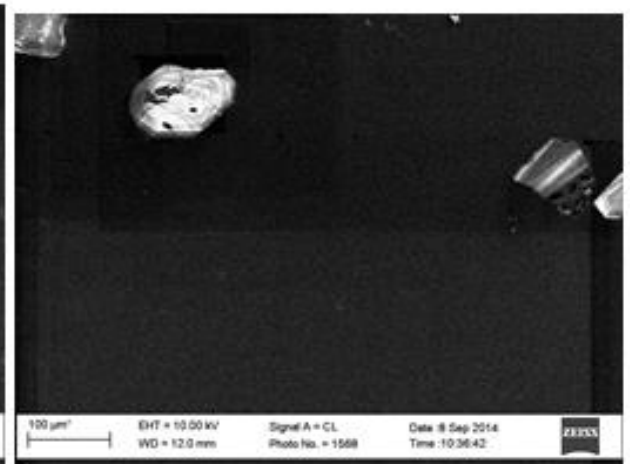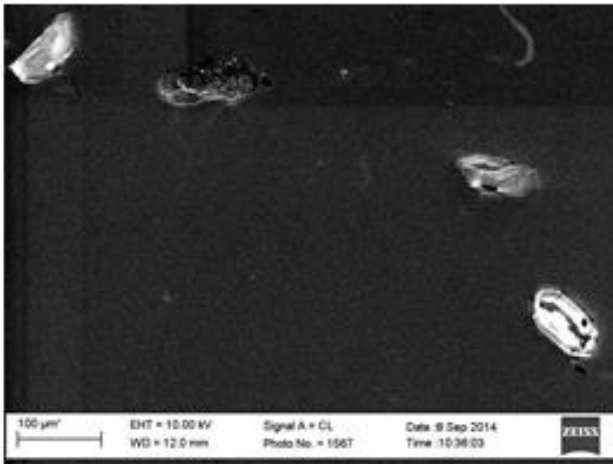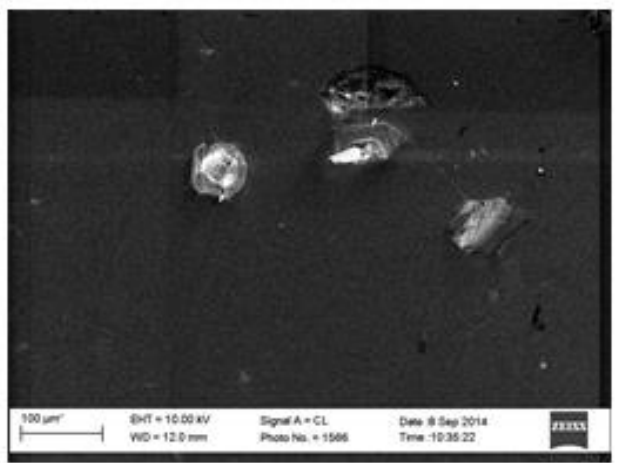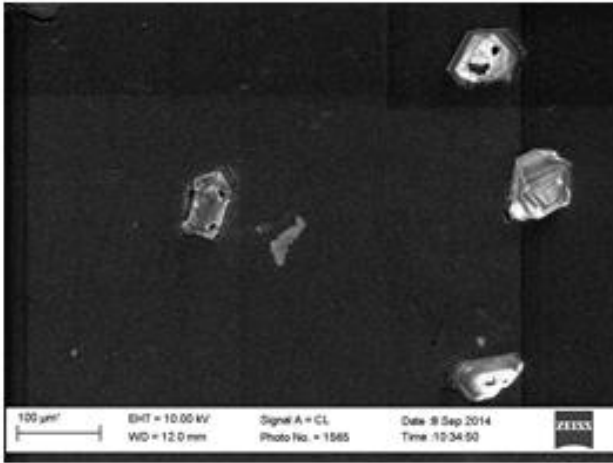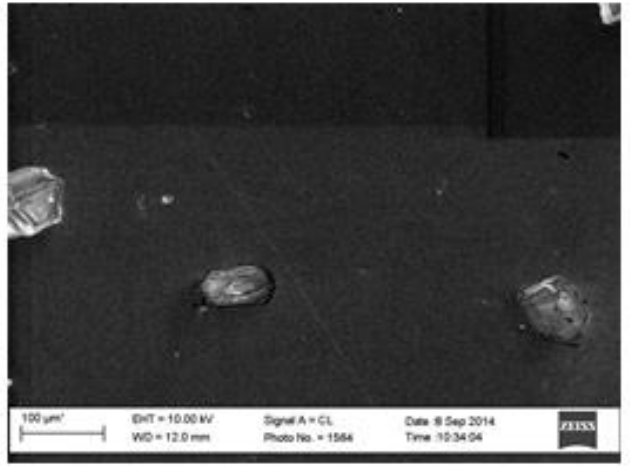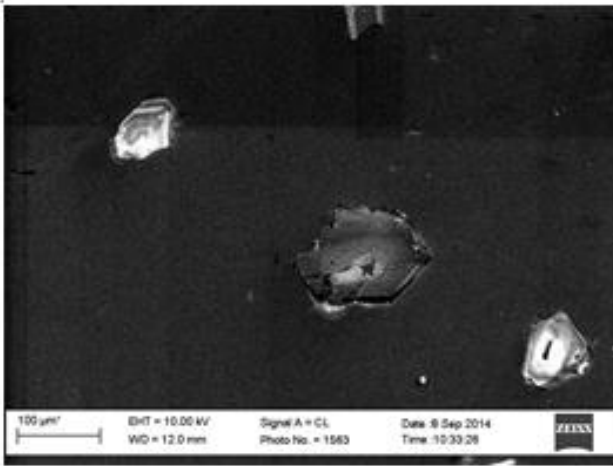
## Part 3 – SHRIMP U/Pb age data

N.B., table continues lengthways across the following pages

| Labels | U/ ppm | Th/ ppm | Th/ U | ± Th/U | Pb*/ ppm | 204/ ppb | 204Pb/ 206Pb | ± 204/ 206 | f206 | ± f206 |
|---|---|---|---|---|---|---|---|---|---|---|
| PCF-1.1 | 227.5 | 64.0 | 0.3 | 0.004 | 16 | 2 | 0.0002 | 0.00009 | 0.0030 | 0.00157 |
| PCF-2.1 | 317.8 | 99.6 | 0.3 | 0.004 | 23 | 4 | 0.0002 | 0.00008 | 0.0035 | 0.00147 |
| PCF-3.1 | 1134.2 | 493.6 | 0.4 | 0.011 | 82 | 6 | 0.0001 | 0.00003 | 0.0016 | 0.00054 |
| PCF-5.1 | 135.8 | 55.8 | 0.4 | 0.009 | 9 | 6 | 0.0008 | 0.00032 | 0.0138 | 0.00571 |
| PCF-6.1 | 572.4 | 238.9 | 0.4 | 0.008 | 43 | 3 | 0.0001 | 0.00004 | 0.0017 | 0.00075 |
| PCF-7.1 | 1227.9 | 564.5 | 0.5 | 0.004 | 91 | 1 | 0.0000 | 0.00002 | 0.0003 | 0.00035 |
| PCF-8.1 | 389.2 | 107.7 | 0.3 | 0.002 | 28 | 4 | 0.0002 | 0.00007 | 0.0028 | 0.00132 |
| PCF-9.1 | 399.4 | 161.6 | 0.4 | 0.014 | 28 | 2 | 0.0001 | 0.00006 | 0.0012 | 0.00112 |
| PCF-10.1 | 822.4 | 292.7 | 0.4 | 0.002 | 60 | 3 | 0.0001 | 0.00003 | 0.0010 | 0.0005 |
| PCF-11.1 | 213.6 | 52.8 | 0.2 | 0.002 | 14 | 0 | 0.0000 | 0.00008 | 0.0000 | 0.00141 |
| PCF-12.1 | 466.7 | 126.7 | 0.3 | 0.005 | 31 | 4 | 0.0001 | 0.00007 | 0.0024 | 0.00118 |
| PCF-12.2 | 343.0 | 72.9 | 0.2 | 0.003 | 23 | 0 | 0.0000 | 0.00005 | 0.0000 | 0.00086 |
| PCF-13.1 | 179.5 | 80.4 | 0.4 | 0.007 | 12 | 5 | 0.0004 | 0.00015 | 0.0080 | 0.00274 |
| PCF-13.2 | 164.4 | 57.8 | 0.4 | 0.010 | 10 | 3 | 0.0003 | 0.00014 | 0.0054 | 0.0026 |
| PCF-14.1 | 939.1 | 365.2 | 0.4 | 0.002 | 68 | 0 | 0.0000 | 0.00001 | 0.0001 | 0.00025 |
| PCF-15.1 | 297.3 | 76.9 | 0.3 | 0.002 | 22 | 2 | 0.0001 | 0.00007 | 0.0016 | 0.00123 |
| PCF-16.1 | 473.7 | 172.5 | 0.4 | 0.038 | 32 | 5 | 0.0002 | 0.00006 | 0.0032 | 0.00102 |
| PCF-17.1 | 279.9 | 107.1 | 0.4 | 0.004 | 21 | 2 | 0.0001 | 0.00009 | 0.0022 | 0.00171 |
| PCF-18.1 | 1948.4 | 1084.4 | 0.6 | 0.003 | 145 | 5 | 0.0000 | 0.00002 | 0.0007 | 0.0004 |
| PCF-19.1 | 1396.5 | 624.5 | 0.4 | 0.003 | 102 | 3 | 0.0000 | 0.00001 | 0.0006 | 0.00026 |
| PCF-20.1 | 353.2 | 137.4 | 0.4 | 0.004 | 26 | 4 | 0.0002 | 0.00007 | 0.0036 | 0.00122 |
| PCF-21.1 | 516.2 | 188.3 | 0.4 | 0.003 | 38 | 0 | 0.0000 | 0.00003 | 0.0001 | 0.0006 |
| PCF-22.1 | 2697.4 | 1431.9 | 0.5 | 0.003 | 202 | 2 | 0.0000 | 0.00001 | 0.0002 | 0.00017 |
| PCF-23.1 | 445.4 | 146.8 | 0.3 | 0.004 | 32 | 1 | 0.0000 | 0.00003 | 0.0008 | 0.00059 |
| PCF-24.1 | 347.2 | 93.1 | 0.3 | 0.001 | 25 | 2 | 0.0001 | 0.00005 | 0.0016 | 0.00082 |
| PCF-25.1 | 417.3 | 112.0 | 0.3 | 0.002 | 28 | 0 | 0.0000 | 0.00003 | 0.0002 | 0.0006 |
| PCF-26.1 | 240.8 | 65.8 | 0.3 | 0.008 | 16 | 3 | 0.0002 | 0.00012 | 0.0035 | 0.00222 |
| PCF-26.2 | 197.3 | 48.7 | 0.2 | 0.010 | 13 | 10 | 0.0009 | 0.00021 | 0.0161 | 0.00372 |
| PCF-27.1 | 606.7 | 289.1 | 0.5 | 0.006 | 45 | 5 | 0.0001 | 0.00006 | 0.0022 | 0.00109 |
| PCF-28.1 | 212.8 | 81.9 | 0.4 | 0.007 | 13 | 44 | 0.0037 | 0.00049 | 0.0675 | 0.00885 |
| PCF-29.1 | 560.3 | 214.2 | 0.4 | 0.003 | 41 | 1 | 0.0000 | 0.00004 | 0.0008 | 0.00073 |
| PCF-30.1 | 330.5 | 121.7 | 0.4 | 0.004 | 23 | 2 | 0.0001 | 0.00006 | 0.0016 | 0.00116 |
| PCF-31.1 | 340.4 | 103.0 | 0.3 | 0.004 | 24 | 4 | 0.0002 | 0.00008 | 0.0036 | 0.00143 |
| PCF-32.1 | 657.9 | 230.7 | 0.4 | 0.017 | 49 | 0 | 0.0000 | 0.00001 | 0.0002 | 0.00014 |
| PCF-33.1 | 793.8 | 292.0 | 0.4 | 0.002 | 58 | 1 | 0.0000 | 0.00002 | 0.0005 | 0.00032 |
| PCF-34.1 | 497.1 | 170.4 | 0.3 | 0.003 | 34 | 0 | 0.0000 | 0.00003 | 0.0001 | 0.00063 |
| PCF-35.1 | 368.9 | 113.3 | 0.3 | 0.004 | 26 | 0 | 0.0000 | 0.00003 | 0.0003 | 0.00054 |
| PCF-36.1 | 186.4 | 65.6 | 0.4 | 0.005 | 13 | 2 | 0.0002 | 0.00010 | 0.0037 | 0.00189 |
| PCF-37.1 | 404.1 | 134.9 | 0.3 | 0.003 | 29 | 0 | 0.0000 | 0.00000 | 0.0000 | 0.00004 |
| PCF-38.1 | 593.4 | 213.6 | 0.4 | 0.003 | 43 | 2 | 0.0001 | 0.00006 | 0.0011 | 0.00116 |
| PCF-39.1 | 2637.2 | 1467.3 | 0.6 | 0.002 | 194 | 4 | 0.0000 | 0.00002 | 0.0004 | 0.00027 |
| PCF-40.1 | 381.6 | 123.4 | 0.3 | 0.005 | 26 | 1 | 0.0000 | 0.00003 | 0.0006 | 0.00052 |
| PCF-41.1 | 764.1 | 266.1 | 0.3 | 0.002 | 57 | 0 | 0.0000 | 0.00000 | 0.0001 | 0.00009 |
| PCF-42.1 | 731.3 | 238.4 | 0.3 | 0.003 | 52 | 0 | 0.0000 | 0.00003 | 0.0000 | 0.00051 |
| PCF-43.1 | 572.5 | 190.5 | 0.3 | 0.003 | 41 | 2 | 0.0000 | 0.00003 | 0.0009 | 0.00058 |

| f207 | f208 | Y | ± Y | com8/6 | ± com8/6 | 6*/38m | ± 6*/38m | UO/U | ± UO/U | 208Pb/ 206Pb | ± 8/6 |
|---|---|---|---|---|---|---|---|---|---|---|---|
| 0.045 | 0.071 | 0.001 | 0.003 | 0.311 | 0.951 | 0.11 | 0.001 | 4.62 | 0.03 | 0.08 | 0.004 |
| 0.051 | 0.065 | 0.017 | 0.003 | 4.880 | 2.207 | 0.10 | 0.002 | 4.53 | 0.02 | 0.11 | 0.004 |
| 0.024 | 0.024 | 0.005 | 0.004 | 3.086 | 2.889 | 0.11 | 0.002 | 4.70 | 0.02 | 0.14 | 0.003 |
| 0.167 | 0.222 | 0.005 | 0.009 | 0.370 | 0.663 | 0.10 | 0.003 | 4.56 | 0.04 | 0.10 | 0.015 |
| 0.026 | 0.027 | 0.000 | 0.000 | 0.000 | 0.000 | 0.12 | 0.002 | 4.73 | 0.02 | 0.13 | 0.004 |
| 0.005 | 0.005 | 0.004 | 0.002 | 13.115 | 14.447 | 0.12 | 0.002 | 4.86 | 0.03 | 0.15 | 0.002 |
| 0.043 | 0.065 | 0.004 | 0.002 | 1.390 | 1.007 | 0.12 | 0.002 | 4.85 | 0.02 | 0.08 | 0.003 |
| 0.018 | 0.020 | 0.000 | 0.000 | 0.000 | 0.000 | 0.09 | 0.003 | 4.18 | 0.07 | 0.12 | 0.004 |
| 0.015 | 0.018 | 0.001 | 0.002 | 1.187 | 2.081 | 0.11 | 0.001 | 4.69 | 0.02 | 0.11 | 0.002 |
| 0.000 | 0.000 | 0.001 | 0.003 | 68.411 | 5386.1 | 0.10 | 0.002 | 4.65 | 0.01 | 0.08 | 0.004 |
| 0.037 | 0.058 | 0.003 | 0.002 | 1.285 | 1.172 | 0.12 | 0.001 | 4.90 | 0.03 | 0.08 | 0.003 |
| 0.000 | 0.001 | 0.000 | 0.000 | 0.000 | 0.000 | 0.10 | 0.002 | 4.49 | 0.04 | 0.06 | 0.003 |
| 0.123 | 0.199 | 0.000 | 0.000 | 0.000 | 0.000 | 0.11 | 0.001 | 4.83 | 0.02 | 0.07 | 0.007 |
| 0.073 | 0.158 | 0.000 | 0.000 | 0.000 | 0.000 | 0.10 | 0.002 | 4.69 | 0.03 | 0.06 | 0.006 |
| 0.001 | 0.001 | 0.000 | 0.000 | 0.000 | 0.000 | 0.12 | 0.001 | 4.86 | 0.01 | 0.12 | 0.002 |
| 0.024 | 0.040 | 0.003 | 0.002 | 1.591 | 1.918 | 0.11 | 0.002 | 4.58 | 0.02 | 0.08 | 0.003 |
| 0.048 | 0.055 | 0.011 | 0.014 | 3.285 | 4.444 | 0.11 | 0.007 | 4.90 | 0.36 | 0.12 | 0.008 |
| 0.033 | 0.037 | 0.004 | 0.004 | 2.050 | 2.435 | 0.11 | 0.003 | 4.65 | 0.05 | 0.12 | 0.005 |
| 0.011 | 0.009 | 0.000 | 0.000 | 0.000 | 0.000 | 0.12 | 0.001 | 4.93 | 0.02 | 0.17 | 0.002 |
| 0.010 | 0.010 | 0.003 | 0.002 | 5.176 | 4.075 | 0.12 | 0.001 | 4.86 | 0.02 | 0.14 | 0.002 |
| 0.055 | 0.061 | 0.001 | 0.004 | 0.410 | 1.157 | 0.12 | 0.002 | 4.76 | 0.03 | 0.11 | 0.005 |
| 0.002 | 0.002 | 0.001 | 0.003 | 4.332 | 29.167 | 0.12 | 0.001 | 4.88 | 0.02 | 0.11 | 0.003 |
| 0.003 | 0.003 | 0.003 | 0.002 | 13.024 | 12.637 | 0.12 | 0.002 | 4.80 | 0.03 | 0.17 | 0.001 |
| 0.012 | 0.016 | 0.001 | 0.002 | 1.566 | 3.268 | 0.11 | 0.002 | 4.60 | 0.02 | 0.10 | 0.002 |
| 0.025 | 0.040 | 0.002 | 0.003 | 1.272 | 1.874 | 0.12 | 0.001 | 4.74 | 0.02 | 0.08 | 0.003 |
| 0.004 | 0.006 | 0.000 | 0.000 | 0.000 | 0.000 | 0.10 | 0.001 | 4.46 | 0.02 | 0.08 | 0.003 |
| 0.054 | 0.090 | 0.000 | 0.000 | 0.000 | 0.000 | 0.11 | 0.002 | 4.86 | 0.03 | 0.08 | 0.007 |
| 0.205 | 0.303 | 0.036 | 0.009 | 2.262 | 0.749 | 0.10 | 0.004 | 4.71 | 0.12 | 0.08 | 0.011 |
| 0.035 | 0.031 | 0.005 | 0.003 | 2.201 | 1.773 | 0.12 | 0.002 | 4.81 | 0.03 | 0.15 | 0.003 |
| 0.528 | 0.622 | 0.117 | 0.011 | 1.736 | 0.279 | 0.10 | 0.001 | 4.76 | 0.04 | 0.09 | 0.022 |
| 0.012 | 0.013 | 0.005 | 0.002 | 6.558 | 7.120 | 0.12 | 0.002 | 4.82 | 0.03 | 0.12 | 0.003 |
| 0.024 | 0.033 | 0.000 | 0.000 | 0.000 | 0.000 | 0.11 | 0.001 | 4.61 | 0.02 | 0.10 | 0.004 |
| 0.056 | 0.082 | 0.000 | 0.000 | 0.000 | 0.000 | 0.11 | 0.002 | 4.70 | 0.04 | 0.09 | 0.004 |
| 0.003 | 0.003 | 0.000 | 0.000 | 0.000 | 0.000 | 0.12 | 0.005 | 4.82 | 0.15 | 0.10 | 0.008 |
| 0.008 | 0.009 | 0.001 | 0.002 | 1.029 | 4.413 | 0.12 | 0.001 | 4.84 | 0.02 | 0.11 | 0.002 |
| 0.001 | 0.002 | 0.004 | 0.002 | 39.185 | 266.716 | 0.10 | 0.002 | 4.53 | 0.03 | 0.11 | 0.003 |
| 0.004 | 0.006 | 0.004 | 0.004 | 16.416 | 36.894 | 0.12 | 0.002 | 4.80 | 0.03 | 0.10 | 0.004 |
| 0.057 | 0.066 | 0.008 | 0.008 | 2.286 | 2.413 | 0.11 | 0.001 | 4.74 | 0.04 | 0.11 | 0.009 |
| 0.000 | 0.000 | 0.002 | 0.002 | 97.612 | 234.654 | 0.12 | 0.002 | 4.74 | 0.03 | 0.10 | 0.002 |
| 0.017 | 0.020 | 0.005 | 0.003 | 4.764 | 5.381 | 0.11 | 0.001 | 4.63 | 0.03 | 0.11 | 0.003 |
| 0.006 | 0.005 | 0.003 | 0.002 | 8.473 | 7.129 | 0.11 | 0.000 | 4.79 | 0.01 | 0.17 | 0.002 |
| 0.008 | 0.011 | 0.008 | 0.004 | 14.086 | 15.194 | 0.08 | 0.002 | 4.12 | 0.05 | 0.11 | 0.004 |
| 0.002 | 0.003 | 0.005 | 0.002 | 33.641 | 26.592 | 0.11 | 0.002 | 4.53 | 0.03 | 0.11 | 0.002 |
| 0.000 | 0.000 | 0.004 | 0.002 | 0.000 | 0.000 | 0.11 | 0.002 | 4.57 | 0.03 | 0.10 | 0.002 |
| 0.013 | 0.018 | 0.003 | 0.002 | 3.705 | 3.414 | 0.12 | 0.001 | 4.79 | 0.02 | 0.10 | 0.002 |

| 208Pb/232Th | ± 8/32 | 206Pb/238U | ± 6/38 | 207Pb/235U | ± 7/35 | 207Pb/206Pb | ± 7/6 | 238U/206Pb | ± 38/6 | 235U/207Pb | ± 35/7 | 206Pb/207Pb |
|---|---|---|---|---|---|---|---|---|---|---|---|---|
| 0.0211 | 0.00127 | 0.073 | 0.0021 | 0.55 | 0.02 | 0.05 | 0.002 | 13.8 | 0.4 | 1.8 | 0.08 | 18.3 |
| 0.024 | 0.00128 | 0.072 | 0.002 | 0.56 | 0.03 | 0.06 | 0.002 | 14.0 | 0.5 | 1.8 | 0.08 | 17.8 |
| 0.022 | 0.00104 | 0.071 | 0.002 | 0.55 | 0.02 | 0.06 | 0.001 | 14.1 | 0.5 | 1.8 | 0.07 | 17.9 |
| 0.017 | 0.0026 | 0.068 | 0.003 | 0.57 | 0.06 | 0.06 | 0.005 | 14.6 | 0.7 | 1.8 | 0.18 | 16.6 |
| 0.022 | 0.00102 | 0.073 | 0.002 | 0.56 | 0.02 | 0.06 | 0.001 | 13.6 | 0.4 | 1.8 | 0.07 | 18.2 |
| 0.023 | 0.00084 | 0.071 | 0.002 | 0.55 | 0.02 | 0.06 | 0.001 | 14.0 | 0.5 | 1.8 | 0.07 | 17.8 |
| 0.022 | 0.00114 | 0.073 | 0.002 | 0.54 | 0.02 | 0.05 | 0.001 | 13.7 | 0.4 | 1.8 | 0.08 | 18.6 |
| 0.021 | 0.00142 | 0.070 | 0.004 | 0.53 | 0.03 | 0.06 | 0.001 | 14.2 | 0.7 | 1.9 | 0.11 | 18.2 |
| 0.022 | 0.00079 | 0.072 | 0.002 | 0.56 | 0.02 | 0.06 | 0.001 | 13.8 | 0.4 | 1.8 | 0.06 | 18.0 |
| 0.021 | 0.00128 | 0.068 | 0.002 | 0.55 | 0.03 | 0.06 | 0.002 | 14.7 | 0.5 | 1.8 | 0.08 | 17.0 |
| 0.021 | 0.00105 | 0.069 | 0.002 | 0.51 | 0.02 | 0.05 | 0.002 | 14.5 | 0.4 | 1.9 | 0.09 | 18.5 |
| 0.021 | 0.00129 | 0.070 | 0.003 | 0.55 | 0.02 | 0.06 | 0.001 | 14.3 | 0.5 | 1.8 | 0.08 | 17.7 |
| 0.010 | 0.00105 | 0.068 | 0.002 | 0.47 | 0.03 | 0.05 | 0.003 | 14.7 | 0.4 | 2.1 | 0.14 | 20.0 |
| 0.011 | 0.00132 | 0.066 | 0.002 | 0.54 | 0.03 | 0.06 | 0.003 | 15.1 | 0.6 | 1.8 | 0.11 | 16.8 |
| 0.022 | 0.0007 | 0.072 | 0.002 | 0.55 | 0.02 | 0.06 | 0.001 | 13.9 | 0.4 | 1.8 | 0.06 | 18.0 |
| 0.023 | 0.00124 | 0.075 | 0.002 | 0.58 | 0.03 | 0.06 | 0.002 | 13.4 | 0.4 | 1.7 | 0.08 | 17.8 |
| 0.021 | 0.00434 | 0.066 | 0.011 | 0.51 | 0.09 | 0.06 | 0.003 | 15.1 | 2.5 | 2.0 | 0.35 | 18.1 |
| 0.023 | 0.00137 | 0.073 | 0.003 | 0.56 | 0.03 | 0.06 | 0.002 | 13.7 | 0.6 | 1.8 | 0.10 | 18.1 |
| 0.022 | 0.00069 | 0.071 | 0.002 | 0.54 | 0.02 | 0.06 | 0.001 | 14.2 | 0.4 | 1.9 | 0.06 | 18.0 |
| 0.022 | 0.00075 | 0.071 | 0.002 | 0.53 | 0.02 | 0.05 | 0.001 | 14.1 | 0.4 | 1.9 | 0.06 | 18.4 |
| 0.021 | 0.00113 | 0.072 | 0.002 | 0.53 | 0.02 | 0.05 | 0.001 | 13.8 | 0.4 | 1.9 | 0.08 | 18.9 |
| 0.023 | 0.00089 | 0.074 | 0.002 | 0.57 | 0.02 | 0.06 | 0.001 | 13.6 | 0.4 | 1.8 | 0.06 | 18.0 |
| 0.022 | 0.00076 | 0.071 | 0.002 | 0.55 | 0.02 | 0.06 | 0.000 | 14.1 | 0.5 | 1.8 | 0.06 | 17.7 |
| 0.022 | 0.00092 | 0.072 | 0.002 | 0.56 | 0.02 | 0.06 | 0.001 | 13.8 | 0.4 | 1.8 | 0.07 | 17.8 |
| 0.022 | 0.00111 | 0.073 | 0.002 | 0.55 | 0.02 | 0.05 | 0.001 | 13.7 | 0.4 | 1.8 | 0.07 | 18.5 |
| 0.020 | 0.00097 | 0.069 | 0.002 | 0.54 | 0.02 | 0.06 | 0.001 | 14.6 | 0.4 | 1.9 | 0.07 | 17.6 |
| 0.019 | 0.00182 | 0.068 | 0.002 | 0.51 | 0.03 | 0.05 | 0.002 | 14.7 | 0.5 | 2.0 | 0.11 | 18.5 |
| 0.021 | 0.00343 | 0.065 | 0.004 | 0.49 | 0.06 | 0.05 | 0.005 | 15.3 | 1.0 | 2.0 | 0.24 | 18.2 |
| 0.022 | 0.00093 | 0.072 | 0.002 | 0.53 | 0.02 | 0.05 | 0.001 | 13.9 | 0.4 | 1.9 | 0.08 | 18.6 |
| 0.015 | 0.0035 | 0.060 | 0.002 | 0.47 | 0.08 | 0.06 | 0.009 | 16.5 | 0.5 | 2.1 | 0.35 | 17.9 |
| 0.023 | 0.00095 | 0.072 | 0.002 | 0.55 | 0.02 | 0.06 | 0.001 | 14.0 | 0.5 | 1.8 | 0.08 | 17.9 |
| 0.018 | 0.00095 | 0.070 | 0.002 | 0.54 | 0.02 | 0.06 | 0.001 | 14.4 | 0.4 | 1.9 | 0.08 | 17.9 |
| 0.020 | 0.00124 | 0.072 | 0.003 | 0.54 | 0.03 | 0.05 | 0.001 | 13.8 | 0.5 | 1.9 | 0.09 | 18.7 |
| 0.022 | 0.00265 | 0.074 | 0.006 | 0.54 | 0.05 | 0.05 | 0.003 | 13.4 | 1.1 | 1.9 | 0.18 | 19.0 |
| 0.022 | 0.0008 | 0.072 | 0.002 | 0.57 | 0.02 | 0.06 | 0.001 | 13.8 | 0.4 | 1.8 | 0.06 | 17.6 |
| 0.022 | 0.00097 | 0.069 | 0.003 | 0.54 | 0.02 | 0.06 | 0.001 | 14.5 | 0.5 | 1.9 | 0.08 | 17.6 |
| 0.023 | 0.00121 | 0.072 | 0.002 | 0.55 | 0.02 | 0.05 | 0.001 | 13.9 | 0.5 | 1.8 | 0.08 | 18.2 |
| 0.021 | 0.0018 | 0.068 | 0.002 | 0.49 | 0.03 | 0.05 | 0.002 | 14.8 | 0.5 | 2.0 | 0.11 | 18.9 |
| 0.023 | 0.0009 | 0.073 | 0.002 | 0.56 | 0.02 | 0.06 | 0.001 | 13.7 | 0.5 | 1.8 | 0.07 | 17.9 |
| 0.023 | 0.00098 | 0.072 | 0.002 | 0.55 | 0.02 | 0.06 | 0.001 | 14.0 | 0.4 | 1.8 | 0.07 | 17.8 |
| 0.022 | 0.00062 | 0.069 | 0.002 | 0.53 | 0.01 | 0.06 | 0.000 | 14.4 | 0.4 | 1.9 | 0.05 | 18.0 |
| 0.022 | 0.00127 | 0.068 | 0.003 | 0.53 | 0.03 | 0.06 | 0.001 | 14.8 | 0.6 | 1.9 | 0.09 | 17.7 |
| 0.024 | 0.00093 | 0.074 | 0.002 | 0.57 | 0.02 | 0.06 | 0.001 | 13.5 | 0.4 | 1.7 | 0.06 | 17.8 |
| 0.023 | 0.001 | 0.071 | 0.003 | 0.54 | 0.02 | 0.06 | 0.001 | 14.1 | 0.5 | 1.8 | 0.07 | 17.9 |
| 0.023 | 0.00086 | 0.072 | 0.002 | 0.56 | 0.02 | 0.06 | 0.001 | 13.8 | 0.4 | 1.8 | 0.06 | 17.7 |

| ± 6/7 | AGE 8/32 | ± age 8/32 | AGE 6/38 | ± age 6/38 | AGE 7/35 | ± age 7/35 | AGE 7/6 | ± age 7/6 | % CONC | Time |
|---|---|---|---|---|---|---|---|---|---|---|
| 0.5 | 421.3 | 25.2 | 451.4 | 12.8 | 443.1 | 16.0 | 400.6 | 67.8 | 112.7 | 11.73 |
| 0.5 | 487.3 | 25.3 | 446.2 | 14.7 | 448.3 | 16.8 | 459.0 | 60.4 | 97.2 | 12.1 |
| 0.3 | 443.1 | 20.5 | 441.2 | 14.4 | 442.5 | 14.0 | 449.0 | 34.5 | 98.3 | 12.47 |
| 1.4 | 342.9 | 51.7 | 425.9 | 18.9 | 456.9 | 38.5 | 616.1 | 198.4 | 69.1 | 13.55 |
| 0.4 | 440.2 | 20.3 | 456.5 | 13.4 | 449.5 | 14.4 | 414.0 | 48.7 | 110.3 | 13.88 |
| 0.2 | 452.8 | 16.6 | 444.4 | 14.8 | 446.3 | 13.4 | 456.3 | 21.1 | 97.4 | 14.23 |
| 0.5 | 441.7 | 22.5 | 454.8 | 13.3 | 440.2 | 14.9 | 364.4 | 56.5 | 124.8 | 14.97 |
| 0.4 | 416.4 | 28.1 | 438.9 | 21.2 | 434.8 | 20.5 | 413.3 | 52.0 | 106.2 | 15.33 |
| 0.2 | 444.6 | 15.6 | 451.1 | 12.7 | 448.9 | 12.2 | 437.8 | 29.8 | 103.0 | 15.67 |
| 0.5 | 426.6 | 25.3 | 423.4 | 13.4 | 445.7 | 16.6 | 562.3 | 62.1 | 75.3 | 17.62 |
| 0.6 | 415.5 | 20.9 | 428.6 | 12.1 | 420.3 | 15.4 | 375.3 | 69.2 | 114.2 | 17.93 |
| 0.4 | 416.3 | 25.5 | 436.6 | 16.0 | 441.8 | 16.5 | 469.2 | 47.7 | 93.1 | 9.03 |
| 1.1 | 209.0 | 21.1 | 423.5 | 12.4 | 389.7 | 21.4 | 193.7 | 131.9 | 218.7 | 18.23 |
| 0.7 | 230.2 | 26.3 | 412.4 | 15.0 | 439.9 | 21.9 | 586.1 | 96.5 | 70.4 | 8.72 |
| 0.2 | 436.9 | 13.8 | 446.7 | 12.3 | 444.0 | 11.6 | 430.0 | 25.6 | 103.9 | 18.88 |
| 0.5 | 458.2 | 24.5 | 465.4 | 14.2 | 464.5 | 16.7 | 459.6 | 62.5 | 101.3 | 19.2 |
| 0.9 | 424.2 | 86.1 | 413.8 | 65.6 | 415.6 | 62.0 | 425.7 | 116.3 | 97.2 | 19.5 |
| 0.6 | 450.5 | 27.0 | 453.7 | 17.9 | 449.0 | 19.8 | 424.7 | 70.5 | 106.8 | 20.15 |
| 0.2 | 432.3 | 13.6 | 439.2 | 12.6 | 438.4 | 11.9 | 434.6 | 25.8 | 101.0 | 20.47 |
| 0.2 | 444.5 | 14.9 | 441.4 | 12.6 | 433.4 | 11.4 | 391.1 | 21.5 | 112.9 | 20.78 |
| 0.5 | 425.9 | 22.4 | 451.0 | 14.2 | 431.5 | 15.5 | 328.4 | 59.1 | 137.4 | 21.42 |
| 0.4 | 456.6 | 17.7 | 458.2 | 12.2 | 455.2 | 13.2 | 440.1 | 44.5 | 104.1 | 21.73 |
| 0.1 | 446.1 | 15.0 | 442.8 | 13.8 | 447.2 | 12.4 | 469.9 | 16.9 | 94.2 | 22.03 |
| 0.3 | 445.8 | 18.3 | 450.6 | 13.7 | 452.4 | 13.5 | 461.7 | 34.4 | 97.6 | 22.68 |
| 0.3 | 445.6 | 22.0 | 455.7 | 12.8 | 442.8 | 13.2 | 376.5 | 42.6 | 121.0 | 22.98 |
| 0.3 | 409.8 | 19.3 | 427.2 | 12.7 | 437.1 | 13.0 | 489.6 | 36.0 | 87.3 | 23.3 |
| 0.8 | 376.6 | 36.2 | 424.4 | 13.6 | 417.2 | 19.6 | 378.1 | 98.0 | 112.2 | 23.62 |
| 1.6 | 419.1 | 68.0 | 408.9 | 27.2 | 408.3 | 40.0 | 404.4 | 206.0 | 101.1 | 8.4 |
| 0.4 | 447.0 | 18.3 | 449.2 | 13.9 | 434.8 | 15.1 | 358.9 | 54.8 | 125.2 | 0.25 |
| 2.8 | 291.5 | 69.9 | 378.4 | 12.1 | 389.0 | 54.8 | 452.8 | 394.8 | 83.6 | 0.57 |
| 0.4 | 455.5 | 18.8 | 445.9 | 14.6 | 446.9 | 15.4 | 451.9 | 48.1 | 98.7 | 0.88 |
| 0.5 | 367.4 | 19.0 | 433.8 | 12.8 | 436.5 | 15.1 | 450.8 | 57.7 | 96.2 | 1.52 |
| 0.5 | 409.5 | 24.6 | 450.8 | 16.7 | 435.3 | 17.7 | 354.1 | 62.8 | 127.3 | 1.83 |
| 1.0 | 434.8 | 52.5 | 462.3 | 35.1 | 438.6 | 36.1 | 315.8 | 123.5 | 146.4 | 2.15 |
| 0.2 | 445.6 | 15.8 | 450.7 | 12.8 | 455.5 | 12.5 | 480.0 | 29.5 | 93.9 | 2.47 |
| 0.2 | 439.0 | 19.1 | 428.7 | 15.2 | 437.4 | 14.6 | 483.8 | 31.6 | 88.6 | 3.1 |
| 0.4 | 463.6 | 23.9 | 449.2 | 14.2 | 442.9 | 14.9 | 409.9 | 48.0 | 109.6 | 3.42 |
| 0.8 | 421.2 | 35.7 | 422.0 | 13.1 | 407.1 | 18.7 | 323.1 | 95.9 | 130.6 | 3.72 |
| 0.2 | 457.5 | 17.8 | 452.9 | 14.5 | 451.5 | 13.7 | 444.3 | 30.4 | 101.9 | 4.37 |
| 0.4 | 454.3 | 19.4 | 445.4 | 13.0 | 448.2 | 14.6 | 462.3 | 51.5 | 96.4 | 4.67 |
| 0.1 | 435.3 | 12.4 | 432.1 | 11.1 | 433.1 | 10.0 | 438.0 | 14.0 | 98.6 | 4.98 |
| 0.3 | 445.1 | 25.1 | 421.4 | 17.4 | 429.3 | 17.1 | 471.7 | 41.4 | 89.3 | 5.62 |
| 0.2 | 476.8 | 18.4 | 460.5 | 14.5 | 460.5 | 13.1 | 460.7 | 21.9 | 100.0 | 5.93 |
| 0.2 | 452.9 | 19.8 | 440.4 | 15.7 | 440.8 | 14.6 | 442.9 | 29.3 | 99.4 | 6.25 |
| 0.3 | 454.1 | 16.9 | 450.9 | 12.9 | 453.8 | 13.3 | 468.5 | 39.1 | 96.2 | 6.57 |

# Appendix 3

**Geochemical Data**

| Sample | Clast Map(s) |
|--------|--------------|
| PCF5 |  |
| PCF5.1 |  |
| PCF5.2 |  |
| | |

| | |
|---|---|
| PCF5.3 |  |
| PCF5.4 |  |
| PCF5.6 |  |
| PCF5.7<br><br>N.B., This sample is the opposite half of PCF5.6 |  |
| PCF5.8 |  |

| | |
|---|---|
| CD1.6 |  |
| CR19 |  |
| CR20 |  |

**Part 2 – HH-XRF Data**

| Limestone Clasts | | Fe2O3 | MnO | TiO2 | CaO | K2O | Al2O3 | SiO2 | MgO | V | Zn | Rb | Sr | Zr | Nb | Pb | Ba | Ti |
|---|---|---|---|---|---|---|---|---|---|---|---|---|---|---|---|---|---|---|
| PCF1c | | 0.8 | 0.1 | 0.1 | 54.2 | 0.9 | 2.2 | 16.7 | | | 5.7 | 11.9 | 506.3 | 21.4 | | | 207.4 | 843.0 |
| CR19a | | 0.6 | 0.1 | 0.1 | 61.7 | | 1.1 | 5.1 | | | | | 242.8 | | 1.9 | | 160.3 | 388.2 |
| PCF5.1h | | 0.6 | 0.1 | 0.1 | 53.8 | 0.6 | 1.3 | 21.1 | | | 5.7 | 7.8 | 473.4 | 14.1 | | 18.1 | 205.5 | 555.7 |
| PCF5.7b | | 0.6 | 0.2 | 0.1 | 65.6 | 0.2 | 1.0 | 7.8 | | | | | 324.9 | | 1.2 | 11.8 | 214.4 | 656.9 |
| PCF5.2d | | 0.1 | 0.0 | 0.1 | 64.7 | 0.1 | 0.4 | 2.5 | | | | 3.2 | 156.6 | | | | 180.2 | 458.2 |
| PCF5.6d | | 0.5 | 0.2 | 0.1 | 66.2 | 0.2 | 1.3 | 8.2 | | | | 4.5 | 330.1 | 5.0 | | 13.8 | 199.8 | 579.7 |
| **Mafic Igneous Rocks** | | | | | | | | | | | | | | | | | | |
| PCF1a | V - Andesite | 11.6 | 0.3 | 1.1 | 3.8 | 0.2 | 12.2 | 58.7 | 1.5 | 188.7 | 71.6 | 5.1 | 176.6 | 129.5 | 4.8 | | 188.7 | 6555.0 |
| PCF1f | V - Basalt | 9.9 | 0.3 | 0.7 | 8.4 | 1.0 | 11.6 | 46.8 | 3.4 | 208.5 | 54.0 | 11.3 | 240.7 | 52.9 | | 9.9 | 267.2 | 4193.6 |
| PCF1i | V - Basaltic Andesite | 4.1 | 0.1 | 0.7 | 4.8 | 2.9 | 10.6 | 52.4 | 0.8 | 107.4 | 23.0 | 32.8 | 295.5 | 110.0 | 2.7 | 18.9 | 396.9 | 4379.9 |
| PCF1j | V - Andesite | 9.8 | 0.2 | 0.8 | 5.3 | 1.4 | 15.5 | 55.7 | 2.6 | 262.4 | 50.6 | 26.0 | 403.2 | 68.0 | | | 357.6 | 5033.2 |
| CR20a | V - Andesite | 8.2 | 0.1 | 0.5 | 1.5 | 0.7 | 15.4 | 54.4 | 2.5 | 210.5 | 40.3 | 5.0 | 129.6 | 31.9 | | | 335.2 | 3139.1 |
| CR20b | V - Andesite | 7.2 | 0.1 | 0.5 | 1.2 | 0.6 | 15.2 | 54.0 | 1.7 | 148.7 | 36.8 | 4.4 | 149.4 | 33.0 | | 4.2 | 287.9 | 2878.8 |
| CR20d | V - Basalt | 10.0 | 0.2 | 0.4 | 3.7 | 0.4 | 13.2 | 44.3 | 2.2 | 380.1 | 41.5 | 4.5 | 131.0 | 28.4 | | | 252.0 | 2594.2 |
| PCF5.1a | V - Basalt | 9.9 | 0.3 | 0.2 | 9.2 | 1.2 | 14.0 | 45.2 | 6.8 | 230.5 | 64.6 | 20.9 | 44.5 | 7.0 | | | 220.3 | 1355.4 |
| PCF5.1e | V - Andesite | 6.0 | 0.1 | 0.6 | 5.8 | 1.8 | 11.5 | 61.9 | 1.8 | 188.3 | 26.3 | 37.2 | 356.1 | 45.5 | 1.6 | 14.4 | 266.5 | 3355.1 |
| PCF5.1d | V - Andesite | 5.4 | 0.2 | 0.4 | 9.2 | 1.8 | 11.4 | 57.9 | 1.3 | 70.4 | 32.9 | 30.4 | 233.4 | 100.3 | | 11.4 | 420.4 | 2524.8 |
| PCF5.8b | V - Basalt | 11.6 | 0.2 | 0.9 | 3.4 | 1.9 | 16.1 | 48.6 | 4.7 | 279.2 | 63.4 | 16.9 | 142.8 | 63.0 | 4.0 | 5.1 | 316.2 | 5248.6 |
| PCF5.7f | V - Basalt | 2.8 | 0.1 | 0.4 | 9.1 | 0.5 | 8.5 | 48.0 | 1.2 | | 20.4 | 5.8 | 65.2 | 34.3 | 1.7 | 9.3 | 211.4 | 2315.4 |
| PCF5.7d | V - Andesite | 5.1 | 0.1 | 1.0 | 4.0 | 2.1 | 13.6 | 53.7 | 1.2 | 196.7 | 38.8 | 13.6 | 410.1 | 63.5 | 3.0 | 18.9 | 405.3 | 6026.2 |
| PCF5.2b | V - Basalt | 8.5 | 0.2 | 0.6 | 6.3 | 1.6 | 14.5 | 48.3 | 2.8 | 196.6 | 48.3 | 17.4 | 239.7 | 51.8 | 2.3 | 11.3 | 314.1 | 3548.2 |
| PCF5.6c | V - Andesite | 4.9 | 0.1 | 0.9 | 3.7 | 2.0 | 14.1 | 54.1 | 2.8 | 178.7 | 40.2 | 15.1 | 425.7 | 58.9 | 3.8 | 17.0 | 427.8 | 5348.5 |
| PCF5.3a | V - basalt | 9.3 | 0.3 | 0.2 | 9.2 | 1.6 | 12.9 | 45.0 | 6.0 | 212.7 | 47.5 | 26.1 | 42.7 | 7.5 | | 4.2 | 256.7 | 1324.4 |
| PCF5.3c | V - Andesite | 5.0 | 0.2 | 0.4 | 7.9 | 1.9 | 11.1 | 56.7 | 0.9 | | 34.5 | 20.2 | 164.9 | 100.3 | 4.3 | 15.5 | 445.6 | 2400.7 |
| PCF5.3j | V - Basalt | 7.7 | 0.2 | 1.1 | 5.6 | 3.0 | 16.4 | 50.8 | 2.6 | 267.3 | 47.7 | 16.9 | 369.0 | 69.4 | 5.1 | 10.0 | 434.6 | 6418.9 |
| PCF1d | P - Gabbro | 7.4 | 0.2 | 0.8 | 8.2 | 1.6 | 13.9 | 49.2 | 1.2 | 241.7 | 27.9 | 33.6 | 561.9 | 56.7 | | 9.2 | 420.5 | 4962.5 |
| PCF1h | P - Gabbro | 6.8 | 0.2 | 0.8 | 7.2 | 1.4 | 12.6 | 48.0 | 3.3 | 248.0 | 32.4 | 21.0 | 467.4 | 68.8 | 2.5 | | 328.3 | 5027.5 |
| PCF5.1g | P - Gabbro | 7.6 | 0.2 | 0.5 | 6.4 | 1.6 | 7.4 | 46.4 | 1.9 | 118.8 | 39.6 | 14.6 | 244.3 | 58.9 | | | 230.1 | 3021.4 |
| **Felsic Igneous Rocks** | | | | | | | | | | | | | | | | | | |
| PCF1b | P - diorite | 4.1 | 0.1 | 0.3 | 8.9 | 2.8 | 10.3 | 60.4 | | 65.7 | 18.2 | 31.9 | 191.0 | 135.9 | 4.3 | 6.8 | 457.2 | 1953.3 |

155

| | | | | | | | | | | | | | | | | | | |
|---|---|---|---|---|---|---|---|---|---|---|---|---|---|---|---|---|---|---|
| **PCF1g** | P - diorite | 9.1 | 0.2 | 0.9 | 8.2 | 1.6 | 14.7 | 51.9 | 4.0 | 374.5 | 38.3 | 24.0 | 332.3 | 39.6 | 2.7 | 10.9 | 320.3 | 5565.1 |
| **CD1.6a** | FV - dacite | 3.9 | 0.1 | 0.7 | 1.0 | 2.7 | 11.2 | 64.4 | 1.0 | 121.4 | 28.9 | 24.4 | 165.2 | 121.6 | 1.9 | 8.9 | 450.8 | 3970.9 |
| **CD1.6d** | FV - rhyolite | 3.2 | 0.0 | 0.6 | 0.7 | 1.1 | 8.2 | 76.2 | | 102.2 | 21.6 | 17.6 | 130.4 | 107.8 | 1.2 | 10.0 | 176.9 | 3495.4 |
| **CD1.6c** | FV - dacite | 5.7 | 0.1 | 0.8 | 0.8 | 1.6 | 9.9 | 66.2 | | 141.0 | 60.3 | 17.9 | 170.9 | 110.5 | 1.9 | 22.1 | 315.2 | 4659.6 |
| **CD1.6b** | FV - rhyolite | 5.6 | 0.1 | 0.6 | 1.0 | 1.2 | 9.7 | 71.1 | 0.6 | 116.1 | 41.6 | 13.1 | 135.4 | 117.3 | | 16.2 | 280.4 | 3720.2 |
| **CR20c** | FV - dacite | 3.0 | 0.1 | 0.5 | 3.3 | 1.7 | 11.8 | 65.4 | 0.9 | 218.5 | 91.1 | 18.1 | 157.7 | 40.4 | | | 539.8 | 3061.2 |
| **PCF5.4a** | P - Granodiorite | 2.1 | 0.1 | 0.2 | 5.0 | 3.4 | 9.8 | 68.9 | | | 6.4 | 38.1 | 86.0 | 174.3 | 4.5 | 13.3 | 486.3 | 1301.3 |
| **PCF5.1c** | P - diorite | 8.4 | 0.2 | 0.6 | 5.0 | 1.7 | 16.0 | 57.1 | 2.6 | 195.3 | 34.3 | 25.5 | 510.0 | 52.4 | 2.5 | 8.6 | 412.4 | 3643.0 |
| **PCF5.1b** | P - Granodiorite | 4.4 | 0.1 | 0.4 | 4.2 | 2.4 | 13.1 | 66.8 | 1.2 | 87.2 | 22.0 | 35.4 | 262.7 | 189.8 | | 11.7 | 448.4 | 2573.2 |
| **PCF5.1f** | P - diorite | 7.4 | 0.2 | 0.6 | 4.6 | 1.5 | 14.7 | 56.3 | 2.2 | 142.8 | 29.5 | 23.1 | 420.2 | 78.9 | 2.5 | 9.1 | 346.5 | 3583.2 |
| **PCF5.1i** | P - Granodiorite | 5.3 | 0.1 | 0.1 | 6.2 | 1.6 | 10.8 | 68.1 | 2.8 | 123.7 | 18.3 | 39.2 | 171.1 | 24.6 | | | 283.0 | 497.9 |
| **PCF5.8a** | P - diorite | 5.2 | 0.1 | 0.1 | 4.4 | 0.8 | 7.1 | 61.9 | 2.7 | 109.2 | 8.3 | 15.8 | 85.9 | 43.3 | | 7.0 | 199.3 | 605.5 |
| **PCF5.7a** | P - diorite | 8.3 | 0.2 | 0.6 | 4.9 | 1.7 | 14.3 | 54.2 | 1.8 | 230.0 | 33.6 | 38.2 | 525.6 | 36.3 | | 10.0 | 459.2 | 3787.0 |
| **PCF5.2a** | P - Granodiorite | 2.6 | 0.1 | 0.3 | 2.6 | 3.4 | 10.1 | 69.0 | | | 8.9 | 30.2 | 88.8 | 166.3 | 5.0 | 12.1 | 470.8 | 1902.2 |
| **PCF5.6a** | P - diorite | 9.0 | 0.2 | 0.6 | 5.8 | 1.6 | 15.1 | 54.4 | 3.1 | 248.0 | 40.0 | 27.3 | 487.7 | 46.1 | 4.3 | 10.5 | 396.0 | 3624.8 |
| **PCF5.3b** | P - diorite | 8.5 | 0.2 | 0.6 | 3.8 | 1.6 | 13.5 | 54.1 | 2.0 | 146.4 | 34.5 | 30.1 | 362.2 | 92.0 | 1.2 | 4.4 | 358.2 | 3583.9 |
| **PCF5.3g** | P - diorite | 6.9 | 0.2 | 0.4 | 5.6 | 3.4 | 15.2 | 54.6 | 2.3 | 135.2 | 27.7 | 54.6 | 517.3 | 21.9 | | 15.0 | 440.3 | 2122.1 |

**Part 3 – WR-XRF:** Major Element Data (wt %)

| Sample | Rock Type | Na2O | MgO | Al2O3 | SiO2 | P2O5 | SO3 | K2O | CaO | TiO2 | MnO | Fe2O3 | LOI | Total |
|---|---|---|---|---|---|---|---|---|---|---|---|---|---|---|
| **Sedimentary Samples** | | | | | | | | | | | | | | |
| **CR10** | Sediment | 8.70 | 0.91 | 18.87 | 62.14 | 0.10 | 0.01 | 0.07 | 1.67 | 0.38 | 0.04 | 5.86 | 1.32 | 100.05 |
| **CR11** | Sediment | 4.14 | 4.24 | 15.68 | 56.76 | 0.15 | 0.03 | 0.10 | 4.80 | 0.59 | 0.10 | 9.29 | 4.75 | 100.63 |
| **CR12** | Sediment | 3.64 | 4.21 | 18.10 | 53.28 | 0.13 | 0.03 | 1.67 | 5.30 | 0.43 | 0.14 | 9.16 | 4.72 | 100.79 |
| **CR14** | Sediment | 5.26 | 4.34 | 13.95 | 53.49 | 0.14 | 0.05 | 0.23 | 8.09 | 0.46 | 0.23 | 10.99 | 3.04 | 100.28 |
| **CR15** | Sediment | 4.88 | 3.83 | 14.16 | 61.51 | 0.08 | 0.19 | 1.25 | 2.18 | 0.34 | 0.12 | 7.05 | 3.79 | 99.37 |
| **CR17** | Sediment | 4.00 | 3.50 | 16.35 | 56.51 | 0.17 | 0.02 | 0.65 | 5.55 | 0.56 | 0.15 | 9.34 | 4.01 | 100.80 |
| **CR18** | Sediment | 3.20 | 3.61 | 15.78 | 56.45 | 0.14 | 0.02 | 0.69 | 5.71 | 0.66 | 0.15 | 9.38 | 3.83 | 99.62 |
| **CD1.6** | Sediment | 2.61 | 0.19 | 8.76 | 78.14 | 0.27 | 0.01 | 2.02 | 1.30 | 0.52 | 0.04 | 3.81 | 1.84 | 99.51 |
| **CD3.4** | Sediment | 3.70 | 0.63 | 12.49 | 72.82 | 0.09 | 0.25 | 1.71 | 1.62 | 0.45 | 0.11 | 4.34 | 1.25 | 99.44 |
| **Mafic Samples** | | | | | | | | | | | | | | |
| **CR01** | V - Andesite | 5.69 | 2.92 | 16.38 | 52.46 | 0.25 | 0.01 | 1.39 | 5.48 | 0.83 | 0.24 | 11.00 | 2.38 | 99.03 |
| **CR03** | V - Andesite | 4.68 | 3.77 | 15.33 | 56.25 | 0.22 | 0.05 | 0.62 | 6.36 | 0.79 | 0.13 | 9.85 | 2.48 | 100.52 |
| **CR24** | V - Andesite | 4.42 | 3.59 | 14.11 | 57.52 | 0.22 | 0.06 | 1.10 | 5.77 | 0.78 | 0.14 | 9.74 | 3.11 | 100.57 |
| **PCF1a** | V - Andesite | 3.72 | 1.15 | 12.19 | 59.61 | 0.12 | 0.01 | 2.86 | 6.88 | 0.44 | 0.13 | 4.83 | 8.21 | 100.15 |
| **PCF5.1a** | V - Basalt | 2.11 | 8.66 | 15.42 | 46.68 | 0.03 | 0.02 | 1.07 | 7.88 | 0.24 | 0.31 | 10.55 | 7.70 | 100.67 |
| **PCF5.1c** | P - Diorite | 3.96 | 3.83 | 16.32 | 55.39 | 0.28 | 0.03 | 1.89 | 4.72 | 0.90 | 0.18 | 10.05 | 2.80 | 100.35 |
| **PCF5.3a** | V - Basalt | 2.28 | 8.40 | 15.32 | 46.04 | 0.02 | 0.00 | 0.93 | 8.29 | 0.23 | 0.31 | 10.12 | 8.78 | 100.72 |
| **PCF5.6** | V - Andesite | 3.89 | 3.64 | 16.05 | 55.06 | 0.28 | 0.02 | 1.89 | 4.68 | 0.93 | 0.18 | 10.06 | 2.81 | 99.48 |
| **PCF5.6a** | P - Diorite | 4.13 | 1.56 | 14.86 | 50.67 | 0.38 | 0.05 | 4.15 | 11.16 | 1.07 | 0.31 | 5.71 | 6.70 | 100.75 |
| **PCF5.8a** | P - Diorite | 3.33 | 3.90 | 10.79 | 69.16 | 0.05 | 0.00 | 1.13 | 3.65 | 0.10 | 0.07 | 5.41 | 2.07 | 99.67 |
| **Felsic Samples** | | | | | | | | | | | | | | |
| **CD2.3** | V - Dacite | 5.81 | 0.48 | 13.97 | 69.92 | 0.30 | 0.01 | 0.42 | 2.66 | 0.66 | 0.06 | 3.23 | 1.98 | 99.50 |
| **CD3.13** | V - Dacite | 6.14 | 0.76 | 14.04 | 69.57 | 0.32 | 0.03 | 0.90 | 2.78 | 0.66 | 0.08 | 3.91 | 1.71 | 100.91 |

**WR-XRF:** Trace Element Data (ppm)

| Sedimentary Samples | | Cl | V | Cu | Zn | Ga | Ge | As | Se | Br | Rb | Sr | Y | Zr |
|---|---|---|---|---|---|---|---|---|---|---|---|---|---|---|
| CR10 | Sediment | 80 | 275 | 106 | 90 | 14 | 1 | 1 | < 1 | < 1 | 1 | 44 | 8 | 26 |
| CR11 | Sediment | 98 | 261 | 108 | 96 | 13 | 2 | 2 | < 1 | < 1 | 2 | 128 | 18 | 48 |
| CR12 | Sediment | 127 | 315 | 138 | 79 | 13 | 1 | 1 | < 1 | < 1 | 16 | 339 | 10 | 26 |
| CR14 | Sediment | 95 | 347 | 165 | 78 | 13 | 2 | < 1 | < 1 | < 1 | 3 | 119 | 14 | 26 |
| CR15 | Sediment | 124 | 225 | 92 | 66 | 12 | 2 | 3 | < 1 | < 1 | 13 | 151 | 11 | 48 |
| CR17 | Sediment | 113 | 252 | 78 | 130 | 14 | 1 | 2 | < 1 | < 1 | 8 | 294 | 17 | 40 |
| CR18 | Sediment | 111 | 260 | 92 | 94 | 14 | 2 | 2 | < 1 | < 1 | 9 | 693 | 20 | 57 |
| CD1.6 | Sediment | 130 | 68 | 12 | 49 | 10 | < 1 | 2 | < 1 | < 1 | 17 | 190 | 23 | 93 |
| CD3.4 | Sediment | 57 | 32 | 14 | 85 | 12 | 2 | 2 | < 1 | < 1 | 29 | 176 | 48 | 121 |
| | | | | | | | | | | | | | | |
| Mafic Samples | | | | | | | | | | | | | | |
| CR01 | P - Gabbro | 188 | 250 | 81 | 100 | 16 | 3 | 2 | < 1 | < 1 | 14 | 210 | 27 | 63 |
| CR03 | V - Andesite | 133 | 379 | 199 | 89 | 15 | 2 | 2 | < 1 | < 1 | 4 | 128 | 21 | 73 |
| CR24 | V - Andesite | 149 | 373 | 188 | 84 | 12 | 1 | 2 | < 1 | < 1 | 7 | 174 | 21 | 75 |
| PCF1a | V - Andesite | 27 | 76 | 17 | 43 | 12 | 1 | 1 | < 1 | < 1 | 34 | 257 | 30 | 151 |
| PCF5.1a | V - Basalt | 29 | 246 | 32 | 164 | 10 | < 1 | < 1 | < 1 | < 1 | 20 | 63 | 11 | 8 |
| PCF5.1c | P - Diorite | 130 | 232 | 86 | 100 | 16 | 2 | 1 | < 1 | < 1 | 33 | 488 | 27 | 76 |
| PCF5.3a | V - Basalt | 26 | 249 | 6 | 172 | 9 | < 1 | < 1 | < 1 | < 1 | 17 | 64 | 11 | 7 |
| PCF5.6 | V - Andesite | 156 | 248 | 76 | 98 | 16 | 1 | < 1 | < 1 | < 1 | 33 | 491 | 28 | 86 |
| PCF5.6a | P - Diorite | 35 | 272 | 123 | 123 | 12 | 1 | 1 | < 1 | < 1 | 36 | 300 | 37 | 63 |
| PCF5.8a | P - Diorite | 79 | 106 | 12 | 16 | 10 | 1 | < 1 | < 1 | < 1 | 22 | 155 | 4 | 45 |
| | | | | | | | | | | | | | | |
| Felsic Samples | | | | | | | | | | | | | | |
| CD2.3 | V - Dacite | 108 | 82 | 24 | 83 | 14 | 2 | 4 | < 1 | < 1 | 6 | 92 | 29 | 128 |
| CD3.13 | V - Dacite | 110 | 67 | 26 | 106 | 11 | 1 | 1 | < 1 | < 1 | 6 | 379 | 31 | 106 |
| | | | | | | | | | | | | | | |

| Sedimentary Samples | | Nb | Mo | Cd | Sn | Sb | Cs | Ba | La | Ce | Hf | W | Hg | Pb | Bi | Th | U |
|---|---|---|---|---|---|---|---|---|---|---|---|---|---|---|---|---|---|
| **CR10** | Sediment | 1 | < 1 | < 2 | < 3 | < 3 | < 4 | 67 | 29 | < 0.3 | < 2 | < 1 | < 1 | < 1 | < 1 | < 0.4 | < 1.0 |
| **CR11** | Sediment | 1 | < 1 | < 2 | < 3 | < 3 | < 4 | 53 | < 4 | 12 | < 2 | < 1 | < 1 | 7 | < 1 | < 0.2 | < 1.0 |
| **CR12** | Sediment | 1 | < 1 | < 2 | < 3 | < 3 | < 4 | 835 | < 4 | 15 | < 2 | < 1 | < 1 | 3 | < 1 | 0.8 | < 1.0 |
| **CR14** | Sediment | 1 | < 1 | < 2 | < 3 | < 3 | < 4 | 96 | < 4 | 16 | < 2 | < 1 | < 1 | 4 | < 1 | < 0.3 | < 1.0 |
| **CR15** | Sediment | 2 | < 1 | < 2 | < 3 | < 3 | < 4 | 382 | 25 | < 4 | < 2 | < 1 | < 1 | 3 | < 1 | 0.9 | < 1.0 |
| **CR17** | Sediment | 1 | < 1 | < 2 | < 3 | < 3 | < 4 | 256 | 15 | < 4 | < 2 | < 1 | < 1 | 4 | < 1 | < 0.3 | < 1.0 |
| **CR18** | Sediment | 1 | < 1 | < 2 | < 3 | < 3 | < 4 | 294 | 14 | 4 | < 2 | < 1 | < 1 | 8 | < 1 | 2 | < 1.0 |
| **CD1.6** | Sediment | 3 | < 1 | < 2 | < 3 | 7 | < 4 | 389 | < 4 | < 4 | < 2 | < 1 | < 1 | 2 | < 1 | 1.8 | 2.4 |
| **CD3.4** | Sediment | 3 | < 1 | < 2 | < 3 | 4 | < 4 | 294 | < 4 | 23 | < 2 | < 1 | < 1 | 6 | < 1 | 2.2 | 0.6 |
| | | | | | | | | | | | | | | | | | |
| **Mafic Samples** | | | | | | | | | | | | | | | | | |
| **CR01** | P - Gabbro | 2 | < 1 | < 2 | < 3 | < 3 | < 4 | 636 | < 4 | < 4 | < 2 | < 1 | < 1 | 2 | < 1 | 1.6 | < 1.0 |
| **CR03** | V - Andesite | 1 | < 1 | < 2 | < 3 | < 3 | < 4 | 214 | 11 | < 1.1 | < 2 | < 1 | < 1 | 9 | < 1 | 1.1 | < 1.0 |
| **CR24** | V - Andesite | 2 | < 1 | < 2 | < 3 | < 3 | < 4 | 327 | 21 | 31 | < 2 | < 1 | < 1 | 6 | < 1 | 1.4 | < 1.0 |
| **PCF1a** | V - Andesite | 5 | < 1 | < 2 | < 3 | < 3 | < 4 | 503 | 18 | 31 | < 2 | < 1 | < 1 | 5 | < 1 | 3 | 2.3 |
| **PCF5.1a** | V - Basalt | < 1 | < 1 | < 2 | < 3 | 3 | < 4 | 107 | 19 | 9 | < 2 | < 1 | < 1 | < 1 | < 1 | < 1.0 | < 1.0 |
| **PCF5.1c** | P - Diorite | 2 | < 1 | < 2 | < 3 | < 3 | < 4 | 441 | 17 | 20 | < 2 | < 1 | < 1 | 4 | < 1 | 2.3 | 0.8 |
| **PCF5.3a** | V - Basalt | < 1 | < 1 | < 2 | < 3 | < 3 | < 4 | 79 | 8 | < 4 | < 2 | < 1 | < 1 | 1 | < 1 | < 1.0 | < 1.0 |
| **PCF5.6** | V - Andesite | 2 | < 1 | < 2 | < 3 | 5 | < 4 | 424 | 9 | < 4 | < 2 | < 1 | < 1 | 4 | < 1 | 1.4 | < 1.0 |
| **PCF5.6a** | P - Diorite | 1 | < 1 | < 2 | < 3 | < 3 | < 4 | 465 | < 4 | 38 | < 2 | < 1 | < 1 | 4 | < 1 | 1.6 | 1 |
| **PCF5.8a** | P - Diorite | 3 | < 1 | < 2 | < 3 | < 3 | < 4 | 170 | < 4 | 24 | < 2 | < 1 | < 1 | 3 | < 1 | 2.8 | 1.1 |
| | | | | | | | | | | | | | | | | | |
| **Felsic Samples** | | | | | | | | | | | | | | | | | |
| **CD2.3** | V - Dacite | 4 | < 1 | < 2 | < 3 | < 3 | < 4 | 154 | 18 | 36 | < 2 | < 1 | < 1 | 3 | < 1 | 1.5 | 1.4 |
| **CD3.13** | V - Dacite | 4 | < 1 | < 2 | < 3 | < 3 | < 4 | 439 | < 4 | 75 | < 2 | < 1 | < 1 | 12 | < 1 | 3.3 | 3.9 |

**Part 4 – REE Data**

| SAMPLE | Ba | Ce | Cr | Cs | Dy | Er | Eu | Ga | Gd | Hf | Ho | La | Lu | Nb | Nd |
|---|---|---|---|---|---|---|---|---|---|---|---|---|---|---|---|
| CR03 | 181 | 20.5 | 110 | 0.16 | 3.16 | 2.06 | 1.1 | 15.9 | 3.41 | 2.1 | 0.69 | 10.1 | 0.3 | 1.8 | 13.9 |
| CR10 | 45.8 | 9.7 | 130 | 0.02 | 1.32 | 0.82 | 0.51 | 14.1 | 1.49 | 0.9 | 0.27 | 4.7 | 0.11 | 1.3 | 6.1 |
| CR11 | 52.5 | 16.2 | 70 | 0.04 | 2.74 | 1.78 | 0.88 | 12.8 | 2.66 | 1.3 | 0.55 | 7.7 | 0.22 | 1.1 | 10.7 |
| CR14 | 76.3 | 11.1 | 140 | 0.13 | 2.01 | 1.42 | 0.69 | 15.2 | 2 | 0.8 | 0.43 | 5.5 | 0.2 | 0.8 | 7.1 |
| CR15 | 346 | 14.9 | 120 | 0.23 | 1.56 | 1.02 | 0.55 | 12.5 | 1.52 | 1.3 | 0.32 | 7.3 | 0.15 | 2.3 | 7.8 |
| CR17 | 225 | 13.6 | 90 | 0.2 | 2.52 | 1.68 | 0.89 | 14.1 | 2.64 | 1.2 | 0.53 | 6.3 | 0.24 | 1.1 | 9.4 |
| CR18 | 271 | 14.6 | 120 | 0.29 | 2.78 | 1.96 | 0.82 | 14.5 | 2.44 | 1.6 | 0.58 | 6.5 | 0.28 | 1.5 | 9.2 |
| CR24 | 300 | 23.1 | 100 | 0.08 | 3.23 | 2.14 | 1.13 | 14 | 3.65 | 2.1 | 0.69 | 11.2 | 0.27 | 1.9 | 14.5 |
| CD2.3 | 148.5 | 49.4 | 130 | 0.41 | 4.46 | 2.89 | 1.75 | 15.2 | 5.03 | 2.8 | 0.89 | 25.5 | 0.35 | 4.3 | 26.6 |
| CD3.13 | 431 | 50.3 | 170 | 0.23 | 4.45 | 3.01 | 1.98 | 11.2 | 5.46 | 2.9 | 0.95 | 26.2 | 0.36 | 4.3 | 29.3 |
| CD3.4 | 296 | 25.4 | 180 | 1.05 | 6.87 | 4.84 | 1.29 | 13.5 | 5.79 | 3.5 | 1.53 | 12.4 | 0.68 | 2.9 | 16.7 |
| PCF5b | 525 | 34.5 | 160 | 0.66 | 5.07 | 3.39 | 1.04 | 13.3 | 4.89 | 4.8 | 1.05 | 17.3 | 0.5 | 4.7 | 21.1 |
| PCF5.1a | 101.5 | 1.2 | 510 | 0.48 | 1.54 | 1.36 | 0.35 | 11.7 | 0.84 | 0.4 | 0.36 | 0.7 | 0.23 | 0.4 | 1 |
| PCF5.1c | 422 | 27 | 100 | 2.15 | 4.61 | 3.09 | 1.21 | 17.6 | 4.49 | 2.5 | 0.91 | 13.2 | 0.38 | 2.8 | 18.3 |
| PCF5.3a | 92.8 | 1.1 | 490 | 0.42 | 1.74 | 1.37 | 0.37 | 11.2 | 0.91 | 0.3 | 0.39 | 0.6 | 0.22 | 0.3 | 1 |
| PCF5.6 | 406 | 24.9 | 120 | 2.1 | 4.45 | 3.07 | 1.11 | 17.3 | 4.33 | 2.9 | 0.92 | 12 | 0.37 | 3.1 | 16.7 |
| PCF5.6a | 486 | 30 | 80 | 0.69 | 5.88 | 4.06 | 1.61 | 13.4 | 5.29 | 2.1 | 1.19 | 15.6 | 0.52 | 1.8 | 19 |
| PCF5.8 | 159 | 13.7 | 410 | 0.13 | 0.73 | 0.4 | 0.32 | 9.9 | 1.06 | 1.2 | 0.13 | 6.9 | 0.07 | 2.8 | 6.2 |

Continued…

| SAMPLE | Pr | Rb | Sm | Sn | Sr | Ta | Tb | Th | Tm | U | V | W | Y | Yb | Zr |
|---|---|---|---|---|---|---|---|---|---|---|---|---|---|---|---|
| CR03 | 3.13 | 2.8 | 3.33 | 1 | 109 | 0.1 | 0.53 | 1.92 | 0.28 | 0.82 | 363 | 2 | 17.2 | 1.83 | 63 |
| CR10 | 1.42 | 0.4 | 1.47 | 1 | 40.2 | 0.2 | 0.23 | 1.25 | 0.1 | 0.34 | 264 | 3 | 7.1 | 0.69 | 26 |
| CR11 | 2.36 | 0.9 | 2.81 | 1 | 110.5 | <0.1 | 0.44 | 1.12 | 0.23 | 0.67 | 230 | 3 | 14.8 | 1.61 | 42 |
| CR14 | 1.63 | 2.5 | 1.97 | 1 | 111 | <0.1 | 0.31 | 0.63 | 0.2 | 0.44 | 349 | 2 | 13.2 | 1.35 | 26 |
| CR15 | 1.92 | 12 | 1.85 | 1 | 136.5 | <0.1 | 0.27 | 1.7 | 0.13 | 0.48 | 208 | 4 | 9.2 | 1.01 | 44 |
| CR17 | 2.07 | 7.2 | 2.3 | 1 | 279 | <0.1 | 0.38 | 1 | 0.23 | 0.53 | 246 | 1 | 14.8 | 1.48 | 38 |
| CR18 | 2.24 | 8.6 | 2.6 | 1 | 644 | <0.1 | 0.44 | 1.55 | 0.26 | 0.66 | 243 | 2 | 17.1 | 1.74 | 54 |

| | | | | | | | | | | | | | | | |
|---|---|---|---|---|---|---|---|---|---|---|---|---|---|---|---|
| **CR24** | 3.4 | 6 | 3.56 | 1 | 157.5 | 0.1 | 0.53 | 2.01 | 0.27 | 0.82 | 372 | 6 | 18.6 | 1.88 | 70 |
| **CD2.3** | 6.55 | 5.8 | 5.93 | 1 | 86.4 | 0.1 | 0.72 | 3.76 | 0.36 | 2.05 | 78 | 2 | 26.3 | 2.34 | 106 |
| **CD3.13** | 7.09 | 5.6 | 6.3 | 1 | 356 | 0.2 | 0.78 | 3.76 | 0.41 | 2.34 | 67 | 4 | 27.5 | 2.51 | 97 |
| **CD3.4** | 3.8 | 27.1 | 5 | 2 | 166 | 0.2 | 0.99 | 2.98 | 0.66 | 0.86 | 24 | 4 | 42.9 | 4.74 | 108 |
| **PCF5b** | 5.18 | 33.3 | 4.83 | 2 | 249 | 0.3 | 0.77 | 3.58 | 0.5 | 1.87 | 79 | 3 | 28.3 | 3.41 | 142 |
| **PCF5.1a** | 0.18 | 19.3 | 0.61 | 1 | 64.6 | <0.1 | 0.19 | 0.05 | 0.21 | 0.06 | 241 | 4 | 11.4 | 1.43 | 11 |
| **PCF5.1c** | 4.03 | 30.3 | 4.48 | 1 | 461 | 0.1 | 0.71 | 1.69 | 0.38 | 0.84 | 246 | 2 | 25.2 | 2.5 | 83 |
| **PCF5.3a** | 0.21 | 17.7 | 0.58 | 1 | 67.8 | <0.1 | 0.2 | <0.05 | 0.2 | <0.05 | 235 | 5 | 11.3 | 1.45 | 10 |
| **PCF5.6** | 3.72 | 31.4 | 4.28 | 1 | 471 | 0.1 | 0.68 | 1.87 | 0.41 | 0.92 | 267 | 3 | 25.7 | 2.62 | 95 |
| **PCF5.6a** | 4.45 | 35.6 | 4.9 | 1 | 296 | <0.1 | 0.9 | 2.39 | 0.55 | 0.95 | 293 | 5 | 35.3 | 3.38 | 63 |
| **PCF5.8** | 1.66 | 20.3 | 1.37 | 1 | 145.5 | 0.1 | 0.13 | 3.36 | 0.08 | 0.59 | 111 | 4 | 3.7 | 0.4 | 41 |